Species interactions in a changing ocean: A study of inducible traits to understand community responses

Sasha Katya Seroy

A dissertation

submitted in partial fulfillment of the

requirements for the degree of

Doctor of Philosophy

University of Washington

2021

Reading Committee:

Daniel Grünbaum, Chair

Julie E. Keister

Terrie Klinger

Program Authorized to Offer Degree:

Oceanography

University of Washington

Abstract

Species interactions in a changing ocean: A study of inducible traits to understand community responses

Sasha Katya Seroy

Chair of the Supervisory Committee:
Professor Emeritus Daniel Grünbaum
Oceanography

Marine communities are experiencing rapid environmental changes including warming temperatures and ocean acidification (OA). For organisms within these communities, responses to ocean change are shaped by population- and community-level interactions which may modify their responses. This dissertation integrates experimental, field, and modeling approaches to understand how marine communities are responding to ocean change by studying species interactions and understanding propagating effects. Organisms with inducible morphologies, physical characteristics that can change based on exposure to specific predators (inducible defenses) or food sources (inducible offenses), can be a tool to track and quantify interactions in a changing ocean. In this dissertation, I present research on two marine invertebrates that exhibit inducible morphologies to demonstrate how studies of inducible traits provide a tool to

understand community responses to ocean change. In Chapters 2 and 3, I explored the individual- and population-level effects of OA on inducible defenses in the calcifying bryozoan, *Membranipora membranacea*. Predator exposure continued to induce defenses and modify *M. membranacea* colony growth in OA conditions. Population-level space competition also modulated costs of inducible defenses in OA conditions. In Chapters 4 and 5, I investigated the effects of an inducible offense on responses to warming temperatures in the marine snail, *Lacuna vincta*. Field surveys of inducible morphology documented frequent adult dispersal between eelgrass and macroalgal habitats, and experiments revealed that consequences of dispersal influenced *L. vincta* response to warming temperatures. Overall, *M. membranacea* and *L. vincta* were largely robust to the stressors they were exposed to and species interactions, documented using inducible traits, greatly influenced responses to ocean change in both organisms. In Chapter 6, I developed and evaluated a K-12 sensor-building module inspired by methods used in my own scientific research to create authentic STEM experiences for high school students. Using hands-on sensor building and local environmental change helped contextualize basic chemistry concepts and increased student learning. This dissertation provides insight into how integrated studies of inducible traits can help shed light on community responses to environmental change and provides ways to integrate ocean change research and educational initiatives through placed-based sensor building programs.

TABLE OF CONTENTS

LIST OF FIGURES

LIST OF TABLES

ACKNOWLEDGEMENTS

Thank you to Danny Grünbaum, my advisor, for his encouragement and support over my six years as a graduate student. He patiently fostered my development both as an educator and researcher, provided me opportunities to learn new skills like sensor building and modeling, and enabled me to follow my interests. I am very grateful to have had the opportunity to learn from him (and sass him) over the years.

Thank you to my committee members, Julie Keister, Terrie Klinger, and Alex Gagnon who helped me plan my research, interpret my data, and provided lots of helpful feedback on my work along the way.

This work would not have been possible without Dianna Padilla, who mentored me as an undergraduate at Stony Brook University, helped me navigate the graduate school application process, and served as an unofficial second advisor to me by continuing to help me in my summer research at Friday Harbor Labs. She was instrumental in developing my interest in invertebrates and taught me everything I know about “snail dentistry”.

I have been so fortunate to have been a part of a wonderful lab group and UW Seattle community. Thank you to my lab mates Robert, Amy, Deana, Katie and Owen, and my academic big sisters Tansy and Karen for always looking out for me, listening to me complain, and celebrating my little and big victories. Thank you to my wonderful friends Isaiah, Tamuka, Max, Zac, Anna, Claire, Rosalind, Theresa, Andrew, Christina, my whole Ocean’s Eleven cohort, the IGERT Program on Ocean Change group, and Oceanography graduate student community for keeping me sane.

I am also grateful for my second community at Friday Harbor Labs. I am appreciative of the graduate students, faculty, staff, and visiting scientists who helped me in my research. Special thanks to my FHL friends Alyssa, Mo, Will, Katie, Maria, Cassandra, Abigail, Karly, Kayla, and Olivia for fun times in Dorm Q and to Becca for always helping me put out fires in the OA lab.

I am also appreciative of the opportunity to mentor several undergraduate students during my ecological and education research. Thank you to Kim, Anik, Hanis, and Jose who let me learn with them and taught me how to be a good mentor. Thank you to Martha Groom for connecting me with wonderful Doris Duke Conservation Scholars Program students.

Thank you to the organizations that funded my work over the years: NSF GRFP, NSF IGERT Program on Ocean Change, Friday Harbor Labs, Conchologists of America, and the Pacific Northwest Shell Club.

Thank you to my family, Mom, Dad, Raoul, and Abuelita, and my unofficial extended family, Louda, Daniel, Sasha, Trevor, and Saletta. I am eternally grateful to my partner Ann who lived this Ph.D. every day with me, helping with fieldwork, building experimental rigs, caring for lab animals, testing lesson plans, and so much more. I love you all. This research would not have been possible without your support.

Finally, I'd like to thank Barbra Streisand for always reminding me to never let anything rain on my parade, which was especially useful for this New Yorker in Seattle.

DEDICATION

For Ann, whose continuous and unwavering support made all this work possible.

Chapter 1. INTRODUCTION

Marine communities are experiencing several rapidly occurring and concurrent environmental changes due to increasing atmospheric carbon dioxide (CO_2) concentrations. Rising CO_2 concentrations in the atmosphere trap heat, warming both the atmosphere and the ocean. Ocean temperatures have been increasing, with projected temperature increases of 2-4˚C within the next century (IPCC, 2014). In addition, increased atmospheric CO_2 drives increases in oceanic CO_2 uptake, resulting in ocean acidification (OA) that is characterized by a suite of chemical reactions decreasing pH and altering other chemical parameters of seawater (Zeebe & Wolf-Gladrow 2001). Ocean acidification is expected to intensify over the next century with projected pH decreases of 0.3-0.4 units (Feely et al. 2004, 2009). A main motivating objective of this dissertation is to understand how marine communities respond to these current environmental changes and near-future projections.

Both OA and warming temperatures present direct physiological stress for marine organisms. OA has documented effects on organism fitness including impairments on growth, development, survival, and behavior across a wide range of taxa and life stages (Ross et al. 2011, Kroeker et al. 2013, Nagelkerken & Munday 2016). Calcifying organisms, those that form shells or skeletons from calcium carbonate ($CaCO_3$), have been identified as particularly vulnerable because acidifying conditions make it more energetically difficult for organisms to precipitate $CaCO_3$ while also increasing $CaCO_3$ dissolution (Orr et al. 2005). Similarly, warming also has demonstrated direct effects on organisms because physiological processes, especially of ectotherms, are foundationally dependent on temperature-sensitive biochemical and cellular processes. Documented effects of warming temperatures across a wide range of taxa include

increased metabolism, respiration, and development (Sanford 2002, Przeslawski 2004, O'Connor 2009, Carr & Bruno 2013).

Direct effects of these environmental changes are well documented for organisms in isolation, but indirect effects driven by species interactions and feedbacks between organisms, populations, and communities modify direct effects of stress (Davis et al. 1998, Kordas et al. 2011, Kroeker et al. 2017). Community responses occur as the result of propagating organism- and population-level responses, but organism-level responses may be modified by population- (competition, population density) and community-level processes (trophic interactions). Indirect effects can modulate effects of ocean change, and carry implications for both community dynamics and the individual fitness of organisms within those communities. These types of population- and community-level processes, interactions, and feedbacks are often less studied because they are more difficult to measure using field and laboratory approaches.

Previous studies have found that indirect effects have amplified or diminished effects of ocean change. OA and warming have resulted in both strengthening and weakening of interactions between predators and prey or grazers and producers (Sanford 1999, O'Connor et al. 2009, Kroeker et al. 2014, Dodd et al. 2015). Contrasting impacts of ocean change variables on various trophic levels can result in differential cumulative effects, for instance if a predator is more vulnerable to stress than its prey species, or stress induces a positive effect on one trophic level but a negative effect on another (King & Sebens 2018). Ocean change can also shift competitive interactions to alter community structure (Sunday et al. 2017), and trophic cascades can cause changes in food web linkages and community dynamics (Alsterberg et al 2013). Therefore, even species that are more tolerant of ocean change can influence community responses via these indirect effects, trophic interactions, and feedbacks. Therefore, predicting

resulting community-level responses to ocean change requires the ability to quantify both direct and indirect effects, and to understand the ecological feedbacks that regulate them.

To understand how community responses to ocean change may be mediated by interactions between organism-, population-, and community-level processes, I use an integrative approach in this dissertation that combines experimental, field and modeling methods. By employing empirical methods to collect data about organism function, I inform models to make inferences about population-level processes that are difficult to measure in the field or manipulate in the lab. Models informed by experimental and field data can give insight into how individual-level responses propagate to higher levels and how higher-level processes shape individual fitness in a changing ocean (Queirós et al 2015, Nagelkerken & Munday 2016).

Inducible traits are those that can change based on a relevant environmental cue without associated genetic changes. Inducibility is common, with a wide variety of organisms exhibiting behavioral, morphological, chemical, or life history plasticity. Inducible traits can often be easily measured with associated costs and benefits quantified at multiple levels of organization. Specifically, inducible offenses and defenses are adaptive mechanisms, occurring from bottom-up or top-down trophic pressures respectively, that enable organisms to increase feeding or protect against predators. When offenses or defenses incur significant costs, inducibility allows organisms to maximize the benefit of the inducible morphology when needed while avoiding the cost when unnecessary (Tollrian & Harvell 1999, Ferrari et al. 2010). Inducible defenses are common in marine organisms, e.g. predator-induced shell thickening in oysters (Lord & Whitlatch 2012, Scherer et al. 2018), snails (Trussell & Nicklin 2002, Bourdeau 2010), and mussels (Leonard et al. 1999). Inducible offenses are less studied but examples are known e.g., gape size in predatory ciliates (Kopp & Tollrian 2003) or claw size in crabs (Smith & Palmer

1994) in response to available prey types. Thus, a fundamental aspect of these types of induble traits are that they modify relationships across trophic levels.

Inducible traits can provide a lens through which to investigate community responses to ocean change. Because they can modulate trophic interactions, it is beneficial to study impacts of ocean change across trophic levels in concert with the effects of inducibility. Potential adaptive advantages of inducibility may shift depending on novel environmental conditions. OA and high temperatures have been found to affect inducible traits and their cost-benefit tradeoffs in some species. The effectiveness, adaptive benefits, and relative costs of an inducible trait can be highly dependent on environmental conditions with the potential for propagating community effects. High pCO_2 conditions reduced predator-induced shell thickening in a marine snail (Bibby et al. 2007), neck teeth in freshwater *Daphnia* spp. (Weiss et al. 2018), anti-predator morphology and behavior in various mussel species (Kong et al. 2019). In contrast, high pCO_2 enhanced protective inducible colony formation in freshwater phytoplankton (Zhang et al. 2021). Warming reduced inducible growth rates in mussels (Freytes-Ortiz & Stallings, 2018) and decreased inducible colony formation in freshwater phytoplankton (Zhang et al. 2021), but reduced the cost of inducible behavior in mosquito larvae (van Uitregt at al. 2013). Studying such inducible organismal systems and measuring effects of ocean change on the individual level can provide a basis for integrative studies of how communities are responding to ocean change.

This dissertation uses two inducible marine invertebrate systems to investigate population- and community-level effects of ocean change: the encrusting calcifying bryozoan, *Membranipora membranacea*, and the snail, *Lacuna vincta*. Both organisms exhibit measurable inducible traits with effects that span multiple levels of organization. *M. membranacea* exhibits an inducible defense, defensive spines formed in response to chemical cues from predators.

These spines offer some protection from predators, but inhibit colony growth rates and space competition (Harvell 1984). Pelagic *M.membrancea* larvae settle on macroalgal blades, then colonize blade area by growing radially to outcompete conspecifics for space which intersects with the effects of these tradeoffs. *L. vincta* exhibits an inducible offense, plastic tooth morphology, in response to cues from different food resources which can influence reproductive output (Padilla 1998). Therefore, these two systems present distinct but informative opportunities to investigate the community effects of two different environmental stressors (*M. membranacea*: OA, *L. vincta*: warming). Studying both species provides an opportunity to consider both top-down and bottom-up examples of interactions between inducibility and ocean change induced stresses.

In Chapters 2 and 3, I ask how inducible defenses and OA affect individual fitness and population-level space competition in the bryozoan *M. membranacea*. Chapter 2 experimentally determines individual-level responses and evaluates them on the population level via the construction of an experimentally-informed spatially-explicit model. This integrative model quantifies competitive interactions among conspecifics that would otherwise be difficult to measure experimentally to make inferences about population-level processes affected by OA and inducibility. Chapter 3 further explores the model developed in Chapter 2 to ask how variable larval settlement time and population density affect the fitness consequences of inducible defenses in OA conditions. This chapter also validates the model using comparisons with bryozoan spatial distribution observations from the field.

Chapters 4 and 5 focus on the marine snail *L. vincta* including how inducible offenses affect responses to warming temperatures and what they can reveal about population-level processes. Chapter 4 investigates the effects of warming on important *L. vincta* ecological

interactions using an experimental approach. Chapter 5 utilizes inducible radula morphology to document population-level patterns of adult dispersal between eelgrass and macroalgal habitats using field and modeling approaches.

Chapter 6 developed from my commitment to STEM education and teaching experiences in the undergraduate course, *Ocean 351: Foundations of Ocean Sensors*, that provided me the opportunity to develop, adapt, and evaluate a sensor-based STEM education module for high school students. Students build, calibrate, and test environmental samples using simple spectrometric pH sensors based on modified but analogous methods to those used in Chapter 2 to monitor OA conditions. I investigate how teaching ocean change using student-built pH sensors can improve student learning by helping to contextualize foundational chemistry concepts.

In Chapter 7, I present conclusions, explore the implications of this body of work and identify avenues for future investigation.

References

Alsterberg C, Eklöf JS, Gamfeldt L, Havenhand JN, Sundbäck K (2013) Consumers mediate the effects of experimental ocean acidification and warming on primary producers. P Nat Acad Sci USA 110:8603-8608.

Bibby R, Cleall-Harding P, Rundle S, Widdicombe S, Spicer J (2007) Ocean acidification disrupts induced defenses in the intertidal gastropod *Littorina littorea*. Biol Letters 3:699-701

Bourdeau PE (2010) Cue reliability, risk sensitivity and inducible morphological defense in a marine snail. Oecologia 162: 987−994

Davis AJ, Lawton JH, Shorrocks B, Jenkinson LS (1998) Individualistic species responses invalidate simple physiological models of community dynamics under global environmental change. J Anim Ecol 67: 600-612

Dodd LF, Grabowski JH, Piehler MF, Westfield I, Ries JB (2015). Ocean acidification impairs crab foraging behaviour. Proc R Soc B Biol Sci 282:20150333

Feely RA, Sabine CL, Lee K, Berelson W, Kleypas J, Fabry VJ, & Millero FJ (2004) Impact of anthropogenic CO_2 on the $CaCO_3$ system in the oceans. Science 305:362-366

Feely RA, Doney SC, Cooley SR (2009) Ocean acidification: Present conditions and future changes in a high-CO_2 world. Oceanography 22:36-47

Ferrari MC, Wisenden BD, Chivers, DP (2010) Chemical ecology of predator–prey interactions in aquatic ecosystems: a review and prospectus. Can J Zool 88:698-724

Freytes-Ortiz IM, Stallings CD (2018) Elevated temperatures suppress inducible defenses and alter shell shape of intertidal mussel. Mar Biol, 165: 113.

Harvell CD (1984) Predator-induced defense in a marine bryozoan. Science 224:1357–1359

IPCC (2014) Climate change 2014: synthesis report. In: Core Writing Team, Pachauri RK, Meyer LA (eds) Contribution of working groups I, II and III to the fifth assessment report of the intergovernmental panel on climate change. IPCC, Geneva, p. 151

King W, Sebens KP (2018) Non-additive effects of air and water warming on an intertidal predator–prey interaction. Mar Biol 165:64

Kong H, Clements JC, Dupont S, Wang T, and others (2019) Seawater acidification and temperature modulate anti-predator defenses in two co-existing *Mytilus* species. Mar Pollut Bull 145:118-125

Kopp M, Tollrian, R (2003). Reciprocal phenotypic plasticity in a predator–prey system: inducible offences against inducible defences? Ecol Lett, 6:742-748

Kordas RL, Harley CDG, O'Connor MI (2011) Community ecology in a warming world: the influence of temperature on interspecific interactions in marine systems. J Exp Mar Biol Ecol 400: 218–226

Kroeker KJ, Kordas RL, Crim R, Hendriks IE, Ramajo L, Singh GS, Gattuso JP (2013) Impacts of ocean acidification on marine organisms: Quantifying sensitivities and interaction with warming. Glob Chang Biol 19:1884-1896

Kroeker KJ, Sanford E, Jellison BM, Gaylord B (2014) Predicting the effects of ocean acidification on predator-prey interactions: a conceptual framework based on coastal molluscs. Biol Bull 226:211-222

Kroeker KJ, Kordas RL, Harley CD (2017) Embracing interactions in ocean acidification research: confronting multiple stressor scenarios and context dependence. Biol Lett 13:20160802

Leonard GH, Bertness MD, Yund PO (1999) Crab predation, waterborne cues, and inducible defenses in the blue mussel, *Mytilus edulis*. Ecology 80:1-14

Lord JP, Whitlatch RB (2012) Inducible defenses in the eastern oyster *Crassostrea virginica Gmelin* in response to the presence of the predatory oyster drill *Urosalpinx cinerea Say* in Long Island Sound. Mar Biol 159:1177-1182

Nagelkerken I, Munday PL (2016) Animal behaviour shapes the ecological effects of ocean acidification and warming: moving from individual to community-level responses. Glob Change Biol 22:974-989.

O'Connor MI (2009) Warming strengthens an herbivore–plant interaction. Ecology 90:388-398.

Orr JC, Fabry VJ, Aumont O, Bopp L and others (2005) Anthropogenic ocean acidification over the twenty-first century and its impact on calcifying organisms. Nature 437:681

Padilla DK (1998) Inducible phenotypic plasticity of the radula in Lacuna (Gastropoda: Littorinidae). Veliger 41:201-204

Queirós AM, Fernandes JA, Faulwetter S, Nunes J and others (2015) Scaling up experimental ocean acidification and warming research: from individuals to the ecosystem. Glob Change Biol 21:130-143

Ross PM, Parker L, O'Connor WA, Bailey EA (2011) The impact of ocean acidification on reproduction, early development, and settlement of marine organisms. Water 3:1005-1030

Sanford E (1999) Regulation of keystone predation by small changes in ocean temperature. Science 283:2095–2096

Scherer AE, Bird CE, McCutcheon MR, Hu X, Smee DL (2018) Two-tiered defense strategy may compensate for predator avoidance costs of an ecosystem engineer. Mar Biol 165:131

Smith LD, Palmer AR (1994) Effects of manipulated diet on size and performance of brachyuran crab claws. Science 264:710-712.

Sunday JM, Fabricius KE, Kroeker KJ, Anderson KM and others (2017) Ocean acidification can mediate biodiversity shifts by changing biogenic habitat. Nat Clim Change 7:81-85

Tollrian R, Harvell CD (1999) The ecology and evolution of inducible defenses. Princeton University Press, Princeton, NJ

Trussell GC, Nicklin MO (2002) Cue sensitivity, inducible defense, and trade-offs in a marine snail. Ecology 83:1635-1647

van Uitregt VO, Hurst TP, Wilson RS (2013) Greater costs of inducible behavioural defences at cooler temperatures in larvae of the mosquito, *Aedes notoscriptus*. Evol Ecol 27:13-26

Zeebe RE, Wolf-Gladrow D (2001). CO_2 in seawater: equilibrium, kinetics, isotopes (No. 65). Gulf Professional Publishing.

Zhang L, Sun Y, Cheng J, Cui G, Huang Y, Yang Z (2021) Warming mitigates the enhancement effect of elevated air CO_2 on anti-grazer morphological defense in *Scenedesmus obliquus*. Sci Tot Environ 770:145341

Chapter 2. INDIVIDUAL AND POPULATION LEVEL EFFECTS OF OCEAN ACIDIFICATION ON A PREDATOR-PREY SYSTEM WITH INDUCIBLE DEFENSES: BRYOZOAN-NUDIBRANCH INTERACTIONS IN THE SALISH SEA

This manuscript has been previously published as: Seroy, S. K., Grünbaum, D. (2018) Individual and population level effects of ocean acidification on a predator-prey system with inducible defenses: bryozoan-nudibranch interactions in the Salish Sea. Marine Ecology Progress Series 607: 1-18. https://doi.org/10.3354/meps12793

2.1 ABSTRACT

Ocean acidification (OA) from increased oceanic CO_2 concentrations imposes significant physiological stresses on many calcifying organisms. OA effects on individual organisms may be synergistically amplified or reduced by inter- and intraspecies interactions as they propagate up to population and community levels, altering predictions by studies of calcifier responses in isolation. The calcifying colonial bryozoan, *Membranipora membranacea*, and the predatory nudibranch, *Corambe steinbergae*, comprise a trophic system strongly regulated by predator-induced defensive responses and space limitation, presenting a unique system to investigate OA effects on these regulatory mechanisms at individual and population levels. We experimentally quantified OA effects across a range of pH from 7.0 to 7.9 on growth, calcification, senescence, and predator-induced spine formation in *Membranipora*, with or without waterborne predator

cue, and on zooid consumption rates in *Corambe* at Friday Harbor Laboratories, San Juan Island, WA. *Membranipora* exhibited maximum growth and calcification at moderately low pH (7.6), and continued spine formation in all pH treatments. Spines reduced *Corambe* zooid consumption rates, with lower pH weakening this effect. Using a spatially-explicit model of colony growth, where colony area serves as a proxy for colony fitness, we assessed the population-level impacts of these experimentally-determined individual-level effects in the context of space limitation. The area-based fitness costs associated with defense measured at the individual level led to amplified effects predicted for the population level due to competition. Our coupled experimental and modeling results demonstrate the need to consider population-level processes when assessing ecological responses to stresses from changing environments.

2.2 INTRODUCTION

Ocean acidification (OA) resulting from increased oceanic uptake of atmospheric carbon dioxide presents a variety of environmental stresses to marine organisms and ecosystems (Hofmann et al. 2010, Kroeker et al. 2013). OA causes a decrease in both pH and carbonate ion availability (Feely et al. 2009), with often negative physiological implications for many organisms (Kroeker et al. 2013). Global pH levels have been declining, with continued projections of 0.3-0.4 units within the next century (Feely et al. 2004, 2009). Coastal areas however, often experience natural pH fluctuations in CO_2 that currently exceed these predicted changes (Hofmann et al. 2010, Doney 2010). In the Salish Sea and San Juan Archipelago, WA, USA, naturally low seawater pH levels result from regular upwelling and river input (Murray et al. 2015). While open ocean pH averages well above 8.0 (Doney 2010), the San Juan Archipelago experiences pH around 7.8 and can reach as low as 7.67 in San Juan Channel during

seasonal upwelling (Sullivan 2012, Murray et al. 2015). Consequently, the Salish Sea is a natural laboratory to investigate OA effects where organisms already experience pH values that open ocean organisms will likely not experience until the end of the century.

Organisms that make shells or skeletons from $CaCO_3$ are common in the Salish Sea, with a third of Puget Sound species identified as calcifiers (Busch & McElhany 2017). Calcifying organisms have been demonstrated to be generally vulnerable to acidification (Kroeker et al. 2013). Decreasing availability of CO_3^{2-} can impede calcification (Feely et al. 2009). In conjunction, the dissolution of calcified structures is favored by the low saturation states of $CaCO_3$ polymorphs calcite and aragonite that often accompany OA (Orr et al. 2005). Calcifier responses to OA have been generally negative with many organisms exhibiting decreased growth, survival and calcification rates (Kroeker et al. 2013). Some taxa, however, display no effect or even positive effects, demonstrating the importance of quantifying species-specific responses in diverse taxa (Ries et al. 2009). Variable OA responses have been attributed to a number of potential causes, including diversity of calcification mechanisms, presence and thickness of protective organic membranes and solubility of different $CaCO_3$ polymorphs in addition to differences in capacity for plasticity and prior exposure to low pH (Ries et al. 2009).

While most studies document OA effects on calcifiers in isolation, the true ecological consequences of these stresses occur within interconnected species networks that ultimately structure populations and communities. Skeletal mineralogy alone is an incomplete predictor of OA sensitivity, especially in the context of trophic interactions where direct and indirect effects associated with species interactions may be significant (Busch & McElhany 2017). Physiological and behavioral processes in both predators and prey may be impacted differently by OA. These alterations potentially amplify or reduce organism-level effects of OA on

population and community levels, highlighting the importance of considering predator-prey interactions when conducting OA studies (Kroeker et al. 2014). For example, OA may impair predator detection mechanisms, resulting in reduced predator avoidance behavior in fish (Dixson et al. 2010) and marine snails (Manriquez et al. 2013), but can reduce predation by crabs on oysters (Dodd et al. 2015). In these examples, the differential effects of OA on distinct trophic levels indicate a potential for environmental stress to impact populations and communities to different extents and in different directions than suggested by studies of species in isolation. The potential of OA to alter predator-prey interactions, and how these effects may propagate to populations and communities, however, remains poorly understood.

Inducible defenses are an important subset of predator-prey interactions that confer protection to organisms upon the detection of environmental cues of impending predation (Harvell 1990). When defenses incur significant costs, inducibility allows organisms to maximize the benefit of being defended when under attack while avoiding the cost of defense when predation risks are low (Tollrian & Harvell 1999, Ferarri et al. 2010). Predator-induced defenses are common in marine calcifiers, e.g. shell thickening in oysters (Lord et al. 2002, Scherer et al. 2018), snails (Trussell & Nicklin 2002, Bourdeau 2010), and mussels (Leonard et al. 1999). OA has been found to affect inducible defenses in some species. Both induced shell thickening in the snail *Littorina obtusata* (Bibby et al. 2007) and predator-induced neck teeth in freshwater *Daphnia* spp. were reduced by high pCO_2 (Weiss et al. 2018). While these studies have investigated the effects of acidification on inducible defenses, few have done so in the context of multiple levels of biological organization.

Inducible defenses can have effects beyond the organism level with potential propagating effects through food webs and population dynamics of both predators and prey (Miner et al.

2005), which suggests that OA effects on these interactions must then be assessed at population and community levels. Scaling organism-level interactions to estimate population-level responses can provide quantitative assessments of propagating effects of OA. In this study we use a well-known inducible defense system to develop a strategy for assessing OA effects in which we empirically measure individual-level responses and use a numerical model to infer population-level effects.

The encrusting bryozoan *Membranipora membranacea* (hereafter *Membranipora*) is an abundant colonial epibiont on kelp in the Salish Sea and San Juan archipelago (Figure 2.1). Larval recruitment occurs in late spring, with populations colonizing kelp blades as they grow throughout the summer (Seed, 1976). Colonies do not typically overgrow each other, and instead divert energy to reproduction when occluded (Harvell & Padilla, 1990). *Membranipora* population dynamics are ecologically significant invasive biofouling organisms along the east coast of North America where overgrowth on kelp can cause kelp deforestation (Scheibling & Gagnon 2009, Saunders et al. 2010), especially where specialist nudibranch predators are not prevalent (Lambert et al. 1992) and other predators prefer different bryozoans (Pratt & Grason 2007). *Membranipora* colonies consist of multiple, genetically identical zooids (Harvell 1984) partially encased in a calcium carbonate skeleton (Smith et al. 2006, Taylor et al. 2014). Larger colonies consist of more zooids, leading to higher reproductive output than colonies with fewer zooids making space an important limiting resource for *Membranipora* (Yoshioka 1982a). The cryptic nudibranch, *Corambe steinbergae* (hereafter *Corambe*), exerts strong episodic predation pressure on *Membranipora*, feeding by sucking individuals out of zooids, leaving them empty (Yoshioka, 1982b). In response, *Membranipora* exhibits an inducible defense by forming protective chitinous spines upon detecting waterborne chemical cues from *Corambe*. Spines are

produced only on newly formed zooids at the growing margin of the colony requiring the formation of new calcified zooids (Harvell, 1984). Spination begins with formation of corner spines on zooid vertices, followed by additional spines along the walls of the zooids (Harvell 1984). Spines have been demonstrated to be effective in reducing predation (Harvell 1986). However, spines also have associated costs, including reduced colony growth as resources are allocated for defense (Harvell 1986, 1992) and disruption of feeding currents (Grünbaum 1997).

The *Membranipora-Corambe* system presents a uniquely informative opportunity to understand the consequences of OA effects and predator-prey interactions across multiple scales of biological organization. *Membranipora* colonies are primarily mineralogically composed of aragonite and low-Mg calcite (Smith et al. 2006) which may affect their ability to grow and calcify in OA conditions. Aragonite is a highly soluble polymorph of $CaCO_3$, and some heavily calcified bryozoans have been identified as potential bioindicators of OA given their vulnerabilities (Fortunato 2015, Taylor et al. 2014, Smith 2009). *Membranipora* is a tractable experimental system, as its modular architecture allows for a single genotype to be divided into multiple experimental treatments. This effective control for genetic variation facilitates quantifying the plastic capabilities of specific genotypes (Harvell 1990). Both the deployment of defense - inducible spine formation - and the degree of predation - consumed zooids - are easily and non-destructively quantifiable. Finally, organizational levels of this system, from zooid to population, are inherently linked by zooid-level processes such as spine formation, which alter colony growth dynamics and ultimately influence space competition and consequently fitness.

Membranipora presents a good system for constructing population dynamics models because space competition and reproductive potential, mediated by variations in predation and colony growth rates, can be represented as a spatially-explicit process analogous to observable

distributions in the field. Using this system to explore connections between individuals and populations, modeled growth patterns which scale up individual responses can provide some insight on OA impacts on predicted area-based fitness and costs of defense under space limitation. Therefore, *Membranipora* presents an exceptional opportunity to understand population-level implications of an organism-level anti-predator mechanism under OA stress.

The goals of this study were: (1) to experimentally quantify the colony-level effects of OA on *Membranipora* growth, $CaCO_3$ production and formation of defensive spines, and rate of predation by *Corambe* and, (2) to use modeling approaches to infer the consequences of observed colony-level impacts at the population level. We addressed the following questions:

1. How does a range of pH reflecting mild to severe OA affect *Membranipora* colony growth, $CaCO_3$ production, and inducible spine formation, and *Corambe* predation rates on *Membranipora*?
2. How are predicted organism-level effects of OA and predator cues altered by the inclusion of population-level processes (e.g. space competition among *Membranipora* colonies)?

We hypothesized that at the colony level, growth and $CaCO_3$ production would be reduced by OA in the absence of predator cues, and that reductions in growth would be compounded in the presence of predator cue due to the cost of defense. On the population level, we predicted the associated costs of these growth rate reductions would be further amplified by space competition. We also hypothesized that inducible spines, although chitinous, would be reduced by OA since they form on areas of new growth which require the formation of new

calcified skeleton, and that predation rates would be reduced due to direct effects of OA stress on organisms.

2.3 METHODS

Bryozoan collection and preparation

Membranipora colonies were collected off the floating dock at Friday Harbor Laboratories (FHL) (48.546° N, 123.013° W) in Spring 2017. Racks of several plastic plates each (8" x 16" x 1/16") were deployed for one month beginning in late April to collect settling larvae. Plates were recovered in late May and transferred to laboratory sea tables reflecting collection site conditions. Colonies with at least a 5cm radius of free space were selected as target colonies and cut from the plastic plate using a bandsaw, to produce 10cm x 10cm plates with one colony at the center. To minimize shock, colonies were returned to sea tables for three days. Other colonies surrounding the target colony were cleared from the plastic plate to prevent interference. This allowed sufficient area for new growth throughout the duration of the experiment, such that no colony was space limited. Target colonies were dyed with a 200mg/l solution of Alizarin Red S (Sigma Aldrich) in filtered seawater for 18 hours and flushed for 6 hours, to mark the initial colony area (Saunders & Metaxas 2009). 10cm x10cm plastic plates with target colonies were scored with a razor blade, broken into separate quarters and returned to sea tables for 24 hours prior to the experiment. A total of 24 colonies (distinct genotypes) were included in the experiment. Twelve colonies were exposed to waterborne predator cue of *Corambe*, and twelve received no predator cue, with each colony genotype fully replicated (roughly equal colony sections) across four nominal pH treatments: 7.0, 7.3, 7.6, and 7.9

(Appendix A Figure S1). We used regression-based approaches to establish *Membranipora* response curves, which could be easily integrated into a population dynamics model.

Experimental setup

Four tanks were used in the FHL Ocean Acidification Environmental Laboratory (OAEL) to establish each of these pH conditions by bubbling CO_2 as described by O'Donnell et al. (2013). Temperature in tanks was maintained at 13˚C reflecting typical ambient temperature at the collection site during the summer months (Murray et al. 2015). Weekly water samples were taken for carbonate chemistry measurements including spectrophotometric pH (total scale) and total alkalinity in accordance with best practices (Reibesell et al. 2010). CO_2Sys v. 1.05 (Pierrot et al. 2006) was used to calculate additional carbonate system parameters from measured pH, total alkalinity, salinity and temperature (Table 2.1). Temperature and pH were monitored continuously throughout the experiment using Durafet electrodes, which were calibrated weekly. Tanks included a total of eight isolated chambers, six of which were used to contain four *Membranipora* colony sections each. Within each tank, three chambers received water pre-treated with predator cue from a separate chamber which housed *Corambe* to induce defensive spines without actual predation. The predator chambers contained 12 nudibranchs for a final concentration of 4 nudibranchs/L, exceeding the threshold concentration required to induce a defensive response (Harvell 1986). Surface area of each nudibranch was measured prior to the experiment, and distributed such that each predator chamber had 12 similarly-sized nudibranchs with a total surface area of approximately 130 mm^2. Another three chambers served as controls, receiving water not treated with predator cue. All chambers received source water from the main tank with independent inflow and outflow lines such that chambers did not share water which

allowed us to restrict predator cue to only predator cue treatments. However, we potentially experienced minor contamination of predator cue in control treatments due to occasional overflows of predator cue chambers into the main water source which may have created diffuse predator cue water for control treatments. Four colony sections were randomly assigned to each tank chamber and rotated among chambers within a treatment every two days to control for chamber effects. One predator-exposed colony section was damaged during the experiment and all corresponding sections of that colony were removed. The flow-through system was plumbed with unfiltered seawater and each chamber was fed 50,000 cells/ml of *Isochrysis galbana* and 5,000 cells/ml of *Dunaliella* sp. three times daily to encourage bryozoan growth.

Part 1: Bryozoan growth, senescence, and inducible defense formation

A paddle system constructed from PVC pipe and a motor (Strathmann 2014) above each OAEL tank generated mixing in each chamber sufficient to keep algal cells suspended to ensure effective *Membranipora* feeding. Colony sections on plastic squares were attached to swinging paddles using rubber bands (four colony sections per chamber) and exposed to experimental treatments for 15 days. Growth and zooid senescence were monitored for each colony section using photographs taken every 5 days using a Nikon D3400 camera with macro lens. Colony section surface area was measured in ImageJ. Colony section growth rates were calculated as the exponential rate of increase in surface area, because colony area increases roughly in proportion to the number of feeding zooids. Growth rates were calculated by solving for *r* using the equation below where $A_{t_{15}}$ is the colony surface area after 15 days, A_{t_0} is the initial colony surface area and *t* is the duration of the experiment (15 days).

$$A_{t_{15}} = A_{t_0} e^{rt} \quad (2.1)$$

Zooids in photos were classified as feeding (fully developed), developing, or degenerated (brown body), and counted using the ImageJ cell counter plugin. Fully developed zooids had a full gut (see center zooids in Figure 2.1, photo 2) while developing zooids could not yet feed and did not yet have a developed gut (see peripheral zooids in Figure 2.1, photo 2). Degenerated zooids referred to senesced zooids not those consumed via predation. To assess spine length and quantity, a Lumenera Infinity microscope camera mounted on a dissecting microscope was used to take photo transects for each colony section. Colonies were held at a 45˚ angle for photographing using a 3D printed mount and a micromanipulator. For each colony section, three uniform transect lines 1cm apart were photographed through the new growth area and stitched together. The length of the closest corner spine to each of 5 randomly selected locations along each transect line was measured and corrected for the photographing angle.

Part 2: Nudibranch feeding rates

After colonies received a 15 day predator cue or control treatment and growth rates were measured in the absence of predation, one nudibranch was released on each colony section in each pH condition to determine feeding rates. Nudibranchs were starved and acclimated for 24 hours in their respective feeding pH treatments before being placed on *Membranipora* colony sections. We measured nudibranch length (diameter in mm from photographs), sorted nudibranchs from shortest to longest and paired them with colony sections such that the longest nudibranch was placed with the colony section of the largest surface area. Nudibranch lengths ranged 2.52 mm - 8.73 mm with a mean length of 5.30 mm. Initial photographs of colonies were taken to establish baseline conditions of zooids. All nudibranchs were initially placed on the center of the target colony's margin and confined by adding 300 µm mesh cages with a 3D

printed frame cable-tied to the swinging plastic paddles above each colony to prevent predation on colonies other than the target colony. Nudibranchs were allowed to consume zooids for a 24-hour period, after which final photographs were taken and the number of empty zooids, from predation, were quantified.

Part 3: Quantification of bulk calcium content in bryozoan skeletons using ICP-MS

One skeleton sample was taken from the new area grown during the experiment from each colony section. Skeleton samples were roughly 100mm^2 but were variable depending on available area of new growth in each colony section. Samples were transferred to a 35mm petri dish, and sequentially rinsed with milliQ water, a 10% bleach solution, a final milliQ rinse and 95% ethanol to dry out the sample. Areas of skeleton samples were measured in ImageJ. Each rinsed and dried skeleton sample was prepared in two parts (A and B) for elemental analysis to quantify Ca content as a proxy for bulk skeletal $CaCO_3$ (similar to methods in Wood et al. 2008 and Findlay et al. 2011 that quantified total Ca). For part A, skeletal samples were removed from their respective petri dishes, weighed on a microbalance, dissolved in 2.5 ml of 5% HNO_3 and diluted to a final 5 ml with milliQ water in a 15ml falcon tube. For part B, residual skeletal material was rinsed into a 2.5 ml 5% HNO_3 solution and diluted to a final 5ml solution with milliQ water. A 10 ml solution composed of 1 ml Part A or B, 100 µl of 100 ppb Sc, Rh, and Y (used as an internal standard spike), and 8.9 ml 2% HNO_3 was analyzed using an Inductively Coupled Plasma Mass Spectrometer (ICP-MS), Thermo model iCAP RQ, for bulk Ca determination. Samples were analyzed for ^{43}Ca and ^{44}Ca. Raw elemental intensities in counts per second were blank corrected, further corrected for $^{87}Sr^{2+}$ interference and instrumental drift with internal standardization before conversion to concentrations (ppm). ^{43}Ca intensities were used to

calculate final Ca concentrations and were converted to total Ca (mg) using exact dilution factors for each sample, and normalized to either weight of skeleton (Part A), as an assessment of skeletal composition, or to area of the sample (Part A + B), as a measure of skeletal density.

Statistical analysis (Parts 1-3)

For each experimental response variable, a series of linear or generalized linear mixed effects models were used to test pH and predation cue as fixed effects and included colony as a random effect to account for variation across genotypes. Quadratic relationships, using pH^2 as a fixed effect, were also tested for the response variables growth rate, zooid senescence and skeletal density which displayed non-linear trends with respect to pH. AIC was used to determine the best fitting model for all analyses (see Appendix A). For growth rate analysis, linear mixed effects models with identity link functions and Gaussian response distributions tested main effects of pH, pH^2 and predation cue. Zooid senescence was presented as a proportion of degenerated zooids relative to total colony zooids and generalized linear mixed effects models with logit link functions and binomal response distributions tested main effects of pH, pH^2 and predator cue. For spine length analysis, linear mixed effects models with identity link functions and Gaussian response distributions with an additional nested random effect of colony section within colony tested for fixed effects of pH and predator cue. For *Corambe* zooid consumption rate analysis, generalized linear mixed effects models with log link functions and a Poisson distribution tested the main effects of pH and previous colony predator exposure (defended vs. undefended colonies) with nudibranch length as a covariate and colony, nudibranch and colony size included as random effects. For skeletal density analysis, linear mixed effects models with an identity link function and a Gaussian distribution tested the fixed

effects of pH, pH^2 and predation cue. Statistical analyses were conducted in R v3.4.1 (R Core Team, 2017) using the lme4 package (Bates et al. 2014) to construct mixed effects models.

Part 4: Integrating experimental data into a model of bryozoan population dynamics

A spatially-explicit population dynamics model was constructed to investigate the implications of empirically-determined colony growth rates for *Membranipora* population structure, distributions and space competition. The model approximates *Membranipora* colonies as aggregations of repeating hexagons representing zooids. These hexagons, with side length *p* and acute angle θ, fit together in an approximately circular form if π/θ is an integer (Figure 2.2; Grünbaum & Shepard 1987). Modeled zooids are not exact replicates of zooid geometry, but are the most similar polygons that can fully tile the plane without gaps or alterations in shape.

The model accounts for the key processes of energy acquisition by mature feeding zooids, translocation of that energy to the growing edge to support formation and development of new zooids, and occlusion by neighboring colonies preventing new zooid formation. Colony growth is mediated through zooid-level algorithms for energy translocation. A system of ordinary differential equations is used to describe changes in zooid energy content, mass and developmental state over time. The rate of change of energy content of the *jth* zooid is defined as

$$\frac{dE_{tot_j}}{dt} = q_{in_j} + q_{f_j} - q_{out_j} - q_{g_j} - q_{m_j} \quad (2.2)$$

where E_{tot_j} is the total available energy content of zooid z_j. q_{in_j} is the rate of energy translocated into zooid z_j from upstream neighboring zooids, q_{out_j} is the rate of energy translocated out of zooid z_j to downstream neighbors, q_{f_j} is the rate of energy intake from feeding, q_{g_j} is the rate of

energy allocated for the production of zooid tissue and q_{m_j} is the rate of energy allocation for basal metabolism. All rates have units of J/day. Additional equations and parameters specifying how each term is calculated are presented in Appendix A Text S1 and Table S1.

Model parameters

The model, implemented in Python 2.7, establishes a two-dimensional domain which simulates a kelp blade randomly seeded with *Membranipora* colonies that grow and compete for space. Colony growth rate is not an explicitly designated parameter in the model, but is an emergent property of energy and growth dynamics within colonies. Model parameters were adjusted to achieve the correct range of growth rates determined from experiments (Table 2.2). Model colony growth rates were calculated using the slope of log-transformed colony area versus time between days 20 – 35 of the simulation, corresponding to the method by which growth rates were experimentally determined. In the model, colony growth rates were driven by the combined parameter $\Delta q = q_f - q_m$, i.e., the difference between energy input from feeding and basal metabolic rate. Therefore, we adjusted Δq to generate simulated growth rates for several single, unoccluded colonies (Figure 2.3). We then linearly interpolated across calculated Δq values to find values resulting in growth rates that matched experimentally determined values for each pH and predator condition (Table 2.2).

We used model simulations to test consequences of space limitation and competition on the cost of defense and OA effects. These simulations contained 16 simultaneously-settled colonies. We used two types of simulations, one set with all 16 colonies growing with the defended colony growth rate or undefended colony growth rate at each pH (10 replicate runs), and a second set of simulations containing 8 colonies with pH-specific undefended colony

growth rates and another 8 colonies with the defended colony growth rates (25 replicate runs). Simulations were 75 days long with 0.5 day time step intervals, approximating the length of *Membranipora* growing season. Model domain dimensions were 50mm x 100mm, a smaller scaled estimate of typical kelp blade area, with typical settlement densities (Seed 1976, Yoshioka 1982a). Smaller domain sizes allowed us to acquire similar space competition data without the computational expense required for larger domain sizes representative of actual kelp blade sizes. Colony areas at each time step were averaged to account for edge effects, and plotted as growth trajectories over 75 days. Growth trajectories from both types of simulations were compared to establish the cost of defense in the context of competition with colonies of identical growth rates, versus competition between colonies of different growth rates.

Using average colony growth trajectories over time, we calculated two metrics to compare the cost of defense in simulations with colonies of identical growth rates versus simulations with undefended and defended colony competition. We defined the intra-population cost of defense as the difference in mean colony area from populations of uniform growth rate, corresponding to either all defended or undefended colonies, at the time when undefended colonies have filled the domain. We defined a full domain at the time at which the increase in mean colony area decreased below 0.5 mm^2. We defined the inter-population cost of defense as the difference in mean colony area between undefended and defended colonies at the end of a 75 day duration, from model simulations where equal numbers of both colony types competed against each other for space. These cost metrics were used as area-based fitness proxies for each pH.

2.4 RESULTS

Part 1a: Bryozoan growth rates

Membranipora colony sections grew in all treatments (mean growth rate = 0.076 day^{-1}, sd = 0.019 day^{-1}, n = 92, Table 2.2, Figure 2.4a). Predator-exposed colonies exhibited slower growth rates compared with control colonies (predator cue: $p = 0.0003$), representing the cost of defense; however, this effect depended on pH (pH x predator cue: $p = 0.0003$). The reduction of growth rates in predator-exposed colonies was observed in all pH treatments except 7.0 (Figure 2.4a). Growth rates responded to pH treatments parabolically (pH^2: $p < 0.0001$, pH: $p < 0.0001$), with the shapes of the curves dependent on predator cue (pH^2 x predator cue: $p = 0.0004$). Both inferred growth peaks occurred at lower than ambient pH: 7.63 (control colonies) and 7.59 (predator-exposed colonies). Control colonies exhibited faster growth rates than predator-exposed colonies at pH 7.9, 7.6 and 7.3 (0.016 day^{-1}, 0.022 $day^{-1}$and 0.013 day^{-1} faster respectively), with a peak at pH 7.6. At pH 7.0, model trends showed growth rates were substantially reduced in both cue and no cue treatments (Figure 2.4a). Average growth rates presented in Table 2.2 were used to inform parameter inputs for model simulations. Complete mixed effects model analysis and best fit model output presented in Appendix A Tables S2.1 and S2.2.

Part 1b: Zooid senescence

Zooid senescence was quantified as the number of degenerated zooids formed during the experiment as a proportion of the total zooids in the colony section (mean proportion degenerated = 0.14, sd = 0.18, n = 92, Figure 2.4b). pH affected zooid senescence trends (pH: $p < 0.0001$), but was dependent on predator cue (predator cue x pH: $p < 0.0001$). Both control and

predator-exposed colonies exhibited parabolic senescence patterns (pH^2: $p < 0.0001$) demonstrating dramatic increases in senescence at pH 7.0 with curves specific to predator-exposure treatment (pH^2 x predation cue: $p < 0.0001$). Control colonies expressed a 2.16x greater proportion of degenerated zooids than predator-exposed colonies only at this lowest pH level; senescence rates were similar across higher pH values (Figure 2.4b). Senescence trends reflected the complement of growth rate trends observed in both predator and no predator cue treatments: lower average growth rates were associated with higher proportions of degenerated zooids (Figure 2.4b). Complete mixed effects model analysis and best fit model output presented in Appendix A Tables S3.1 and S3.2.

Part 1c: Inducible defense formation

Spines were formed in all treatments (mean length = 76.33 µm, sd = 71.94 µm, n = 1350), but were 117.43 µm longer on average in predator cue treatments than in control treatments (Figure 2.4c). Spines were produced in some control colonies (mean length = 19.79 µm) but were significantly shorter than those produced by predator-exposed colonies (predator cue: $p < 0.0001$). A weak but significant effect of pH was detected for both control and predator-exposed colonies indicating that spine length at lower pH was slightly decreased (pH: $p = 0.01$). Abundance of spines per treatment is presented in Appendix A Figure S1. Complete mixed effects model analysis and best fit model output presented in Appendix A Tables S4.1 and S4.2.

Part 2: Nudibranch consumption rates

Consumption rates of *Membranipora* zooids by *Corambe* were measured as the number of zooids consumed over a 24 hour period (mean consumption = 74.29 zooids, sd = 49.69

zooids, n = 92, Figure 2.5). Spines deterred feeding in nudibranchs (spine presence: $p = 0.022$) but this effect was dependent on pH with reduced zooid consumption rates in higher pH treatments but not in lower pH treatments (spine presence x pH: $p = 0.016$). As pH decreased, zooid consumption rates on control colonies decreased, while consumption rates on predator-exposed colonies increased (Figure 2.5), essentially removing the benefit of defense. Nudibranch length also significantly influenced zooid consumption rate with larger nudibranchs consuming more zooids (nudibranch length: $p = 0.001$). Complete mixed effects model analysis and best fit model output presented in Appendix A Tables S6.1 and S6.2.

Part 3: Bulk calcium content quantification of bryozoan skeletons using ICP-MS

Total mg Ca per sample was calculated and normalized to skeletal area as a metric of skeletal density (Figure 2.4d). Skeletal density (mean density = 0.0023 mg Ca/mm^2, sd = 0.0007 mg Ca/mm^2, n = 90) was significantly affected by pH (pH: $p < 0.0001$) and displayed a parabolic trend (pH^2: $p < 0.0001$) with a weak peak at target pH 7.6. This peak pH was similar to pH values associated with maximum growth (7.63, control; 7.59, predator-exposed). There was no significant difference between skeletal density of control and predator-exposed colony sections. Complete mixed effects model analysis and best fit model output presented in Appendix A Tables S7.1 and S7.2. Bulk calcium content normalized to skeletal weight is presented in Appendix A Figure S3.

Part 4: *Membranipora* population dynamics model results

Model output (Figure 2.6) enabled visualization and quantification of predicted population-level costs of defense at different OA conditions. The cost of defense was dependent

on space competition between colonies and the variations in their growth rates. In simulations where all colonies grew with identical growth rates (either defended or undefended) all colonies eventually approached the same average colony size of 250 mm^2, regardless of growth rate (Figure 2.7). As expected, slower-growing colonies required a longer time to reach this average size. In this case, the intra-population cost of defense demonstrated the area deficit of a slower growing colony at the time at which the faster-growing colonies have filled the domain. However, this trend was dramatically altered when colonies from mixed populations containing both undefended and defended colonies competed for space. The inter-population cost of defense demonstrated the area deficit of defended colonies in comparison with undefended colonies at the end of the simulation duration. Defended, slower-growing colonies were prevented from reaching the average size by competing undefended, faster-growing colonies which exceeded the average size. Mixed population competition increased the cost of defense with inter-population costs of defense exceeding intra-population costs of defense between pH 7.9 – 7.3. At pH 7.0, all colonies grew too slowly to fill the domain over a 75 day simulation, thus costs of slower growth using these two metrics could not be calculated. In addition, undefended colonies at pH 7.0 grew slower than defended colonies and did not exhibit a cost of defense.

Inter-population costs of defense were higher than intra-population costs of defense at pH 7.9 – 7.3. The intra-population costs of defense were calculated as 37.9 mm^2, 58.4 mm^2, and 17.2 mm^2 for pH values 7.9, 7.6 and 7.3 respectively (label a. in Figure 2.7). In comparison, the inter-population costs of defense were much higher at 183.2 mm^2, 207.5 mm^2, and 121.9 mm^2 for pH values 7.9, 7.6 and 7.3 respectively (label b. in Figure 2.7). Costs of defense initially increased at mild OA conditions (pH 7.6) but were reduced in severe OA conditions (pH 7.3).

Compounding costs of slow growth in the context of competition resulted from a reduced growth rate and the inability to grow into space already occupied by faster-growing colonies.

In model simulations, all colonies settled simultaneously, to control for the effect of settlement time which likely influences colony competitiveness. Faster growing colonies quickly gained an early competitive advantage over slower growing colonies which was maintained throughout the simulations. Overall, smaller colony growth rates yielded smaller population size structures. Population size structures are represented as density plots displaying the frequency of different sized colonies at the beginning, middle and end of model simulations (Figure 2.8).

2.5 DISCUSSION

We sought to understand the impacts of OA-related stress on both the organism and population level using the bryozoan *Membranipora* and its specialist nudibranch predator *Corambe* as a case study. Using this organismal system, we developed a spatially-explicit model to infer population-level consequences of experimentally-determined individual-level responses to OA, that would otherwise be difficult to assess. Key characteristics of bryozoan life-history such as the cost of defense and the importance of space limitation were maintained within the range of near-future seawater pH projections (7.6, 7.3). At pH 7.0, likely not representative of conditions that are or will soon be experienced, we observed apparent physiological limits in *Membranipora*; colonies at this low pH suffered low growth rates and high zooid senescence. Here, we focus on responses and ecological interactions for pH 7.9 – 7.3, above this apparent toxicity limit. When scaled to population levels in the context of space competition, individual-level reductions in growth rate associated with the cost of defense were amplified, resulting in multiplicative decreases in colony area, and likely reduced fitness since reproduction is generally

proportional to area. The population-level cost of defense increased at moderate OA conditions but decreased at more severe OA conditions likely due to interacting effects of increased growth of undefended colonies at moderately low pH and space competition. Our results demonstrated the need to consider population-level mechanisms such as space competition when making assessments of ecological consequences of environmental stress.

Membranipora growth rates and calcification under ocean acidification

Contrary to our hypotheses, we observed maximum growth rates near target pH 7.6, corresponding to a moderately high pCO_2 of 985µatm. This is lower than current average ambient conditions in the Salish Sea, but not outside the range normally experienced by *Membranipora* in the field (Murray et al. 2015). Previous studies have also documented increased growth in bryozoans at moderately low pH conditions. The calcifying bryozoans *Electra pilosa* (Saderne & Wahl 2013), *Celleporella cornuta* (Swezey et al. 2017a), and *Jellyella tuberculata* (Swezey et al. 2017b) exhibited increased growth in response to moderately high pCO_2, corresponding with moderately low pH conditions, relative to ambient (*E. pilosa*, 1200µatm; *C. cornuta*, 1150µatm; *J. tuberculata*, 1050 µatm). *E. pilosa* displayed a parabolic growth response curve exhibiting maximum growth at 1200 µatm (Saderne & Wahl 2013), similar to our results, suggesting these types of response curves may not be unusual in bryozoans.

Maximum skeletal density also occurred near target pH 7.6, reflecting observed trends in growth rate and implying a positive relationship between growth rate and skeletal density with a possible physiological link. Observed trends in growth and calcium production could reflect the calcification mechanism used by *Membranipora*, which is currently poorly understood. Many

calcifiers secrete $CaCO_3$ from a calcifying fluid space of elevated pH, making it energetically favorable to convert HCO_3^- to CO_3^{2-} rather than extracting CO_3^{2-} directly from seawater. Microelectrode studies have shown calcifying fluids to be upwards of 2 units above ambient seawater pH (Al-Horani et al. 2003). Ries (2009) documented increases in calcification with respect to acidification in multiple taxa of marine calcifiers, and suggested that these increases could be due to strong control over calcifying fluid pH and H^+ regulation at the calcification site used to convert HCO_3^- to CO_3^{2-}. In *C. cornuta*, OA also increased the expression of protective organic coverings in areas of new growth, which can prevent dissolution while allowing calcification to continue (Swezey et al. 2017a). A combination of strong chemical control over a calcifying space and protective membranes might be responsible for *Membranipora's* robust calcification response to OA.

In the bryozoan *C. cornuta*, increased growth was associated with costs including reduced investment in reproduction and lighter skeletons (Swezey et al. 2017a). We did not find a cost associated with calcification in *Membranipora*. However, it is possible that our observed increases in growth and skeletal density in *Membranipora* are associated with costs that were not measured in this study, such as reduced per-zooid reproduction or altered metabolic costs.

Spine formation in ocean acidification conditions

Inducible spine formation was sustained across the entire range of pH conditions we investigated, with low pH correlated with slightly shorter spines. In particular, spination varied less than other colony response metrics we measured, including growth rate, calcification and senescence. *Membranipora* spines are chitinous (Harvell 1984), rather than calcified, so their chemical composition may be less vulnerable to pH changes than zooids' $CaCO_3$ skeletons.

Predator cues in all pH conditions induced spines in consistent patterns, and were deposited concurrently with new skeleton formation. Induction of spines suggests that *Membranipora* colonies were able to detect predator cues in seawater with pH as low as pH 7.0. Shorter spines in lower pH may imply slight impairment of predator detection mechanisms in *Membranipora* due to OA. If so, this would be consistent with diminished chemosensitivity observed in other taxa (Dixson et al. 2010, Manriquez et al. 2013, Dodd et al. 2015, Weiss et al. 2018). Our observations are perhaps most analogous to Weiss et al. (2018), who documented decreases in the length of induced neck teeth in *Daphnia* spp. due to decreased predator-detection ability at higher pCO_2. While our data do not suggest strongly impaired predator detection in *Membranipora*, predator cue concentrations in our treatments may have been so high such that cues were detected despite decreased sensitivity to OA. By using high levels of cue, we effectively tested for physiological limits to spine formation, but not cue detection thresholds. Spine formation occurred in some control colonies due to likely diffuse cross contamination of predator cue that made it effectively a "low predation cue" treatment. In these low-level induction conditions, abundance of corner spines decreased with decreasing pH. This is consistent with the hypothesis that OA may affect defense formation, but only at very diffuse predator cue concentrations.

Nudibranch consumption rate responses

Zooid consumption rates by nudibranchs were slightly affected by pH, as shown by a significant interaction of spine presence and pH. With decreasing pH, nudibranch consumption increased in the absence of spines. Lower pH conditions apparently reduced the benefit conferred by induced spines in higher pH conditions, with nudibranchs consuming nearly equal numbers of

zooids from defended and undefended colonies at the lowest pH. This trend suggests that OA stress fundamentally compromised the benefit of defenses in *Membranipora*, and represents potential differential effects of pH on predators and prey. This could have resulted from a variety of mechanisms acting on nudibranchs, bryozoans or both. OA could have effects on feeding physiology and energetic requirements in *Corambe*. OA stress has been shown to decrease the energetic content of some prey taxa, potentially increasing feeding rates in predators to meet their energetic requirements (Kroeker et al. 2014). Future experiments are needed to establish effects of OA on both *Corambe* and *Membranipora* physiological processes as we did not measure them in our study. Effectiveness of protective spines in *Membranipora* could also have been altered by OA. Consistent with the slight decrease in spine length at lower pH, shorter spines may not confer the same protective advantage as the longer spines induced at higher pH. Alternatively, OA stress may have compromised the structural integrity of spines, enabling higher consumption rates of defended zooids. OA has been shown to negatively affect defensive polymorphs in the bryozoan *Schizoporella errata* (Lombardi et al. 2011). While prey detection in *Corambe* may be sensitive to OA like in other molluscs that have exhibited decreased sensory ability in OA conditions (Manriquez et al. 2013), our experiments did not test for impaired prey detection as *Corambe* was confined to a small area on top of colonies requiring only short-range detection of prey. Therefore, differences in consumption rates across pH are not likely due to impaired prey detection, but this mechanism may be relevant in the field and merits further investigation.

Population-level insights from experimental data: inferences from a spatially-explicit model

Our experiments quantified the roughly exponential growth patterns exhibited by isolated colonies in the absence of geometric constraints on growth. The model provides insight into the implications of these different growth rates in a more realistic context where space is frequently limiting and where colony growth is constricted by dynamically interacting competitive neighbors. Compared to experimentally-determined growth rates in the absence of space competition, simulated space limitation in our model reduced area-based colony fitness. Our results reaffirm and add quantitative detail to the importance of density-dependence in assessing *Membranipora* area-based colony fitness. Modeling provided new insights into effects of environmental stress, allowing us to consider population-level processes in evaluating the relative effects of pH and predation pressure on area-based colony fitness and competitiveness. Within the pH range 7.9 – 7.3, our model results show potential amplification of the cost of defense due to space competition pressure, demonstrating how growth patterns of competing colonies shape individual area-based fitness. Specifically, the cost of defense increased in mixed populations containing defended and undefended colonies, representing both the costs incurred by reduced growth and space occupied by faster-growing colonies. In addition to emphasizing the need to assess fitness in the context of populations, our results also highlight the selective advantages of inducibility such that these high costs of reduced growth are minimized and only incurred when predation pressure is sufficiently high. Our model only considers intraspecific competition, however if *Membranipora* is less vulnerable to OA, this may confer competitive advantage over other species with which it shares a common substrate such as other bryozoans, tunicates and epibionts experiencing space limitation.

Our model simulations most accurately represent competition between colonies that are undefended or defended throughout the entirety of their growing period to evaluate the extremes

of fitness tradeoffs associated with defenses. In the field, predation cue concentrations would need to be regularly high to maintain constant production of defenses and positions of defended colonies would likely be dictated by predator placement in the field and not random, as used in our model. Therefore, our model simulations most accurately represent competition between constitutively spined colonies, those that are spined even in the absence of predators, which constitute 6.2% of the population (Harvell 1986) and unspined colonies to evaluate the extremes of potential fitness tradeoffs. The high cost of defense in the context of space competition emphasizes the benefit of inducibility where costs are only incurred when necessary. Predation was not included in our model, so we did not quantify the benefits of defense across OA conditions which may offset some of the predicted costs. Beyond demonstrating that both predator-prey relationships and intraspecies competition can influence OA responses in *Membranipora* and *Corambe,* our modeling results also suggest that organismal-level effects are often times insufficient to estimate population-level effects of environmental stress in space-limited species.

Membranipora is relatively robust to ocean acidification

Given the metrics measured in our experiments and modeled population-level effects, *Membranipora* in the Salish Sea appear to be less vulnerable to OA than many other calcifiers, particularly within the range of near-future predictions, and may be well-suited to tolerate changes in ocean chemistry. This relative robustness may be in part attributable to the frequency of naturally low and fluctuating pH in the Salish Sea, and to conditions in their immediate microhabitats on kelp. pH values in the Salish Sea fluctuate seasonally between 7.9 to 7.6 (Murray et al. 2015) and have been recorded as low as 7.3 in Washington state coastal

environments (Wooton & Pfister 2012). Diffusional boundary layers on kelp can create distinctly different microenvironments for *Membranipora*, modulated by photosynthesis and respiration, which may provide a partial refuge from chemical changes occurring in ambient seawater (Cornwall et al. 2014). Fluctuations of oxygen concentrations and pH within this micro-environment may also exceed ambient conditions serving to pre-condition bryozoans to low pH environments, especially in slow flow environments where boundary layers are thicker (Noisette & Hurd 2018). While we considered conditions of pH 7.6 to be suboptimal, this may not in fact be very stressful for *Membranipora* if it is within the pH range normally experienced within the boundary layer.

Implications for *Membranipora* population dynamics

On the east coast of North America, *Membranipora* is a significant invasive biofouling organism in kelp forests that contributes to defoliation events in kelp forests (Scheibling & Gagnon 2009, Saunders et al. 2010). Population-level size structures in our simulations may have implications for kelp forest health, which are culturally and ecologically important ecosystems. From our study, *Membranipora* does not appear particularly vulnerable to OA having maintained growth, $CaCO_3$ production, and spine formation at least to pH 7.3, with maximum growth and calcification near pH 7.6. Predicted population structures of undefended colonies were larger under pH 7.6 conditions suggesting *Membranipora* may have an invasive edge at lower pH conditions. As *Corambe* is not prevalent on the east coast to reduce growth our observations and simulations of undefended colonies are most relevant (Lambert et al. 1992). *Membranipora* may represent an example of a relatively resilient species to ocean change as studies of increased

temperature have demonstrated increased growth as well (Saunders et al. 2010), although potential interactions of OA and warming have not been investigated.

Conclusion

Our study demonstrates the need to consider both inter-specific interactions and intra-specific interactions on both organism and population levels in assessments of effects of ocean acidification. Overall, *Membranipora* colonies were less vulnerable to moderate OA conditions than hypothesized but responses were heavily influenced by predator exposure and space competition among conspecifics. By modeling population-level processes we were able to understand effects of individual-level experimental responses to OA under the pressures of space limitation. More broadly, these environmentally-induced geometric tradeoffs associated with space limitation can be applicable to other modular encrusting organisms affected by changing environments.

2.6 ACKNOWLEDGEMENTS

The authors gratefully acknowledge Rebecca Guenther for assistance in in the FHL OAEL, Alexander Gagnon, Tamas Ugrai and Anne Gothmann for ICP-MS assistance and data interpretation, Dianna Padilla, Drew Harvell, Terrie Klinger, Julie Keister, and Michael Temkin for help with experimental design and lab techniques, Jason Hodin for assistance with algal culturing, Alyssa Liguori, Will King, Cassandra Donatelli, Robert Levine, Mo Turner, Katie Dobkowski, Hilary Hayford and Ann Stanbrough for organism collection and laboratory assistance, Sarah Converse for statistical advice, Anna McLaskey for manuscript comments, four anonymous reviewers who provided helpful feedback, and the FHL director and community.

Calcium measurements were conducted at the University of Washington's TraceLab, a mass spectrometry facility for the analysis of trace elements in natural materials. TraceLab was established through the generous support of the M.J. Murdock Charitable Trust. This work was funded by FHL student support fellowships (Beatrice Crosby Booth Endowed Scholarship, Alan J. Kohn Endowed Fellowship, Richard and Megumi Strathmann Fellowship), NSF IGERT Program on Ocean Change, NSF Graduate Research Fellowship Program and Washington Sea Grant.

References

Al-Horani FA, Al-Moghrabi SM, De Beer D (2003) The mechanism of calcification and its relation to photosynthesis and respiration in the scleractinian coral *Galaxea fascicularis.* Mar Biol 142:419-426

Bates D, Maechler M, Bolker B, Walker S (2014) lme4: Linear mixed-effects models using 'Eigen' and S4. http:// CRAN. R-project. org/package = lme 4

Bibby R, Cleall-Harding P, Rundle S, Widdicombe S, Spicer J (2007) Ocean acidification disrupts induced defenses in the intertidal gastropod *Littorina littorea*. Biol Letters 3:699-701

Bourdeau PE (2010) Cue reliability, risk sensitivity and inducible morphological defense in a marine snail. Oecologia 162:987-994

Busch S, McElhany P (2017) Using mineralogy and higher-level taxonomy as indicators of species sensitivity to pH: A case-study of Puget Sound. Elem Sci Anth 5:53

Cornwall CE, Boyd PW, McGraw CM, Hepburn CD, Pilditch CA, Morris JN, Smith AM, Hurd CL (2014) Diffusion boundary layers ameliorate the negative effects of ocean acidification on the temperate coralline macroalga *Arthrocardia corymbosa*. PLOS ONE 9:e97235

Dickson AG (1990) Standard potential of the reaction: AgCl(s) + 12H2(g) = Ag(s) + HCl(aq), and the standard acidity constant of the ion HSO_4 – in synthetic sea water from 273.15 to 318.15 K. J Chem Thermodyn 22:113–127

Dickson AG, Millero FJ (1987) A comparison of the equilibrium constants for the dissociation of carbonic acid in seawater media. Deep Sea Res A, Oceanogr Res Pap 34:1733–1743

Dixson DL, Munday PL, Jones GP (2010) Ocean acidification disrupts the innate ability of fish to detect predator olfactory cues. Ecol Lett 13:68-75

Dodd LF, Grabowski JH, Piehler MF, Westfield I, Ries JB (2015). Ocean acidification impairs crab foraging behaviour. Proc R Soc B Biol Sci 282:20150333

Doney SC (2010) The growing human footprint on coastal and open-ocean biogeochemistry. Science 328:1512-1516

Feely RA, Sabine CL, Lee K, Berelson W, Kleypas J, Fabry VJ, & Millero FJ (2004) Impact of anthropogenic CO_2 on the $CaCO_3$ system in the oceans. Science 305:362-366

Feely RA, Doney SC, Cooley SR (2009) Ocean acidification: Present conditions and future changes in a high-CO_2 world. Oceanography 22:36-47

Ferrari MC, Wisenden BD, Chivers, DP (2010) Chemical ecology of predator–prey interactions in aquatic ecosystems: a review and prospectus. Can J Zool 88:698-724

Findlay HS, Wood HL, Kendall MA, Spicer JI, Twitchett RJ, Widdicombe S (2011) Comparing the impact of high CO_2 on calcium carbonate structures in different marine organisms. Mar Biol Res 7:565-575

Fortunato H (2015) Bryozoans in climate and ocean acidification research: A reappraisal of an under-used tool. Reg Stud Mar Sci 2:32-44

Grünbaum D (1997) Hydromechanical mechanisms of colony organization and cost of defense in an encrusting bryozoan, *Membranipora membranacea*. Limnol Oceanogr 42:741-752

Grünbaum B, Shephard GC (1987) *Tilings and patterns*. WH Freeman & Company, New York, NY

Harvell CD (1984) Predator-induced defense in a marine bryozoan. Science 224:1357–1359

Harvell CD (1986) The ecology and evolution of inducible defenses in a marine bryozoan: cues, costs, and consequences. Am Nat 128:810-823

Harvell CD (1990) The ecology and evolution of inducible defenses. Q Rev Biol 65:323-340

Harvell CD (1992) Inducible defenses and allocation in a marine bryozoan. Ecology 73:1567 -1576

Harvell CD, Padilla DK (1990) Inducible morphology, heterochrony, and size hierarchies in a colonial invertebrate monoculture. Proc Natl Acad Sci USA 87:508-512

Hofmann GE, Barry JP, Edmunds PJ, Gates RD, Hutchins DA, Klinger T, Sewell MA (2010) The effect of ocean acidification on calcifying organisms in marine ecosystems: an organism-to-ecosystem perspective. Annu Rev Ecol Syst 41:127-147

Kroeker KJ, Kordas RL, Crim R, Hendriks IE, Ramajo L, Singh GS, Gattuso JP (2013) Impacts of ocean acidification on marine organisms: Quantifying sensitivities and interaction with warming. Glob Chang Biol 19:1884-1896

Kroeker KJ, Sanford E, Jellison BM, Gaylord B (2014) Predicting the effects of ocean acidification on predator-prey interactions: a conceptual framework based on coastal molluscs. Biol Bull 226:211-222

Lambert WJ, Levin PS, Berman J (1992) Changes in the structure of a New England (USA) kelp bed: the effects of an introduced species? Mar Ecol Prog Ser 88: 303-307

Lee K, Kim TW, Byrne RH, Millero FJ, Feely RA, Liu YM (2010) The universal ratio of boron to chlorinity for the North Pacific and North Atlantic oceans. Geochim Cosmochim Acta 74:1801–1811

Leonard GH, Bertness MD, Yund PO (1999) Crab predation, waterborne cues, and inducible defenses in the blue mussel, *Mytilus edulis*. Ecology 80:1-14

Lombardi C, Gambi MC, Vasapollo C, Taylor P, Cocito S (2011) Skeletal alterations and polymorphism in a Mediterranean bryozoan at natural CO_2 vents. Zoomorphology 130:135-145

Lord JP, Whitlatch RB (2012) Inducible defenses in the eastern oyster *Crassostrea virginica Gmelin* in response to the presence of the predatory oyster drill *Urosalpinx cinerea Say* in Long Island Sound. Mar Biol 159:1177-1182

Manríquez PH, Jara ME, Mardones ML, Navarro JM and others (2013) Ocean acidification disrupts prey responses to predator cues but not net prey shell growth in *Concholepas concholepas* (loco). PLoS One 8:e68643

Miner BG, Sultan SE, Morgan SG, Padilla DK, Relyea RA (2005) Ecological consequences of phenotypic plasticity. Trends Ecol Evol 20:685-692

Murray JW, Roberts E, Howard E, O'Donnell M, Bantam C, Carrington E, Fay A (2015) An inland sea high nitrate-low chlorophyll (HNLC) region with naturally high pCO_2. Limnol Oceanogr 60:957-966.

Noisette F, Hurd C (2018) Abiotic and biotic interactions in the diffusive boundary layer of kelp blades create a potential refuge from ocean acidification. Funct Ecol. 32:1329-1342

O'Donnell MJ, George MN, Carrington E (2013) Mussel byssus attachment weakened by ocean acidification. Nat Clim Chang 3:587

Orr JC, Fabry VJ, Aumont O, Bopp L and others (2005) Anthropogenic ocean acidification over the twenty-first century and its impact on calcifying organisms. Nature 437:681

Pierrot D, Lewis E, Wallace DWR (2006) MS Excel Program Developed for CO_2 System Calculations. ORNL/CDIAC-105a. Carbon Dioxide Information Analysis Center, Oak Ridge National Laboratory, U.S. Department of Energy, Oak Ridge, Tennessee.

Pratt MC, Grason EW (2007) Invasive species as a new food source: does a nudibranch predator prefer eating an invasive bryozoan? Biol Invasions 9:645-655

R Core Team (2017) R: a language and environment for statistical computing. R Foundation for Statistical Computing, Vienna. www.r-project.org

Reibesell U, Fabry VJ, Hansson L, Gattuso JP (2010) Guide to best practices for ocean acidification research and data reporting. Publications Office of the European Union, Luxembourg

Ries JB, Cohen AL, McCorkle DC (2009) Marine calcifiers exhibit mixed responses to CO_2-induced ocean acidification. Geology 37:1131-1134

Saderne V, Wahl M (2013) Differential responses of calcifying and non-calcifying epibionts of a brown macroalga to present-day and future upwelling pCO_2. PLOS ONE 8:e70455

Saunders MI, Metaxas A (2009) Effects of temperature, size, and food on the growth of *Membranipora membranacea* in laboratory and field studies. Mar Biol 156: 2267-2276

Saunders MI, Metaxas A, Filgueira R (2010) Implications of warming temperatures for population outbreaks of a nonindigenous species (*Membranipora membranacea*, Bryozoa) in rocky subtidal ecosystems. Limnol Oceanogr 55:1627–1642

Scheibling RE, Gagnon P (2009) Temperature-mediated outbreak dynamics of the invasive bryozoan *Membranipora membranacea* in Nova Scotian kelp beds. Mar Ecol Prog Ser 390: 1-13

Scherer AE, Bird CE, McCutcheon MR, Hu X, Smee DL (2018) Two-tiered defense strategy may compensate for predator avoidance costs of an ecosystem engineer. Mar Biol 165:131

Seed R (1976) Observations on the ecology of *Membranipora* (Bryozoa) and a major predator *Doridella steinbergae* (Nudibranchiata) along the fronds of *Laminaria saccharina* at Friday Harbor, Washington. J Exp Mar Biol Ecol 24:1-17

Smith AM (2009) Bryozoans as southern sentinels of ocean acidification: A major role for a minor phylum. Mar Freshwater Res 60:475–482

Smith AM, Key MM Jr, Gordon DP (2006) Skeletal mineralogy of bryozoans: taxonomic and temporal patterns. Earth Sci Rev 78:287-306

Strathmann RR (2014) Culturing larvae of marine invertebrates. In: Carroll D, Stricker S (eds) Developmental biology of the sea urchin and other marine invertebrates. Methods in molecular biology: methods and protocols. Humana Press, Totowa, NJ, p 1-26

Sullivan CA (2012) Carbonate chemistry in the San Juan Channel: Characterization and suggestions for mitigation. Masters Thesis. University of Washington, Seattle, WA

Swezey DS, Bean JR, Hill TM, Gaylord B, Ninokawa AT, Sanford E (2017a) Plastic responses of bryozoans to ocean acidification. J Exp Biol 220:4399-4409

Swezey DS, Bean JR, Ninokawa AT, Hill TM, Gaylord B, Sanford E (2017b) Interactive effects of temperature, food and skeletal mineralogy mediate biological responses to ocean acidification in a widely distributed bryozoan. Proc R Soc B Biol Sci 284:20162349

Taylor PD, Lombardi C, Cocito S (2014) Biomineralization in bryozoans: present, past and future. Biol Rev Camb Philos Soc 90:1118-1150

Tollrian R, Harvell CD (1999) The ecology and evolution of inducible defenses. Princeton University Press, Princeton, NJ

Trussell GC, Nicklin MO (2002) Cue sensitivity, inducible defense, and trade-offs in a marine snail. Ecology 83:1635-1647

Weiss LC, Pötter L, Steiger A, Kruppert S, Frost U, Tollrian R (2018) Rising pCO_2 in freshwater ecosystems has the potential to negatively affect predator-induced defenses in *Daphnia*. Curr Biol 28:327-332

Wood HL, Spicer JI, Widdicombe S (2008) Ocean acidification may increase calcification rates, but at a cost. Proc R Soc B Biol Sci 275:1767-1773

Wootton JT, Pfister CA (2012) Carbon system measurements and potential climatic drivers at a site of rapidly declining ocean pH. PLOS ONE 7:e53396

Yoshioka PM (1982a) Role of planktonic and benthic factors in the population dynamics of the bryozoan *Membranipora membranacea*. Ecology 63:457-468

Yoshioka PM (1982b) Predator-induced polymorphism in the bryozoan *Membranipora membranacea* (L.). J Exp Mar Biol Ecol 61: 233-242

Figure 2.1. Tightly linked multiple levels of biological organization in the bryozoan, *Membranipora membranacea*, make it a uniquely informative organismal system in which to investigate OA effects at multiple levels. Individual zooids within a colony: 1a) feeding, undefended zooids (with no spines), 1b) spines formed along zooids walls of defended zooids. 2) One *Membranipora* colony comprising many genetically identical zooids with older, developed zooids at the center and younger developing zooids along the perimeter. 3) Multiple colonies competing for space on a kelp blade, with larger colonies occluding smaller colonies. From left to right scale bars are 300 µm, 250 µm, 3 mm and 5 cm.

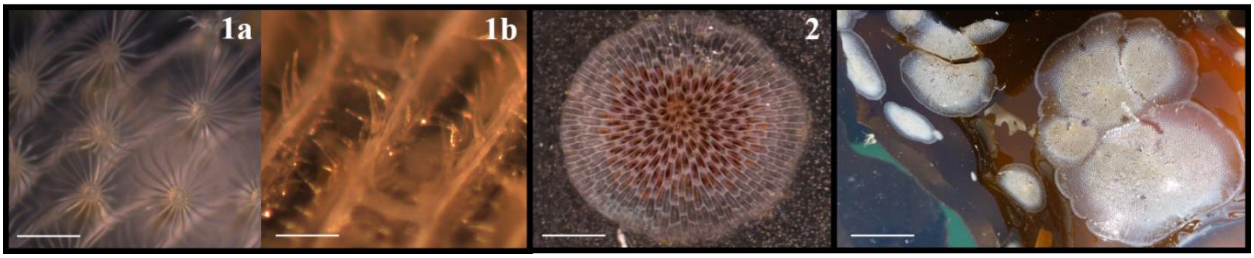

Figure 2.2. Diagram showing the basic zooid connection pattern within a simulated colony, and a schematic of connections between zooids within the colony. All zooid sides are of length *p*, and all acute angles are θ radians. Inset image: Focal zooid z_j has two designated types of neighbors for approximating energy translocation through a colony, axial (dark grey) and lateral (light grey). "Upstream" neighbors (sources of translocated metabolites) of z_j are axial neighbors z_{j-1}, z_{j-2}, and lateral neighbors z_{lat1} and z_{lat2}. "Downstream" neighbors (sinks of translocated metabolites) of z_j are axial neighbors z_{j+1}, z_{j+2}, and lateral neighbors z_{lat1} and z_{lat2}. (Note the bidirectional connections between lateral neighbors.)

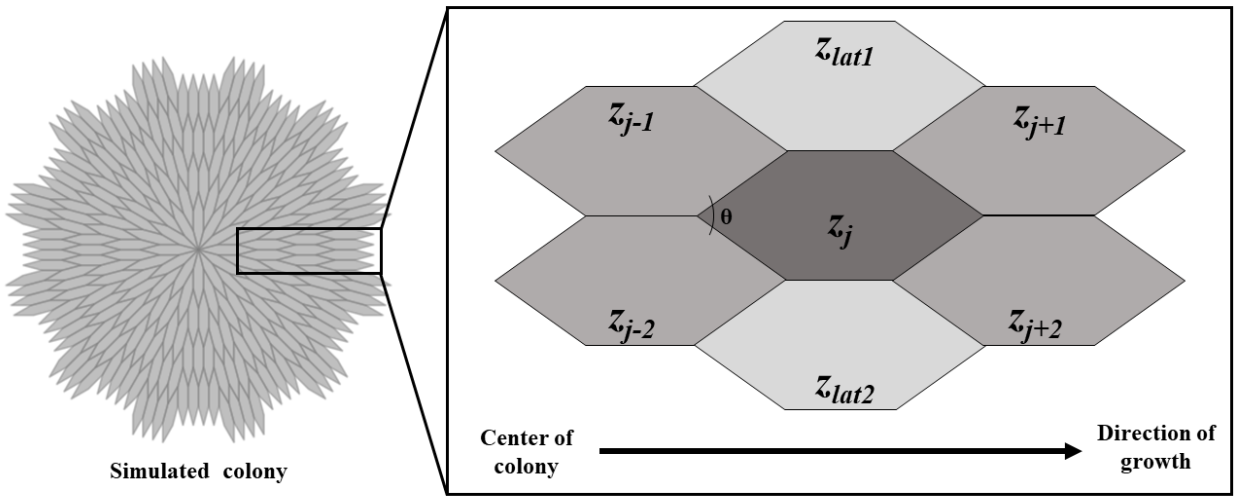

Figure 2.3 Relationship between Δq (difference between energy input from feeding and energy output to basal metabolic rate) and colony growth rate in modeled colonies. This plot shows simulated growth rates in single unoccluded (non-space limited) colonies across a range of Δq values. Other parameters are fixed as described in Appendix A Table S1.

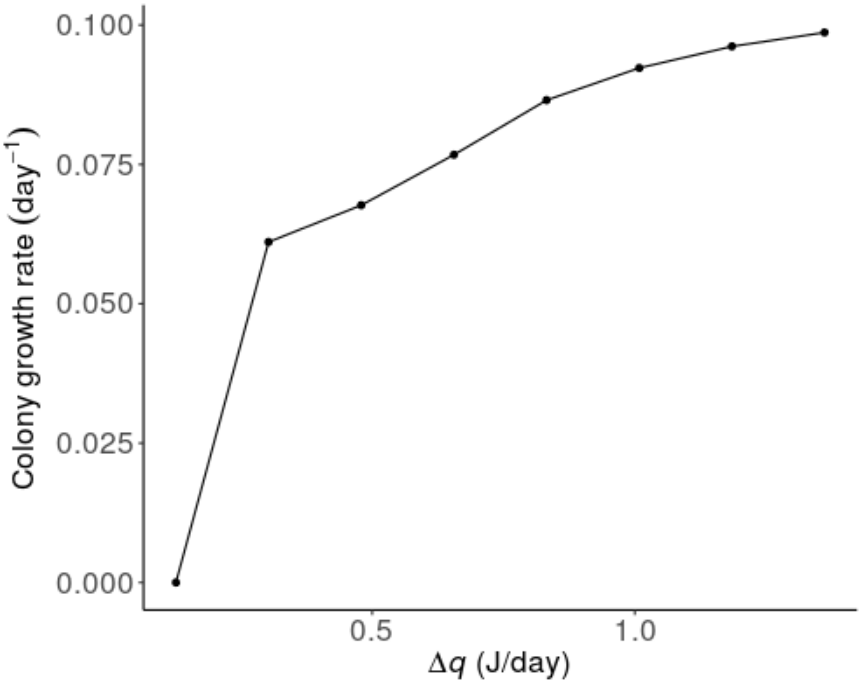

Figure 2.4 *Membranipora* (a) growth rates in day^{-1}, (b) colony senescence represented as a proportion (degenerated zooids/total zooids), (c) spine length in µm and (d) skeletal density in mg Ca/mm^2 for control and predator exposed colony sections from pH 7.0 – 7.9. Trendlines for each response variable show predictions for control and predator-exposed colonies from the best fit linear or generalized linear mixed effects model. In (d) only one trendline is presented since the best fit model does not designate a significant difference between skeletal density of control and predator-exposed colonies.

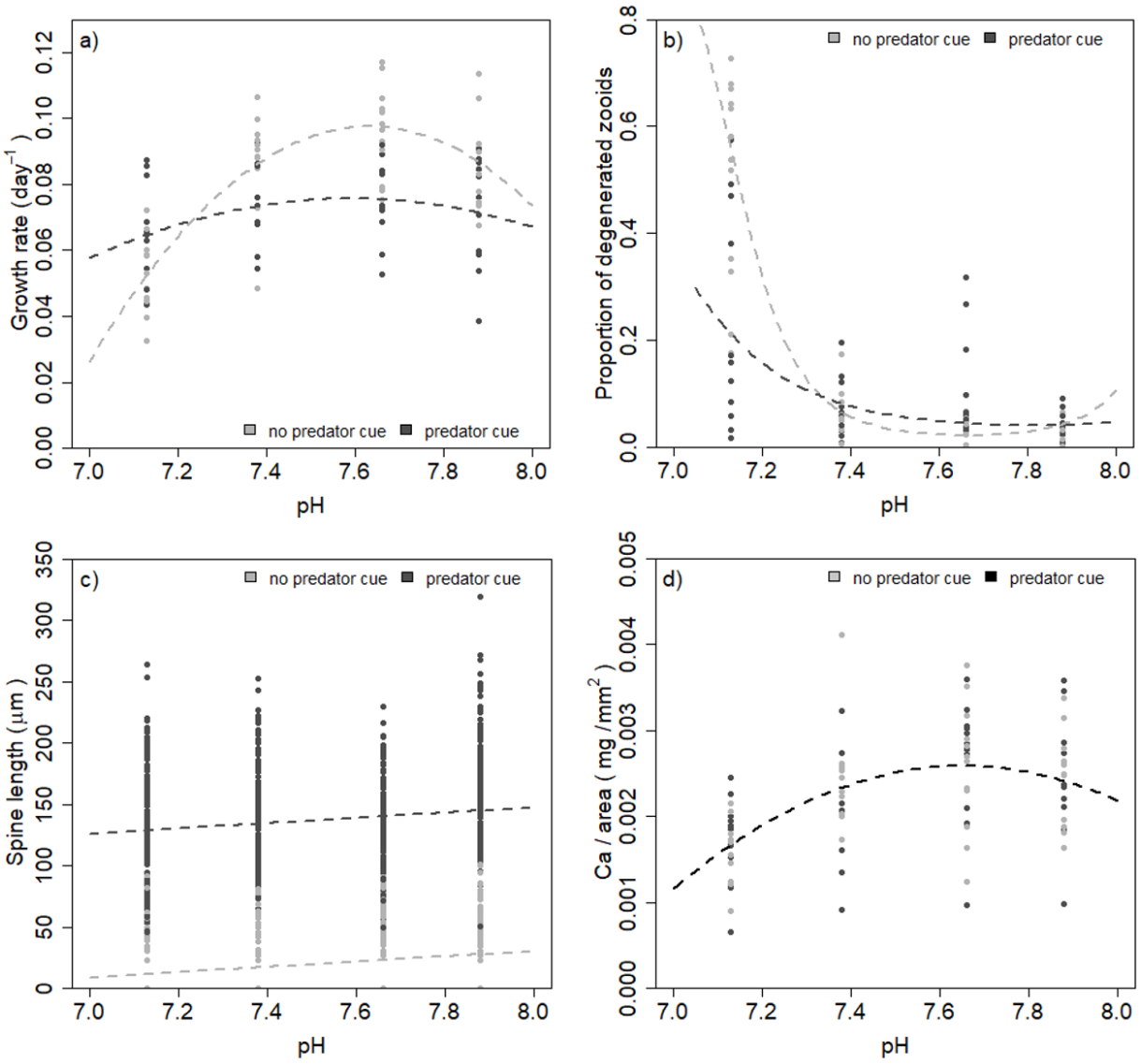

Figure 2.5 *Corambe* consumption rates plotted as the number of *Membranipora* zooids consumed over 24 hours, normalized by nudibranch length in mm. Defended colonies formed spines in the same pH treatments at which they were consumed. Plotted points represent the means and error bars represent +/- standard error.

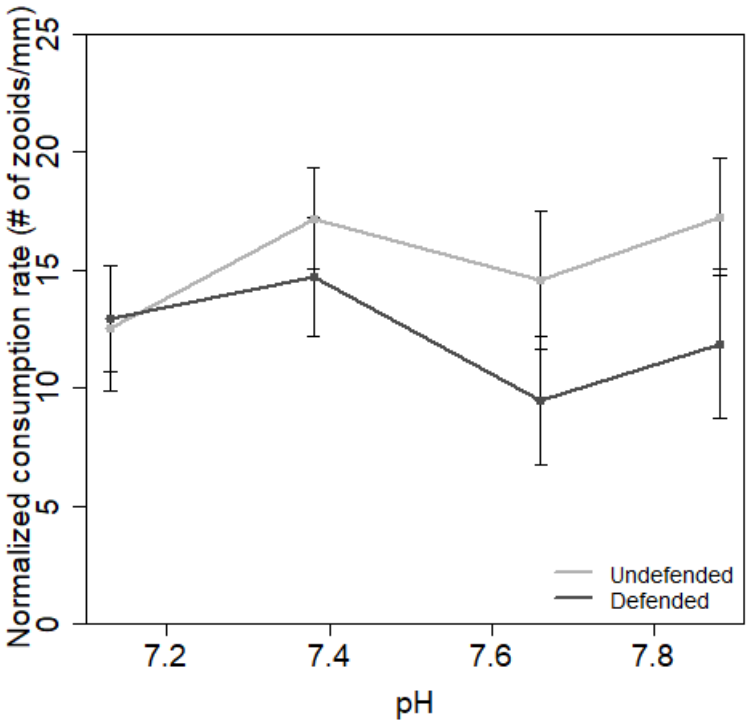

Figure 2.6 Typical model output showing 16 colonies, 8 with experimentally-determined undefended (blue) and 8 with experimentally-determined defended (pink) colony growth rates at pH 7.9. Model output is from a representative simulation run using average growth rates from pH 7.9 experimental treatments at A) 10 days, B) 30 days and C) 75 days. Light blue and pink areas signify developing zooids along the colony perimeter. Model animations are presented in published online supplement: http://www.int-res.com/articles/suppl/m607p001_supp/

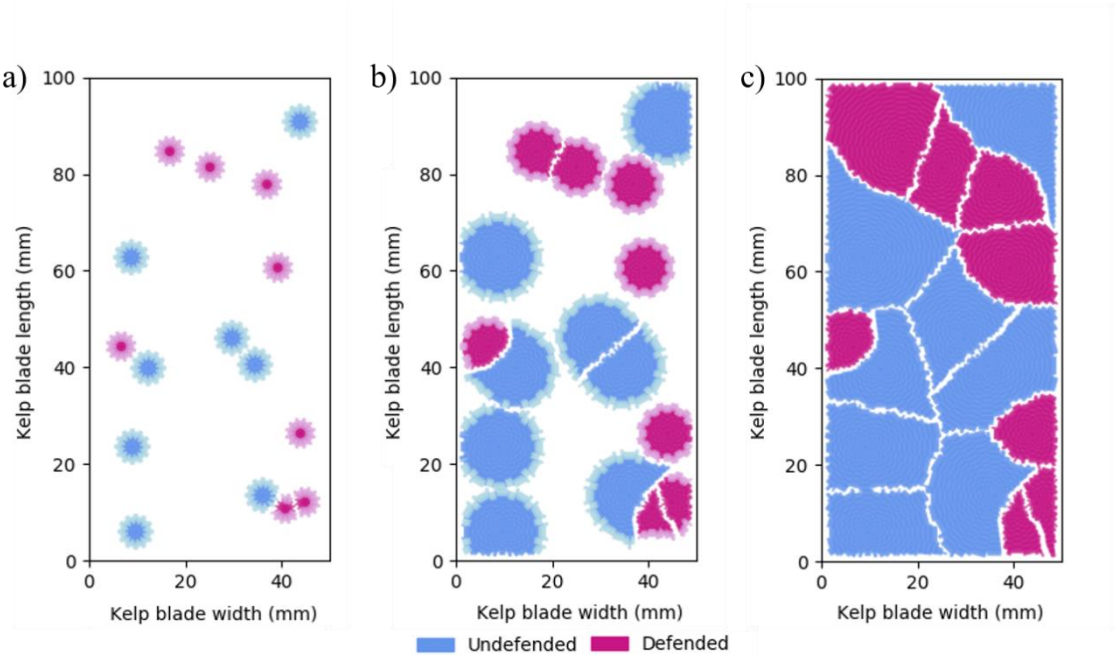

Figure 2.7 Average growth trajectories of a single *Membranipora* colony area over a 75 d simulation for each pH condition. Dashed lines: mean colony areas from simulations of 16 colonies, all growing with either the undefended (blue) or defended (pink) colony growth rates. Colonies from these simulations ultimately approach a similar maximum size of 250 mm^2, but differ in the time necessary to reach maximum size. Solid lines: mean colony areas for simulations where equal numbers of undefended and defended colonies (mixed population) competed for space. Plots show a comparison of the intra-population cost of defense (a) and the interpopulation costs of defense (b). Colony competition in mixed populations drives the increase in the inter-population cost of defense. At pH 7.0, the domain was not filled after 75 d due to slow colony growth rates, so costs of defense are not displayed

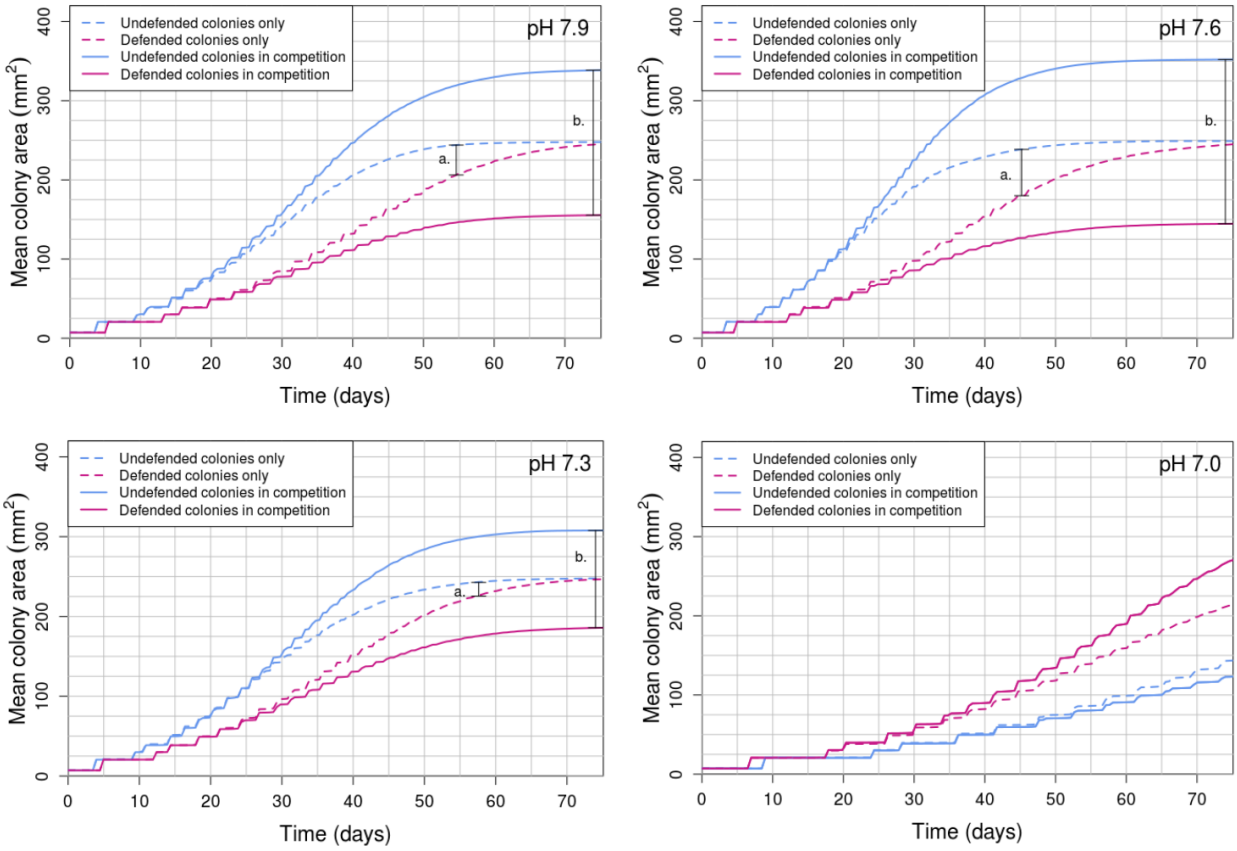

Figure 2.8 Colony size distributions under space limitation at each pH condition. Comparison of model simulations of mixed populations of 8 defended (pink) and 8 undefended (blue) colonies after (a) 20 days, (b) 40 days and (c) 75 days, using growth rates from each experimental treatment (Table 2.2). Within each pH, all colonies of a given type (defended or undefended) have equal growth rates and settled at the same time. Hence, variations in size reflect only the consequences of space competition, mediated by pH effects and cost of defense. Each distribution represents aggregated data from all mixed population model runs. Histograms were created to establish the frequency of colony sizes at given time steps, and then converted to density plots to better visualize distributions.

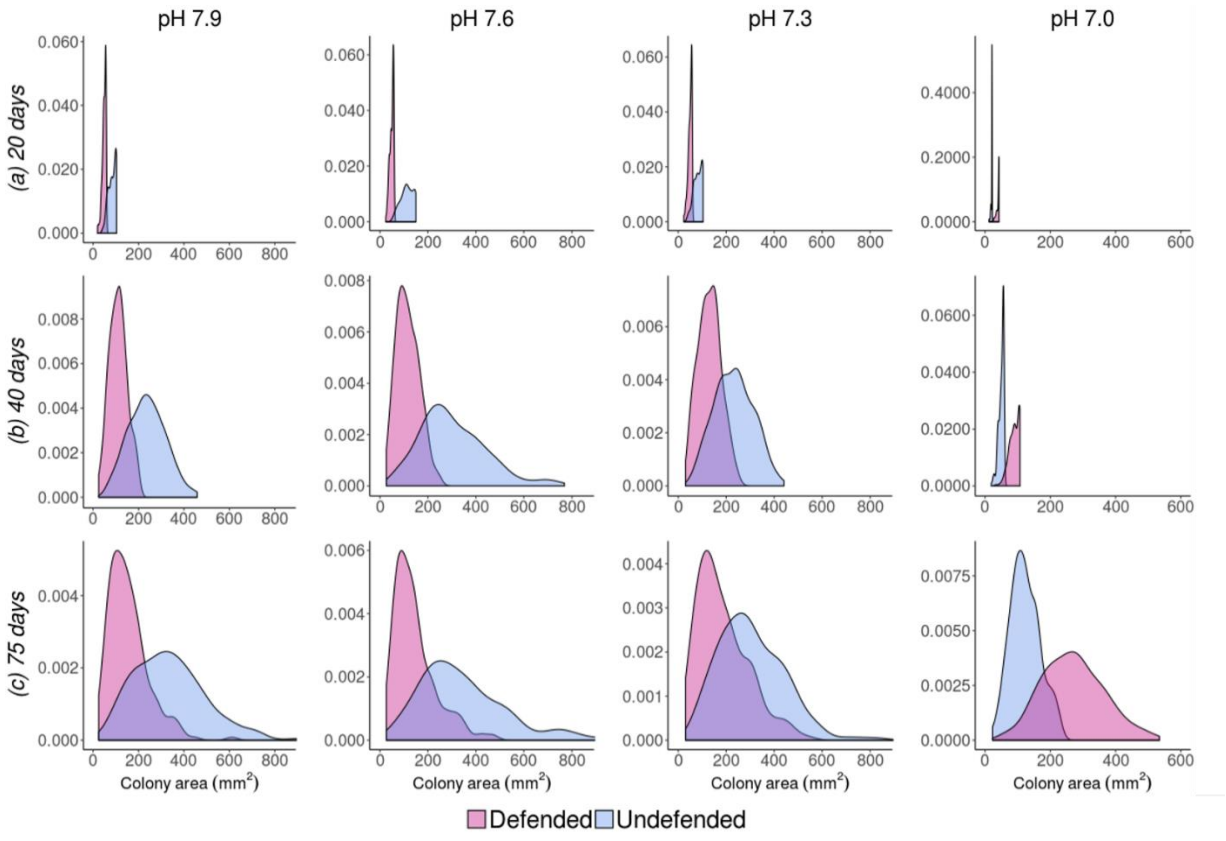

Table 2.1. Average carbonate chemistry data ± one standard deviation for OAEL tank treatments. Total alkalinity (TA) and salinity were measured weekly and pH (total scale) in tank chambers was monitored daily throughout the study. Additional carbonate system parameters (DIC, pCO_2, Ω_{arg}) were calculated using CO_2Sys with the following constants: CO_2 K1, K2 from Mehrbach et al. 1973 refit by Dickson and Millero, 1987; $KHSO_4$ Dickson, 1990; Boron Lee et al. 2010.

Target treatment pH	Temp (°c)	Salinity (psu)	pH (total scale)	TA (µmol/kg sw)	DIC (µmol/kg sw)	Pco_2 (µatm)	Ω argonite
7.0	12.8 ±0.1	28.6 ±0.1	7.13 ±0.06	2022 ±19	2141 ±32	3462 ±504	0.23 ±0.03
7.3	13.3 ±0.3	29.2 ±0.1	7.38 ±0.02	2024 ±25	2060 ±27	1937 ±94	0.44 ±0.02
7.6	13.3 ±0.2	28.9 ±0.1	7.66 ±0.03	2022 ±19	1984 ±21	986 ±74	0.81 ±0.05
7.9	13.2 ±0.1	29.0 ±0.3	7.88 ±0.02	2023 ±20	1920 ±21	5589 ±28	1.30 ±0.05

Table 2.2. Average *Membranipora* growth rates for each treatment determined by experiments which were later replicated in a spatially-explicit bryozoan population model. Corresponding Δq values used to replicate specific treatment growth rates in the model determined using Figure 3 are listed.

pH	Predator treatment	Mean (day^{-1})	SD	N	Δq (j/day) used for model
7.9	Control	0.087	0.013	12	0.852
	Predator-exposed	0.071	0.017	11	0.554
7.6	Control	0.096	0.014	12	1.193
	Predator-exposed	0.074	0.012	11	0.613
7.3	Control	0.087	0.015	12	0.858
	Predator-exposed	0.074	0.012	11	0.608
7.0	Control	0.052	0.012	12	0.277
	Predator-exposed	0.065	0.016	11	0.402

Chapter 3. SPACE COMPETITION MODULATES THE COST OF INDUCIBLE DEFENSE IN A MARINE BRYOZOAN

3.1 ABSTRACT

Space competition among conspecifics structures populations of many organisms. Among these organisms the fitness of individual strategies is ultimately determined in the context of space competition. Space-limited organisms may be impacted by bidirectional feedbacks between individuals and populations, in which individual strategies collectively shape the competitive environment, which conversely modulates fitness consequences of these strategies. The encrusting bryozoan, *Membranipora membranacea*, is an informative system to study bidirectional feedbacks, because it has quantifiable links between individual fitness and space competition. *M. membranacea* colonizes kelp blades with colony area as a fitness proxy. *M. membranacea* deploys an inducible defense upon detecting predators that provides protection but incurs the cost of reduced colony growth. We combined modeling, laboratory, and field methods to quantify the realized costs of defense in the context of space competition. We validated a spatial *M. membranacea* population model with field observations and used it to calculate effects of population density and settlement timing on colony area and costs of defense. Field and model analyses showed colony density and settlement time significantly impacted colony area. Surprisingly, increased colony density decreased costs of defense. In simulations using previously measured ocean acidification induced growth rates, costs of defense were largest at moderately acidified conditions, with lower costs at present-day and very acidified conditions. Interactive effects of space competition, growth, and defensive strategies in

modulating realized fitness may be common across marine communities. Integrated studies can help quantify feedbacks between organisms and populations, which may be applicable to other space-limited communities.

3.2 INTRODUCTION

Space is a critical resource for many sessile marine organisms, necessary for growth, resource acquisition and survival but often limited due to the presence of competitors (Connell 1961, Dayton 1971, Buss 1979, Sebens 1982, Goldberg & Barton 1992). Crowding can limit growth in both aquatic and terrestrial organisms, resulting in population size structures that are shaped by competitive interactions among individuals (bryozoans: Buss 1980; corals: Lang & Chornesky 1990, Connolly & Muko 2003; lichens: Armstrong & Welch 2007; plants: Dickinson & Miller 1998, Schwinning & Weiner 1998; sponges: López-Victoria et al. 2006). To compete for limited space, many organisms employ what appear to be fitness-enhancing strategies, such as regulating allocation to somatic or reproductive tissues to meet requirements for growth and survival. These strategies often present tradeoffs, where employing some fitness-enhancing traits entails a cost in others (Harvell 1986, Herms & Mattson 1992). The costs and benefits associated with a fitness-enhancing strategy may differ for isolated individuals compared with those in strong competition for space. If so, space competition results in population-level modulation of realized fitness effects of allocation strategies. Conversely, strategies exhibited by individual organisms collectively structure populations and shape the competitive environment.

The situation in which population-level frequencies of alternative strategies result from the fitness of those strategies, but the realized fitness of a given strategy depends on the frequencies of those strategies within a population, represents a bidirectional feedback. Because

they appear to be common across many habitats and taxa, such feedbacks may be central to compelling "big-picture" ecological questions, such as: How do characteristics of individual organisms collectively determine emergent properties like space competition? How do population-level processes like space competition alter the effects of individual-level fitness strategies?

Bidirectional feedbacks between individual-level traits and population-driven conditions are probably frequent in aquatic and terrestrial ecosystems, but are generally difficult to characterize and quantify. Spatially-explicit modeling approaches potentially serve a number of important purposes in understanding dynamics of bidirectional feedbacks. These models present means of testing key underlying hypotheses, e.g., that mechanistic models of individual organisms can be used to predict and interpret population-level dynamics, and that potentially dominant ecological mechanisms have been identified and quantified. Models are also tools with which to conduct numerical experiments, simulating manipulations or observations that are impractical to carry out empirically. In the context of space-limited populations, spatially-explicit models provide a means to systematically explore fitness consequences of observed or hypothetical resource allocation strategies across broad variations in population density and environmental conditions.

The quantifiable links between space limitation due to competition and individual fitness make the encrusting marine bryozoan, *Membranipora membranacea,* an informative system to investigate how space competition results in realized effects of fitness strategies. *M. membranacea* also shares important traits with other colonial invertebrates, plants, lichens, and other space-limited organismal systems. These include modular, distributed organizational structures; population-mediated space competition; inducible and constitutive defenses

associated with fitness costs; and variability in phenology of growth, gamete-formation and recruitment.

M. membranacea larvae spend roughly four weeks in the water column before settling on kelp blades (Yoshioka 1982). In the San Juan Archipelago, Washington, USA, a settlement pulse typically occurs in late spring, with larvae continuing to settle throughout the summer (Seed 1976, Harvell 1986). Controls on settlement time have been attributed to large-scale oceanographic processes, temperature (Saunders & Metaxas 2007, 2009), larval supply (Saunders & Metaxas 2010) and larval behavior (Matson et al. 2010). *M. membranacea* larvae are selective in choosing a substrate, exhibiting searching behaviors to identify high-quality habitats, that can result in delayed settlement (Matson et al. 2010). Once settlement occurs, colonies grow via the addition of new genetically identical zooids (Harvell 1984) while competing to occupy limited kelp blade area (Harvell et al. 1990). Colony growth rates vary with environmental conditions such as temperature (Saunders & Metaxas 2009), food availability (Saunders & Metaxas 2009), and ocean acidification (OA) conditions (Seroy & Grünbaum 2018). *M. membranacea* are commonly found in monocultures, and experience competitive pressure mainly from conspecifics (Harvell et al. 1990). Higher population densities result in less available space and can reduce colony sizes because colony growth stops once occluded by conspecifics, and zooids instead divert resources to reproduction (Harvell et al. 1990, Harvell and Padilla 1990). *M. membranacea* colony area therefore serves as a proxy for fitness, with larger colonies having higher reproductive output in proportion to their number of gamete-producing zooids (Yoshioka 1982).

M. membranacea exhibits an inducible defense against the predatory nudibranch, *Corambe steinbergae* (Harvell 1984). Upon chemical detection of *C. steinbergae*, *M.*

membranacea colonies produce protective spines on newly forming zooids along growing colony margins. While these spines reduce predation, defended colonies incur the cost of reduced growth rates. Reduced growth is a result of resource allocation for defense (Harvell 1986, 1992) and reduced feeding due, at least in part, to hydrodynamical interference by spines (Grünbaum 1997). Area-based costs of defense for *M. membranacea* colonies in the absence of space competition have been well established in the laboratory (Harvell 1984, Seroy & Grünbaum 2018).

While costs of defense are well-documented for isolated *M. membranacea* colonies, realized costs in the context of space competition that varies strongly from blade to blade are still poorly understood. A modeling study suggested that area-based costs of defense, in the absence of predation, are modified when considered in the context of conspecifics competing for space (Seroy & Grünbaum 2018). While space competition generally modifies this cost of defense, the cost is likely also dependent both on variable population-level characteristics like population density and on individual-level strategies like settlement timing and allocation to growth.

We used *M. membranacea* as a model system to investigate bidirectional feedbacks between organisms and populations. We asked:

1. How do population density and the timing of settlement affect individual colony size (a fitness proxy)?
2. How do population density and settlement time alter the cost to colonies of inducible defensive spines?
3. How do variations in OA conditions, reflecting predictions of ocean change, alter the cost of inducible defenses?

We hypothesized that increased population density and late settlement times would both decrease colony sizes due to increased impacts of space competition. We also hypothesized that stronger space competition would amplify the cost of defense. If true, implications include that increasing population density and later settlement times would increase the cost of defense. Similarly, we hypothesized that under OA conditions associated with faster colony growth, the cost of defense would increase because of stronger competition for space.

To address these hypotheses, we used an integrative approach combining modeling, laboratory, and field methods to quantitatively estimate the realized cost of defense across variation in the intensity of population-level space competition. We validated a previously constructed spatial model, informed by experimentally-determined growth rates (Seroy & Grünbaum 2018), by comparing sizes of colonies growing in the field with model predictions. We then used that model to explore how various population-level parameters influence fitness and the cost of inducible defenses in *M. membranacea*. In addition, we simulated effects on costs of defense of stress-induced growth rates across a range of predicted ocean acidification conditions.

3.3 METHODS

Part 1: Effects of population density and settlement time on colony area in the field

Thirty acrylic plates (406.4 mm x 203.2 mm x 1.5 mm) were deployed in late April 2018 off the dock at Friday Harbor Laboratories (Washington, USA) to enable pelagic *M. membranacea* larvae to settle. Larvae were allowed to settle on plates for a 46-day period. 29 days after deployment, plates were removed, and initial photographs of each plate were captured. On day 46, plates were photographed a second time. Photographs from these first two time

points were used to record colony settlement locations and initial areas. After the 46-day settlement period, selected colonies were removed to manipulate population densities such that each plate had either 8, 16 or 24 colonies present. Ten plates were selected for each density treatment. Only the smallest colonies (those that had most recently settled) were removed, such that manipulated densities reflected only the first colonies to settle on a given plate. Plates were subsequently monitored and photographed once a week until they were completely covered with *M. membranacea*, at which time they were removed from the field. During weekly monitoring, manipulated density treatments were maintained by removing any newly settled colonies. Plates that maintained healthy colonies throughout the summer (i.e., those on which colonies did not die or have significant portions damaged) were selected for analysis. After careful inspection, 12 plates met these criteria: three with 8 colonies, five with 16 colonies, and four with 24 colonies.

From these plates, we measured final colony areas and settlement positions and estimated settlement times. The final area occupied by each colony was measured with ImageJ from final time point photographs. Colony settlement positions (*x* and *y* positions of the first settled zooids, i.e., the ancestrula) were also measured with ImageJ from settlement period photographs. We used only unoccluded colonies (those that remained undisturbed by competitors) across all plates to calculate a population-wide average colony growth rate between the first two photographing time points, 29 days and 46 days. This growth rate was calculated for each individual unoccluded colony by solving for *r* in the equation

$$A_1 = A_0 e^{r(t_1 - t_0)} \tag{3.1}$$

where $A_0$was the colony area measured at time t_0(29 days) and A_1 was the colony area at t_1 (46 days) and then calculating the mean *r* value (0.198 $^{-d}$).

To estimate a settlement time for each colony, we used the same equation but instead solved for t_0 (settlement time). In this calculation $A_1$was the colony area at t_1 at the first time point the colony was recorded (either 29 days or 46 days,), A_0 was the initial colony size at settlement (assumed to be 1 mm^2 for all colonies), and r was the mean colony growth rate previously calculated.

A series of linear models were constructed to test the fixed effects of population density and settlement time on final colony area. Both population density and settlement time were included as continuous fixed effects. Colony area data were log-transformed to meet the assumptions of the model. Models were compared using the Akaike Information Criterion (AIC), and the model with the lowest AIC value was selected as the best fitting model here and for all analyses below (see Appendix B). When ΔAIC between two models was within two units, the most parsimonious model was chosen here and for all analyses described below (Burnham & Anderson 2002). A Likelihood Ratio Test (in R library RLRsim) showed that the addition of a random effect of settling plate did not significantly improve the selected model. All statistical tests were conducted in R v.3.4.1 (R Core Team 2017).

Part 2: Comparison of field distributions and model predictions

We compared spatial distributions observed from field plates in Part 1 with modeled spatial distributions using a previously-constructed spatial bryozoan growth model (Seroy & Grünbaum 2018). The model, implemented in Python 2.7, spatially simulates a bryozoan population on a two-dimensional domain where colonies can compete for space. Colony-level parameters include settlement time, growth rate based on experimental conditions, and an option to designate a specific colony settlement position or a random settlement position within the

domain. Colonies are spatially approximated using aggregated polygons to represent individual zooids and colony growth results from equations representing zooid-level processes of energy acquisition.

We simulated the 12 focal plates selected in Part 1, using observed settlement times and relative colony settlement positions as model inputs. All colonies were given the same experimentally-determined growth rate in typical ambient conditions (Seroy & Grünbaum 2018). Because the model is computationally expensive, a scaled down simulation domain was used in which 1 mm in the model represented 4.06 mm on the plates. Settlement positions were scaled accordingly. Simulations were run until the model domain was filled, and final colony areas were calculated. Percent area occupied by colonies was used to compare model and field colony area measurements. Percent area occupied measured from field observations and percent occupied predicted by the model were compared using linear regression to quantify predictive skill of the model. A linear regression was constructed with log-transformed field and model percent areas and a forced intercept at zero to reflect biological limitations.

Part 3: Effects of population density, settlement time, and pH on the cost of defense in the model

Model metrics

All model simulations used a model domain of 50 mm x 100 mm, and simulation parameters and empirical bryozoan growth rates experimentally from Seroy and Grünbaum (2018). Simulations were for 75 days, chosen such that populations in most runs filled the model domain. Colonies in the model were designated as undefended or defended by assignment of the respective growth rates. The mean undefended colony size ($\bar{a}_{u,t}$) was calculated from colonies with equivalent settlement times at the end of each replicate run using the equation,

$$\bar{a}_{u,t} = \frac{1}{n_{u,t}} \sum_{i=0}^{n} a_{i,u,t} \tag{3.2}$$

where $n_{u,t}$ is the number of undefended colonies that settled at the focal settlement time *t*, and $a_{i,u,t}$ is the area of colony *i*. The mean defended colony size ($\bar{a}_{d,t}$) for each replicate model run was calculated in the same way.

Cost of defense (COD) was calculated as the difference between the mean undefended ($\bar{a}_{u,t}$) and mean defended ($\bar{a}_{d,t}$) colony size for each replicate run as in Seroy and Grünbaum (2018). COD values were analyzed in two ways:

1) *normalized COD (nCOD)*, in which raw COD values were normalized to the simulated kelp blade area using the equation

$$nCOD = \frac{\bar{a}_{u,t} - \bar{a}_{d,t}}{A} \tag{3.3}$$

where *A* is the model domain area.

2) *relative COD (rCOD)*, in which raw COD values were normalized by mean undefended colony size using the equation

$$rCOD = \frac{\bar{a}_{u,t} - \bar{a}_{d,t}}{\bar{a}_{u,t}} \tag{3.4}$$

Mean defended colony size was also analyzed using two metrics:

1) *normalized defended colony size ($N_{d,t}$)*, in which mean defended colony sizes were normalized to the simulated kelp blade area using the equation

$$N_{d,t} = \frac{\bar{a}_{d,t}}{A} \tag{3.5}$$

2) *relative defended colony size* ($R_{d,t}$), in which mean defended colony sizes were normalized to mean undefended colony size:

$$R_{d,t} = \frac{\bar{a}_{d,t}}{\bar{a}_{u,t}} \quad (3.6)$$

These metrics were calculated to evaluate the realized fitness of defense strategies in two relevant ecological contexts: direct within-blade competition between defended and undefended neighbors (*rCOD*) and habitat-level competition, including indirect competition across kelp blades with variable colony densities (*nCOD*). See Appendix B for complete equations that explicitly connect these metrics to their population-level fitness implications. These metrics vary as functions of the ratio of defended and undefended colonies. The results presented here correspond to simulation conditions, in which numbers of defended and undefended colonies per algal blade were equal.

Population density manipulations

The model was used to systematically investigate the effects of population density on the cost of defense. Model simulations of different population densities (16, 20, 24, 28, 32 and 36 colonies) were conducted with half the colonies defended and the other half undefended. Fifty replicate model runs were conducted for each population density. All colonies settled at 0 days. To explore effects of ocean acidification, we replicated these model simulations with defended and undefended *M. membranacea* growth rates measured at pH 7.6 and pH 7.3 in laboratory experiments (Seroy & Grünbaum 2018). These pH values are lower than typical ambient pH of 7.9 during the *M. membranacea* growing season in Friday Harbor, WA (Murray et al. 2015).

A series of generalized linear models were used to determine the effect of population density and pH on *normalized COD* and *normalized defended colony size* calculated from these model simulations. Linear models used a gamma distribution, which is appropriate for continuous positive skewed data (Faraway 2016), and a log link. For *relative COD* and *relative*

defended colony size, a series of linear models using a Gaussian distribution with an identity link was used. Linear models were compared using AIC values to select a best fit model (see Appendix B). Population density was treated as a continuous fixed effect and pH was treated as a factor.

Settlement time and population density manipulations

We also used the model to investigate the effect of settlement time and population density on the cost of defense. Within selected population densities (16, 24, 32 colonies), we tested the effects of a range of delayed settlement times. In these simulations, half of the colonies settled at $t = 0$ days and the other half settled at the designated late settlement time ($t = 5$, 10, or 20 days). Within each settlement time, half of the colonies were assigned the undefended growth rate and the other half were assigned the defended growth rate. Raw COD values were calculated for the late settling colonies. COD and mean defended colony sizes were analyzed as both normalized and relative metrics, as described above. These model simulations were also replicated with growth rates from pH 7.6 and pH 7.3. Fifty replicate model simulations were conducted for each set of settlement time, density and pH conditions.

A series of linear models were constructed to test the fixed effects of settlement time, population density and pH on both *normalized COD* and *relative COD*. Models used a Gaussian distribution with an identity link. Models of similar structure were also used to test above effects on *normalized defended colony size* and *relative defended colony size*. Both population density and settlement time were included in models as continuous predictors. Models were compared using AIC values to select the best fit model (see Appendix B).

3.4 RESULTS

Part 1: Field analysis of settlement time and population density

Colony size in the field was highly variable with final colonies areas ranging from 56.7 mm^2 to 29,968.5 mm^2 across all plates (mean = 5077 mm^2, *sd* = 5052 mm^2, *n* = 200) (Figure 3.1). Both settlement time and density independently influenced colony area in the field, without a significant interaction. Increasing population density significantly reduced colony size ($p < 0.0001$). Later settlement times also reduced colony size in the field ($p < 0.0001$). This analysis identified both factors as important controls on colony size and justified their inclusion in later analyses of their effects on COD.

Part 2: Model and field comparison

Colony areas were presented as percent area of the domain occupied by corresponding colonies in the model and in the field (Figure 3.2, Figure 3.3). Area occupied in the model and the field showed a close positive relationship. Modeled colony areas resulting from settlement time and settlement position inputs predicted colony field areas well ($R^2 = 0.834$, $p < 0.0001$) with a slope of 1.05, where the model slightly but consistently underestimated field areas.

Part 3: Modeled effects of population density, settlement time, and pH on COD

Population density manipulations

For model runs with only manipulated population densities (16, 20, 24, 28, 32 and 36 colonies) and pH (7.9, 7.6, 7.3), *nCOD* calculations showed cost of defense (COD) was small in comparison to the model domain size (mean = 0.021, *sd* = 0.012, *n* = 900) (Figure 3.4a). However, *rCOD* calculations indicated that COD was, on average, a large fraction of colony size

(mean = 0.479, *sd* = 0.136, *n* = 900) (Figure 3.4c). Population density significantly decreased *nCOD* ($p < 0.0001$) and *rCOD* ($p < 0.0001$). pH also significantly affected both *nCOD* ($p < 0.0001$) and *rCOD* ($p < 0.0001$), with significantly larger COD at pH 7.6 than typically ambient pH 7.9 conditions, and significantly smaller COD at pH 7.3 than pH 7.9. Across all densities, the largest *rCOD* and *nCOD* both occurred at pH 7.6 where undefended colony growth rates were the fastest, and the difference between undefended and defended growth rates was the largest. Across all densities, the smallest *rCOD* and *nCOD* both occurred at pH 7.3, where the difference between defended and undefended growth rates was the smallest (Figure 3.4).

Normalized defended colony sizes ($N_{d,t}$), showed colony sizes were also generally small compared with the domain area (mean = 0.021, *sd* = 0.007, *n* = 900) (Figure 3.4b), typically <10% of the area simulated for an isolated defended colony (a normalized maximum size of 0.27). This is expected because colony areas are normalized by the large domain size. The indicated costs are nonetheless important, because these metrics combine to determine habitat-wide costs of defense, integrating across diverse blades that range from sparse to crowded (Appendix B). Relative defended colony sizes ($R_{d,t}$) showed defended colonies were on average approximately half the size of undefended colonies at the end of model simulations (mean = 0.521, *sd* = 0.136, *n* = 900) (Figure 3.4d). Both $N_{d,t}$ and $R_{d,t}$ were significantly decreased by increasing population density ($p < 0.0001$). pH also significantly affected both $N_{d,t}$ ($p < 0.0001$) and $R_{d,t}$ ($p < 0.0001$), with smaller defended colonies at pH 7.6 than at typically ambient pH 7.9, and larger defended colony sizes at pH 7.3 than at pH 7.9 across all population densities (Figure 3.4). Best fit statistical models for *rCOD*, *nCOD*, $N_{d,t}$ and $R_{d,t}$ contained no significant interactions between population density and pH.

Settlement time and population density manipulations

In model runs with manipulated population densities (16, 24, and 32 colonies), late settlement times (5, 10, and 20 days) and pH (7.9, 7.6, 7.3), *nCOD* (mean = 0.016, *sd* = 0.013, *n* = 1800) was significantly affected by all three factors (Figure 3.5a). The best-fit linear model contained all fixed effects (population density, settlement time and pH) as well as all possible pairwise interactions between the predictors. Later settlement decreased *nCOD* ($p < 0.0001$), but the relationship was dependent on population density and pH. $N_{d,t}$ (mean = 0.020, *sd* = 0.008, *n* = 1800) was also affected by all three factors (Figure 3.5b). Like the best fit model describing effects on *nCOD*, the best fit linear model for $N_{d,t}$ also included all three fixed effects and all pairwise interactions. $N_{d,t}$ decreased with later settlement times ($p < 0.0001$) but was dependent on population density and pH.

rCOD calculated from these model simulations (mean = 0.405, *sd* = 0.219, *n* = 1800), significantly decreased with increasing population density ($p = 0.0009$) (Figure 3.5c). Later settlement time also decreased *rCOD* ($p < 0.0001$). Similar to analyses of density manipulation model runs, greater *rCOD* was observed at pH 7.6 ($p < 0.0001$) and smaller *rCOD* was observed at pH 7.3 ($p < 0.0001$) in comparison with ambient pH parameter conditions. $R_{d,t}$ (mean = 0.595, *sd* = 0.219, *n* = 1800) were also significantly decreased by increasing population density ($p < 0.0001$) and later settlement time ($p < 0.0001$) (Figure 3.5d). Within these trends, defended colonies were smallest at pH 7.6 where the difference between undefended and defended growth rates was the greatest, and largest at pH 7.3 where this difference was the smallest (Figure 3.5). There were no significant interactions between the three factors in determining *rCOD* or $R_{d,t}$.

3.5 DISCUSSION

We used an integrative modeling and in situ empirical approach to investigate bidirectional feedbacks between population-level space competition and individual fitness strategies, including growth and defense. We used a marine bryozoan that shares similar traits with a diversity of other space-limited organisms, *M. membranacea*, as a model organismal system to illustrate the utility of this approach. Our study used *M. membranacea* to ask how space competition modified colony fitness and the cost of inducible defenses, and how these costs changed across a range of environmental change conditions.

Feedbacks from organismal-level to population-level responses

To understand ways that organism-level processes cross scales to structure populations, we asked how characteristics of individual organisms collectively determine emergent properties like space competition. In comparing field and modeled *M. membranacea* populations, we found that overall field distributions, and specific details like individual colony size and shape, could be predicted with remarkable accuracy from observed settlement times and positions (Figure 3.2, Figure 3.3). The model had a strong predictive correlation. It slightly under-predicted field colony areas, probably because the smaller model domain size exaggerated the exclusion area between neighboring colonies. However, the relationship between field observations and the predictive capacity of the model remains clear, and the regression analysis provides a simple correction factor that could be applied to the model-field relationship to predict actual colony sizes in the field in future studies. These findings largely support the hypotheses that, in *M. membranacea* and perhaps other space-limited organisms, mechanistic models of individual organisms can predict population-level dynamics, and that (in this case) the dominant ecological

mechanisms were identified and quantified. Our results provide evidence that outcomes of spatial competition among bryozoans were predictable from first principles using measured organism-level characteristics.

Feedbacks from population-level to organismal-level responses

To understand feedbacks from populations to individuals, we asked how population-level processes like space competition alter the fitness effects of individual-level growth and defense strategies in *M. membanacea*. Our field data suggested that space competition, modulated by population density and settlement time, strongly regulated colony size. Model simulations supported the importance of this regulation, and provided quantitative insight into how population density and settlement time factors influence colony size and modulate competitive interactions. Building upon previous work that has documented reduced colony sizes with increasing population density (e.g. Harvell et al. 1990), our work further quantified the relationships between density and size-frequency distributions. In particular, we quantified the fitness costs of crowding and delayed larval settlement. According to our best-fit equation (Figure 3.1), for example, colonies that settled on Day 0 on plates with 16 colonies have about 65% the estimated fitness of colonies that settled on Day 0 on plates with 8 colonies. By comparison, colonies that settled on Day 7 on plates with 8 colonies have only about 52% the estimated fitness of colonies that settled on Day 0 on plates with 8 colonies. These results suggest, for *M. membranacea* and perhaps for many other space-limited organisms, fitness reductions due to late settlement can be on a par with or exceed those due to settlement in areas with high colony density.

We also used model investigations to assess and quantify the realized fitness effects of defensive strategies, given variations in space competition. To bracket the spectrum of inducible (partially defended) cases, we calculated the cost of defense from colonies that were assigned defended or undefended growth rates for the entire simulation. This enabled us to calculate the maximum possible cost of an inducible defense over the lifetime of a colony, and the corresponding maximum benefit of an inducible defense compared to a constitutive one.

We quantified the costs of defensive strategies in *M. membranacea* as reductions in colony area on the organism level. The fitness implications of these costs can be evaluated in multiple ways when considered in the context of a population of competing conspecifics (see Appendix B Equations). On the scale of a single kelp blade that hosts multiple colonies, the fitness implications of defensive costs can be evaluated in the context of direct local interactions of defended colonies relative to neighboring colonies without defenses (*rCOD*). On the scale of a habitat that may include multiple kelp blades of varying densities, accounting for defensive costs must include the fact that colonies on different kelp blades in the same habitat are also in indirect competition to contribute to the next generation (*nCOD*).

We found both normalized (*nCOD*) and relative (*rCOD*) cost of defense metrics to be modulated by competitive interactions with similar directional trends (Figures 3.4 and 3.5). This suggests the experimentally more tractable *rCOD* metric may also be informative about larger scale dynamics characterized by *nCOD*. Space competition exerted significant controls on the cost of defense: *rCOD* calculations suggested that space limitation reduced the competitive disadvantage of defended colonies, in comparison with undefended counterparts. The mechanism underlying this decrease was likely that, on crowded blades, differences in exponential growth rates could operate for relatively shorter periods before further growth was halted by occlusion,

limiting the ultimate differences in colony areas. We did not simulate predation, but these results suggest that the threshold of predation at which deployment of defenses improves reproductive success by lowering zooid mortality may be lower on crowded blades than sparse blades.

Normalized cost of defense (*nCOD*) calculations suggest that high colony density also reduced expected differences in reproductive output between defended and undefended colonies on a kelp blade. Calculating *nCOD* requires specifying the relative frequency of blades with different colony densities. On the habitat scale, colonies on sparse blades grew much larger than colonies on dense blades, and hence had disproportionately large reproductive contributions. Colonies on sparse blades also had relatively higher costs of defense than colonies on dense blades. Under our assumption that sparse (8-colony), medium (16-colony) and dense (24-colony) blades were equally prevalent, the *nCOD* metric in our calculations showed a relatively high habitat-scale cost of defense. This suggests that, in general, costs of defense on sparsely populated blades may disproportionately impact costs and benefits of defensive spines for a population as a whole, and that increased frequency of sparse blades magnifies cost of defense while increased frequency of crowded blades reduces it.

One of our motivating hypotheses stemmed in part from results in Seroy and Grünbaum (2018), where two competitive scenarios were compared. In one scenario, 16 defended colonies and 16 undefended colonies grew on separate blades, and their areas were evaluated at a time point when blades were substantially but incompletely covered. In the second scenario, 8 defended and 8 undefended colonies grew in competition on the same blades. Seroy and Grünbaum (2018) observed that decrements in the areas of defended colonies relative to undefended colonies were much greater when the two morphs directly competed on the same

blade, compared to when they competed indirectly on different blades. This suggested the hypothesis that, more generally, more intense space competition would increase cost of defense.

The distinction between direct and indirect competition was made more explicit in the present study by the metrics *rCOD* and *nCOD*, by systematic variation across colony densities on blades, and by running simulations to steady state -- that is, to a "late-season" time point when habitats were fully or nearly fully occupied. In this scenario, space competition has run its course and potential growth time is not limiting. Our results suggest that, under this scenario, increased numbers of conspecifics reduced the cost of defense compared to isolated colonies.

Our results highlight how inducible defenses benefit colonies in the field by enabling them to grow quickly before deploying defenses, avoiding high costs of defense in habitats where space is readily available. The large costs of defense on sparse blades, upwards of 50% of colony size as indicated by *rCOD* calculations, emphasizes the importance of inducibility, through which colonies incur this high cost only when necessary to avoid heavy predation. Conversely, on more densely populated blades where space is more limited, colonies may benefit more by deploying defenses, because costs are lower.

Because costs of defense are strongly modulated by crowding, colonies may benefit from potential mechanisms for detecting conspecifics. *M. membranipora* colonies contacting space competitors along a growing edge are known to sometimes deploy stolons, which are undifferentiated extensions of tissue projected across the growing edge of a neighbor to inhibit its advance (Harvell & Padilla 1990). Beyond this response to contact, there is thus far no evidence that *M. membranipora* colonies have a remote mechanism for anticipating future crowding. However, such a mechanism could exist, for example responses to chemical cues of conspecifics akin to the known induced defensive responses to cues of incipient predation. The

strong effects of incipient crowding suggest that regulation of defensive spines by chemical cues of conspecifics, in addition to predators, may be worth investigation.

Maintenance of diverse defensive strategies in *M. membranacea*

In many marine and terrestrial species, individuals may exhibit inducible or constitutive defenses. However, the ecological mechanisms maintaining these multiple strategies are unclear (Karban & Baldwin 1997, Tollrian & Harvell 1999). Evidence from previous studies has shown that a diversity of defensive strategies exists among *M. membranacea* colonies: Most exhibit inducible defenses, but a small fraction of colonies are either constitutively defended (always exhibit spines) or undefended (never exhibit spines) (Harvell 1986). Inducible defenses typically appear to be potent generalist strategies, combining the advantages of both defended and undefended constitutive strategies while minimizing their disadvantages (Tollrian & Harvell 1999). Why then are these constitutive strategies maintained in wild populations?

The variation in costs of defense with blade-level crowding suggests a mechanism for maintaining this diversity. We found that even in the absence of predation, the cost of defense is minimized on crowded blades, on which colony growth is greatly reduced. Because only developing zooids along colony growing margins can deploy defensive spines (Harvell 1984), growth reduction likely suppresses effective responses to predator cues. This suggests that in more crowded habitats, fewer benefits are conferred by induced responses to predator chemical cues. We hypothesize that this potential insufficiency of predator cues on crowded blades provides a context in which constitutive strategies may confer fitness benefits, e.g. on crowded blades with heavy predation. If true, this interpretation suggests additional potential links

between defensive strategies and population densities across the diverse environments in which *M. membranacea* is found.

Cost of defense in a changing ocean

Many ecological communities are experiencing changing environments (Kordas et al. 2011, Gaylord et al. 2015, Franklin et al. 2016). Understanding bidirectional feedbacks shaping populations can help provide a more holistic view of predicted organism responses. In *M. membranacea*, we sought to understand how consequences of these feedbacks resulted in realized fitness across a range of predicted future environmental conditions. *M. membranacea* has a relatively wide pH tolerance (Seroy & Grünbaum 2018), unlike other more sensitive calcifying organisms (Kroeker et al. 2013). Across the range of ocean acidification conditions simulated in our model, the observed effects of population density and settlement timing on colony area and cost of defense changed modestly. The cost of defense was largely determined by the competitive advantage of undefended colonies across the range of OA conditions, indicated by the difference in growth rate between undefended and defended colonies. At pH 7.6, faster undefended growth rates increased the competitive advantage of undefended colonies which, in turn, increased the cost of defense. At pH 7.3, the smaller competitive advantage of undefended colonies reduced the cost of defense. Increasing competitive advantage was characterized by an increased tendency of faster-growing undefended colonies to occupy space quickly, making it unavailable for slower-growing defended colonies. Consistent with results for typical ambient conditions, cost of defense under predicted future OA regimes were tightly coupled to competitive ability and maximum colony size. This suggests that space competition will continue to modify organismal responses even in changing environments, until pH

reductions become extreme. While we simulated different pH conditions in the model, this conclusion appears likely to also apply to other environmental changes, like temperature, that can have similar effects on growth rates in *M. membranacea* (Saunders & Metaxas 2009).

Life history implications

In life history analysis of marine invertebrates with planktonic larvae, and of many other organismal systems, prolonged development times that delay recruitment are typically found to incur costs such as losses to predation, depletion of maternally-provided resources, transport away from favorable habitats and loss of settlement opportunities (Smith & Fretwell 1974, McEdward 1997, Jorgensen et al. 2011). These costs may be offset by benefits such as increased fecundity, made possible by smaller propagules. The costs are typically difficult to quantify, making life history analysis integrating propagule stages through adulthood a challenge.

Our coupled model-field approach quantified benefits of early settlement and costs of late settlement under the pressures of space limitation. For *M. membranipora* larvae, early settlement times potentially enable individuals to outcompete conspecifics for space, and may also provide the benefit of growth before predatory nudibranchs become abundant (Yoshioka 1986). This reduces zooid predation in critical early growth and avoids the need for induction of defenses, which may be costly early in the season when space is readily available.

Despite costs of late settlement, larvae often exhibit selective behaviors and preferences that can delay metamorphosis and settlement (Pechenik 1990). *M. membranacea* larvae exhibit substrate-specific behaviors and algal substrate preferences (Matson et al. 2010). Our study quantifies some of the risks and tradeoffs for larvae between early settlement in a crowded habitat and later settlement in a sparse habitat. *M. membranacea* larvae have also exhibited

settlement preferences across an algal substrate, preferring younger, proximal, and typically less crowded areas of kelp blades (Denley et al. 2014).

Our work illustrates how space limitation modulates tradeoffs between settling early and identifying favorable substrates. Our field data show that late-settling larvae in low density areas can attain similar colony sizes to those settling earlier in higher density areas. Trendlines associated with Figure 3.1 enable predictions of conditions under which it would be beneficial for a larva to wait for another habitat. For example, suppose a larva that encounters a crowded kelp blade at time t_0 can choose between settling, or abandoning it to find a sparse blade after a search time Δt. For the latter choice to enhance fitness, the expected fitness on a sparse blade must exceed the expected fitness on a crowded blade after discounting both for the Δt delay in settlement time and the mortality risk associated with the prolonged planktonic period. Forgoing a crowded habitat where space competition is likely to be intense would then be predicted to enhance the fitness of choosy larvae.

If population density influences possible suitability of a substrate, a question emerges: do *M. membranacea* larvae have mechanisms to assess competitor density upon settlement? Many marine invertebrate larvae have been shown to detect adult conspecifics or competitors, including attraction to adult conspecific cues like gregarious settlement in oysters (Tamburri et al. 2007), gastropods (Cahill & Koury 2016), and barnacles (Pineda & Caswell 1997) or avoidance of established competitors in bryozoans (Young & Chia 1981). Substrate preferences may also enable larvae to indirectly locate lower-density settlement sites. *M. membranacea* larvae exhibit settlement preferences for younger ends of kelp blades (Denley et al. 2014), which likely have less crowding and fewer larger colonies that would occlude new settlers quickly. Whether *M. membranacea* larvae can detect adult populations during settlement remains poorly

understood, but the hypothesis that they may have direct or indirect mechanisms to detect adult conspecifics merits further investigation.

Conclusions

We evaluated potential bidirectional feedbacks between space competition, a population-level mechanism, and individual-level strategies for growth, defense, and habitat selectivity by competing space-limited modular organisms in the context of variations in competitor density and environmental stresses. To quantify feedbacks, we used an experimentally-informed, spatially-explicit population model validated with field data to quantify indirect population-level effects that are otherwise difficult to measure. Coupling field distributions with modeling also provided a method to infer dominant ecological processes governing space competition from field observations. In our focal organism, the bryozoan *M. membrancea*, we demonstrated that bidirectional feedbacks are significant. Individual fitness consequences of alternative growth, defense and larval settlement strategies were strongly modulated by population-level characteristics such as size-frequency distributions and intensity of space competition. In general, conditions under which colony growth could proceed further before occlusion by neighbors increased the cost of inducible defensive spines. This included sparser populations of colonies on kelp blades, and earlier larval settlement times. Conversely, denser populations of colonies on kelp blades and later settlement resulted in smaller, more space-limited colonies but reduced the cost of defense relative to competing undefended colonies. These conclusions also applied across a spectrum of an environmental stress, ocean acidification, that affects growth rates, emphasizing that bidirectional feedbacks also likely modulate how these organisms will respond to changing environments. By identifying population density and settlement time as

potential drivers of the outcomes of competitive interactions and quantifying their effects, our results demonstrate how integration of organismal responses across multiple organizational scales and life history stages can be characterized and quantified. Our approach, which may be broadly applicable to other space-limited organisms, highlights the benefit in considering multiple levels of organization in context to quantify the realized effects of individual-level fitness strategies.

3.6 ACKNOWLEDGEMENTS

The authors thank Ann Stanbrough, Rachel Snow, Kim Stewart, Anik Mutsuddy, Jackelyn Garcia, and Faustino Hampson-Medina for field assistance, Drew Harvell and Dianna Padilla for advice, Katie Dobkowski for manuscript comments, and Robert Levine and Amy Wyeth for feedback on study design and interpretation. This work was funded by the Patricia L. Dudley Endowed Scholarship (Friday Harbor Laboratories) and NSF Graduate Research Fellowship to SKS. DG gratefully acknowledges support from Washington State Sea Grant (NA10OAR-4170057) and NSF (OCE-1657992).

References

Armstrong RA, Welch AR (2007) Competition in lichen communities. Symbiosis 43(1): 1-12

Burnham KP, Anderson DR (2002) Model selection and multi -model inference: a practical information-theoretic approach, 2nd edn. Springer, New York, New York, USA.

Buss LW (1979) Bryozoan overgrowth interactions - the interdependence of competition for space and food. Nature 281:475-477

Buss LW (1980) Competitive intransitivity and size-frequency distributions of interacting populations. P Nat Acad Sci USA 77:5355-5359

Connell JH (1961) The influence of interspecific competition and other factors on the distribution of the barnacle *Chthamalus stellatus*. Ecology 42:710-723

Connolly SR, Muko S (2003) Space preemption, size-dependent competition, and the coexistence of clonal growth forms. Ecology 84:2979-2988

Cahill AE, Koury SA (2016) Larval settlement and metamorphosis in a marine gastropod in response to multiple conspecific cues. PeerJ 4:e2295

Dayton PK (1971) Competition, disturbance, and community organization: the provision and subsequent utilization of space in a rocky intertidal community. Ecol Monogr 41:351-389

Denley DA, Metaxas A, Short J (2014) Selective settlement by larvae of *Membranipora membranacea* and *Electra pilosa* (Ectoprocta) along kelp blades in Nova Scotia, Canada. Aquat Biol 21:47-56

Dickinson MB, Miller TE (1998) Competition among small, free-floating, aquatic plants. Am Midl Nat 140:55-67

Faraway JJ (2016) Extending the linear model with R: generalized linear, mixed effects and nonparametric regression models. Chapman and Hall/CRC, London, United Kingdom.

Franklin J, Serra-Diaz JM, Syphard AD, Regan HM (2016) Global change and terrestrial plant community dynamics. P Nat Acad Sci USA 113: 3725-3734

Gaylord B, Kroeker KJ, Sunday JM, Anderson KM and others (2015) Ocean acidification through the lens of ecological theory. Ecology 96:3-15

Goldberg DE, Barton AM (1992) Patterns and consequences of interspecific competition in natural communities: a review of field experiments with plants. Am Nat 139: 771-801

Grünbaum D (1997) Hydromechanical mechanisms of colony organization and cost of defense in an encrusting bryozoan, *Membranipora membranacea*. Limnol Oceanogr 42: 741-752

Harvell CD (1984) Predator-induced defense in a marine bryozoan. Science 224:1357-1359

Harvell CD (1986) The ecology and evolution of inducible defenses in a marine bryozoan: cues, costs, and consequences. Am Nat 128:810-823

Harvell CD, Padilla DK (1990) Inducible morphology, heterochrony, and size hierarchies in a colonial invertebrate monoculture. P Nat Acad Sci 87:508-512

Harvell CD, Caswell H, Simpson P (1990) Density effects in a colonial monoculture: experimental studies with a marine bryozoan (*Membranipora membranacea L.*). Oecologia 82:227-237

Harvell CD (1992) Inducible defenses and allocation shifts in a marine bryozoan. Ecology 73: 1567-1576

Herms DA, Mattson W (1992) The dilemma of plants: to grow or defend. Q Rev Biol 67:1689–1699

Jørgensen C, Auer SK, Reznick DN (2011) A model for optimal offspring size in fish, including live-bearing and parental effects. Am Nat 177: E119-E135.

Karban R, Baldwin IT (1997) Induced responses to herbivory. University of Chicago Press, Chicago, Illinois, USA.

Kordas RL, Harley CD, O'Connor MI (2011) Community ecology in a warming world: the influence of temperature on interspecific interactions in marine systems. J Exp Mar Biol Ecol 400:218-226.

Kroeker KJ, Kordas RL, Crim R, Hendriks IE, Ramajo L, Singh GS, Duarte CM, Gattuso JP (2013) Impacts of ocean acidification on marine organisms: quantifying sensitivities and interaction with warming. Glob Change Biol 19:1884-1896.

Lang JC, Chornesky EA (1990) Competition between scleractinians reef corals—a review of mechanisms and effects. In: Z. Dubinsky (ed) Coral reefs. Ecosystems of the World. Vol 25. Elsevier, Amsterdam, The Netherlands, p209–252

López-Victoria M, Zea S, Weil E (2006) Competition for space between encrusting excavating Caribbean sponges and other coral reef organisms. Mar Ecol Prog Ser 312:113-121.

McEdward LR (1997) Reproductive strategies of marine benthic invertebrates revisited: facultative feeding by planktotrophic larvae. Am Nat 150: 48-72.

Matson PG, Steffen BT, Allen RM (2010) Settlement behavior of cyphonautes larvae of the bryozoan *Membranipora membranacea* in response to two algal substrata. Invertebr Biol 129:277-283.

Murray JW, Roberts E, Howard E, O'Donnell M, Bantam C, Carrington E, Fay A (2015) An inland sea high nitrate-low chlorophyll (HNLC) region with naturally high pCO_2. Limnol Oceanogr 60:957-966.

Pechenik JA (1990) Delayed metamorphosis by larvae of benthic marine invertebrates: does it occur? Is there a price to pay? Ophelia 32:63-94.

Pineda J, Caswell H (1997) Dependence of settlement rate on suitable substrate area. Mar Biol 129:541-548.

R Core Team (2017) R: a language and environment for statistical computing. R Foundation for Statistical Computing, Vienna. www.r-project.org

Saunders MI, Metaxas A (2007) Temperature explains settlement patterns of the introduced bryozoan *Membranipora membranacea* in Nova Scotia, Canada. Mar Ecol Prog Ser 344:95-106

Saunders MI, Metaxas A (2009) Effects of temperature, size, and food on the growth of *Membranipora membranacea* in laboratory and field studies. Mar Biol 156:2267-2276

Saunders MI, Metaxas A (2010) Physical forcing of distributions of bryozoan cyphonautes larvae in a coastal embayment. Mar Ecol Prog Ser 418:131-145

Schwinning S, Weiner J (1998) Mechanisms determining the degree of size asymmetry in competition among plants. Oecologia 113:447-455

Sebens KP (1982) Competition for space: growth rate, reproductive output, and escape in size. Am Nat 120:189-197

Seed R (1976) Observations on the ecology of *Membranipora* (Bryozoa) and a major predator *Doridella steinbergae* (Nudibranchiata) along the fronds of *Laminaria saccharina* at Friday Harbor, Washington. J Exp Mar Biol Ecol 24:1-17

Seroy SK, Grünbaum D (2018) Individual and population level effects of ocean acidification on a predator-prey system with inducible defenses: bryozoan-nudibranch interactions in the Salish Sea. Mar Ecol Prog Ser 607:1-18

Smith CC, Fretwell SD (1974) The optimal balance between size and number of offspring. Am Nat 108: 499-506

Tamburri MN, Zimmer RK, Zimmer CA (2007) Mechanisms reconciling gregarious larval settlement with adult cannibalism. Ecol Monogr 77:255-268

Tollrian R, Harvell CD (1999) The ecology and evolution of inducible defenses. Princeton University Press, Princeton, New Jersey, USA.

Yoshioka PM (1982) Role of planktonic and benthic factors in the population dynamics of the bryozoan *Membranipora membranacea*. Ecology 63:457-468.

Yoshioka PM (1986) Life history patterns of the dorid nudibranchs *Doridella steinbergae* and *Corambe pacifica*. Mar Ecol Prog Ser 31:179-184

Young CM, Chia FS (1981) Laboratory evidence for delay of larval settlement in response to a dominant competitor. Int J Inver Rep Dev 3:221-226

Figure 3.1 Final colony area measured from settling plates in the field with manipulated densities with respect to estimated colony settlement time. Trendlines show predictions for each density from a linear model. Trendline equation: $\ln(a_j) = -0.054c - 0.093s_j + 10.193$, where a_j is the area of a given colony j, c is number of colonies on the plate, and s_j is settlement time of colony j.

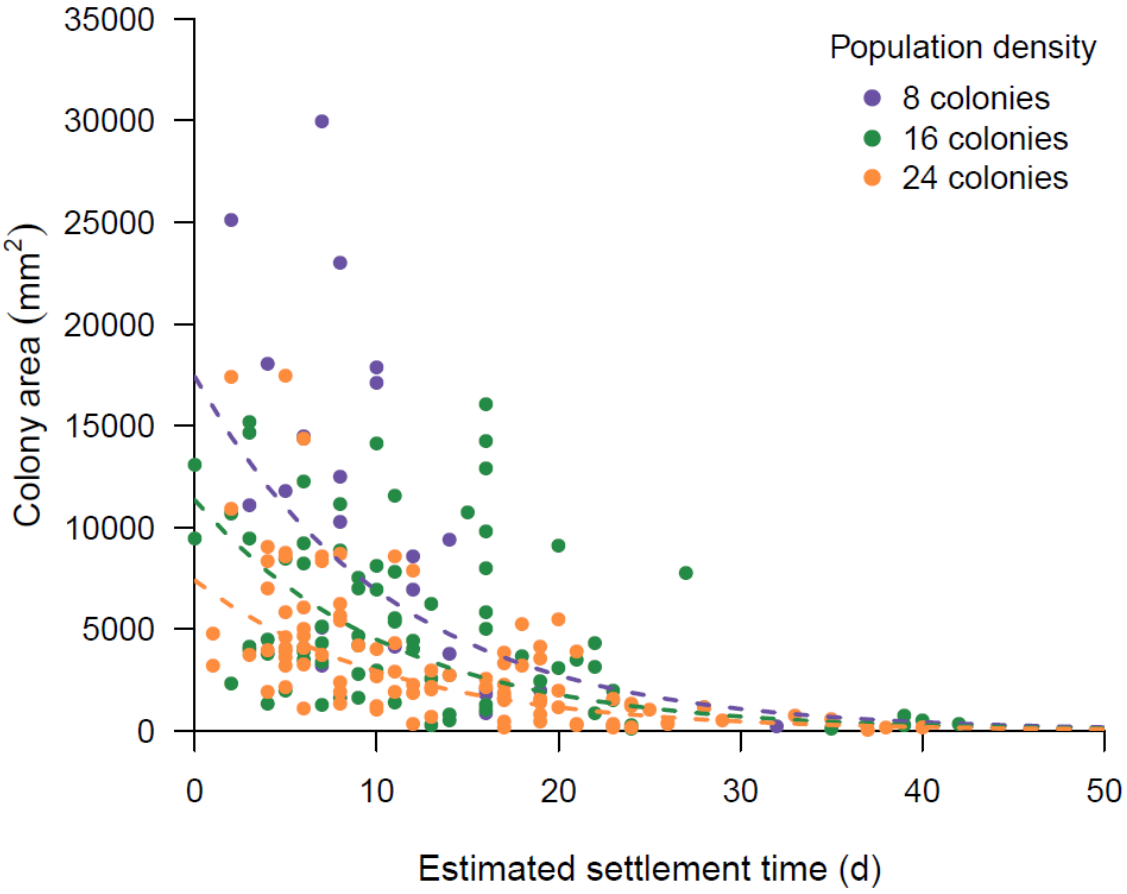

Figure 3.2 Colony area as a percentage of the total available area measured from field plates and replicated in the model using colony position and settlement time. Trendline shows the model's ability to quantitatively predict colony area in field. Colonies are color coded by which plate they came from. Manipulated plate densities are in parentheses.

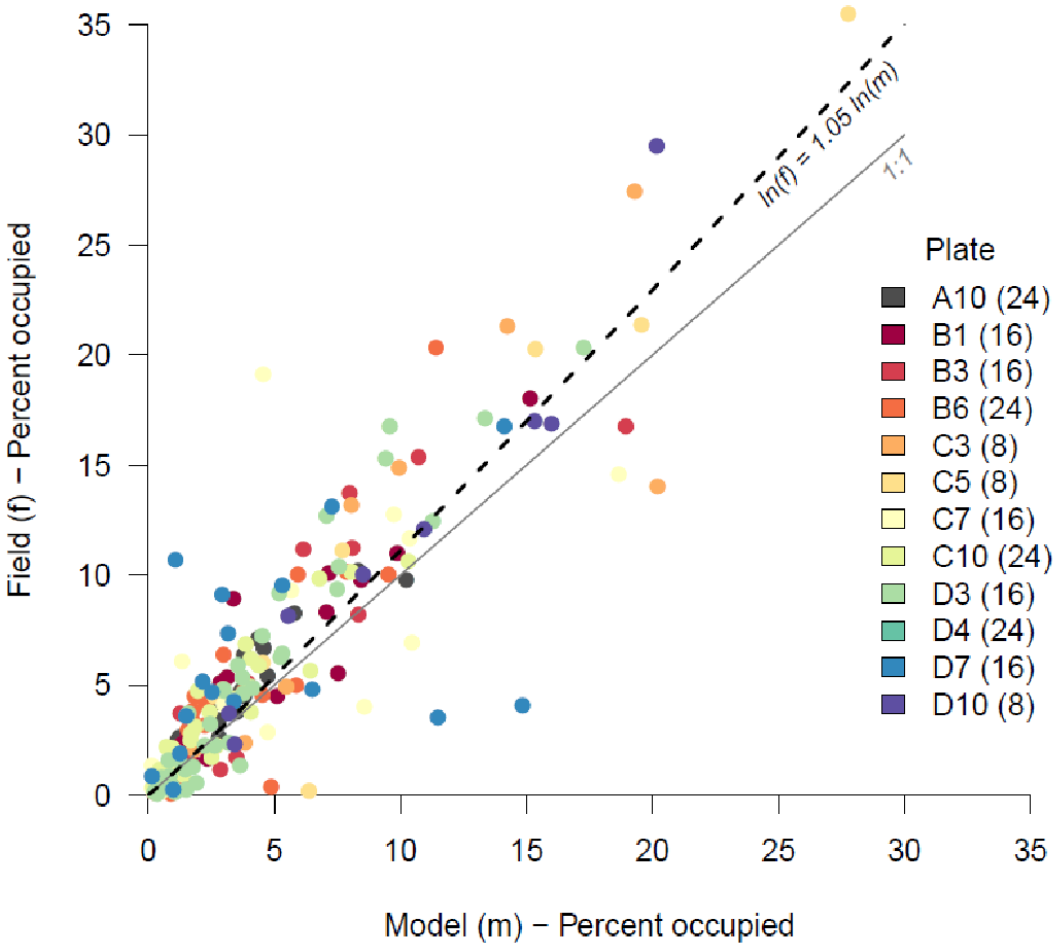

Figure 3.3 Example settling plates, showing a range of population densities, with *M. membranacea* distributions in the field and the same plates replicated in the model using colony settlement times and relative center points. Field plate dimensions were 406.4 mm x 203.2 mm. (a) Plate A10 (24 colonies) field distribution and (d) corresponding model simulation. (b) Plate B1 (16 colonies) field distribution and (e) corresponding model simulation. (c) Plate D10 (8 colonies) field distribution and (f) corresponding model simulation.

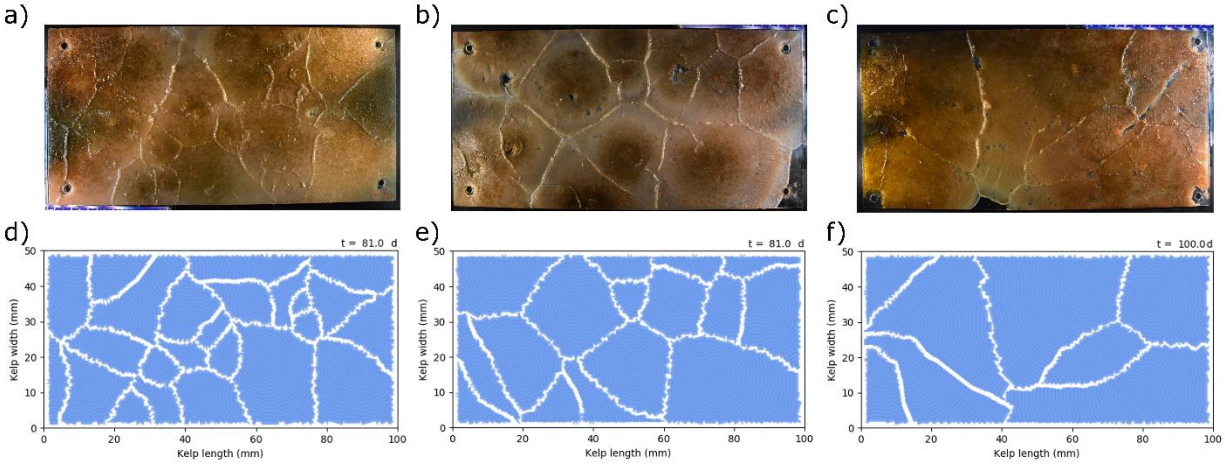

Figure 3.4 (a) Normalized COD (*nCOD*) and (b) normalized defended colony sizes ($N_{d,t}$) with respect to population density for each OA condition, indicated by pH, calculated from model simulations. pH 7.9 is reflective of ambient conditions during the *M.membranacea* growing season in Friday Harbor, WA, with pH 7.6 and pH 7.3 indicating possible future conditions. (c) Relative COD (*rCOD*) and (d) relative defended colony sizes ($R_{d,t}$) calculated from the same model simulations Trendlines show predictions from linear models. Error bars denote standard error.

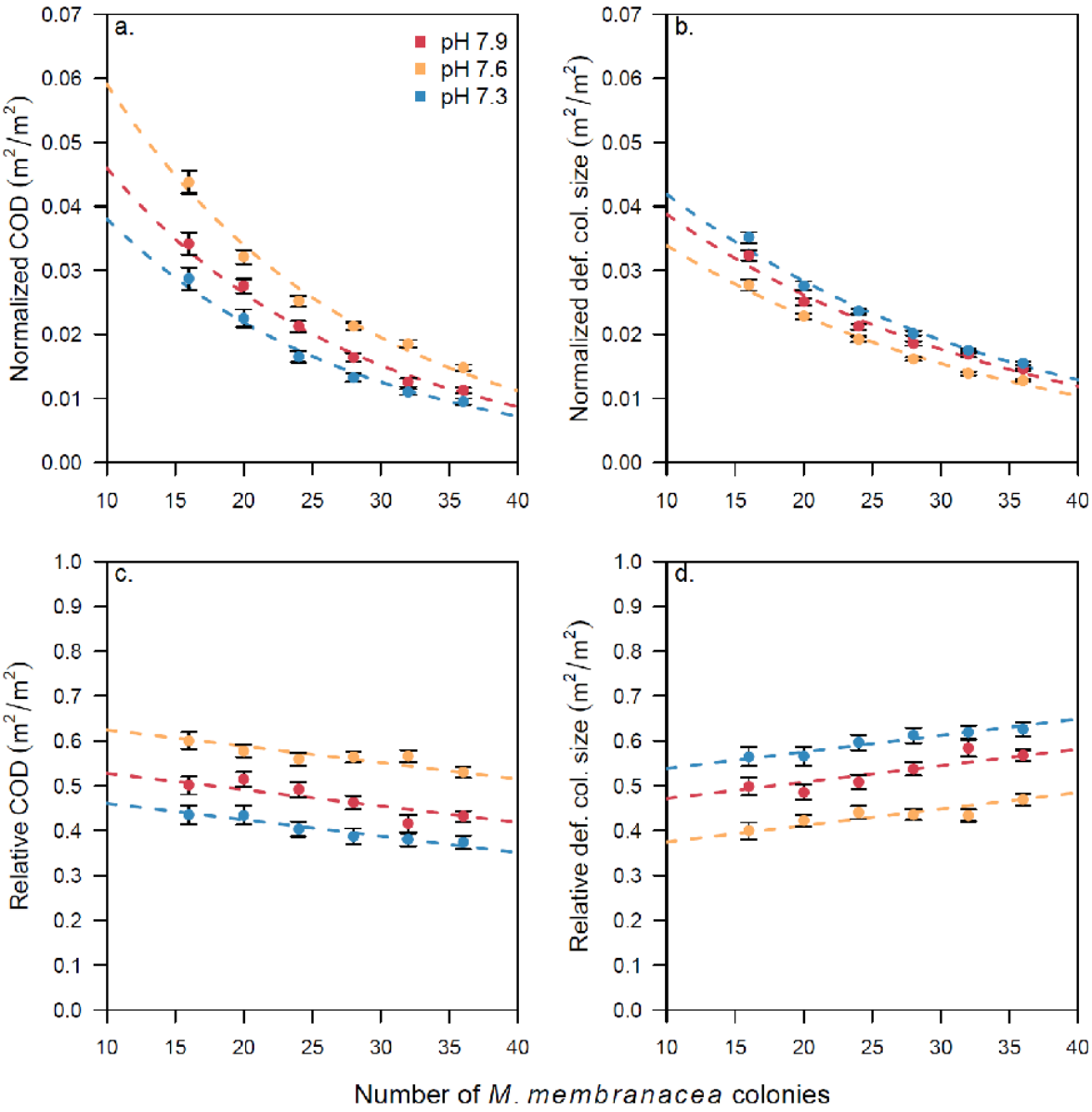

Figure 3.5 (a) Normalized COD (*nCOD*) and (b) normalized defended colony sizes ($N_{d,t}$) with respect to population density and settlement time for each OA condition, indicated by pH, calculated from model simulations. pH 7.9 is representative of ambient conditions with pH 7.6 and pH 7.3 representing potential future conditions. (c) Relative COD (*rCOD*) and (d) relative defended colony sizes ($R_{d,t}$) calculated from the same model simulations.

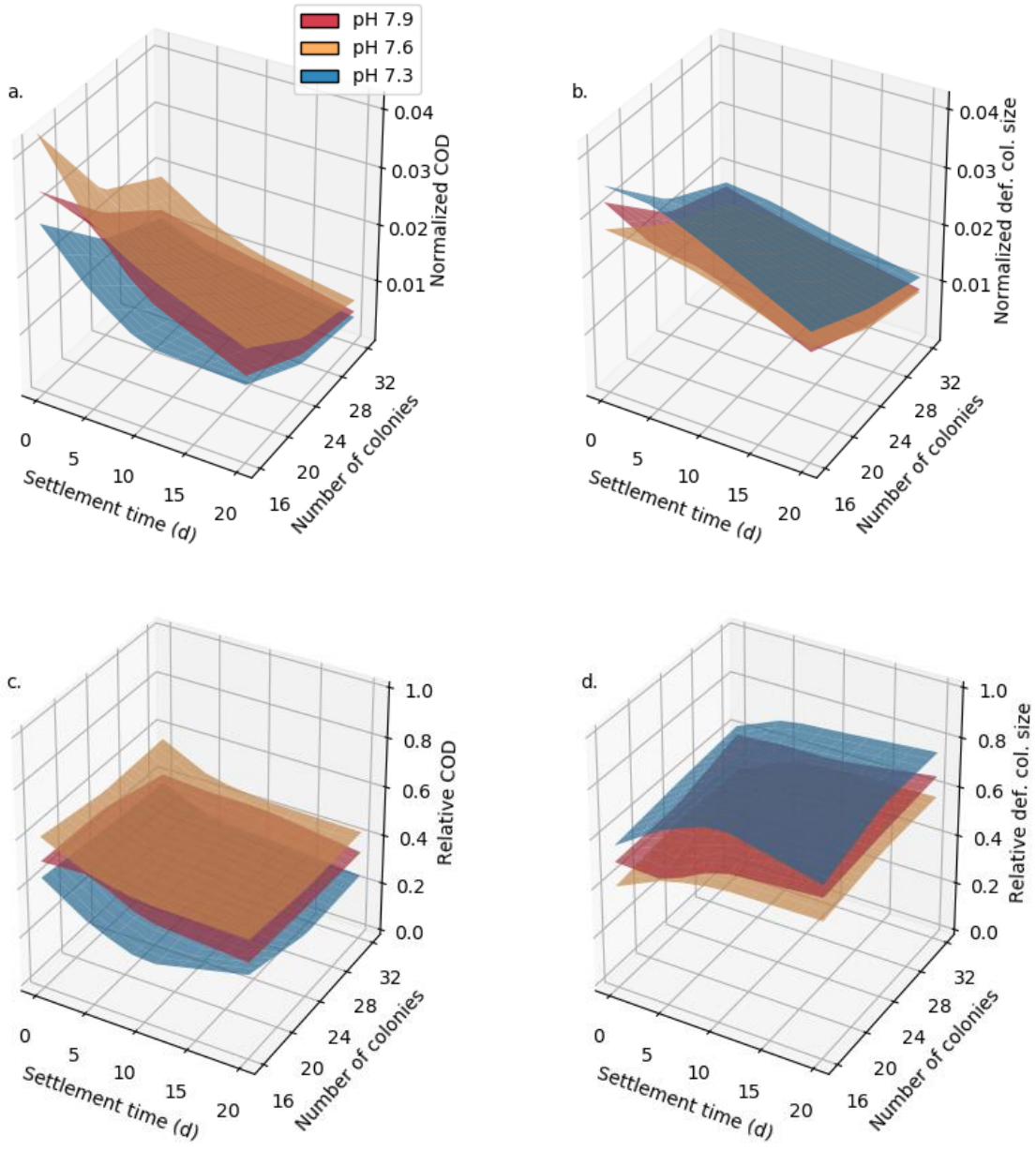

Chapter 4. ECOLOGICAL INTERACTIONS OF THE MARINE SNAIL, *LACUNA VINCTA*, EXHIBIT RESILIENCE TO WARMING TEMPERATURES

4.1 ABSTRACT

Marine communities are exposed to warming temperatures due to climate change. Temperature-induced effects on individuals have the potential to cause shifts in community structure via altered species interactions. We investigated the effects of warming temperatures on trophic interactions of the marine snail, *Lacuna vincta*, to understand how such interactions could modify organism-level responses to warming ocean temperatures. *L. vincta* is common in coastal macroalgal and eelgrass habitats of the Pacific Northwest and exhibits an inducible radula morphology in which tooth shape depends on habitat type. We experimentally explored the effects of temperature (12˚C, 16˚C and 20˚C) on *L. vincta* interactions with macroalgal and eelgrass food sources and whether tooth shape affected snail responses to warming. To elucidate the role of predators, we measured the effect of these three temperature treatments on the predation rates of two common predators, the crab *Pugettia gracilis* and the sea star *Leptasterias spp*. To elucidate effects on snail reproduction, we measured *L. vincta* egg mass production, hatching time and success at these three temperatures. Snails in eelgrass treatments had higher reproductive output and produced more fecal pellets, a proxy for feeding rate, than snails in macroalgal treatments, with no significant effects of temperature. Temperature did not significantly affect predation rates on *L. vincta*. However, increased temperature did increase the mortality of egg masses. Our results suggest that *L. vincta*'s trophic interactions are generally

tolerant of moderate warming temperatures, but reproduction may be more sensitive to near-future warming with potential demographic impacts of increasing egg mortality.

4.2 INTRODUCTION

Marine communities are exposed to a variety of stresses due to climate change, including rising ocean temperatures. Current ocean temperatures have been rising, and are projected to continue to increase 2-4˚C over the next century (IPCC 2014). Temperature is an important factor with demonstrated effects on organismal physiology, fitness, and ecology. Organisms typically function on thermal performance curves where rates of biochemical and physiological processes increase with temperature up to a critical temperature, after which physiological functions become too costly to maintain and rates decline dramatically (Huey & Kingsolver 1989). As ocean temperatures increase, many marine organisms are predicted to shift their thermal performance curves upward or move beyond their critical temperatures, depending on their thermal tolerances and limits (Sinclair et al. 2016). Increased temperatures cause direct effects on organisms that include increased metabolism, higher respiration rates, faster development, and increased food consumption (McMahon & Russell-Hunter 1977, Sanford 1999, Sanford 2002, O'Connor 2009, Przeslawski 2004, Carr & Bruno 2013). These effects can manifest in diverse ways, including growth, development, and reproduction because they impact many other physiological processes. For example, increased metabolism causes increased growth due to increased consumption in some organisms, but in others increased energetic costs may outweigh increases in consumption and reduce growth (Sanford 2002, Freitas et al. 2010, Iles 2014).

Modeling and experimental studies suggest that temperature-induced organism-level effects may mediate larger changes in community structure, via altered species interactions (O'Connor et al. 2009, O'Connor et al. 2011, Carr et al. 2018). Quantifying how community interactions are affected by temperature can help illustrate how such interactions could modify marine community dynamics in response to climate change (Kordas et al. 2011, Harley et al. 2013). Temperature changes can influence the strength of food web interactions like herbivory and predation, both modifying individual organism-level responses to change and propagating effects through communities (O'Connor et al. 2009, Schiel et al 2004). For example, direct stress on a producer due to increasing temperature can be compounded by more intense grazing pressure (Vergés et al. 2014, Rothäusler et al. 2009). Alternatively, increased food or nutrient availability can offset negative impacts of environmental stress relative to food-limited organisms (Vilchis et al. 2005, Torres & Giménez 2020).

For organisms within these communities, inducible traits can influence ecological interactions (Miner et al. 2005) and may modulate responses to stress. Inducible morphologies are adaptive mechanisms that are typically triggered by relevant environmental cues but are often costly (Tollrian & Harvell 1999). Chemical cues signalling the presence of a predator can trigger an inducible defense, e.g., protective spines in bryozoans (Harvell 1984) or shell thickening in snails (Appleton & Palmer 1988). Similarly, the presence of a particular food source can trigger an inducible offense, e.g., gape size in predatory ciliates (Kopp & Tollrian 2003) or claw size in crabs (Smith & Palmer 1994). Organisms with inducible morphologies have demonstrated a range of responses to environmental stress differing between organisms with and without exposure to inducing cues (Bibby et al. 2007, Freytes-Ortiz & Stallings 2018, Seroy & Grünbaum 2018). This suggests that the adaptive advantage of inducible traits may shift based

on abiotic conditions such as temperature. For example, in the ribbed mussel *Guekensia granosissima*, predator exposure induces faster growth rates that reduce the time necessary to reach a size refuge from predation. However, high temperatures suppress these inducible growth rates, limiting their benefits in a warming world (Freytes-Ortiz & Stallings 2018). Examples like this suggest that understanding the roles of inducibility in determining responses to ocean change can provide important context for predictions of marine community responses to climate change.

The goals of this study were to quantify the relative positive and negative impacts of increased temperature on rates of interaction with both higher and lower trophic levels, and to assess the potential for interactions between temperature stresses and inducible morphologies and behaviors in an important marine grazer. To address these goals, we evaluated the trophic relationships of the marine snail, *Lacuna vincta. L. vincta* is a common and dominant grazer in low intertidal and shallow subtidal coastal eelgrass and macroalgal beds of North America (Brady-Campbell et. al 1984, Nelson & Waaland 1997, Krumhansl & Scheibling 2011). *L. vincta* is prevalent in these areas throughout the year, with significant increases in population size during the summer months (Nelson 1995, Nelson & Waaland 1997). In Washington state, shallow subtidal habitats exhibit variable temperature on tidal and seasonal scales with extremes reaching below 5˚C and above 20˚C (Ruesink 2010, O. Graham, L. Aoki & M. Eisenlord unpublished data), and surface tissue temperatures of low intertidal macroalgae when exposed at low summer tides can be significantly hotter (Van Alstyne & Olsen 2014).

In macroalgae-dominated habitats, *L. vincta* feeds directly on macroalgal tissue. In eelgrass-dominated habitats, they feed by scraping eelgrass-associated epiphytic diatoms, which are abundant only in the summer (Nelson 1995, Nelson & Waaland 1997). *L. vincta* grazes using a conveyor-belt like radula, in which new rows of teeth are continuously produced, and old worn

rows of teeth are continuously shed. *L. vincta* produces an average of 3 rows of teeth/day and has typical radula lengths of 65-100 rows of teeth (Padilla et al. 1996). *L. vincta* exhibits inducible radula morphology dependent on the dominant available food source. Diet-related chemical cues shift radula morphology from the default pointed teeth in macroalgal habitats to induced blunt teeth in eelgrass habitats (Padilla 1998, Padilla 2001, Van Alstyne et. al 2017).

L. vincta also exhibit an inducible defensive behavior, releasing themselves from their substrate to escape predators or unfavorable food environments (Martel & Diefenbach 1993). Detachment can result in transport by currents, causing snails to disperse between habitat types. Primary predators of *L. vincta* that induce escape behavior include the kelp crab *Pugettia gracilis*, sea stars in the genus *Leptasterias* (Menge 1972) and fish. Predator-induced escape behavior is initiated by voluntary foot-raising, followed by creation of mucus threads enabling snails to drift away from threats via water currents (Martel & Chia 1991a). Due to escape-driven dispersal, snails may land in a place in which their radula morphology does not match their habitat.

We experimentally explored the effects of a temperature range experienced in situ (12˚C - 20˚C), a range relevant to near-future warming conditions, on *L. vincta* trophic interactions. We measured interactions with two common food sources, by measuring reproductive output and herbivory. We measured interactions with two common predators by measuring predation rates to identify any sublethal effects of warming. We tested whether having matched or mismatched radular morphology affected snail responses to temperature. In addition, we also investigated temperature effects on *L. vincta* life history, by measuring effects of temperature stress on egg mass success.

We hypothesized that increasing temperatures would increase herbivory, but reduce reproductive output due to increased energy needed to meet higher metabolic needs. We hypothesized that habitat mismatch would exacerbate the net metabolic deficit, further reducing reproductive output. We also hypothesized that increased temperature would accelerate *L. vincta* egg development, until sustained high temperatures became too stressful for development. Finally, we hypothesized that increased temperature would increase predation rates on *L. vincta*, because predators would need to meet increased metabolic demands at higher temperatures.

4.3 METHODS

Experiment 1: Temperature effects on *L. vincta* reproductive output and feeding

Organism collection and preparation

Lacuna vincta snails were collected from macroalgal blades growing on the Friday Harbor Laboratories dock in June 2019. The sex of each snail was determined, and females were retained and transferred to laboratory tanks containing flowing ambient sea water. To establish radular morphology prior to the experiment, snails were fed either macroalgae (*Ulva lactuca*) or eelgrass (*Zostera marina*) with epiphytic diatoms for two weeks. Following Padilla et al. (1996) and Bear & Padilla (2015), *U. lactuca* was used for the macroalgae food treatment, because it is easily tractable in the laboratory and maintains or induces pointed radular morphology. Snails in different food treatments were isolated from each other to prevent cross-exposure to cues. Food was changed every two days to ensure snails were not food limited.

Experimental setup

To test effects of temperature, food and radular morphology, snails were distributed across three temperature treatments and four food treatments. Target temperatures were 12, 16 and 20˚C. We chose these temperatures to reflect a range of in situ subtidal temperatures. Although 12℃ and 16℃ are typical summer temperatures, 20℃ is at the edge of the subtidal temperature range and sustained temperatures this high would likely be more reflective of a near-future warming scenario. Within these temperature treatments, snails were assigned to the following food treatments: *macroalgae matched* (snails with macroalgal radula morphology consuming macroalgae), *macroalgae mismatched* (snails with macroalgal radula morphology consuming eelgrass epiphytes), *eelgrass matched* (snails with eelgrass radula morphology consuming eelgrass epiphytes) and *eelgrass mismatched* (snails with eelgrass radula morphology consuming macroalgae). We replicated each treatment four times using a total of 96 snails.

To create these treatment conditions, a flow-through seawater system was established using four 54-quart plastic tubs nested across two large sea tables. One tub served as a header tank which received incoming filtered sea water. The other three served as water baths to create target temperature treatments. Water baths consisted of fresh water that was either cooled using a chiller (12˚C treatment) or heated using an aquarium heater (16 and 20˚C treatments) to maintain target temperatures. Water bath positions in sea tables were rotated every three days throughout the duration of the experiment such that each water bath experienced all locations, to control for potential location effects. Each water bath tub contained eight ¾ quart buckets that received seawater continually pumped from the header tub. Buckets were partially submerged in the bath water to enable the incoming seawater to reach target temperatures. Each bucket had its own outflow line to which directed overflow water to the exterior of the tub, to maintain water height and prevent bucket overflow. Buckets had equal flow rates with a seawater residence time of

roughly 20 minutes. Each bucket was bubbled with air to ensure mixing and temperature consistency within a bucket.

Within temperature treatment tubs, four buckets were designated as macroalgae food treatment replicates and the other four buckets were designated as eelgrass food treatment replicates. Each bucket contained two 4oz plastic containers with 330 μm mesh windows. One mesh container held snails with a prior diet that matched the bucket food treatment and the other mesh container held snails with an opposite prior diet to the bucket food treatment. Each mesh container held two snails. Mesh containers were rotated across buckets of the same food and temperature conditions every two days to control for potential bucket effects. See Appendix C Figure S1 for diagram of the experimental setup.

Experimental methods

Snails were acclimated to temperature treatments for two days prior to initiation of the 14-day experiment. Water temperature was recorded twice a day using a Fluke 16 temperature probe. Snails were measured (mean shell length = 6.41 mm, sd =1.19 mm) and distributed evenly across temperature treatments by size. During this period, snails consumed food that matched their prior food condition. After the acclimation period, snails were placed into their assigned food treatments, and food sources were switched if required by the diet treatment. During the acclimation period and experimental duration, snails in all food treatments were fed the same surface area of food. For macroalgae treatments, snails were fed 5 cm x 5 cm squares of *U. lactuca*. For eelgrass treatments, snails were fed five 1 cm x 5 cm *Z. marina* strips that were densely covered in epiphytes. *U. lactuca* and *Z. marina* were collected off the FHL dock or from a nearby subtidal site. Food was changed every two days and food quantities ensured that snails

were not food limited. Mesh cages were rinsed of fecal material daily. Any dead snails were removed from treatments. Mesh cages were also rotated between buckets of replicate food and temperature treatments every two days to control for potential bucket effects.

Snail reproductive output throughout the experiment was quantified by monitoring the production of egg masses in each mesh container every two days. Egg masses were removed and photographed with a Lumenera Infinity 2 microscope camera. Egg mass area was measured in ImageJ from photographs. Total egg mass area produced by snails in each mesh cage was calculated for the duration of the experiment to compare reproductive output across treatments.

Fecal pellet production was used as a proxy to quantify food consumption in treatments. Fecal pellets produced during a 24-hour period were quantified after 1 day, 8 days and 14 days of the experiment. Mesh containers were rinsed out to collect fecal pellets on 330 μm mesh and pellets were counted under a dissecting microscope.

Statistics

Differences in reproductive output were assessed using a two-way ANOVA with fixed factors of temperature and diet treatment. Differences in fecal pellet production for each time point were also assessed using a two-way ANOVA with fixed factors of temperature and diet treatment. Data for both reproductive output and fecal pellet production were square-root transformed to meet the homogeneity of variances assumption. We tested for homogeneity of variances using a Levene's Test (car Library in R). Pairwise differences between treatments were assessed with a Tukey's HSD post hoc test. All statistics were done in R version 3.6.1 (R Core Team 2019) and ANOVA tables are presented in the Appendix C.

Egg mass area regression

To establish that egg mass area was a valid metric for assessing reproductive output, we quantified the relationship between egg mass area and the number of eggs contained within egg masses. We collected 50 egg masses across a broad size range that were laid by snails in the laboratory. Egg masses were imaged to measure area, then opened using a scalpel and flattened onto a microscope slide to view individual eggs. Opened egg masses were imaged and eggs were counted in ImageJ using the cell counter plugin. We then calculated a regression between egg mass size and number of eggs.

Experiment 2: Temperature effects on *L. vincta* egg development time

Eggs laid during Experiment 1 were collected and monitored in the temperature treatments in which they were laid to determine hatching time and success. The same temperature treatments setup was used as in Experiment 1. Temperatures were recorded twice a day. We collected and monitored eggs in cohorts laid every two days. The first cohort was collected between the fourth and sixth day of Experiment 1 and cohort collection continued every two days until the completion of Experiment 1. Only egg masses that were laid on a substrate (eelgrass or macroalgae) were followed through the experiment; others, e.g. those laid on aquarium walls, were removed. Substrates were cut to just the area surrounding the egg mass and epiphytes on eelgrass blades were removed to prevent any cue chemical contamination. Once egg masses were collected from the mesh containers that housed snails, each egg mass was transferred to small egg holders where it could be isolated and monitored. Egg holders were made from thinly sliced ¾” tubing that was covered with 1 mm mesh to enable water flow. Egg holders were hung with clothespins from bucket edges in the temperature treatments the egg

mass was laid in. Egg masses were rotated haphazardly around buckets to control for potential bucket effects. Egg masses were checked daily to determine the day of hatching. Egg masses were classified as hatched once the gelatinous egg mass case had broken open completely. If egg masses remained unhatched after 14 days, they were checked for mortality. Mortality was confirmed by inspection under a dissection scope to look for larval movement within the egg mass.

Statistics

Differences in hatching time across treatments were assessed using a two-way ANOVA with fixed factors of temperature and substrate. We confirmed homogeneity of variances using a Levene's Test (car Library in R) before proceeding with the ANOVA. We also assessed whether egg mass size influenced hatching time using a linear regression. Statistical tables are presented in Appendix C.

Experiment 3: Temperature effects on predation rates on *L. vincta*

We assessed the predation rates on *L. vincta* by two common predators (the kelp crab, *Pugettia gracilis*, and the sea star, *Leptasterias spp.*) using the same temperature treatments as Experiments 1 and 2. Instead of using eight buckets per temperature water baths, the set up was replumbed with larger buckets such that each temperature treatment had four buckets. This was done to accommodate the increased space needed for predators. Each large bucket held two smaller containers with 1mm mesh windows for water exchange to house predators and snail prey.

Thirty of each predator type were collected from Cattle Point, San Juan Island and maintained in ambient seawater conditions for up to 7 days prior to being placed in experimental treatments. Predators were measured with digital calipers to distribute them roughly evenly across temperature treatments. Crabs were measured using distance between lateral carapace teeth, (mean = 16.46 mm, sd = 4.71 mm) and sea star length was measured using the longest arm tip to arm tip (mean = 41.01 mm, sd = 8.67 mm). *L. vincta* snails for predation experiments (shell length mean = 5.87 mm, sd = 1.40 mm) were collected from various sites around San Juan Island (Merrifield Cove, Cattle Point False Bay and Friday Harbor). To control for possible size preferences of predators, snails were assigned to small containers within buckets, such that all containers had a roughly similar mean snail size. Ten replicates of each treatment were conducted.

Predators were starved in their respective temperature treatments for 28 hours prior to receiving prey. Ten snails were then added to each container to be consumed by predators. Crabs were given two hours to feed, and sea stars were given three hours to feed. After the feeding period, the number of snails consumed was counted, and the remaining snails were measured to determine which snail sizes predators had consumed. Snails that were in a sea star's mouth or arms were scored as consumed.

Statistics

A series of generalized linear models were created to examine the effect of temperature and predator type on the number of snails consumed. Generalized linear models used a Poisson distribution, which is appropriate for count data, and tested fixed effects of predator type and temperature. Models were compared and AIC was used to determine the best model. We also

tested whether the snail sizes consumed differed across temperature treatments and predator types using a two-way ANOVA, and whether predator size covaried with snail size consumed for each predator type using an ANCOVA. We confirmed homogeneity of variances (using the car library in R) for snail size data prior to running ANOVA and ANCOVA tests. Statistical tables are presented in Appendix C.

4.4 RESULTS

Experiment 1: Reproductive output and fecal pellet production

Reproductive output

We found a significant relationship between *L. vincta* egg mass size and the number of eggs contained ($R^2 = 0.785$, Figure 4.1a, Appendix C Table S1.1), which justified the use of egg mass size as a proxy for reproductive output. We calculated reproductive output as the total area of all egg masses produced in each container over the two-week experimental duration divided by the number of surviving adult snails in each container. Mortality in the treatments was low with only 6 of 96 snails dying throughout the two-week exposure. No snails died in 12˚C treatments, two snails died in 16˚C treatments (both in macroalgae mismatched food treatments), and four snails died in 20˚C treatments (one in macroalgae match, one in eelgrass mismatch and two in eelgrass match food treatments). These mortality events were not significantly affected by temperature ($p = 0.16$, Fisher exact test). *R*eproductive output (mean = 15.02 mm^2, sd = 13.91 mm^2, n = 48) was significantly affected by diet treatment ($p < 0.0001$, Two-way ANOVA), but not by temperature ($p = 0.910$) or diet-temperature interactions ($p = 0.663$) (Figure 4.1b, Appendix C Table S1.2). Reproductive output was highest in the eelgrass match treatment and

lowest in the macroalgae match treatment, with intermediate reproductive output in both mismatch treatments. A Tukey's HSD post hoc test indicated significant differences between all diet treatments except between both mismatch treatments ($p = 0.896$, Appendix C Table S1.3).

Fecal pellet production

We found significant effects of diet ($p < 0.0001$, two-way ANOVAs), but not temperature, on *L. vincta* fecal pellet production at all three time points (Figures 4.1c-e, Appendix C Tables S1.4, S1.6 and S1.8). Snails in eelgrass treatments consistently produced more fecal pellets than those in macroalgal treatments throughout the duration of the experiment. In eelgrass treatments, fecal pellet production was significantly higher in the matched treatment than in the mismatched treatment ($p < 0.0001$, Tukey's HSD, Appendix C Table S1.5) only at the first time point. However, there were no significant differences between eelgrass matched and mismatched treatments at time point 2 ($p = 0.9744$, Tukey's HSD, Appendix C Table S1.7) and 3 ($p = 0.09661$, Tukey's HSD, Appendix C Table S1.9). At all three time points, fecal production was lowest in macroalgal treatments, with no significant difference between macroalgal matched and mismatched treatments throughout the duration of the experiment (Appendix C Tables S1.5, S1.7, S1.9).

Experiment 2: Egg mass development

We collected four cohorts of eggs masses, each laid two days apart. We followed the subset of egg masses that met the criteria of being laid on a substrate, which comprised 62 out of 137 total egg masses laid during that time. We observed 39% mortality of egg masses across all treatments. On both substrate types, egg mortality increased at higher temperatures, with

substantially high mortality rates of nearly 50% on both substrate types at 20˚C (Figure 4.2b). Among eggs that hatched (mean hatching time = 11.76 d, sd = 2.07 d, n=38), we found a significant interaction of substrate and temperature on hatching time (p=0.008, two-way ANOVA, Appendix C Table S2.1, Figure 4.2a). The only significant difference in hatching time between substrate types was at 20˚C, with faster hatching on macroalgal substrates (p = 0.002, Tukey post-hoc test, Appendix C l Table 2.2). There was no relationship between egg mass area and hatching time, suggesting that size was not a confounding factor (R^2 = 0.042, p = 0.112, Appendix C Figure S2 and Table 2.3).

Experiment 3: Predation rates

Snail consumption by both crab and sea star predators was unaffected by temperature within the range we measured (Figure 4.3a, Appendix C Tables 3.1 and 3.2). Crabs consumed more snails than sea stars (p < 0.001, GLM with Poisson distribution). Crabs and sea stars consumed similarly sized snails (mean = 5.60 mm, sd = 1.18 mm, n = 102, Figure 4.3b), with no significant difference in the size consumed by either predator (p = 0.460, two-way ANOVA, Appendix C Table 3.3). The size of snails consumed was not significantly affected by temperature (p = 0.323, two-way ANOVA). We found no significant relationship between predator size and snail size consumed (p = 0.396, ANCOVA, Figure 4.3c, Appendix C Table 3.4) or number of snails consumed (crabs: p = 0.428, stars: p = 0.309, GLM with Poisson distribution) for either predator type.

4.5 DISCUSSION

Modeling and experimental studies have suggested temperature-induced changes in community structure are mediated by effects at the organism level (O'Connor et al 2009, O'Connor et al. 2011, Carr et al. 2018), emphasizing the potential insights to be gained from quantifying both direct effects of temperature on organisms and propagating effects on interactions within these communities. We set out to determine whether temperature effects on trophic interactions of an important marine grazer, *L. vincta*, suggest major impacts on food web dynamics in temperate shallow subtidal communities. We found these trophic interactions, and the role of inducible morphologies, to be generally robust across the temperature range we measured, but we identified potential demographic vulnerabilities in temperature-dependence of *L. vincta* egg mass survival.

No observed temperature effects on trophic interactions in *L. vincta*

Marine organisms of diverse taxa have demonstrated sensitivities to warming, including increases in respiration, metabolism, feeding rates, and changes in energy allocation (McMahon & Russell-Hunter 1977, Sanford 1999, Sanford 2002, O'Connor 2003, Carr & Bruno 2013). We hypothesized that higher temperatures would increase herbivory but reduce reproductive output due to increased energetic requirements to satisfy higher metabolic costs, and increase predation rates on *L. vincta* due to increased predator metabolism. Contrary to our hypotheses, we found no significant effects of temperature on *L. vincta* trophic interactions. *L. vincta* reproductive output, fecal pellet production, and rates of predation by two common predators all remained unaffected by temperature across the range we tested.

What underlies the observed robustness of *L. vincta* trophic interactions to moderate increases in temperature? Organisms from fluctuating environments have often demonstrated an increased capacity to manage environmental stress, including warming temperatures, because of their large thermal tolerances (reviewed in Boyd et al. 2016, Marshall & McQuaid 2011). *L. vincta* and its predators inhabit low intertidal and shallow subtidal environments that are thermally variable on daily cycles due to tides, seasonal timescales, and spatial scales where snails may find refuges from short-term extremes. Because of this transient and episodic warming, these organisms have a wide temperature tolerance range. Our temperature treatments were within the range of in situ transient temperature fluctuations and below 27.3˚C, the previously determined lethal thermal thresholds for *L. vincta* in northern Washington (Jurgens and Gaylord, 2018). Instead of studying the effects of temperature extremes, we chose to investigate the effects of moderate but sustained temperature increases, such as those most relevant to near-future projections. Therefore, our results are most applicable to more immediate near-future conditions and not longer-term warming conditions.

L. vincta may display sensitivities to temperature that were masked by other factors in our experiments, such as an unlimited food supply, or that were expressed by metrics we did not measure in our study. A previously established thermal performance curve for *L. vincta* showed respiration rate increased with temperature, peaking at 25˚C (McMahon & Russell-Hunter 1977). This peak is above the maximum temperature used in our experiments, suggesting that we did not expose *L. vincta* to stress associated with their critical temperature. Though we did not measure biochemical or physiological traits that are typically more tightly coupled with temperatures, the cumulative effects we measured are ecologically relevant. Because *L.vincta* has a large thermal range, perhaps snails were able to maintain functions that we measured across a

broad temperature range, especially given that they were not limited by food. Several prior studies have demonstrated that abundant food resources can offset negative effects of environmental stress, such as warming and acidification, with organisms demonstrating the ability to maintain growth and other processes if they are not food limited (Vilchis et al. 2005, Thomsen et al. 2013, Pansch et al. 2014, Ramajo et al. 2016). Our study suggests that community dynamics models parameterized using present-day biological rates appear largely applicable to climate change impact predictions, with the exception of reproductive potential which is significantly reduced by increased egg mass mortality.

Diet and radula morphology effects

Broadly, our study identified eelgrass epiphytes to be a higher quality food source than *U. lactuca* for *L. vincta* snails. Reproductive output was consistently higher in treatments where snails were fed eelgrass epiphytes over the range of temperatures we tested. Fecal pellet production was also higher in eelgrass treatments suggesting that snails were eating higher quantities of food in these treatments. We found this food source to support higher reproductive output likely because epiphytic diatoms are highly nutritious for gastropods (Hayakawa et al. 2010).

We hypothesized that reproductive output and fecal pellet production would be reduced for snails that were mismatched with the food treatment in which they formed their radula. Generally, fecal pellet production was not reduced by mismatches for either food source. Snails were not food-limited so this suggests that rates of herbivory among food treatments remained the same. While we did observe reduced reproductive output in mismatched snails that consumed eelgrass epiphytes, mismatched snails in macroalgae treatments did not exhibit the same effect.

In fact, mismatched snails that consumed macroalgae had higher reproductive output than those that were matched (supported by DK Padilla, unpublished data). This suggests a higher nutritional status in mismatched snails that consumed macroalgae, presenting a possible hypothesis that blunt eelgrass teeth are more efficient than pointed macroalgae teeth in consuming highly nutritious components of food sources, rather than indigestible components, because egg production is higher. Additionally, previously consumed epiphytes may have provided short-term energy reserves sufficient to support higher reproduction of mismatched snails despite unchanged rates of herbivory.

However, an outstanding question from our work remains: if blunt teeth are more efficient, even in mismatched situations, why do snails not make them all the time? It is possible that there is a cost to this inducible morphology, but we did not observe it because we used *U. lactuca* as our macroalgal food source, which is thinner and easier to consume than tougher kelps like *Saccharina latissima* and *Nereocystis luetkeana,* which may have better elicited the benefits of the default pointed morphology. Though *U. lactuca* was more experimentally tractable than kelp, has been used in previous studies, and induces the macroalgal radula morphology (DK Padilla, unpublished data), it may have not enabled us to generalize the effects to common kelps on which *L. vincta* also feeds. While *U. lactuca* is a common substrate and food source for *L.vincta*, consumption of *Saccharina latissima* induces higher snail growth rates, suggesting it may be a more nutritious food source (Chavanich & Harris 2002). Therefore, we hypothesize that pointed macroalgal teeth may be superior for food sources with tougher tissues.

Implications of *L. vincta* egg development results

We observed increases in egg mortality with increasing temperature, suggesting potential demographic impacts on *L.vincta* populations with warming. This is consistent with prior studies that have demonstrated that early life stages are most vulnerable to environmental stress (Pandori & Sorte 2019, Byrne & Przeslawski 2013). We also observed that egg masses laid on *U. lactuca* in the highest temperature treatment had the fastest mean time to hatching, suggesting either that higher temperatures accelerated hatching, or that egg masses with longer hatching times could not survive sustained high temperatures and died. This is also consistent with prior studies showing moderate temperature increases can accelerate development times (Przeslawski 2004). Vulnerability of *L. vincta* egg masses to sustained temperature increases, potentially creating a reproductive bottleneck for the population at this life stage in a warming world, warrants further investigation under more realistic field conditions. Investigating larval performance across this temperature range would also be informative to identify other potential vulnerabilities at early life stages.

There are some limitations in the interpretation of the egg monitoring part of our study. We observed a difference in development time that was dependent on substrate at 20˚C. At this temperature, egg masses on eelgrass did not exhibit accelerated hatching times like those on macroalgae. We noted that after several days, eelgrass substrates had decayed significantly, which could have reduced oxygen availability locally for egg masses. Oxygen limitation has been shown to lengthen development times for gastropod eggs (Strathmann & Strathmann 1995, Przeslawski, 2004). Oxygen for *Lacuna spp.* egg masses is mainly supplied by photosynthesis of the host tissue (Woods & Podolsky 2007), and if eelgrass substrates in our study were not photosynthesizing sufficiently, this could have reduced oxygen availability and extended development time in the highest temperature treatment. Our sample size was also reduced due to

39% mortality of egg masses overall, and to the fact that we limited our measurements to egg masses laid on the food substrate. In future studies, removing egg masses from substrates, or using egg masses on plastic substrates, would avoid these possible confounding factors.

Community-level implications

L. vincta interactions did not exhibit negative responses across the temperature range we tested, suggesting that *L. vincta* may be well-positioned to tolerate near-future warming conditions. The nutritional value of a variety of *L. vincta* food sources has been shown to be unaffected by moderate temperature increases, supporting similar snail growth, reproduction, and survival up to 21˚C (Simonsen et al. 2015b). Therefore, grazing pressure applied by *L. vincta* may remain unchanged as well under near-future warming conditions. However, given the lack of temperature effects observed in *L. vincta*, there still may be community-level impacts of these findings depending on the responses of lower trophic levels to warming. Some kelp species that are common *L. vincta* substrates exhibit reduced growth and rapid deterioration in response to short- and long-term warming (Schiel et al. 2004, Simonsen et al. 2015a), and eelgrass beds are increasingly vulnerable to diseases that tend to be more prevalent at higher temperatures (Dawkins et al. 2018). Increasing temperatures can also exacerbate existing grazing damage to some macroalgae by accelerating the degradation of tissue, further increasing the likelihood of breakage due to water flow (Rothäusler et al. 2009).

Alternatively, other common *L. vincta* substrates like the alga *Sargassum muticum* have not exhibited vulnerabilities to rising temperatures. *S. muticum* is non-native but common along the Washington coast and thrives at temperatures above 20°C (Norton 1977, Britton-Simmons et al. 2011). Therefore, the propagating community-level effects may be highly dependent on

substrate, and it may be possible that more tolerant macroalgae like *S. muticum* will continue to support robust *L. vincta* populations under near-future warming conditions. Our results can be viewed in this community framework to identify both vulnerable and robust ecological links with potential effects within a variety of *L. vincta* habitats

Though our experimental work suggests that *L. vincta* may be a potential "winner" in warming world, *L. vincta* interactions have shown sensitivities to acidification and hypoxia (Young & Gobler 2020), and thus future work should consider combinations of stressors that might also affect the interactions we studied. Future studies could also investigate effects of food limitation on the interactions we observed and measurements of physiological responses that could help contextualize our results.

4.6 ACKNOWLEDGEMENTS

Kim Stewart and Anik Mutsuddy contributed greatly to this work through their experiments on egg development and predation rates. We like to thank Dianna Padilla for lab equipment and advice, Ann Stanbrough, Alyssa Liguori, Katie Dobkowski, Molly Roberts, Maria Rosa, Olivia Graham and Abigail Ames for lab and organism collection assistance, Robert Levine, and Amy Wyeth for help with data interpretation and experimental design. We would also like to thank Salish Sea Sciences summer program high school students and Doris Duke Conservation Scholars undergraduates Jackelyn Garcia and Tino Hampton-Medina for help with pilot studies.

References

Appleton RD, Palmer AR (1988) Water-borne stimuli released by predatory crabs and damaged prey induce more predator-resistant shells in a marine gastropod. P Nat Acad Sci USA 85: 4387-4391

Bear Magallanes SE, Padilla DK (2015) Predator-prey interactions of *Pugettia gracilis* (Dana, 1851) and *Leptasterias spp.*(Verrill, 1866) and two species of *Lacuna* (Turton, 1827). REU thesis, Friday Harbor Laboratories, University of Washington, Friday Harbor, WA.

Bibby R, Cleall-Harding P, Rundle S, Widdicombe S, Spicer J (2007) Ocean acidification disrupts induced defenses in the intertidal gastropod Littorina littorea. Biol Letters 3:699-701

Boyd PW, Cornwall CE, Davison A, Doney SC and others (2016) Biological responses to environmental heterogeneity under future ocean conditions. Glob Change Biol 22:2633-2650

Brady-Campbell MM, Campbell DB, Harlin MM (1984) Productivity of kelp (*Laminaria* spp.) near the southern limit in the northwestern Atlantic Ocean. Mar Ecol Prog Ser 18:79-88

Britton-Simmons KH, Pister B, Sánchez I, Okamoto D (2011) Response of a native, herbivorous snail to the introduced seaweed *Sargassum muticum*. Hydrobiologia, 661:187-196

Byrne M, Przeslawski R (2013) Multistressor impacts of warming and acidification of the ocean on marine invertebrates' life histories. Integr Comp Biol 53:582-596

Carr LA, Bruno JF (2013) Warming increases the top-down effects and metabolism of a subtidal herbivore. PeerJ 1:e109

Carr LA, Gittman RK, Bruno JF (2018) Temperature influences herbivory and algal biomass in the Galápagos Islands. Front Mar Sci 5:279

Chavanich S, Harris LG (2002) The influence of macroalgae on seasonal abundance and feeding preference of a subtidal snail, *Lacuna vincta* (Montagu)(Littorinidae) in the Gulf of Maine. J Mollusc Stud, 68:73-78

Dawkins PD, Eisenlord ME, Yoshioka RM, Fiorenza E and others (2018) Environment, dosage, and pathogen isolate moderate virulence in eelgrass wasting disease. Dis Aquat Org 130:51-63

Freitas V, Cardoso JF, Lika K, Peck MA and others (2010) Temperature tolerance and energetics: a dynamic energy budget-based comparison of North Atlantic marine species. Philos T R Soc B 365:3553-3565

Hayakawa J, Kawamura T, Ohashi S, Horii T, Watanabe Y (2010) Importance of epiphytic diatoms and fronds of two species of red algae as diets for juvenile Japanese turban snail *Turbo cornutus*. J Shellfish Res 29:233-240

Harvell CD (1984) Predator-induced defense in a marine bryozoan. Science 224:1357–1359

Huey RB, Kingsolver JG (1989) Evolution of thermal sensitivity of ectotherm performance. Trends Ecol Evol 4:131-135

Iles AC (2014) Toward predicting community-level effects of climate: Relative temperature scaling of metabolic and ingestion rates. Ecology 95: 2657-2668

IPCC (2014) Climate change 2014: synthesis report. In: Core Writing Team, Pachauri RK, Meyer LA (eds) Contribution of working groups I, II and III to the fifth assessment report of the intergovernmental panel on climate change. IPCC, Geneva, p. 151

Jurgens LJ, Gaylord B (2018) Physical effects of habitat-forming species override latitudinal trends in temperature. Ecol Lett 21:190-196

Krumhansl KA, Scheibling RE (2011) Spatial and temporal variation in grazing damage by the gastropod *Lacuna vincta* in Nova Scotian kelp beds. Aquat Biol 13:163-173

King W, Sebens KP (2018) Non-additive effects of air and water warming on an intertidal predator–prey interaction. Mar Biol 165:64

McMahon RF, Russell-Hunter WD (1977) Temperature relations of aerial and aquatic respiration in six littoral snails in relation to their vertical zonation. Biol Bull 152:182-198

Marshall DJ, McQuaid CD (2011) Warming reduces metabolic rate in marine snails: adaptation to fluctuating high temperatures challenges the metabolic theory of ecology. Proc R Soc B 278: 281-288

Martel A, Diefenbach T (1993) Effects of body size, water current and microhabitat on mucous-thread drifting in post-metamorphic gastropods *Lacuna* spp Mar Ecol Prog Ser 99:215-215

Miner BG, Sultan SE, Morgan SG, Padilla DK, Relyea RA (2005) Ecological consequences of phenotypic plasticity. Trends Ecol Evol 20:685-692

Nelson TA (1995) Interactions and dynamics of eelgrass (*Zostera marina L.*) epiphytes, and grazers in subtidal meadows of Puget Sound. Dissertation. University of Washington, Seattle, WA

Nelson TA, Waaland JR (1997) Seasonality of eelgrass, epiphyte, and grazer biomass and productivity in subtidal eelgrass meadows subjected to moderate tidal amplitude. Aquat Bot 56:51-74

Norton TA (1977) The growth and development of *Sargassum muticum* (Yendo) Fensholt. J Exp Mar Biol Ecol 26:41-53

Pandori LL, Sorte CJ (2019) The weakest link: sensitivity to climate extremes across life stages of marine invertebrates. Oikos 128:621-629

Pansch C, Schaub I, Havenhand J, Wahl M (2014) Habitat traits and food availability determine the response of marine invertebrates to ocean acidification. Glob Change Biol 20:765-777

O'Connor MI (2009) Warming strengthens an herbivore–plant interaction. Ecology 90:388-398.

O'Connor MI, Piehler MF, Leech DM, Anton A, Bruno JF (2009) Warming and resource availability shift food web structure and metabolism. PLOS Biol 7:e1000178

O'Connor MI, Gilbert B, Brown CJ (2011) Theoretical predictions for how temperature affects the dynamics of interacting herbivores and plants. Am Nat 178:626-638

Padilla DK, Dittman DE, Franz J, Sladek R (1996) Radular production rates in two species of *Lacuna* Turton (Gastropoda: Littorinidae). J Mollusc Stud 62:275-280

Padilla DK (1998) Inducible phenotypic plasticity of the radula in Lacuna (Gastropoda: Littorinidae). Veliger 41:201-204

Padilla DK (2001) Food and environmental cues trigger an inducible offense. Evol Ecol Res 3: 15-25

Przeslawski R (2004) A review of the effects of environmental stress on embryonic development within intertidal gastropod egg masses. Molluscan Res 24:43-63

R Core Team (2019). R: a language and environment for statistical computing. R Foundation for Statistical Computing, Vienna. www.r-project.org

Ramajo L, Pérez-León E, Hendriks IE, Marbà N and others (2016) Food supply confers calcifiers resistance to ocean acidification. Sci Rep 6:1-6

Rothäusler E, Gómez I, Hinojosa IA, Karsten U, Tala F, Thiel M (2009) Effect of temperature and grazing on growth and reproduction of floating *Macrocystis spp.*(phaeophyceae) along a latitudinal gradient. J Phycol 45:547-559

Ruesink JL, Hong JS, Wisehart L, Hacker SD, Dumbauld BR, Hessing-Lewis M, Trimble AC (2010) Congener comparison of native (*Zostera marina*) and introduced (*Z. japonica*) eelgrass at multiple scales within a Pacific Northwest estuary. Biol Invasions 12:1773-1789

Sanford E (1999) Regulation of keystone predation by small changes in ocean temperature. Science 283:2095–2096

Sanford E (2002) The feeding, growth, and energetics of two rocky intertidal predators (*Pisaster ochraceus* and *Nucella canaliculata*) under water temperatures simulating episodic upwelling. J Exp Mar Biol Ecol 273:199-218

Schiel DR, Steinbeck JR, Foster MS (2004) Ten years of induced ocean warming causes comprehensive changes in marine benthic communities. Ecology 85:1833-1839

Simonson EJ, Scheibling RE, Metaxas A (2015a) Kelp in hot water: I. Warming seawater temperature induces weakening and loss of kelp tissue. Mar Ecol Prog Ser 537:89-104

Simonson EJ, Metaxas A, Scheibling RE (2015b) Kelp in hot water: II. Effects of warming seawater temperature on kelp quality as a food source and settlement substrate. Mar Ecol Prog Ser 537:105-119

Sinclair BJ, Marshall KE, Sewell MA, Levesque DL and others (2016) Can we predict ectotherm responses to climate change using thermal performance curves and body temperatures? Ecol Lett 19:1372-1385

Smith LD, Palmer AR (1994) Effects of manipulated diet on size and performance of brachyuran crab claws. Science 264:710-712

Strathmann RR, Strathmann MF (1995) Oxygen supply and limits on aggregation of embryos. Mar Biol Assoc UK, 75:413-428

Thomsen J, Casties I, Pansch C, Körtzinger A, Melzner F (2013) Food availability outweighs ocean acidification effects in juvenile Mytilus edulis: laboratory and field experiments. Glob Change Biol 19:1017-1027

Tollrian R, Harvell CD (1999) The ecology and evolution of inducible defenses. Princeton University Press, Princeton, NJ

Torres G, Giménez L (2020) Temperature modulates compensatory responses to food limitation at metamorphosis in a marine invertebrate. Funct Ecol 34:1564-1576

Van Alstyne KL, Olson TK (2014) Estimating variation in surface emissivities of intertidal macroalgae using an infrared thermometer and the effects on temperature measurements. Mar Biol 161:1409-1418

Van Alstyne KL, Padilla DK, Chan M, Yee AK (2017) Do dietary chemical signals cue an inducible offense? Society for Integrative and Comparative Biology, Jan 2017, New Orleans, LA. Abstract 119-5.

Vilchis LI, Tegner MJ, Moore JD, Friedman CS, Riser KL, Robbins TT, Dayton PK (2005) Ocean warming effects on growth, reproduction, and survivorship of southern California abalone. Ecol Appl 15:469-480

Vergés A, Steinberg PD, Hay ME, Poore AGB and others (2014) The tropicalization of temperate marine ecosystems: climate-mediated changes in herbivory and community phase shifts. Proc R Soc B 281: 20140846

Woods HA, Podolsky RD (2007) Photosynthesis drives oxygen levels in macrophyte-associated gastropod egg masses. Biol Bull 213:88-94

Young CS, Gobler CJ (2020) Hypoxia and acidification, individually and in combination, disrupt herbivory and reduce survivorship of the gastropod, *Lacuna vincta*. Front Mar Sci 7:785

Figure 4.1 Results from Experiment 1 on the effects of temperature and diet on reproductive output and feeding in *L. vincta*. (a) Regression analysis to establish that measuring egg mass area is a good proxy for the reproductive output. (b) Total egg mass area per snail summed over the course of the two-week experiment, EG = Eelgrass food treatment, MA = Macroalgae food treatment. (c-e) Fecal pellets produced per snail over a 24-hour period at three time points over the course of the two-week experiment. Error bars denote standard error.

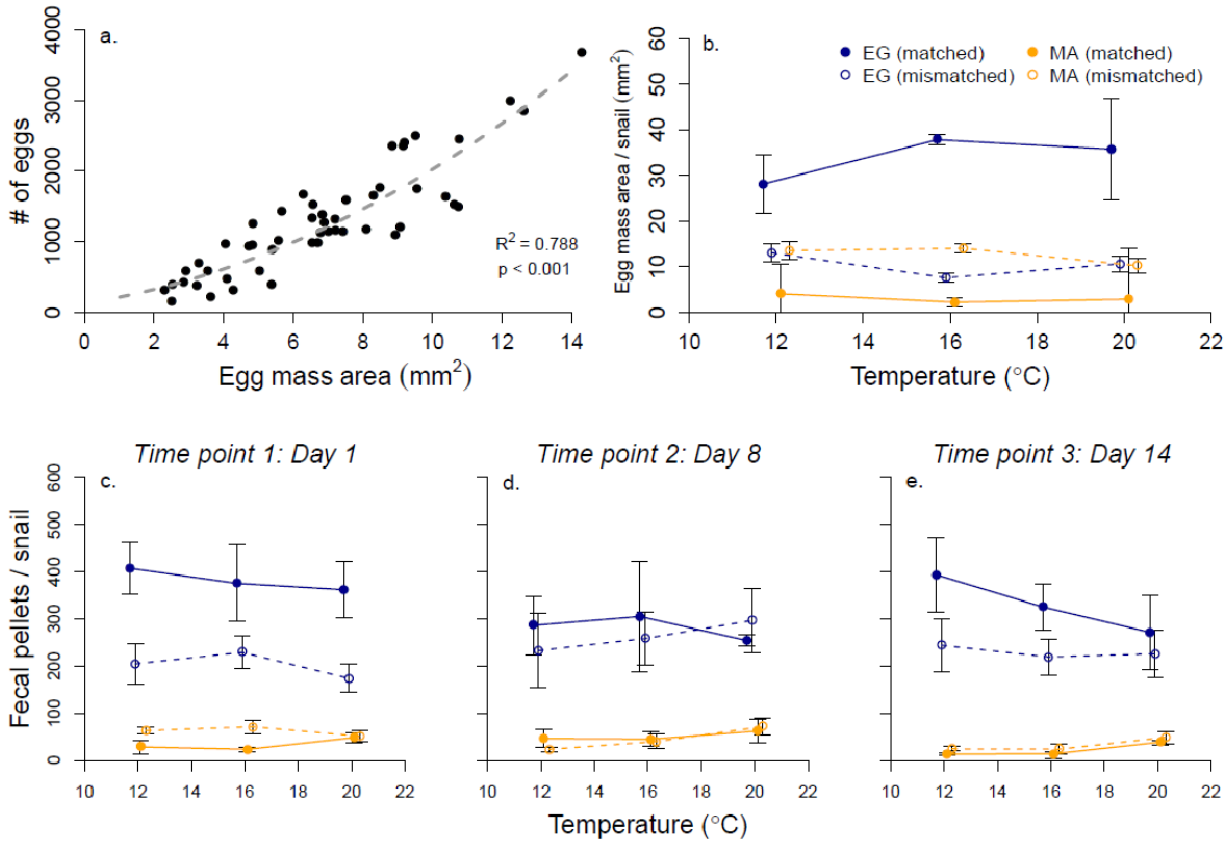

Figure 4.2 Results from Experiment 2 on effects of temperature and substrate on *L. vincta* egg development. (a) Hatching times of the egg masses by substrate and temperature treatment. Error bars denote standard error. (b) Egg mass mortality by temperature and substrate.

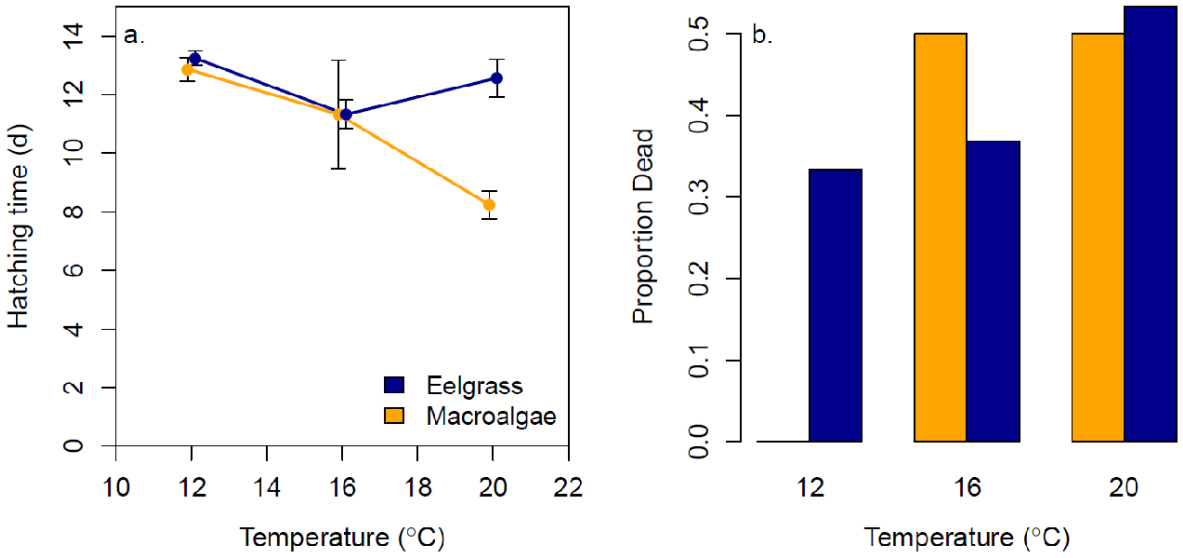

Figure 4.3 Results from Experiment 3 on effects of temperature on predation rates on *L. vincta*. (a) Number of snails eaten by the sea star, *Leptasterias spp.*, and the kelp crab, *Pugettia gracilis*, in different temperature treatments. (b) Comparison of the size of snails consumed by predator type across temperature treatments. (c) Size of predators vs. the size of the prey consumed showing no significant relationship between predator size and prey size. Dark colored symbols denote snails that were consumed by predators. Light colored symbols denote snails that were available to predators but were not consumed. Error bars denote standard error.

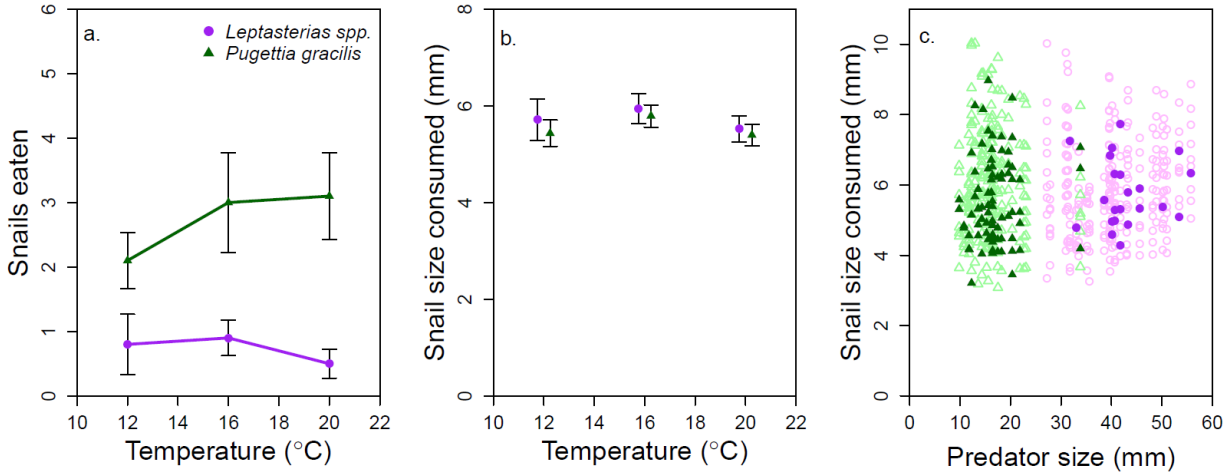

Table 4.1 Target vs. actualized temperature in treatments (mean ± sd) in buckets for each of the three experiments conducted.

Target temperature	Food treatment	Experiment 1	Experiment 2	Experiment 3
12˚C	Macroalgae	11.93 ± 0.30	11.86 ± 0.25	12.18 ± 0.27
	Eelgrass	11.81 ± 0.30		
16 ˚C	Macroalgae	15.80 ± 0.65	15.86 ± 0.68	16.48 ± 0.42
	Eelgrass	15.82 ± 0.55		
20 ˚C	Macroalgae	19.86 ± 0.76	19.88 ± 0.90	20.13 ± 0.67
	Eelgrass	19.63 ± 0.71		

Chapter 5. INDUCIBLE MORPHOLOGY REVEALS ADULT DISPERSAL BETWEEN HABITATS IN A MARINE SNAIL

5.1 ABSTRACT

The marine snail, *Lacuna vincta,* exhibits inducible radula morphology dependent on food source. These snails produce pointed teeth in macroalgal habitats and blunt teeth in response to chemical cues from epiphytes in eelgrass beds. Inducible morphology provides a record of an individual's habitat history. *L. vincta* adults exhibit drifting behavior resulting in dispersal to a habitat that does not match a snail's radula morphology. Though only seasonally available, eelgrass epiphytes promote high snail reproductive output and feeding rates. We used the interaction between individual-level inducibility and dispersal behavior to determine population-level characteristics of *L. vincta* in two eelgrass and two macroalgae sites around San Juan Island, WA. Snails were collected during summer low tides and dissected to extract radulae. Radulae were then classified by tooth type as matched, transitioning or mismatched to their current habitat. We used sequences of tooth types in radulae to parametrize a Markov chain to quantify snail retention and dispersal probabilities in both habitat types. To explore possible controls on observed dispersal patterns, we also deployed collectors to catch dispersing snails in the water column, and characterized flow regimes using novel 3D printed microcontroller-based current speed sensors. In eelgrass beds, proportions of matched and transitioning snails increased over the summer, suggesting immigration to and retention at those sites. In macroalgae sites, matched snails decreased over the summer and we observed very few transitioning snails, indicating potential high migration to and from these sites. Despite faster flow speeds at eelgrass sites than macroalgae sites, matched snails were still largely retained at eelgrass sites. Calculated

retention probabilities indicated snails were more likely to remain in eelgrass than in macroalgal habitats, suggesting they may exhibit a preference for eelgrass habitats. Our work shows how inducible traits can be used to quantify interactions between organism- and habitat-level ecological mechanisms in marine environments.

5.2 INTRODUCTION

The marine snail *Lacuna vincta* is a common grazer in coastal habitats of the Salish Sea, inhabiting both eelgrass and macroalgal beds. In macroalgal beds *L. vincta* feeds directly on macroalgal tissue, but in eelgrass habitats snails consume epiphytic diatoms that are only seasonally available in the summer (Nelson and Waaland 1997). Chapter 4 established clear effects of these different food substrates on *L. vincta* biology. Eelgrass epiphytes were a higher quality food source promoting higher reproductive output than macroalgal substrates. To take advantage of this high quality food environment, snails must either settle there as larvae or disperse as adults to colonize it in the spring, and disperse from it in the fall. *L. vincta* has planktonic larvae that settle after 7-9 weeks in the water column (Martel & Chia 1991c). Current speeds in these shallow coastal habitats, which may facilitate such dispersal, are highly variable on small spatial scales, dependent on abundance of eelgrass or macroalgae, and temporally influenced heavily by tidal cycles (Eckman et al. 2003, Lacy & Wyllie-Echeverria 2011).

While many marine molluscs have pelagic larvae that disperse long distances, some post-metamorphic (juvenile and adult) molluscs can also disperse locally via thread-drifting behavior. This type of dispersal is hypothesized to be an important ecological and life history trait of these organisms (Vahl 1983, Prezant & Chalermwat 1984, Beukema & De Vlas 1989, Martel & Chia 1991b). Post-metamorphic *L. vincta* exhibit this voluntary thread-drifting behavior enabling them

to disperse. To disperse, snails initiate foot-raising behavior such that mucus that has accumulated underneath their foot is stretched by water flow, sometimes reaching up to 160 times the snail's body length (Martel & Chia 1991a). These mucus threads enable snails to release from a substrate, and to be passively transported by currents to other habitats.

Previous studies have identified several mechanisms controlling voluntary foot-raising and drifting behavior. Chemical cues of nearby predators can induce drifting behavior to escape predation risk. In the laboratory, snails exhibited foot raising behavior in flowing water, but not in still water. Current speeds below 10 cm/s are insufficient to induce drifting behavior even when foot raising is initiated (Martel & Chia 1991a, Martel & Diefenbach 1993). Martel & Chia (1991a) determined that the unavailability of food triggered foot raising and drifting behavior. Snails in environments without food initiated dispersal behavior more frequently than those actively feeding on macroalgae. However, it remains unclear whether food preferences or quality differences among algal types induce dispersal behavior in a similar way.

Dispersal behavior, especially between habitat types, has potential fitness consequences for *L. vincta*. Like other marine gastropods, *L. vincta* feeds using its radula, a conveyor belt-like structure on which rows of teeth are continuously worn out and replaced. *L. vincta* produces teeth at a consistent rate of 3 rows/day. Radulae have 65 – 100 total rows of teeth, so that all teeth are replaced every 3-4 weeks (Padilla et al. 1996). *L. vincta* exhibits an inducible offense, described in Chapter 4, whereby radula morphology changes depending on food source. The default tooth morphology is pointed in macroalgal habitats but chemical cues from eelgrass epiphytes shift tooth shape to the induced blunt morphology in eelgrass beds (Padilla 1998, Padilla 2001, Yee & Padilla 2013, Van Alstyne et. al 2017) (Figure 5.1). Radula morphology

mismatch with current food type, a possible result of dispersal behavior, has consequences for key demographic rates, including feeding, growth, and reproduction (Chapter 4).

Because *L. vincta* tooth morphology reflects current food type, the progression of tooth types along the length of a radula can be used as a tool to investigate historical dispersal events between habitat types. Radula morphology records the history of habitat types previously inhabited by an individual, and the length of time those habitats were inhabited for the most recent 3-4 weeks during which teeth are present with identifiable morphologies (Padilla et al. 1996). Therefore, studying inducible tooth morphology across many individuals provides a unique opportunity to gain insight into population-level dispersal across habitat types in *L. vincta*.

The main objective of this study was to use inducible tooth morphology to investigate the frequency of post-metamorphic dispersal between eelgrass and macroalgae habitat types in *L. vincta*, and to assess whether environmental characteristics correlate with increased or decreased dispersal. Given the known fitness consequences of different food types, but the likely high risk associated with passive dispersal between habitats, a question remains as to whether dispersal between habitat types is a common or rare occurrence. It is generally difficult to quantify dispersal by small marine organisms in situ, making this and similar questions in population biology difficult to address.

We hypothesized that snails are more likely to facultatively disperse from lower food quality substrates, like macroalgae, than from higher quality substrates, like eelgrass. To determine the dispersal patterns of *L. vincta* between eelgrass and macroalgal habitats over the course of a summer, we surveyed radula morphology in the field, quantified numbers of snails dispersing in the water column, and modeled probabilities of dispersal between habitats. We

aggregated individual dispersal histories determined by tooth morphology across many individuals within a population, to gain insights into population-level patterns of movement between habitat types.

We also sought to investigate whether current speed influenced dispersal patterns. Because low current speeds limit snails' dispersal behavior and decrease the likelihood of arrival at distant habitats once in the water column, we hypothesized that increased flow speed would increase dispersal between habitats. Testing this hypothesis about this one mechanism would lend insight to whether the other possible drivers of dispersal, predation risk or behavioral preferences for particular food types, might be more dominant.

5.3 METHODS

Field sites and surveys

We surveyed radula morphology of *L. vincta* periodically throughout Summer 2019 to test for adult dispersal between eelgrass and macroalgae habitat types. The study period was limited to summer because that is when eelgrass epiphytes are abundant to induce the blunt tooth morphology. We collected *L. vincta* from two paired eelgrass-macroalgae field sites, Merrifield Cove (MC) and False Bay (FB), on San Juan Island, WA (Figure 5.2). These sites were selected because they had eelgrass and macroalgal habitats in close proximity to each other. At both MC and FB, macroalgal sites were dominated by the kelp, *Saccharina latissima*, and eelgrass sites were dominated by the native eelgrass, *Zostera marina*. Collection sites were separated by 153 m at FB and 126 m at MC. Twenty *L. vincta* were collected haphazardly at each sampling site at the end of four low tide series (total = 320 snails) throughout the summer: (1) 6/16/2019 – 6/20/2019, (2) 6/30/2019 – 7/6/2019, (3) 7/14/2019 – 7/18/2019, and (4) 7/28/2019 – 8/3/2019.

Snails were collected from MC eelgrass and macroalgae habitats on 6/19, 7/4, 7/18, and 8/3. Snails were collected from FB eelgrass and macroalgae habitats on 6/18, 7/5, 7/17, and 8/2. After collection, snails were frozen until they could be dissected to assess radula morphology.

Radula morphology assessments

Collected snails were dissected using the protocol in Padilla et al. (1996) in mid-August 2019 to remove and image radulae (n = 320 snails). The order of snail dissection was randomized, such that snails were dissected blindly without knowledge of their source field sites. Shell length was measured prior to dissection. Radulae were mounted on microscope slides with a drop of milliQ water and covered with a cover slip for viewing. We recorded the morphology of each row of teeth as either having macroalgal morphology (pointed) or eelgrass morphology (blunt), and recorded the total number of rows in each radula. The oldest 10 rows of teeth were not assessed for morphology because tooth wear made it difficult to determine tooth type. Snails were also classified as having radula morphology that either completely *matched* their source habitat, *in transition* to their source habitat or completely *mismatched* with their source habitat.

Projections without continuous dispersal

To assess if continuous dispersal occurred over the course of the summer, we compared observed radula morphologies to theoretical projections which assumed no dispersal beyond the first collection time. We started with observed morphology data from the first field collection time and projected the expected radula morphologies at the three subsequent time points if those snails had not moved habitats after the initial observation. To project expected morphologies from the first time point, we first calculated the number of days required for each current radula

morphology to match the source habitat. We divided the number of unmatched rows by the average *L. vinta* production rate of 3 rows/day (Padilla et al., 1996) to calculate the number of days required to match the source habitat. Using days required to achieve a matched radula for each initial snail, we summarized the expected morphology proportions of matched, transitioning and mismatched snails for the remaining time points. We used Fisher Exact tests to compare these projected proportions with our observed field proportions of matched, transitioning, and mismatched snails at each time point. All statistical analysis was completed in R version 3.6.1 (R Core Team 2019)

Modeling habitat retention probabilities

We constructed a Markov chain analysis in Python 3.8 to estimate snail transition probabilities between eelgrass and macroalgal sites to apply to our radula morphology survey data. The key assumptions in this analysis were that dispersal rates were constant during the sampling period, that dispersal events occurred randomly and independently, and that a snail's dispersal probability depends only on its current food type. We designated two habitat states (0 = eelgrass and 1 = macroalgae) where state history (the sequence of food substrates for each time block) can be inferred from tooth morphology. Because *L. vincta* produces an average of 3 rows of teeth per day (Padilla et al. 1996), we used a time step of 8 hours which represents a transition either to the same or a different habitat. By comparing chronological pairs of adjacent rows of teeth, we calculated the number of each type of transition using the matrix

		Timestep $i + 1$	
Timestep i		N_{00}	N_{01}
		N_{10}	N_{11}

where N_{jk} is the observed number of transitions from habitat *j* to habitat *k*. This enabled us to estimate the probability of transition from eelgrass to macroalgae or vice versa. The total number of transitions for snails in eelgrass habitats is $N_{00} + N_{01}$. Hence, the probability of a snail starting in an eelgrass habitat and staying in eelgrass over an 8-hour time step is $\frac{N_{00}}{N_{00}+ N_{01}}$. The probability of a snail starting in an eelgrass habitat and dispersing to a macroalgae habitat over an 8-hour time step is $\frac{N_{01}}{N_{00}+ N_{01}}$. The same calculations can be made for snails from macroalgal habitats which results in this probability matrix generated from our radula survey data:

$$\bar{P} = \begin{bmatrix} \frac{N_{00}}{N_{00}+ N_{01}} & \frac{N_{10}}{N_{00}+ N_{01}} \\ \frac{N_{10}}{N_{10}+ N_{11}} & \frac{N_{11}}{N_{10}+ N_{11}} \end{bmatrix} = \begin{bmatrix} P_{00} & P_{10} \\ P_{10} & P_{11} \end{bmatrix} \quad (5.1)$$

We used these transition probabilities to predict the probability that a snail stays in its current habitat over a two-month period (60 days) for better comparison with our field collected data which was collected over the course of a summer. To calculate probabilities for retention in both macroalgae and eelgrass, we used the equations below where *d* refers to the number of days in the projection period:

$$P(stay\ in\ Eelgrass) = {P_{00}}^{3d}$$

$$P(stay\ in\ Macroalgae) = {P_{11}}^{3d} \quad (5.2)$$

Here, *d* is multiplied by three because there are three 8-hour time steps in a day. These equations were used to calculate two-week (*d*=60) retention probabilities using subsets of the data grouped by habitat (Eelgrass, Macroalgae), site (False Bay or Merrifield Cove) or both. To calculate the probability of dispersal, which is the opposite of the retention probability, we used the equation below:

$$P(leave\ Eelgrass) = 1 - {P_{00}}^{3d}$$

$$P(leave\ Macroalgae) = 1 - {P_{11}}^{3d} \quad (5.3)$$

Snail catchers

To further explore dispersal in the water column, we constructed "snail catchers" to collect snails that were drifting in the water column at Merrifield Cove. Snail catcher frames were constructed with ½" diameter PVC pipe and an attached mesh net to catch and retain drifting snails. PVC frames had two 18" legs supporting an open 12" x 12" square which was backed with mesh bags to create a net to catch drifting snails. Two snail catcher frames were then attached back-to-back to collect snails on both sides of the catcher. The frame legs were secured in the field with two cinder blocks, one on either side of the snail catcher (Figure 5.4a).

Three snail catchers were deployed at Merrifield Cove, one in the macroalgal habitat, one in the eelgrass habitat and one in the boundary zone between the two habitat types (Figure 5.4b). The boundary zone snail catcher was 80 m from the macroalgae snail catcher and 45 m from the eelgrass snail catcher. All snail catchers were deployed at the same tidal height with the top of the net frame at approximately 25.4 cm below MLLW and were only accessible to monitor at low tides. Snail catchers were censused at 6 time points during three low tide series: 7/2/2019, 7/4/2019, 7/6/2019, 7/16/2019, 7/18/2019 and 7/31/2019. At the beginning of a low tide series, snail catcher nets were filled approximately halfway with *Ulva lactuca* from the site. Nets were filled with *U. lactuca* because it is an easily accessible and common *L. vincta* food source which would retain snails in the nets until we could collect and count them. Newly collected *U. lactuca* was rinsed in fresh water to remove any snails prior to placement in snail catcher nets. Once filled, 1" x 1" mesh was secured over the net frame opening using cable ties to prevent *U.*

lactuca from being washed away but still enable collection of drifting snails. Every two days during low tides series, *U. lactuca* was removed from nets and rinsed in freshwater to collect snails, and new *U. lactuca*, cleaned of snails, was replaced in nets. We counted and collected measured snails from each net. After a low tide series, we emptied snail catchers of *U. lactuca* and did not monitor during high tide series when they were inaccessible. We put snails into two categories, shell lengths >1 mm and shell lengths <1 mm to distinguish snails that had likely newly recruited (<1 mm) from those that were dispersing (>1 mm). We tested for differences in snail counts for both size classes across snail catcher locations using a one-way ANOVA. We square root transformed data to satisfy homogeneity of variances using Levene's Test (car library in R) prior to running the ANOVA.

Current sensors

To characterize water flow speed regimes at each *L. vincta* collection site, we constructed current sensors from low-cost raw electronic components. Briefly, our current sensors utilized hall effect sensors, which detect changes in magnetic field, to count rotations of a 3D printed propeller embedded with magnets over a 30 second sampling period. Sensors were programmed to sample for 30 seconds every 10 minutes. Current sensors used ESP8266 MicroPython-based microcontrollers to log data, with electronics encased in a waterproof PVC housing and powered by a solar battery. Sensors were mounted on foam kickboards to measure water flow at the surface and secured in the field with a rope and cinder block (Figure 5.5).

Current sensors were calibrated in the flume (Model 1520, Rolling Hills Research Corporation) at Friday Harbor Laboratories. We floated each sensor in the flume and collected propellor rotation count data over 30 second intervals at 5 standard speeds (10 cm/s, 12 cm/s, 15

cm/s, 20 cm/s, and 25 cm/s). We conducted ten 30 second samples for each sensor at each speed to ensure rotation speed consistency and used that data to create a calibration curve to translate rotations/30 sec to flow speed for each sensor. The lowest reliable speed that would rotate propellers with consistent results was 10 cm/s. Sensors were calibrated using this procedure before and after deployments (Appendix D, Figure S1).

Current sensors were deployed at each of the four sites for 2-5 days prior to *L. vincta* collection over three low tide series: (1) 6/30/2019 – 7/6/2019, (2) 7/14/2019 – 7/18/2019, and (3) 7/28/2019 – 8/3/2019. We anchored sensors with a cinderblock and a rope long enough to enable the sensor to float at the surface throughout the tidal cycle. Sensors were always floating in at least 0.5m of water and never beached at the lowest tides. Sensors were checked every two days while deployed to clean and ensure the propeller had not been clogged with debris. After retrieving sensor data, we used sensor calibration curves to calculate the proportion of current observations above 10 cm/s, the sensors' minimum detection threshold, to characterize the flow regimes at each site. We compared flow across these four sites using a one-way ANOVA, and log-transformed values prior to running the test to satisfy Levene's Test of homogeneity of variances (car library in R). We compared this flow metric to the corresponding proportion of matched snails (assumed residents), to investigate the relationship between flow rate and dispersal. We created a series of linear models with fixed effects of habitat type (macroalgae, eelgrass) and flow regime and used AIC to determine which model was the best fit. All statistics were done in R version 3.6.1.

5.4 RESULTS

Radula morphology observations and projections

We found strong evidence of *L. vincta* dispersal between eelgrass and macroalgae habitats because we observed many snails with radulae that did not match their collection site habitat. For both eelgrass habitats, we observed similar patterns for the proportions of snails with various radular morphologies (Figure 5.3a-b). In early summer, eelgrass sites exhibited few snails with matched radula morphologies (≤10%) but this increased by 30% over the course of the summer at both sites. At these sites, most early summer snails had mismatched radulae (MC: 90%, FB: 75%) but decreased by 50% at MC and 45% at FB over the course of the summer. Snails with transitioning radula morphology were present in eelgrass sites and increased over the summer.

Macroalgal sites started with high proportions of matched snails in early summer (MC: 100%, FB: 80%) but this decreased by the final tide series by 40% at FB and 20% at MC (Figure 5.4a-b). These sites started with low proportions of mismatched snails (≤20%) but this increased over the summer by 35% at FB and 20% at MC. At the first three tide series MC macroalgae only contained matched snails. Both macroalgae sites had few to no snails (≤10%) with transitioning radula at any time point.

For both MC and FB eelgrass sites and the FB macroalgae site, the observed *L. vincta* radular morphologies significantly differed from the projections assuming no continuous dispersal indicating significant continued adult dispersal over the summer at three of our four sites (Figure 5.3c-d, Figure 5.4c-d). There were significant differences between observations and projections at all time points after the first tide series at FB eelgrass (tide series 2: $p = 0.0002$, tide series 3: $p < 0.0001$, tide series 4: $p < 0.0001$, Fisher exact tests), MC eelgrass (tide series 2: $p < 0.0001$, tides series 3: $p < 0.0001$, tide series 4: $p < 0.0001$, Fisher exact tests), and FB macroalgae (tide series 2: $p = 0.0317$, tide series 3: $p = 0.0202$, tide series 4: $p < 0.0001$, Fisher

exact tests). MC macroalgae was the only site that did not exhibit significant differences between observations and projections at any time point. At this site, radula morphology proportions matched the projections exactly, except at the last time point but this difference in proportions was not significant (tide series 4: $p = 0.1060$, Fisher exact test).

Model probabilities

We found that snails were much more likely to stay in their current habitat than to move to a new habitat during a single 8-hour time step (Equation 5.1). Overall, the probability of a transition over an 8-hour interval was very low. However, in projecting these low transition probabilities over a two-month period, we found that dispersal probabilities (Equation 5.3) grew considerably. We found lower dispersal probabilities away from eelgrass than macroalgae (Table 5.1). In using the entire dataset to inform calculations, the probability of dispersal from eelgrass over two months was 45% versus 59% in macroalgae (Equation 5.3), and the probability of retention over the same time period was 55% in eelgrass and 41% in macroalgae (Equation 5.2, Table 5.1). Though there were variations in these two-month probabilities when estimated using different subsets of the data by habitat or site, retention probabilities were generally higher in eelgrass than in macroalgae, and dispersal probabilities were generally lower away from eelgrass than macroalgae. Additionally, when projected over the course of a typical *Lacuna* lifespan (6-12 months, Martel & Chia 1991c) the likelihood of an individual snail dispersing between habitat types approaches 100% (Equation 5.3, $d = 180*3$).

Snail catchers

We found a significant difference in the number of small snails, those with shell lengths < 1mm, caught across different snail catchers from various sites ($p = 0.020$, ANOVA, Figure 5.5c, Appendix D Tables S1.1 and S1.2). Though most pairwise comparisons between snail catchers were not significantly different, we found trends that suggest there were more small snails in macroalgal snail catchers than eelgrass snail catchers. There were marginally insignificant differences between the macroalgal and eelgrass snail catchers 3A and 1B ($p = 0.057$, Tukey's HSD) and 3A and 1A ($p = 0.088$, Tukey's HSD) but these effects were not strong. The trends for the larger snail size class, shell lengths >1mm, were similar but not as pronounced and we only identified a marginally insignificant effect of snail catcher on the number of larger snails caught ($p = 0.072$, ANOVA, Figure 5.5d, Appendix D S1.3 and S1.4) with the only marginally insignificant pairwise comparison identified between macroalgal and eelgrass snail catchers 3A and 1B ($p = 0.092$, Tukey's HSD). Abundances of both size classes of snails were variable over the course of the summer with more snails caught earlier in the season, especially over the macroalgae site (Figure 5.5e-f).

Current sensors

At both MC sites (macroalgae and eelgrass) and at the FB macroalgae site, flow speeds were typically low with less than 5% of flow observations above the 10cm/s threshold. However, the flow rates at the FB eelgrass site were significantly higher with a mean of 23% of flow observations above 10cm/s ($p = 0.002$, one-way ANOVA, Appendix D Table S2.1). In comparing these measured flow speeds with our radula survey data, AIC analysis determined that the best linear model included flow speed, habitat type, and their interaction. The effect of the flow speed on the number of resident snails (those with radula morphology matched to the

habitat) was dependent on habitat type, with faster flow speeds correlated with fewer resident snails in macroalgal habitats but the opposite trend in eelgrass habitats ($p = 0.01$, linear model, Appendix D Tables S2.2 and S2.3, Figure 5.6c). A higher proportion of resident snails remained in eelgrass habitats even at faster flow speeds.

5.5 DISCUSSION

Dispersal is a common process across a wide range of marine taxa. Most commonly, holoplankton, and organisms with pelagic larval stages but benthic juveniles and adults exhibit dispersal (Grantham et al. 2003). However, examples are known of post-metamorphic dispersal by benthic juvenile and adult life stages via voluntary drifting behaviors (Vahl 1983, Prezant & Chalermwat 1984, Beukema & De Vlas 1989, Martel & Chia 1991b) or dispersal by "rafting" on floating substrates (Gibson et al. 2005). Understanding the prevalence and importance of dispersal in marine organisms can help address questions about life histories, population distributions, and community-level implications.

While dispersal is a critical process shaping marine populations, it is typically not well understood and can be difficult to quantify because of the challenges associated with tracking dispersing individuals in the field (Levin 2006). For this reason, many dispersal studies have used complex methods to track organisms including chemical markers, modeling circulation patterns, and genetic approaches to understand population connectivity (DiBacco & Levin 2000, Levin 2006, Swearer at al. 2019). In *L. vincta* specifically, an inducible morphological trait presents a unique opportunity to track individuals, enabling estimations of population-level dispersal between two habitat types: eelgrass and macroalgal beds. Chapter 4 demonstrated that these two habitats have different effects on *L. vincta* ecology, with eelgrass epiphytes supporting

higher reproductive output and feeding than macroalgae. Therefore, post-metamorphic dispersal between these habitats could be an important factor shaping *L. vincta* ecology and population dynamics.

Inducible morphology documents dispersal

We successfully quantified population-level dispersal between eelgrass and macroalgal habitats using an innovative approach of tracking an individual-level inducible trait. Our field survey data of radula morphology show that post-metamorphic snails disperse frequently between these habitat types as shown by the high proportions of mismatched snails we observed. Using our field data, we were able to project expected radula morphologies assuming no continued dispersal over the course of the summer. These projections were significantly different from our field observations, strongly suggesting that dispersal between habitat types continued throughout the summer. Our results highlight the successful arrival of individuals to a new habitat, which can be just as difficult to quantify as departure from an area. Experimental and field work has shown that snails drift away from their current habitats for various reasons but the likelihood of survival at a new site has been largely unknown (Martel & Chia 1991a, 1991b). Coupled with fitness implications from Chapter 4, tracking this inducible trait provides an avenue to understand *L. vincta* post-dispersal success.

Eelgrass epiphytes are a transient high-quality food source which is only available in the summer. Our results provide insights into how well and by what mechanisms snails can exploit this high quality food source. Radula morphology surveys suggest snails move to eelgrass beds from macroalgal beds. Early summer observations indicated low proportions of resident snails (matched morphology) in eelgrass beds, but this increased over the summer. Likewise,

proportions of newly arrived snails (mismatched morphology) decreased as the summer progressed. Eelgrass sites also exhibited considerable proportions of transitioning snails, in which morphologies of newer teeth matched the food source but older teeth did not. This suggests that snails that arrived from macroalgal sites stayed in their new eelgrass habitat. It might be beneficial for new arrivals to remain in eelgrass habitats because epiphyte consumption supports high reproductive output and feeding even when snails have mismatched radula morphology (Chapter 4). In contrast, transitioning snails were rare in macroalgal habitats, suggesting that snails arriving with mismatched teeth may not stay after arrival at macroalgal sites. Consistency between snail catcher data and tooth morphology metrics also suggest dispersal was a key mechanism in demographic changes. At Merrifield Cove, we observed more snails in the water column above macroalgae early in the summer at the same time as our radula morphology observations suggesting high immigration to eelgrass. This snail catcher data supports the hypothesis that snails were dispersing from macroalgae to eelgrass. Though the radula morphology of snails caught in the water column was not assessed, this information could be helpful to gain insight whether snails caught above macroalgae were leaving or arriving. Additionally, data on adult *L. vincta* abundances at our sites would help determine that immigration patterns suggested by proportion data are not confounded by differences in population sizes across sites.

Chemical cues from eelgrass epiphytes induce blunt tooth morphology in *L. vincta.* Can we distinguish if the morphology patterns we observed were just responding to an increase in induction cue as epiphytes grow over the summer as opposed to being an indicator of recent dispersal from a macroalgal habitat? Epiphytes are in high abundance during the summer, with maximum biomass beginning in early June (Nelson 1995, Nelson & Waaland 1997). If snails

were not dispersing between habitats and radula morphologies were only responding to an increase in epiphyte cue, radulae should have all been matched earlier in the summer than what we observed and should not have varied from the projections of not continued dispersal, assuming the 3-4 week complete radula replacement period. This strongly suggests that the increase in resident snails over the summer quantified by inducible morphology was not just a response to the increase in epiphyte cue in late spring.

Our results suggest that *L. vincta* snails preferentially disperse from macroalgae to eelgrass habitats. *L. vincta* has documented food preferences among species of macroalgae (Chavanich & Harris 2002, Britton-Simmons et al. 2011), but laboratory studies have not tested similar preferences for eelgrass epiphytes. Our radula survey data suggest that eelgrass may be a preferred habitat because newly arrived snails slowly became residents of those sites over the summer, indicated by increasing proportions of transitioning snails, whereas we did not observe this pattern at macroalgal sites. Though our macroalgal sites consisted mostly of *S. latissima* and other kelps, there may be species-specific differences across macroalgal groups that may impact the *L. vincta* responses we measured. For example, the invasive macroalga *Sargassum muticum* is a preferred food of *L. vincta* (Britton-Simmons et al. 2011) and can host large epiphyte loads (Baer & Stengel 2014), and its impact on *L. vincta* tooth morphology is unknown.

We hypothesized that current speed would be a limiting mechanism for dispersal. We found some evidence for this at macroalgal sites where both current speeds and inferred dispersal was low. Though our study suggests that eelgrass is the preferred habitat, we still observed higher proportions of matched (resident) snails at macroalgal sites, especially early in the summer. Observations of high abundances of snails in the water column above macroalgae suggest that snails may have been drifting more, either because of predators or algal preference,

but it did not result in fewer matched snails. Crab predator populations (*Pugettia* sp.) in macroalgal beds are known to increase over the summer (Hines 1982, Daly & Konar 2008, Ohtsuchi et al. 2016) possibly increasing the likelihood of dispersal behavior and providing context for our observations. Both macroalgae sites exhibited slow flow speeds which may have prevented snails from being transported far enough to leave the habitat despite displaying drifting behavior.

In eelgrass habitats, our current speed data provide support that eelgrass may be a preferred habitat. We observed the fastest flow speeds at the False Bay eelgrass site, with observed current speeds within the range measured at nearby eelgrass beds (Lacy & Wyllie-Echeverria 2011). Despite faster flow speeds, we observed increasing proportions of matched and transitioning snails over the summer, suggesting that snails remained in this habitat. Although this was only one site, it suggests that high current speeds do not necessarily imply high dispersal rates. If other factors like predator presence do not induce drifting behavior or if snails exhibit an active behavioral choice to stay in an eelgrass habitat once they arrive, they may remain despite higher flows.

Though we measured flow at the surface, actual speeds experienced by *L. vincta* on substrates may have been lower because near-bed vegetation slows current speeds, further limiting dispersal (Eckman et al. 2003, Lacy & Wyllie-Echeverria 2011). Our flow speed characterizations are limited to small sample sizes with low flow observations across 2-5 days during low tide series. Though these periods experience large tidal exchanges, investigations of current speeds over longer time scales could help better describe flow and correlations with dispersal patterns.

Insights from model dispersal and retention probabilities

Probabilities of dispersal and retention, calculated from sequences of tooth types, showed that dispersal from macroalgae was more likely than dispersal from eelgrass. As descriptors of snail dispersal, these probabilities reflect simplifying assumptions, such as that dispersal rates remained constant during the sampling period and that dispersal events could be approximated as Markov events. Despite these simplifications, our results have important implications for the directions and timescales over which *L. vincta* populations in the field moved between habitats with different food substrates.

We hypothesized that snails preferentially remain in eelgrass habitats for higher food quality and are more likely to disperse away from lower food quality macroalgae habitats. Our results showed that retention probabilities over a two-month period were consistently higher in eelgrass than in macroalgae. Conversely, snails dispersed away from macroalgae with higher probabilities than away from eelgrass habitats (Table 5.1). Therefore, this provides further support that snails are more likely to be retained in eelgrass by some mechanism (i.e., behavioral choice to remain on substrate, lower predator encounter rates). These initial modeling results establish a path forward for an expanded model in which retention probabilities can be used to estimate population distributions, dispersal histories, and calculate fluxes between habitat types which can be compared with our field collected data.

Future directions

This work presents avenues for future research investigating the possible mechanisms determining *L. vincta* dispersal patterns. Snails exhibit drifting behavior that can result in dispersal due to a variety of factors including predator presence, lack of food, and current speeds

(Martel & Chia 1991a, Martel & Chia 1991b, Martel & Diefenbach 1993). We determined that flow speeds may have a partial role in dispersal away from macroalgal sites, but we observed that resident snails remained in eelgrass habitats even during high flow periods suggesting other mechanisms may be contributing. Assessing predator populations to characterize predation risk across sites in combination with radula surveys and current speed measurements as we have conducted, would help provide some context for the likelihood of snails to exhibit drifting behavior. Martel & Diefenbach (1993) determined that snails were more likely to exhibit drifting behavior if they were not actively feeding. Our results suggest this behavior is influenced by algal preferences, therefore, similar laboratory experiments could determine if there are differences in drifting behavior dependent on algal substrate, like eelgrass or various species of macroalgae. It is also still largely unknown if radula morphology influences the likelihood of drifting behavior (e.g. are snails with mismatched radula more likely to exhibit drifting behavior, and does this differ based on habitat type?). This study developed methods that can be applied to test snail dispersal on broader spatial and temporal scales, and can be used in conjunction with other integrative studies on *L. vincta* (Grünbaum & Padilla 2014), to enable more in-depth investigations of the ecological causes and consequences of *L. vincta* dispersal.

5.6 Acknowledgements

Thank you to Ann Stanbrough, Katie Dobkowski, Mo Turner, and Olivia Graham for field assistance, Kim Stewart and Anik Mutsuddy for field assistance and help classifying radula morphologies, Martha Groom and the UW Doris Duke Conservation Scholars Program for making it possible that Kim and Anik participate in this project, Robert Levine and Brian Bare for sensor design and testing assistance. Funding from Friday Harbor Labs Research Fellowship

Endowment, Conchologists of America (Toto Olivera and Donald Dan Award) and the Pacific Northwest Shell Club (Ann Smiley Memorial Award).

References

Baer J, Stengel DB (2014) Can native epiphytes affect establishment success of the alien seaweed *Sargassum muticum* (Phaeophyceae)?. Proc R Ir Acad Biol Environ, 114:41-52

Beukema JJ, De Vlas J (1989) Tidal-current transport of thread-drifting postlarval juveniles of the bivalve *Macoma balthica* from the Wadden Sea to the North Sea. Mar Ecol Prog Ser 52:193-200

Britton-Simmons KH, Pister B, Sánchez I, Okamoto D (2011) Response of a native, herbivorous snail to the introduced seaweed *Sargassum muticum*. Hydrobiologia, 661:187-196

Chavanich S, Harris LG (2002) The influence of macroalgae on seasonal abundance and feeding preference of a subtidal snail, *Lacuna vincta* (Montagu)(Littorinidae) in the Gulf of Maine. J Mollusc Stud, 68:73-78

Daly B, Konar B (2008) Effects of macroalgal structural complexity on nearshore larval and post-larval crab composition. Mar Biol, 153:1055-1064

DiBacco C, Levin LA (2000) Development and application of elemental fingerprinting to track the dispersal of marine invertebrate larvae. Limnol Oceanogr, 45:871-880

Eckman JE, Duggins DO, Siddon CE (2003) Current and wave dynamics in the shallow subtidal: implications to the ecology of understory and surface-canopy kelps. Mar Ecol Prog Ser, 265:45-56.

Gibson RN, Atkinson RJA, Gordon JDM (2005) The ecology of rafting in the marine environment. II. The rafting organisms and community. Oceanogr Mar Biol Annu Rev, 43:279-418

Grantham BA, Eckert GL, Shanks AL (2003) Dispersal potential of marine invertebrates in diverse habitats. Ecol Appl, 13:S108-116

Grünbaum D, Padilla DK (2014) An integrated modeling approach to assessing linkages between environment, organism, and phenotypic plasticity. Integr Comp Biol, 54:323–335

Hines AH (1982). Coexistence in a kelp forest: size, population dynamics, and resource partitioning in a guild of spider crabs (Brachyura, Majidae). Ecol Monogr 52:179-198

Lacy JR, Wyllie-Echeverria S (2011) The influence of current speed and vegetation density on flow structure in two macrotidal eelgrass canopies. Limnol Oceanogr Fluid Environ, 1:38-55

Levin LA (2006) Recent progress in understanding larval dispersal: new directions and digressions. Integr Comp Biol, 46:282–297

Martel A, Chia FS (1991a) Foot-raising behaviour and active participation during the initial phase of post-metamorphic drifting in the gastropod *Lacuna* spp. Mar Ecol Prog Ser 72:247-254

Martel A, Chia FS (1991b) Drifting and dispersal of small bivalves and gastropods with direct development. J Exp Mar Biol Ecol, 150:131-147

Martel A, Chia FS (1991c). Oviposition, larval abundance, in situ larval growth and recruitment of the herbivorous gastropod Lacuna vincta, in kelp canopies in Barkley Sound, Vancouver Island. Mar Biol, 110:237-47

Martel A, Diefenbach T (1993) Effects of body size, water current and microhabitat on mucous-thread drifting in post-metamorphic gastropods *Lacuna* spp. Mar Ecol Prog Ser, 99:215-215

Nelson TA (1995) Interactions and dynamics of eelgrass (*Zostera marina L.*) epiphytes, and grazers in subtidal meadows of Puget Sound. Dissertation. University of Washington, Seattle, WA

Nelson TA, Waaland JR (1997) Seasonality of eelgrass, epiphyte, and grazer biomass and productivity in subtidal eelgrass meadows subjected to moderate tidal amplitude. Aquat Bot 56:51-74

Ohtsuchi N, Kawamura T, Hayakawa J, Kurogi H, Watanabe Y (2016) Growth patterns and population dynamics of the kelp crab *Pugettia vulgaris* (Decapoda, Brachyura, Epialtidae) on the coast of Sagami Bay, Japan. Crustaceana, 89: 645-667

Padilla DK, Dittman DE, Franz J, Sladek R (1996) Radular production rates in two species of *Lacuna* Turton (Gastropoda: Littorinidae). J Mollusc Stud 62:275-280

Padilla DK (1998) Inducible phenotypic plasticity of the radula in Lacuna (Gastropoda: Littorinidae). Veliger 41:201-204

Padilla DK (2001) Food and environmental cues trigger an inducible offense. Evol Ecol Res 3: 15-25

Prezant RS, Chalermwat K (1984) Flotation of the bivalve *Corbicula fluminea* as a means of dispersal. Science, 225:1491-1493

R Core Team (2019). R: a language and environment for statistical computing. R Foundation for Statistical Computing, Vienna. www.r-project.org

Swearer SE, Treml EA, Shima JS (2019) A review of biophysical models of marine larval dispersal. Oceanogr Mar Biol Annu Rev, 57:325-356

Vahl O (1983) Mucus drifting in the limpet *Helcion (= Patina) pellucidus* (Prosobranchia, Patellidae). Sarsia, 68:209-211

Van Alstyne KL, Padilla DK, Chan M, Yee AK (2017) Do dietary chemical signals cue an inducible offense? Society for Integrative and Comparative Biology, Jan 2017, New Orleans, LA. Abstract 119-5.

Yee AK, Padilla DK (2013) Chemical signaling in an inducible offense. REU thesis, Friday Harbor Laboratories, University of Washington.

Figure 5.1 Microscope images, using a high contrast filter, of two different radula morphologies of *L. vincta*. Pointed teeth (left) for consuming macroalgae and inducible blunt teeth (right) for scraping epiphytes from eelgrass blades. Scale bar is 50 μm

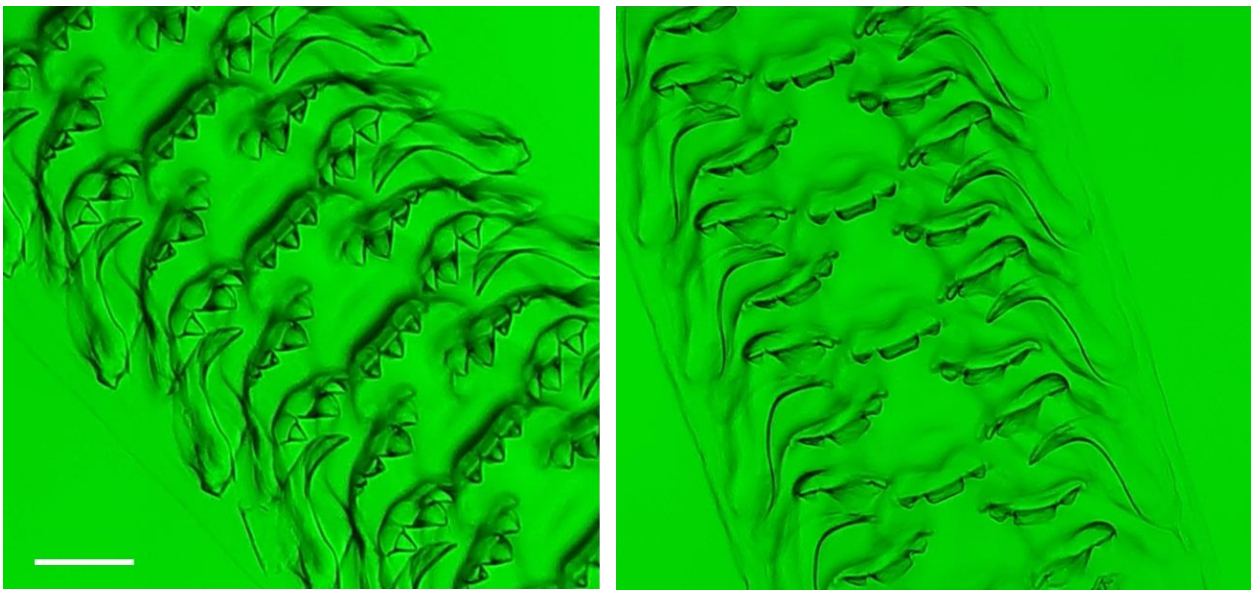

Figure 5.2 Map of field sites on San Juan Island, WA. Aerial images of Merrifield Cove and False Bay from Google Maps.

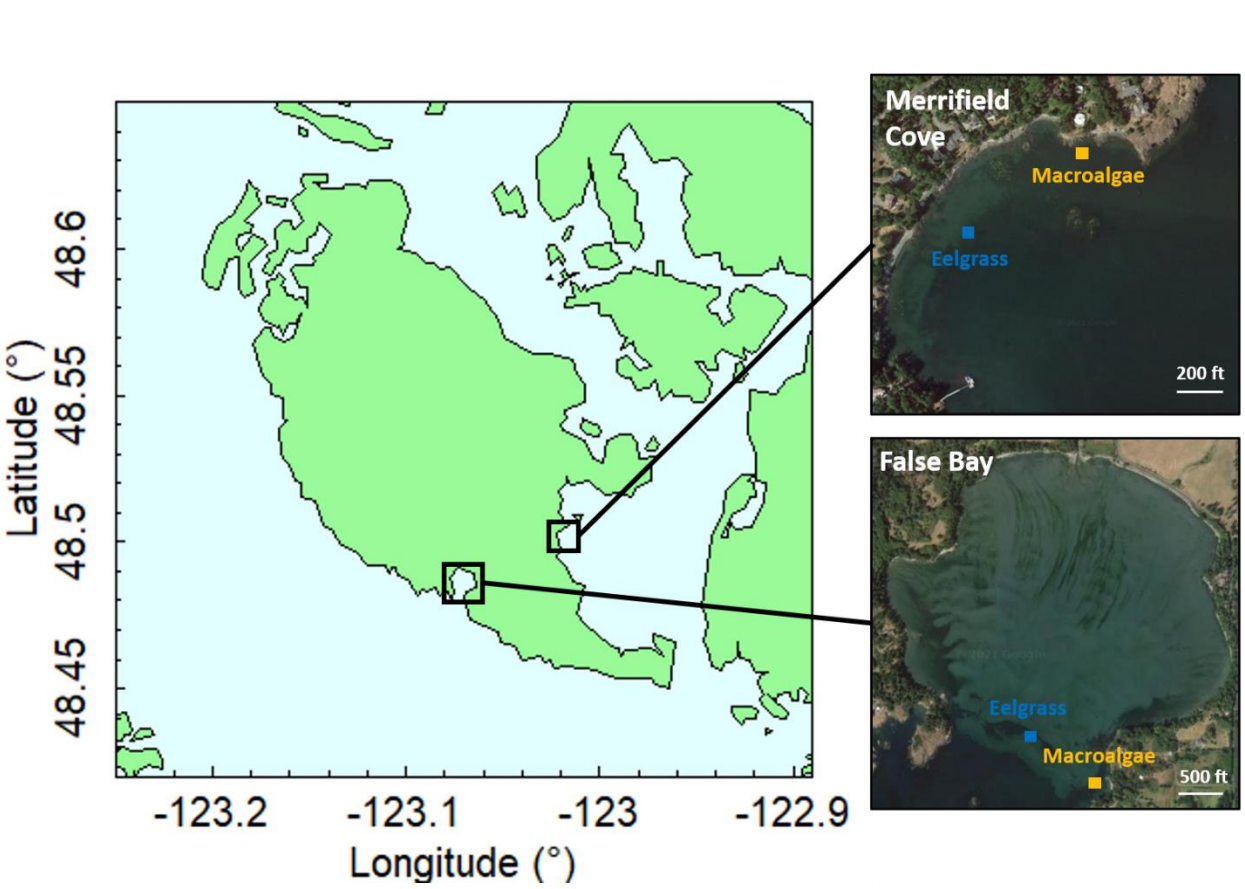

Figure 5.3 Observed radula morphologies at four low tide series throughout the summer at two eelgrass sites, False Bay and Merrifield Cove (top). Expected radula morphologies assuming no continuous dispersal between habitat types after the first sampling time point at the same two eelgrass sites (bottom). Projections were generated by using tide series 1 observations to project expected proportions to the subsequent tide series.

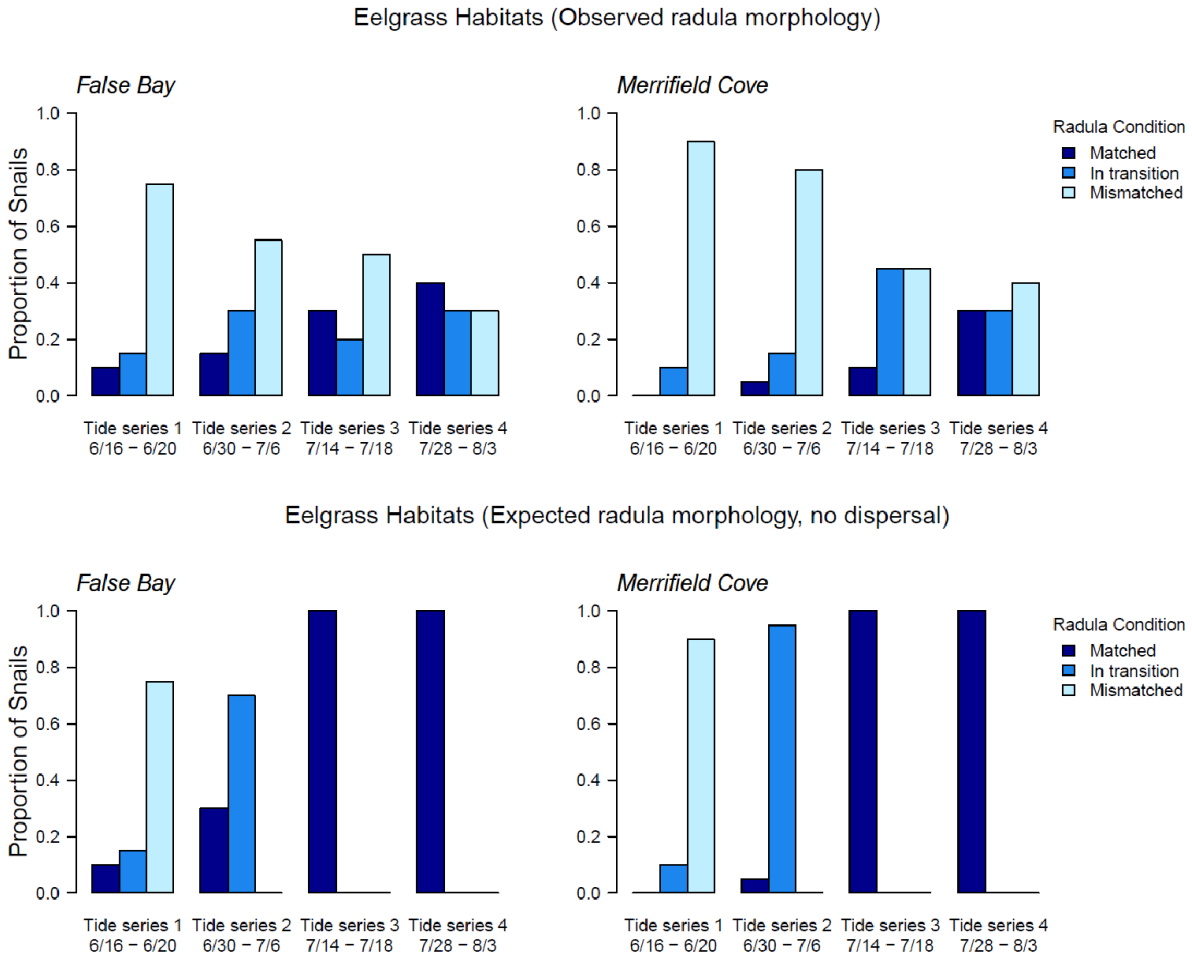

Figure 5.4 Observed radula morphologies at four low tide series throughout the summer at two macroalgae sites, False Bay and Merrifield Cove (top). Expected radula morphologies assuming no continuous dispersal between habitat types after the first sampling time point at the same two macroalgae sites (bottom). Projections were generated by using tide series 1 observations to project expected proportions to the subsequent tide series.

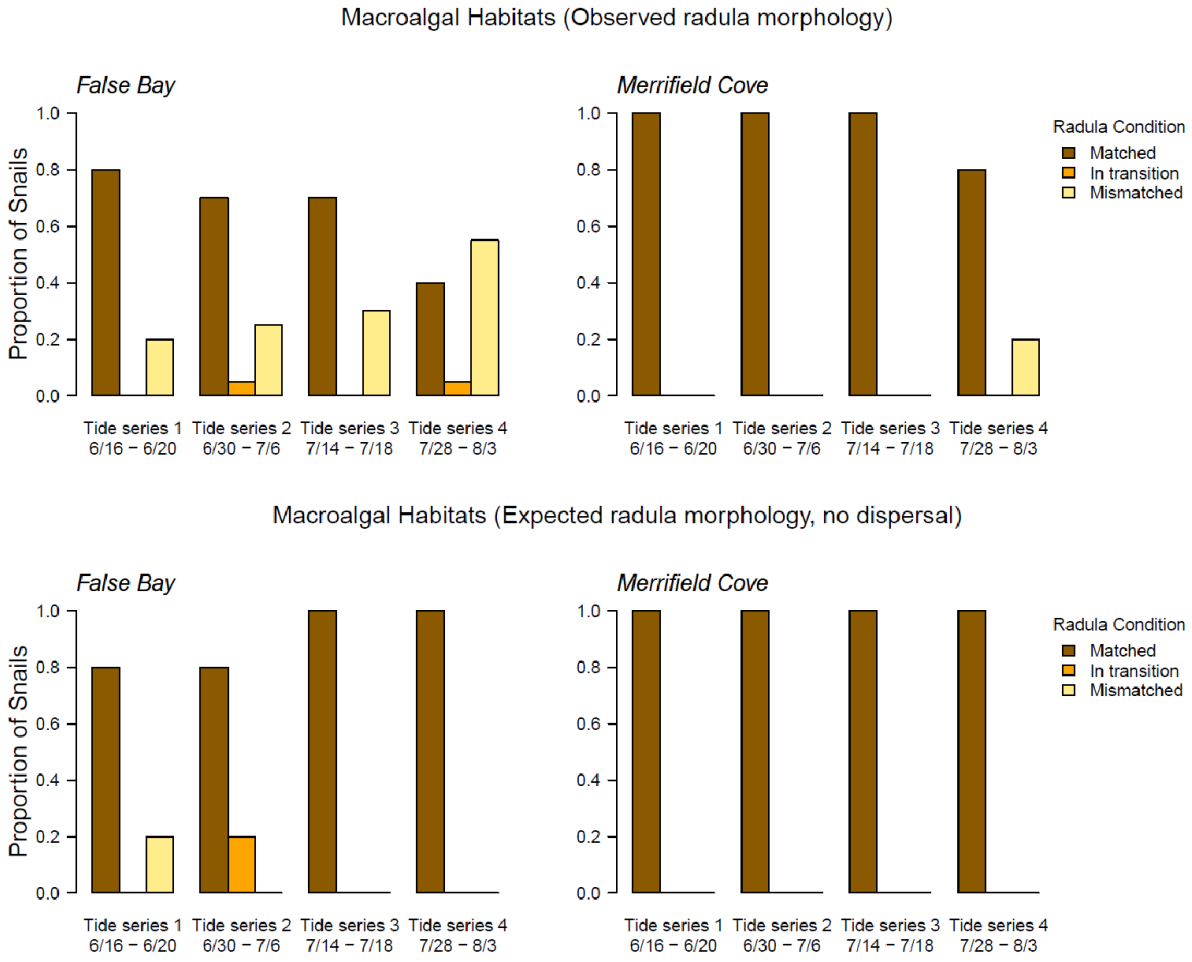

Figure 5.5 Results from snail catchers. (a) Image of a snail catcher in the field. (b) Locations of snail catchers at Merrifield Cove. Image from Google Maps (c) Number of snails (shell lengths < 1 mm) caught in catchers over 6 time points throughout the summer. (d) Number of snails (shell lengths > 1 mm) caught in catchers. Error bars indicate standard error. The same data is presented as a time series of snails caught for (e) shell lengths < 1 mm and (f) shell lengths > 1 mm.

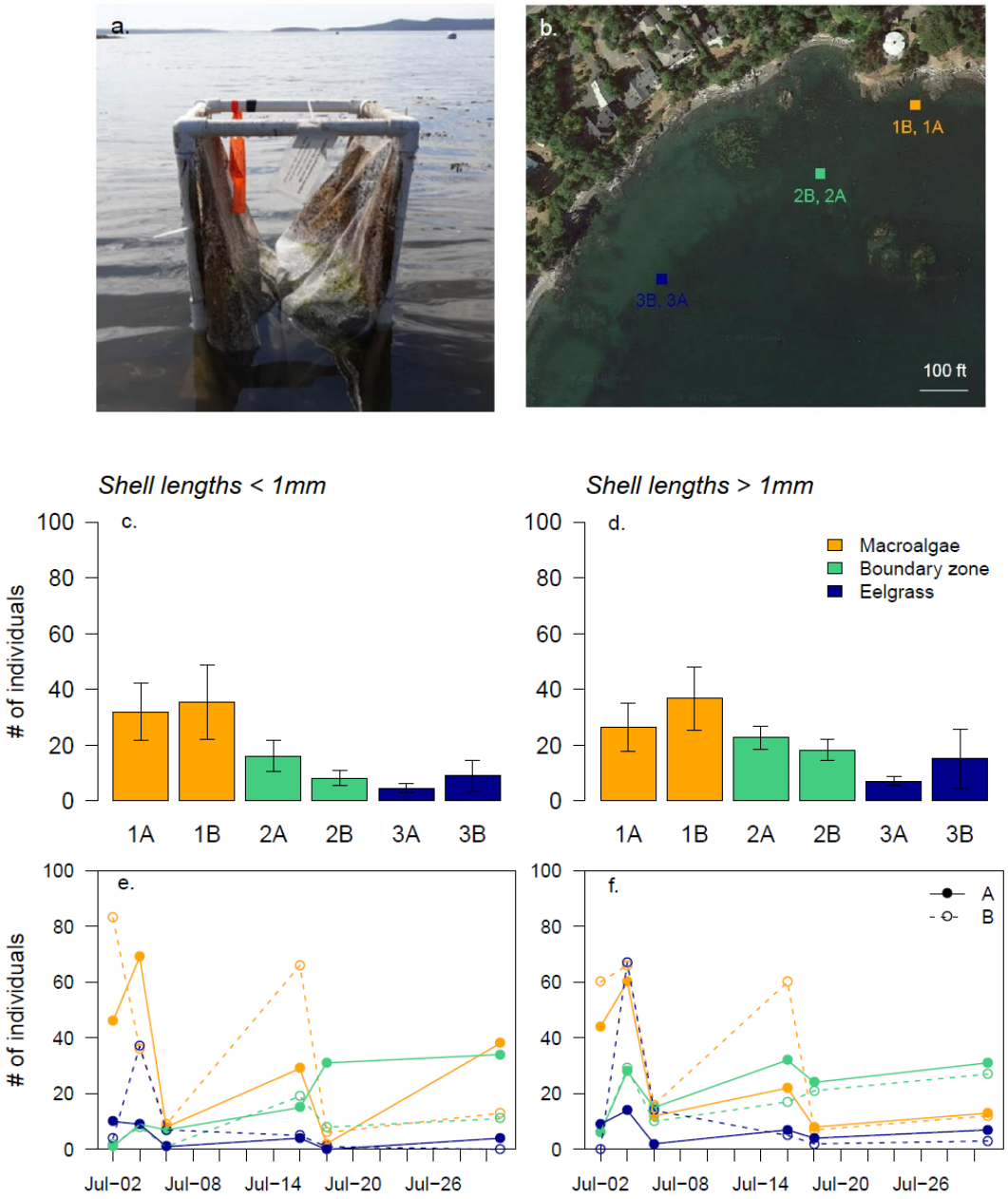

Figure 5.6 (a) Photo of constructed current sensor deployed in field. (b) Bottom view of current sensor displaying the 3D printed propellor mechanism in the flume. (c) Plot showing the relationship between current speed and the proportion of snails with matched radulae (implied residents of the site).

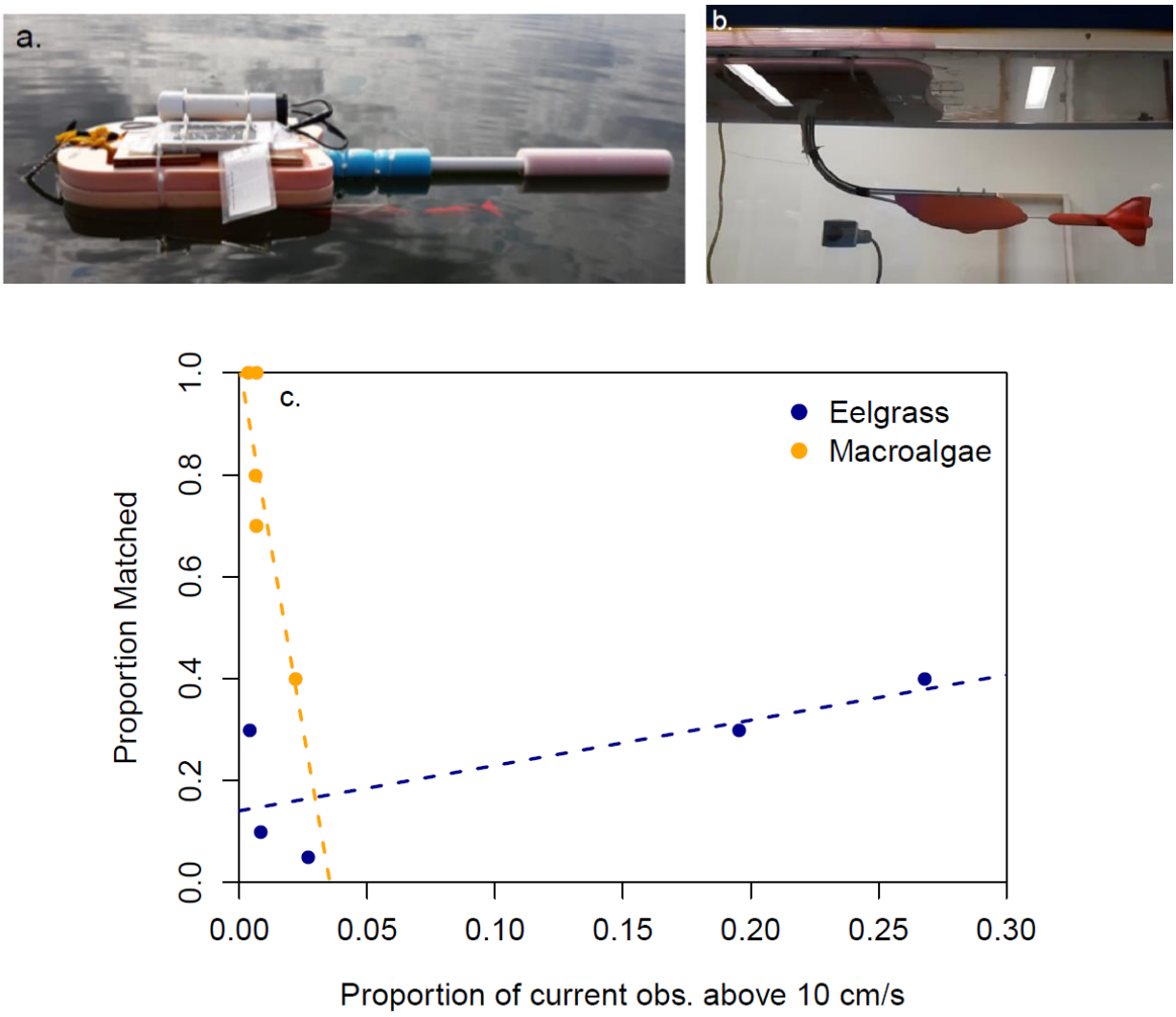

Table 5.1 Probabilities generated from the model. Calculated probabilities are reported using subsets of radula morphology data denoted by habitat type (E=Eelgrass, M=Macroalgae) and site (FB=False Bay, MC= Merrifield Cove). Probabilities are calculated from data from all four tide series collections. P_{00} , P_{01} , P_{10} , P_{11} refer to transition probabilities calculated over a single 8-hour time step where 0=eelgrass and 1=macroalgae (Equation 5.1).Columns 7 and 8 represent retention probabilities of a snail remaining in its current habitat type over the duration of two months (Equation 5.2, *d*=60), representative of our entire collection period. Columns 9 and 10 are the dispersal probabilities given retention probabilities calculated in Columns 7 and 8 (Equation 5.3, *d*=60)

Habitat	**Site**	**P_{00}**	**P_{01}**	**P_{10}**	**P_{11}**	**P(stay in E)**	**P(stay in M)**	**P(leave E)**	**P(leave M)**
E,M	FB,MC	0.9967	0.0033	0.0050	0.9950	55%	41%	45%	59%
E	FB,MC	0.9966	0.0034	0.0073	0.9927	54%	27%	46%	73%
M	FB,MC	0.9970	0.0030	0.0032	0.9968	58%	56%	42%	44%
E,M	FB	0.9977	0.0023	0.0068	0.9932	66%	29%	34%	71%
E,M	MC	0.9948	0.0052	0.0035	0.9965	39%	53%	61%	47%
E	FB	0.9982	0.0018	0.0079	0.9921	73%	24%	27%	76%
M	FB	0.9967	0.0033	0.0059	0.9941	55%	34%	45%	66%
E	MC	0.9944	0.0056	0.0067	0.9933	36%	30%	64%	70%
M	MC	1.0000	0.0000	0.0010	0.9990	100%	83%	0%	17%

Chapter 6. CONNECTING HIGH SCHOOL CHEMISTRY CONCEPTS WITH ENVIRONMENTAL CONTEXT USING STUDENT-BUILT PH SENSORS

This manuscript has been previously published as: Seroy, S.K., Zulmuthi, H., Grünbaum, D. (2019) Connecting chemistry concepts with environmental context using student-built pH sensors. Journal of Geoscience Education 68(4): 334-344. This is an Accepted Manuscript of an article published by Taylor & Francis in Journal of Geoscience Education on Dec 20, 2019 and available online: https://doi.org/10.1080/10899995.2019.1702868

6.1 ABSTRACT

Educational research supports incorporating active engagement into K-12 education using authentic STEM experiences. While there are discipline-specific resources to provide students with such experiences, there are limited transdisciplinary opportunities that integrate engineering education and technological skill-building to contextualize core scientific concepts. Here, we present an adaptable module that integrates hands-on technology education and place-based learning to improve student understanding of key chemistry concepts as they relate to local environmental science. The module also supports disciplinary core ideas, practices, and cross-cutting concepts in accordance with the Next Generation Science Standards. We field-tested our module in three different high school courses: Chemistry, Oceanography and Advanced Placement Environmental Science at schools in Washington, USA. Students built spectrophotometric pH sensors using readily available electronic components and calibrated

them with known pH reference standards. Students then used their sensors to measure the pH of local environmental water samples. Assessments showed significant improvement in content knowledge in all three courses relating to environmental relevance of pH, and to the design, use and environmental application of sensors. Students also reported increased self-confidence in the material, even when their content knowledge remained the same. These findings suggest that classroom sensor building and collection of environmental data increases student understanding and self-confidence by connecting chemistry concepts to local environmental settings.

6.2 INTRODUCTION

Literature context

Recent education reforms have encouraged implementation of authentic STEM (Science, Technology, Engineering and Mathematics) experiences in K-12 education: those with real-world context that reflect actual methods that scientists and engineers use to conduct scientific research (National Research Council 2012, NGSS Lead States 2013). Authentic STEM experiences help students develop scientific knowledge via active engagement in practices which encourage them to think and act like scientists and engineers (Lee & Butler 2003). The Next Generation Science Standards (NGSS) promote authentic STEM experiences through three-dimensional engagement with *disciplinary core ideas, science and engineering practices* and *crosscutting concepts* that span a multitude of scientific fields (NGSS Lead States 2013). While such opportunities for K-12 students are growing, due in part to the increasing development of NGSS-aligned curricula, there are limited transdisciplinary educational modules that integrate STEM concepts across disciplines (National Research Council 2009, Honey et al. 2014).

Therefore, a present need exists for the development and assessment of transdisciplinary STEM curricula, particularly those that incorporate engineering and technology (Honey et al. 2014).

Engineering- and technology-based education help facilitate integrated and authentic STEM experiences. Engineering-based education engages students in active, hands-on learning connecting core STEM concepts through design and building solutions that address scientific challenges (Honey et al. 2014). Moreover, these active, hands-on learning experiences have demonstrated increases in student content knowledge and understanding of scientific concepts (Freeman et al. 2014). Such experiences through engineering activities encourage student creativity and cooperative problem-solving, enhancing student achievement, self-confidence, and attitudes toward STEM (Honey et al. 2014). A technology-based education provides students exposure to and experience with the tools and skills that drive technological advances necessary for STEM innovation to address scientific challenges. Technology-based activities also connect scientific concepts with societal relevance (Bennett et al. 2007), leveraging students' interest in technology in their everyday lives (Walia et al. 2007). Similar to engineering-based education, technology use in the classroom has been shown to positively correlate with student achievement and attitudes towards STEM (Liu 2005). For example, sensor-based lab activities in life sciences (Walia et al. 2007, Iskander & Kapila 2012), computer-assisted instruction in Earth science (Chang, 2000), robotics initiatives (Tims et al. 2011), and use of Makerspaces, student centers with technological tools to support creativity and design, (Hsu et al. 2017) have increased student achievement and helped develop student confidence in STEM. Teaching STEM in a transdisciplinary way, grounded in real-world technologies and context increases the relevance of material for students (National Research Council 2009, Honey et al. 2014)

Place-based educational approaches can help address the need for more integrated authentic K-12 STEM experiences by providing real-world context for scientific concepts. Place-based education emphasizes connections between classroom learning and places that students consider familiar and important (Sobel 2004, Semken et al. 2017). These approaches can be especially meaningful in the geosciences, as they provide students with the environmental context to apply and ground transdisciplinary STEM knowledge (Semken et al. 2017). Locally-relevant environmental phenomena can serve as "anchoring" events that help students frame their understanding of a scientific concept (Theobald et al. 2015; Thompson et al. 2018). Moreover, emphasis on locally relevant, real-world context in previous studies has yielded increased student comprehension, positive attitudes toward science (Bennett et al. 2007), and greater appeal to underrepresented student groups (Semken 2005, DeFelice et al. 2014, Semken et al. 2017). Many communities face locally-relevant environmental challenges that require innovative STEM solutions, which can serve to provide such real-world context. For example, in Washington State, water quality monitoring and development of water treatment systems were implemented to address oyster die-offs at local shellfish farms due to ocean acidification (Barton et al. 2015). Educators can use these challenges as meaningful and informative contexts to engage student interest. As educators work towards incorporating curricula to meet NGSS standards, resources and examples will be needed to support this engagement. Contextualizing learning with engineering, technology, and placed-based approaches offer students and educators unique opportunities for authentic, transdisciplinary STEM experiences that emulate scientific and engineering practices.

Purpose and learning objectives

Our goal was to develop an educational module that combines technology-based and place-based elements to provide students with a transdisciplinary and authentic hands-on STEM experience. Engaging students in hands-on sensor building serves as an excellent means to address this goal because it promotes transdisciplinary learning by introducing students to engineering design, construction and function of technological devices, computer programming and tools to test scientific hypotheses (Hotaling et al. 2012, Kelley & Grünbaum 2018). Sensor building facilitates authentic STEM experiences by engaging students in methods practiced by scientists, who regularly use sensor-based platforms to measure environmental parameters, such as pH in natural waters. Spectrophotometry is the one of the preferred methods used by scientists to measure pH in both freshwater environments (French et al. 2002) and marine environments (Clayton & Byrne 1993, Dickson et al. 2007). Scientists commonly use sensor-based techniques for local and global environmental monitoring and have even built custom low-cost DIY spectrophotometric pH sensors to meet their research needs (Yang et al. 2014). With easily accessible and inexpensive electronic components, it is more feasible than ever before for students to engage in simple sensor building. Furthermore, sensor building initiatives facilitate environmental literacy, lend real-world context to STEM concepts, and enable students to observe and investigate local effects of global environmental change in their own communities (Hotaling et al. 2012, Kelley & Grünbaum 2018).

Here, we present a field-tested sensor building module, adaptable for a variety of subject classes, that integrates hands-on technology education and a place-based approach to enable students to apply chemistry concepts to their local environments. The module is also aligned with NGSS goals (see Table 6.1). Student learning goals include: (1) to describe pH and explain spectrophotometry principles, (2) to develop skills in sensor building and sensor use and (3) to

apply knowledge of pH and sensors to an environmental context. Additionally, we designed our module to 'demystify' technology and make it more approachable for students with varying comfort and prior experience with technology. Constructing sensors from raw components can help address the lack of understanding of the function of commercially available sensors students typically use in the classroom (Hotaling et al. 2012). We emphasized multiple entry points for knowledge acquisition to increase accessibility (e.g. through hands-on design, collaborative group work and the need for a diverse set of skills).

Students built a simple spectrophotometer, used it to describe the relationship between red and blue light absorbance and pH across a range of standards by creating a calibration curve. They then used their calibration curve to assess the pH of a water sample from a local body of water. In the module, students built spectrophotometers and measured pH using a method analogous to, albeit less accurate than, a preferred method of environmental scientists (Clayton & Byrne 1993, French et al. 2002, Dickson et al. 2007). We assessed whether this sensor-building experience presented in a local environmental context helped achieve learning goals by measuring content knowledge and self-confidence in students who completed the module using pre- and post-test assessments.

This module was initially developed for use in an undergraduate introductory ocean technology course, through a graduate student teaching assistantship. It was later adapted for the high school level and piloted at two high schools in 2017, where initial discussion-based feedback was collected from teachers and students to improve the module. Through a collaboration with an undergraduate oceanography service-learning course, a student helped further improve the module and assessment by incorporating collected feedback and helped teach the final module as a course project. Improvements to the module based on student and teacher

feedback included reducing lecture components, simplifying written instructions, adding more visuals to lab guides, and building in more opportunities for discussion among students to process and engage with the material. The implementation described here is the final revised iteration of the module.

6.3 METHODS

Student population

We worked with students from two high schools located in coastal communities near Puget Sound, Washington, USA. At one school, five Chemistry classes (96 students) implemented the module following an acid-base chemistry unit in May 2018. The module was also implemented in January 2019 at another school in two Advanced Placement (AP) Environmental Science classes (45 students) during a unit on bodies of water, and in four Oceanography classes (68 students) as a part of an ocean chemistry unit. At both schools each class consisted of roughly 15-25 students. Additional student demographic data were not collected.

Concept introduction

Students were first introduced to environmental sensors by engaging in a short discussion using the guiding question: *What is a sensor and why might we want to use them to study the environment?* The discussion was facilitated by a teacher with students first discussing the prompt in small groups, then as a whole class. Small student groups (2-3 students each) were organized by the teacher prior to implementing the module and remained the same throughout the duration of the module. Students then watched a video we created on the use of sensors in

oceanographic science explaining how student-built sensors operate in much the same way (video: https://interactiveoceans.washington.edu/story/From_Cruise_to_the_Classroom). After the video, students returned to the guiding question to add to their previous ideas. Small group work and discussion-based learning was emphasized throughout the module as it enables students to process information by giving and receiving feedback, develops social practices of scientists and encourages critical thinking (Driver et al. 2000).

A 15-minute mini-lecture (see *Presentation Slides* in Supplemental Materials) was then presented by the teacher to the students to introduce three major concepts: (1) pH, (2) the environmental relevance of pH and, (3) the properties of light that are foundational to the function of spectrophotometric pH sensors. For concept 1, students were reminded of the pH scale and prompted with questions to discuss their everyday experiences with pH, distinguishing between acids and bases and the importance of measuring pH. For concept 2, pH was given environmental context using ocean acidification as an example. Ocean acidification is of local importance to coastal communities in Washington State, where the schools are located, affecting livelihoods, economies and cultural resources (Feely et al. 2012, Barton et al. 2015). Students were presented time-series data on the CO_2 concentration of the atmosphere from Mauna Loa Observatory, the partial pressure of CO_2 in ocean water and the corresponding ocean pH from oceanographic Station ALOHA (data available through NOAA PMEL Carbon Program: https://www.pmel.noaa.gov/co2/file/Hawaii+Carbon+Dioxide+Time-Series). Students were then prompted to discuss, in small groups and then as a class, the relationship between these variables, and the causes and implications of local environmental pH change. For concept 3, students were introduced to methods used to measure environmental pH, e.g. spectrophotometry, and basic principles of absorbance and transmittance of light through a medium that govern how

spectrophotometers work. Discussion questions for concepts 1-3 are listed in the *Lesson Plan* document in Supplemental Materials.

Students explored the relationship between the absorbance and transmittance of different color light through different color solutions using an online PhET simulation of Beer's Law that was analogous to the spectrophotometric pH sensor design (https://phet.colorado.edu/sims/html/beers-law-lab/latest/beers-law-lab_en.html). PhET simulations have been shown to support authentic STEM experiences by helping students think critically about physics concepts (Wieman et al. 2008). Students explored the online simulation in small groups using an in-class worksheet (*Simulation Worksheet* in Supplemental Materials), enabling them to discover relationships between light absorbance and transmittance they would later use when interpreting their sensor data. Teachers facilitated the concept introduction, mini-lecture, simulation exercise and related discussions.

Sensor construction and application

Students worked together in previously formed small groups. Each student group was provided a color-coded kit containing all the necessary sensor components, such that the technology would be more accessible for students who had not had prior exposure to electronics (Figure 6.1a, *Sensor Parts List* and *Instructor Setup Guide* available in Supplemental Materials). Student groups worked through the *Sensor Assembly Instructions* document (see Supplemental Materials) in a self-guided manner to construct a spectrophotometric pH sensor from the sensor kit (Figure 6.1b). Once assembled, students confirmed their sensor was operational by connecting the sensor to a laptop to communicate with it. Students communicated with sensors using Beagle Term, an app for Google Chrome that emulates a serial terminal enabling students

to send commands directly to the sensor (Han & Lim 2016). Students were prompted to type two lines of code, which returned the transmittance of light from the LED to the light sensor. At this step, students engaged in troubleshooting if necessary by correcting common errors, such as loose or incorrect wire connections (see *Instructor Troubleshooting Guide* and *Presentation Slides* in Supplemental Materials). After confirming sensors were operational, student groups completed a short checkpoint discussion with an instructor (see *Lesson plan* in Supplemental Materials). Students were required to explain how the sensor functioned and the significance of the data returned by their sensor prior to using the sensor. Checkpoint questions were incorporated into the module to facilitate comprehension through informal discussion and enable the instructor to assess student understanding midway through the module.

Student groups then worked through the *Lab Procedure* document (see Supplemental Materials) where the sensor was used to measure the transmittance of red and blue light through five standard pH solutions: pH 3, 5, 7, 9, and 11. The lab procedure was designed to guide students through the use of the sensor with clear visual aids to reduce barriers to understanding the material, and to enable groups to work at their own pace. Standards were colored with red cabbage juice, a pH indicator dye (Figure 6.1c). Students then input their data into the pre-built MS Excel *Student Datasheet* (see Supplemental Materials) to create a calibration curve for their sensor (Figure 6.1d). The datasheet was pre-built to encourage students to focus on the patterns generated from their data and to ensure that a lack of experience using MS Excel would not be a barrier to data interpretation.

Using their calibration curve, students identified the unknown pH of a seawater sample collected locally from Puget Sound (sample collection instructions in *Instructor Setup Guide*). This local seawater sample was also used as a connection to the earlier discussion of ocean

acidification in the concept introduction. After identifying the pH of a local sample, groups reported their measurements to calculate a class average. Students were then asked to discuss findings, the sensors' strengths and limitations, and how the sensor function compared with the online Beer's Law simulation in respective small groups and then as a class. Students also identified additional local environments (e.g. streams, lakes, marine areas) in which to use their sensor, and they proposed sampling regimes of these environments to address questions of interest. Final discussion questions were facilitated by instructors and are listed in the *Lesson plan* (see Supplemental Materials). Total class time needed to implement the module was approximately three hours, one for the concept introduction, one for sensor construction, and one for sensor application and use (more details in *Lesson Plan* in Supplemental Materials). Complete Supplemental Materials to conduct the module can also be found at http://publicsensors.org/K12modules/pHsensor/.

Assessment of student learning

We evaluated student learning over the duration of the module using pre- and post-test assessments (Figure 6.2). Learning assessments were developed through personal communication with a K-12 education research associate at the University of Washington College of Education. Assessment questions prompted both written and diagrammatic explanations related to the application and environmental relevance of pH rather than recalling information from the classroom lecture. Students were also asked to self-report their confidence level when answering content knowledge questions.

Students answered assessment questions on the following concepts: (1) pH basics, (2) environmental pH monitoring tools, (3) impacts of environmental pH changes, (4) causes of

environmental pH changes, (5) properties of light necessary to understand spectrophotometric principles, and (6) sensor design. Pre- and post- assessments were blindly scored, using methods similar to Chan et al. (2012), with a scale of 0-4 for the following criteria: 0 - blank, 1 - attempted but incorrect, 2 - partially correct with some incorrect logic, 3 - correct but incomplete, 4 - correct and complete. Self-reported confidence in the material was also scored on a 0-4 scale, where students were asked which statement they identified with most: 0 - blank, 1 - "I have no idea", 2 - "I have some idea, but mostly unsure", 3 - "I feel comfortable but not confident", 4 - "I feel very confident". One Oceanography class of 17 students did not take the post-assessment so corresponding pre-assessments were removed from the analysis. Comparison of pre- and post-assessment scores were assessed with a non-parametric Wilcoxon rank sum test using R version 3.4.1 (R Core Team, 2017) to detect changes in mean scores before and after students completed the module. Significance was determined at an $\alpha = 0.05$ threshold.

After completing the module, we facilitated discussions and asked students to provide informal feedback on their experience completing the module in small groups, then as a whole class. We also had informal conversations with teachers for anecdotal feedback after the module was completed. Discussions were not formally recorded. Chemistry teachers independently solicited written student feedback on the degree to which they found the module engaging and enjoyable.

6.4 RESULTS

In all courses (Oceanography, AP Environmental Science and Chemistry), assessment scores showed significant increases in student understanding of (1) properties of light governing spectrophotometry principles and (2) sensor design (Figure 6.3a, 6.3c, 6.3e). Students in all

classes exhibited low prior knowledge of properties of light governing spectrophotometry principles with average pre-test scores of 0.78, 0.56 and 1.75, out of a maximum possible score of 4.0, for Oceanography, AP Environmental Science, and Chemistry respectively. Students exhibited similarly low prior knowledge in sensor design with average pre-test scores of 0.98, 0.71 and 1.35 in these courses respectively, suggesting limited prior exposure to spectrophotometric instrumentation and technology. However, post-test scores indicated that students in all courses demonstrated significant improvement in their understanding of these two topics. Average student scores in properties of light governing spectrophotometry principles increased by 1.67, 0.85, and 0.96 in Oceanography, AP Environmental Science and Chemistry classes respectively. Similarly, average scores in sensor design increased by 1.52, 1.31, and 1.53 in these courses.

Students in all courses also exhibited an increased understanding of environmental pH monitoring tools (Figure 6.3a, 6.3c, 6.3e). In this assessment category, average pre-test scores were lower in Oceanography (1.56) and AP Environmental Science (1.87) than in Chemistry (3.28). Despite these differences in prior knowledge across disciplines, students in all courses showed improved content knowledge in this category with significant average score increases of 1.89, 1.42, and 0.48 in Oceanography, AP Environmental Science and Chemistry classes respectively.

Students in all courses reported increased self-confidence in all assessment categories (Figure 6.3b, 6.3d, 6.3f). Students generally exhibited low initial self-confidence in (1) properties of light governing sensor function and (2) sensor design. In these two categories respectively, students demonstrated low average pre-test confidence scores of 1.34 and 1.31 in Oceanography, 1.24 and 1.27 in AP Environmental Science, and 1.74 and 1.32 in Chemistry. After completing

the module, students exhibited increases in self-confidence in both categories, which accompanied the above-described significant increases in content knowledge. In properties of light governing spectrophotometry principles, average confidence scores significantly increased by 0.82, 0.37, and 0.89 in Oceanography, AP Environmental Science, and Chemistry classes respectively. In sensor design, students demonstrated average score increases of 0.91, 0.49, and 1.19 in these classes respectively, with statistically significant increases in Oceanography and Chemistry. Student confidence scores increased significantly in all other assessment categories as well, sometimes even when there was no associated significant increase in content knowledge. Average post-test confidence scores increased by 0.44, 0.46, and 0.33 in fundamental pH concepts, and 0.54, 0.39, and 0.51 in environmental context of pH for Oceanography, AP Environmental Science, and Chemistry classes respectively.

Cross-course comparison

In Oceanography courses, students exhibited significant increases in their content knowledge in all assessment categories with corresponding significant increases in their confidence in the material (Figure 6.3a, 6.3b). Oceanography students demonstrated significant content knowledge gains with average score increases of 1.02 in fundamental pH concepts, 1.89 in environmental pH monitoring tools, 1.23 in environmental pH change impacts, 1.66 in environmental pH change causes, 1.67 in properties of light governing spectrophotometry principles, and 1.52 in sensor design.

In AP Environmental Science, students exhibited significant increases in their content knowledge in all assessment categories except (1) impacts and (2) causes of environmental pH change (Figure 6.3c, 6.3d). Pre-test scores were higher in these categories, 2.47 and 2.38

respectively, than in the other assessment categories where average pre-test scores were below 2.0. Students exhibited increased post-test scores in these categories, but they were not significant. Despite non-significant content knowledge increases in these two categories, students demonstrated significant increases in self-confidence in environmental pH context with an average confidence score increase of 0.39. In the remaining content knowledge categories, students demonstrated significant score increases. Average student scores increased significantly by 0.77 in fundamental pH concepts, 1.42 in pH monitoring tools, 0.85 in properties of light governing spectrophotometry principles and 1.31 in sensor design.

Chemistry students did not demonstrate significant increases in their understanding of (1) fundamental pH concepts, (2) impacts of environmental pH change or (3) causes of environmental pH change (Figure 6.3e, 6.3f). Students showed considerable prior knowledge in these three topics with high pre-test averages of 3.51, 3.6 and 2.89 respectively, unlike in the other two courses. In these categories where content knowledge was already high, Chemistry students did not demonstrate significant score increases after the module. However, students exhibited significant increases in confidence scores in all categories, including those without significant content knowledge increases. In the remaining categories, Chemistry students exhibited significant increases in their understanding of sensors and their application to the environment. Average post-test scores increased significantly by 0.48 in environmental pH monitoring tools, 0.96 in properties of light governing spectrophotometry principles and 1.53 in sensor design.

Feedback

From whole-class discussions conducted after completing the module, students generally found the module enjoyable and engaging. This was supported by written student comments in the Chemistry classes. Quotes reported here refer to written comments which were independently solicited by teachers from Chemistry students only. Chemistry students described the module as "fun", "cool", "awesome" and "interesting". Many students made specific references to enjoying building sensors, reporting that they "liked the hands-on aspect of building the sensors" and "building the spectrophotometer was fun". The integration of technology was also cited as an enjoyable experience with students commenting that "it was fun making electronics and working with programming" and the module "involved using technology that is not usually used which was engaging". However, some students reporting feeling "frustrated" and "confused" with the use of technology because of "technical issues" and the need for troubleshooting, although "enjoying trying to fix things" was also mentioned. Despite some references to frustration, students reported the approachability of the module and the sensor stating it was "easy to understand", "simple and easy to follow" and "not at all hard to do".

Chemistry students also reported that the module was an integrative experience that "combines engineering and science" and provided an authentic STEM opportunity, in which they "felt like a scientist" and "learned how to build a sensor and record different pH levels like scientists". Students also mentioned the relevance and importance of the context provided in the module, citing it was "cool to see a real-life application of what we are learning", "it had applications for future everyday use" and there was a "good connection between class and real-world science". See Appendix E for the complete list of Chemistry student quotes that were received.

In our informal conversations with teachers, they expressed enthusiasm for including hands-on technology opportunities in their courses and noted the broad applicability of the module in other natural and physical science courses. Teachers commented that the nature of the module appealed to a diversity of students and engaged some who were typically more reserved. Though we do not have a formal record of all teacher comments, one teacher expressed in an email that "having students in my class become engineers of their own pH meters helped them understand better how pH works in our oceans and why monitoring pH is important".

6.5 DISCUSSION

Student outcomes

The pH sensor building module provided students with an authentic STEM experience. Through this experience, students were exposed to accessible technology that helped them learn and apply chemistry concepts. Our assessment results suggest that students largely met the learning goals of the module by demonstrating significant learning gains in fundamental pH concepts (significant score increases of 1.02 in Oceanography, 0.77 in AP Environmental Science), spectrophotometry principles (significant score increases of 1.67 in Oceanography, 0.85 in AP Environmental Science, 0.96 in Chemistry), sensor design (significant score increases of 1.52 in Oceanography, 1.31 in AP Environmental Science, 1.53 in Chemistry) and the environmental applications of sensors (significant score increases of 1.89 in Oceanography, 1.42 in AP Environmental Science, 0.48 in Chemistry). Students also developed skills in sensor building, with feedback suggesting that the hands-on experience was important for their learning. Student assessments showed increased self-confidence in both new and familiar material, determined from pre-test responses. This demonstrated the benefit of such active sensor building

experiences, even when students had considerable content knowledge. This adds further evidence that technology-based approaches connect classroom chemistry concepts to environmental contexts and increase student knowledge and self-confidence. Observed increases in student confidence during our module and anecdotal student feedback corroborate previous studies (Bennett et al. 2007) showing that connecting learning to society through technology improved student attitudes towards science.

Comparison of the difference subject courses

Implementations of our sensor building program in high school Chemistry, Oceanography and AP Environmental Science courses enabled us to test its efficacy across multiple disciplines. The module was successfully integrated into three different subject courses with significant student learning gains in all three, demonstrating its ability to support student learning in a diversity of subjects. The module was therefore adaptable and relevant, with the place-based approach contributing real-world context for students in all three courses. Not surprisingly, Chemistry students demonstrated the most prior knowledge of pH, with a high pre-test average of 3.51. The module directly followed an acid-base chemistry unit in this course, suggesting Chemistry students had had the most recent exposure to pH and retained a proportion of this knowledge set. Oceanography students increased their content knowledge in the greatest breadth of topics after completing the module, including foundation pH concepts. AP Environmental Science students also demonstrated increases in content knowledge in foundational pH concepts. pH was likely not a new concept for students in these courses, but it was presented outside of a traditional chemistry course which may have presented an additional challenge in transferring their prior knowledge. Students across all disciplines also increased

their confidence in all assessment categories. This suggests hands-on sensor building opportunities are capable of building student self-confidence in STEM concepts in various disciplinary settings.

Broadening the place-based approach

A key component of our module was its place-based approach. Students tested water samples from their local environment and reflected on specific locations where their sensor would enable them to address scientific questions in their own local communities. Here, the module was presented in the context of ocean acidification, a locally-relevant phenomena common in coastal Washington near the schools. However, students who participated in the module also proposed sensor-based monitoring in non-marine environments such as local streams, lakes, and the school pool. These proposals demonstrated the flexibility of the module to meet local interests of the students. They also demonstrate student understanding of the range of applications even though the module was framed around ocean acidification. To adapt the module to non-marine contexts, instructors can have students test the pH of samples from any local waterway using the student-built sensor. Additionally, instructors can substitute any locally-important example for slide 4 in the *Presentation Slides* (Supplemental Materials) to adapt the module to a local environmental concern in need of ecological monitoring. The adaptability of our module to local environmental needs expands authentic STEM opportunities among diverse student populations, supporting achievement and retention of underrepresented students in the geosciences (Semken 2005, DeFelice et al. 2014, Semken et al. 2017).

Supporting the goals of NGSS

The spectrophotometric pH sensor module provided students with an authentic and integrative STEM experience that emulated how professional scientists investigate environmental change. The module provided students with increased content knowledge in core NGSS physical science, Earth science and engineering concepts through the construction and use of a sensor that enabled them to engage in authentic science and engineering practices. Specifically, the module was modeled after actual scientific protocols used to make spectrophotometric pH measurements and conveyed to students that scientists often build their own instruments, including for this particular purpose (Yang et al. 2014). Overall, the module contributes to a growing body of resources for teachers that incorporate authentic STEM experiences and evidence-based teaching practices which meet NGSS standards.

Limitations

We documented many successes of the module. However, there are some limitations to the data interpretation. Student learning gains were reported across three different disciplinary courses. Differences in learning gains and module effectiveness across the three classes were attributed to specific fields of study associated with the course. However, classes differed in several other ways that may have influenced assessment results, such as different instructional approaches that may have introduced additional variability in our data. Demographic data and student educational history may have also helped explain differences in assessment scores; however, we did not collect these data. Additional data regarding student grades and performance in the course would have been informative to interpret our results and situate the benefits of the module in the larger framework of a course.

Students self-reported increased confidence in the material in all three courses. Confidence scores may have been affected by external variables for which we did not account, such as gender or educational experience (MacPhee et al. 2013). In some instances, students exhibited a significant increase in confidence without an associated significant increase in content knowledge. While we interpreted this positively - that students increased their confidence even in concepts they understood well - this may also be a result of student metacognitive skills and difficulty in self-assessment (Kruger & Dunning 1999).

We used student quotes to support assessment interpretations. However, we received written feedback from Chemistry students only. Oceanography and AP Environmental Science students expressed similar comments in whole class discussions, but these were not formally recorded. We have assumed Chemistry student quotes to be largely representative of the student experience across all three courses. Therefore, caution should be exercised in interpreting our student feedback data for other contexts.

The pH sensor constructed in the module is accurate to approximately +/- 0.5 pH units, if measurements are conducted carefully. However, from our experience in the classroom, accuracy tends to be closer to approximately +/- 1.0 pH units, given the variability in and sources of error introduced during student use. Sources of error can be minimized by ensuring that the LED and light sensor are well secured in the student-built pH sensors and that careful attention is paid to sample preparation and indicator dye use directions in the *Lab Procedure* (Supplemental Materials).

Beyond the high school classroom

The current module is intended to educate a high school audience, but it is further adaptable and has also been used in additional settings aside from the implementation and evaluation described here. The module has been incorporated in professional development workshops for high school science teachers to provide training on connections between climate, chemistry and scientific instrumentation. An adaptation of the module has been used to teach upper-level oceanography undergraduates about sensor construction and function in an introductory ocean technology course, and it has the potential to be adapted for other undergraduate courses.

The module has also been used as a tool to train undergraduates in science communication and pedagogy. In an undergraduate oceanography service-learning course, the module was used as an example to teach students about creating and aligning teaching materials with NGSS standards. Most undergraduate STEM education does not include science communication training, prompting calls for increasing its inclusion for undergraduate STEM majors (Brownell et al. 2013). Engaging in such experiences has demonstrated benefits for undergraduates including skill development and increased confidence as science communicators (Dohaney et al. 2017). Our module can help serve to provide undergraduates with science communication opportunities while simultaneously engaging high school students in valuable sensor building learning experiences.

At present, the model requires visual confirmations to build and communicate with the sensor, and record and interpret data in an MS Excel spreadsheet. However, the module can be made more broadly inclusive, and could be coupled with assisted technologies to support students with visual impairments. Screen readers could be used to read out sensor values and enable interaction with the MS Excel datasheet, and braille tablets could enable students to type

code, though we have not tested this. Modules like ours present diverse avenues for training educators and science communicators, and for educating future scientists and scientifically literate citizens.

6.6 ACKNOWLEDGEMENTS

The authors gratefully acknowledge assistance from Kareen Borders, Tansy Clay Burns, Deb Morrison, Deb Kelley, Katie Bigham, Robert Levine, Isaiah Bolden, Amy Wyeth and Deana Crouser. We thank Chemistry teachers Isaac Rapelje, Brittany Murdach and Lynette Jenne, Oceanography teacher Beverly Painter, and AP Environmental Science teacher Stephanie Winslow for allowing us to work with them in their classrooms. We thank the Washington State Sea Grant (NA10OAR-4170057) and NSF (OCE-1657992) for supporting sensor development, and the Olympic STEM Partnership Program for connecting our group with teachers and providing funding for sensor building materials.

References

Barton A, Waldbusser GG, Feely RA, Weisberg SB, Newton JA *et al*. (2015) Impacts of coastal acidification on the Pacific Northwest shellfish industry and adaptation strategies implemented in response. Oceanography 28:146-159

Bennett J, Lubben F, Hogarth S (2007) Bringing science to life: A synthesis of the research evidence on the effects of context-based and STS approaches to science teaching. Sci Educ 91:347-370

Brownell SE, Price JV, Steinman L (2013) Science Communication to the General Public: Why We Need to Teach Undergraduate and Graduate Students this Skill as Part of Their Formal Scientific Training. J of Undergrad Neurosci Educ 12:E6-E10

Chan KYK, Yang S, Maliska ME, Grünbaum D (2012) An interdisciplinary guided inquiry on estuarine transport using a computer model in high school classrooms. Am Biol Teach 74:26-33.

Chang CY (2000) Enhancing tenth graders' earth science learning through computer-assisted instruction. J Geosci Educ 48:636-640.

Clayton TD, Byrne RH (1993) Spectrophotometric seawater pH measurements: total hydrogen ion concentration scale calibration of m-cresol purple and at-sea results. Deep-Sea Res Part I 40:2115-2129

DeFelice A, Adams JD, Branco B, Pieroni P (2014) Engaging underrepresented high school students in an urban environmental and geoscience place-based curriculum. J Geosci Educ 62:49-60

Dickson AG, Sabine CL, Christian JR (2007) Guide to best practices for ocean CO_2 measurements. North Pacific Marine Science Organization.

Dohaney J, Brogt E, Wilson TM, Kennedy B (2017) Using role-play to improve students' confidence and perceptions of communication in a simulated volcanic crisis. In Observing the Volcano World. Springer, Cham, Switzerland, p 691-714

Driver R, Newton P, Osborne J (2000) Establishing the norms of scientific argumentation in classrooms. Sci Educ 84:287-312

Feely RA, Klinger T, Newton JA, Chadsey M (2012) Scientific summary of ocean acidification in Washington State marine waters. NOAA OAR Special Report

Freeman S, Eddy, SL, McDonough M, Smith MK, Okoroafor N, Jordt H, Wenderoth MP (2014) Active learning increases student performance in science, engineering, and mathematics. P Natl Acad Sci USA 111:8410-8415.

French CR, Carr JJ, Dougherty EM, Eidson LA, Reynolds JC, DeGrandpre MD (2002) Spectrophotometric pH measurements of freshwater. Anal Chim Acta 453:13-20

Han J, Lim S (2016) Beagle Term (1.8.2) [Mobile Application Software]. Retrieved from <https://chrome.google.com/webstore/detail/beagle-term/gkdofhllgfohlddimiiildbgoggdpoea?hl=en>

Honey M, Pearson G, Schweingruber H. (eds) (2014) STEM integration in K-12 education: Status, prospects, and an agenda for research (Vol. 500). National Academies Press, Washington DC

Hotaling L, Lowes S, Stolkin R, Lin P, Bonner J, Kirkey W, Ojo T (2012) SENSE IT: Teaching STEM principles to middle and high school students through the design, construction, and deployment of water quality sensors. Adv Eng Educ 3:n2

Hsu YC, Baldwin S, Ching YH (2017) Learning through making and maker education. TechTrends 61:589-594

Iskander M, Kapila V (2011) Revitalizing achievement by using instrumentation in science education (RAISE), a GK-12 fellows project. J Prof Iss in Eng Edu Pr 138:62-72

Kelley DS, Grünbaum D (2018) Seastate: Experiential C-STEM learning through environmental sensor building. Oceanography 31:147

Kruger J, Dunning D (1999) Unskilled and unaware of it: how difficulties in recognizing one's own incompetence lead to inflated self-assessments. J Pers Soc Psychol 77:1121

Lee HS, Butler N (2003) Making authentic science accessible to students. Int J Sci Educ 25:923-948.

Liu M (2005) The effect of hypermedia learning environment on middle school students' motivation, attitude, and science knowledge. Computers in the Schools, The Haworth Press, Inc. 22:159-171

MacPhee D, Farro S, Canetto SS (2013) Academic self-efficacy and performance of underrepresented STEM majors: Gender, ethnic, and social class patterns. Anal Soc Issues Public Policy 13:347-369

National Research Council (2009). Engineering in K–12 education: Understanding the status and improving the prospects. The National Academies Press, Washington DC

National Research Council (2012) A Framework for K-12 Science Education: Practices, Crosscutting Concepts, and Core Ideas. The National Academies Press, Washington DC

NGSS Lead States (2013) *Next Generation Science Standards: For States, By States*. The National Academies Press, Washington DC

R Core Team (2017) R: a language and environment for statistical computing. R Foundation for Statistical Computing, Vienna. www.r-project.org

Semken S (2005) Sense of place and place-based introductory geoscience teaching for American Indian and Alaska Native undergraduates. J Geosci Educ 53:149-157

Semken S, Ward EG, Moosavi S, Chinn PW (2017) Place-based education in geoscience: Theory, research, practice, and assessment. J Geosci Educ 65:542-562

Sobel D (2004) Place-based education: Connecting classroom and community. Nature and Listening 4:1-7

Theobald EJ, Crowe A, HilleRisLambers J, Wenderoth MP, Freeman S (2015) Women learn more from local than global examples of the biological impacts of climate change. Front Ecol Environ 13:132-137

Thompson JJ, Windschitl M, Braaten M (2018) *Ambitious Science Teaching*. Harvard Education Publishing Group, Cambridge, MA

Tims H, Corbett K, Hall D, Turner G, Harbour D (2011, October). Work in progress - Application of the Boe-Bot in teaching K12 electricity fundamentals. In 2011 Frontiers in Education Conference (FIE) Rapid City, SD p S2D-1

Walia M, Yu E, Iskander M, Kapila V, Kriftcher N (2007) The modern science lab: Integrating technology into the classroom is the solution. In Advances in Computer, Information, and Systems Sciences, and Engineering, Springer, Dordrecht, p. 358-363

Wieman CE, Adams WK, Perkins KK (2008) PhET: Simulations that enhance learning. Science 322:682-683.

Yang B, Patsavas MC, Byrne RH, Ma J (2014) Seawater pH measurements in the field: a DIY photometer with 0.01 unit pH accuracy. Mar Chem 160:75-81

Figure 6.1. (a) Color-coded materials students use to build their spectrophotometric pH sensor, (b) a student-constructed sensor, (c) pH standard solutions mixed with red cabbage juice as a colorimetric pH indicator and (d) the calibration curve generated from the *Student datasheet* MS Excel spreadsheet using above pH standards which described the relationship between the absorbance of red and blue light and the color (pH) of a solution. Pink and blue squares represent the intersection point of the calibration curve with student-generated absorbance data for an environmental sample of unknown pH. Dashed lines on the calibration curve show how students interpolate the pH of their environmental sample from absorbance values. Students take the average pH from their red and blue light approximations.

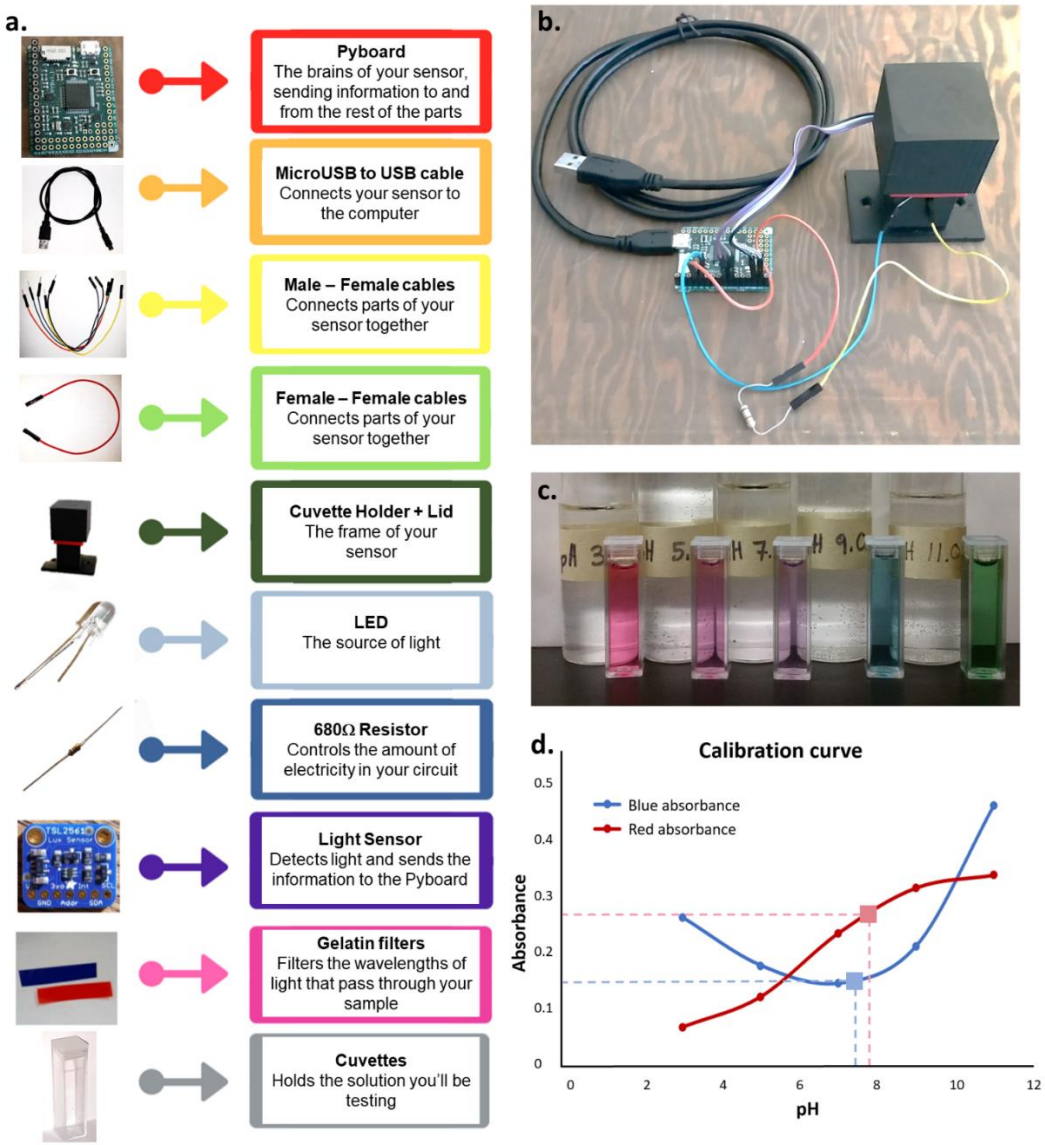

Figure 6.2. Student assessment questions used to collect information on student content knowledge and confidence in the material before and after completing the module.

1. Draw and explain how you use the pH scale to identify acids and bases.

Check the box that best describes your ability to answer this question	
I have no idea	☐
I have some idea but mostly unsure	☐
I feel comfortable but not confident	☐
I feel very confident	☐

2. You are a marine scientist. Your records show that the pH of ocean water is dropping.

   a. As a scientist, what tools would you use to monitor pH?

   b. Why do marine scientists care about ocean pH?

   c. Describe a factor that might cause ocean pH to change.

Check the box that best describes your ability to answer this question	
I have no idea	☐
I have some idea but mostly unsure	☐
I feel comfortable but not confident	☐
I feel very confident	☐

3. Describe what happens when white light goes through a red solution. What color(s) light is absorbed and what color(s) light is transmitted?

Check the box that best describes your ability to answer this question	
I have no idea	☐
I have some idea but mostly unsure	☐
I feel comfortable but not confident	☐
I feel very confident	☐

4. You need to identify the exact pH of a solution. The solution has been mixed with a pH indicator dye and changed color. You are given the following pieces to make a pH sensor:

   • Light sensor • LED (light source)

Draw a diagram of how you would assemble and use these components to measure the pH of your solution. You can add extra components if needed. Label your diagram.

Check the box that best describes your ability to answer this question	
I have no idea	☐
I have some idea but mostly unsure	☐
I feel comfortable but not confident	☐
I feel very confident	☐

Figure 6.3. Student assessment data by course. Light grey bars represent student scores before completing the module and dark grey bars denote student scores after completing the module for each assessment question. Asterisks denote significant improvements in score and confidence. Error bars denote the standard error. Data is presented from 51 students in Oceanography, 45 students in AP Environmental Science and 96 students in Chemistry.

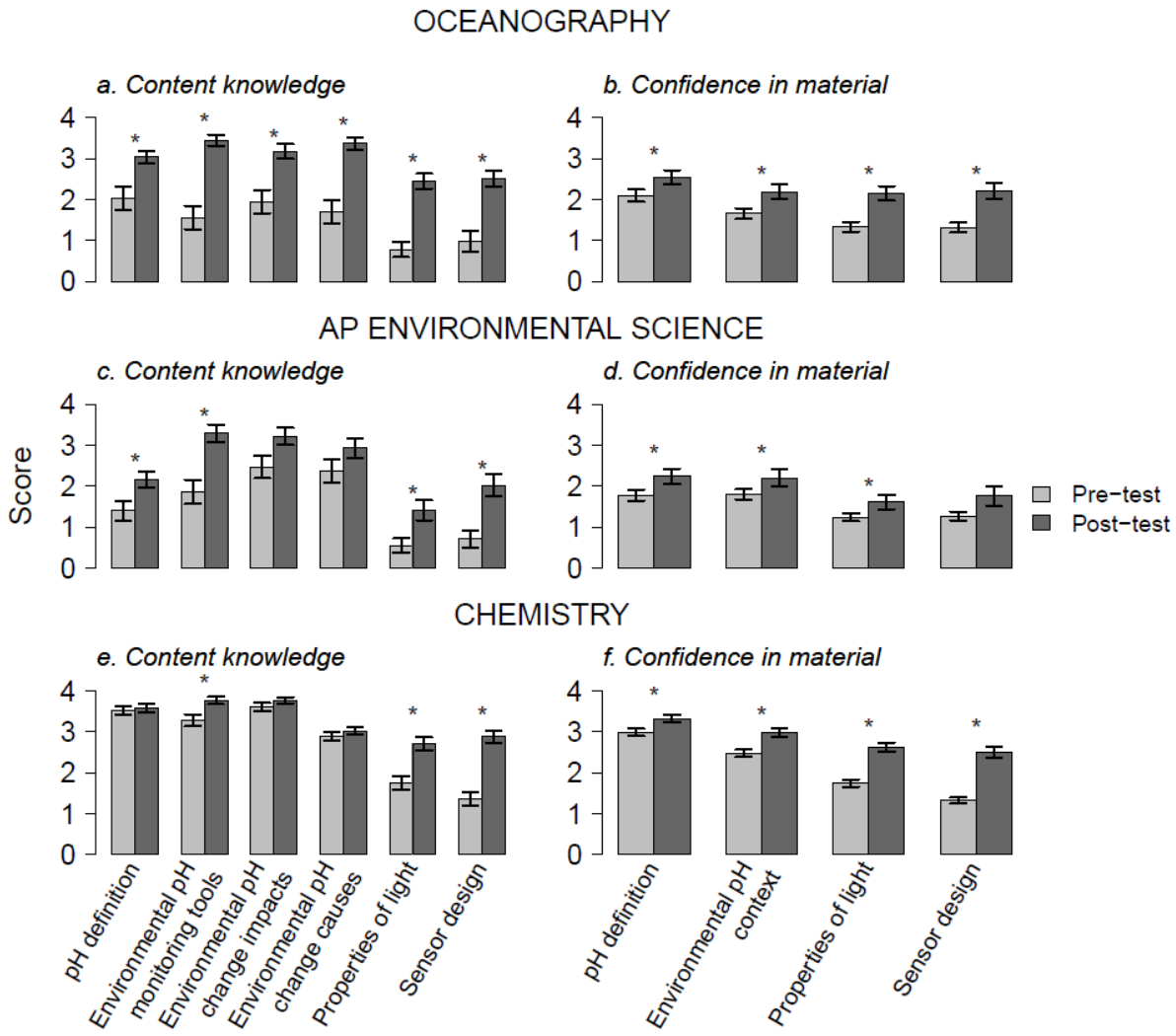

Table 6.1. NGSS disciplinary core ideas, science and engineering practices and crosscutting concepts addressed by the module in conjunction with the corresponding module component that supports that standard.

	NGSS Standard (Grades 9 -12)	Module component
Disciplinary Core Ideas	PS4.B: Electromagnetic Radiation	Students learn about light absorbance and transmittance and use a Beer's law simulation to understand how their spectrophotometric sensor works.
	PS4.C: Information Technologies and Instrumentation	Students build their own sensor and learn how technology and instrumentation support scientific questions.
	ESS3.D: Global Climate Change	Students learn how scientists use sensors to monitor climate change and ocean acidification. Students collect data using their sensor within the framework of monitoring their local environment to record changes.
	ETS1.C: Optimizing the Design Solution	Students build and troubleshoot a sensor to collect environmental data. They consider strengths and limitations of their sensor.
Science and Engineering Practices	Planning and Carrying Out Investigations	Students conduct an investigation using their sensor to identify the pH of an environmental sample.
	Analyzing and Interpreting Data	Students analyze their data using their calibration curve and interpret it in the context of their local environment.
	Using Mathematics and Computational Thinking	Students create a calibration curve and use the relationships they create between pH and light absorbance to assess environmental samples. They are also introduced to basic coding to communicate with their sensor.
Crosscutting concepts	Patterns	Students use their calibration curve to describe the relationship between pH and light absorbance.
	Cause and effect	Students explain how their sensor works and how differences in light intensity cause the sensor readings to change. Students learn about the causes and effects of ocean acidification.
	Stability and Change	Students learn how sensor building and environmental monitoring help detect changes related to natural variability and climate change.

Chapter 7. CONCLUSION

A key objective of this dissertation was to use inducible traits as tools to gain insight into how marine communities are responding to ocean change. Inducible morphologies were particularly useful because they provided a quantifiable marker of species interactions and enabled inferences about ecological interactions across time and space. I demonstrated the value of using these inducible morphologies to understand both population- and community-level ecological interactions in a changing environment, particularly those that would have been difficult to measure otherwise. Inducible defenses -- spine growth due to chemical cues from predators -- in the bryozoan *M. membranacea* enabled tracking of predator-prey interactions in ocean acidification conditions and, coupled with modeling, enabled quantifying costs of defense to fitness in the context of space competition within a population. It is generally difficult to observe exposure to predation over time in epibiont communities but monitoring inducible spines can reveal historical proximity of predators. Inducible offenses -- variable tooth morphologies induced by chemical cues of different food substrates -- in the marine snail *L. vincta* presented a method to document population-level dispersal and experimentally investigate the fitness consequences of dispersal in a warming ocean. Quantifying dispersal between habitats for small marine organisms is very difficult, but these studies have done so successfully using the individual histories recorded in tooth morphology. Inducible traits are common across a wide range of taxa (Tollrian & Harvell 1990, Kishida et al. 2010) and these results suggest that taking advantage of these traits can provide meaningful future studies to understand the causes and consequences of community responses to a variety of environmental stressors.

These studies of inducible morphologies also demonstrated that responses of both *M. membranacea* and *L. vincta* to environmental stresses (OA and warming, respectively) were shaped by population- and community-level interactions. Trophic interactions, competition, and population-level processes modulated organism responses highlighting the importance of interactions in shaping community responses to change. *M. membrancea* responses to OA were dependent on exposure to predators, and their impacts were strongly influenced by space competition imposed by the density of competitors for space in the local community. Similarly, *L. vincta* responses to warming were dependent on community-level abundance and geographic proximity of habitats dominated by different food types. Population-level processes like space competition (*M. membranacea*) and dispersal consequences (*L. vincta*) also exerted pressures that modified individual responses.

For both organismal systems, inducible morphologies influenced responses to ocean change variables. These responses showed both organisms to be largely tolerant of range of OA (*M. membrancea)* and temperature (*L. vincta*) with trophic interactions modifying organism fitness more than changing environmental conditions. This suggests that both organisms may be well-positioned to manage near-future ocean conditions, unlike some other more vulnerable organisms (Kroeker et al. 2013). This is a positive outcome, and it is important to find species and communities that are tolerant of predicted stresses, at least in the near-term. Those organisms may help stabilize future marine communities and understanding characteristics of these resilient organisms will lead to better prediction and mitigation of ocean change impacts. Therefore, understanding the relative magnitudes between direct effects of ocean change and effects of species interactions in shaping organism responses can help shed light on community responses to changing environments (Kordas et al. 2011, Kroker et al. 2017).

The observed tolerance of both organisms to ocean change variables may be due to the naturally variable environments they inhabit, especially with respect to the environmental stressor each was exposed to. Organisms from highly variable environments have been demonstrated to be more tolerant of ocean change conditions (Boyd et al. 2016). As an epibiont, *M. membranacea* experiences significant pH fluctuations within the macroalgal boundary layer where photosynthesis and respiration change pH on daily cycles (Noisette & Hurd 2018). Likewise, as a shallow subtidal and low intertidal organism, *L. vincta* is exposed to daily and seasonal temperature fluctuations (Ruesink et al. 2010) that may pre-adapt these snails to near future warming. Generally, the findings from this dissertation underscore the importance of considering species interactions (Kordas et al. 2011, Kroeker et al 2014).

From this work, the tolerance of near-future pH and temperature conditions exhibited by *M. membrancea* and *L. vincta* may identify these organisms as potential “winners" in response to climate-related changes. However, while these experiments only exposed organisms to a single stressor at a time, in the field organisms are exposed to multiple stressors concurrently. Combined exposure to OA and warming can induce synergistic or antagonistic effects (Byrne & Przeslawski 2013, Kroeker et al. 2013, Kroeker et al. 2017) and future studies should investigate how such compounding stressors influence the organisms and interactions studied in this dissertation. Therefore, future studies should investigate if the responses observed here remain the same in the context of multiple stressors or if these organisms exhibit vulnerabilities that were not measured. In addition, understanding these effects in conjunction with other community members can help lend insight to cumulative community responses to ocean change. For example, while *L. vincta* responses remained unchanged by temperature and *M. membranacea*

exhibited some positive responses to moderate OA, these effects co-occur with other members of marine communities that may exhibit vulnerabilities, potentially leading to propagating effects.

This dissertation also included an educational study using ocean change as a lens through which to bring scientific practices and tools into the K-12 classroom. This experience enabled me to create and inform an educational program with my research experiences, including water chemistry spectrophotometry used in Chapter 2, and technological skills acquired via custom flow speed sensor construction in Chapter 5. Inspired by these research experiences and skills, this program was able to empower high school students to build sensors and use sensors to contextualize basic science concepts which resulted in significant learning gains. This module provides a template, informed by evidence-based teaching and pedagogy scholarship, for sensor design and use in the context of student-driven environmental monitoring. This module has been able to further the growth of the PublicSensors program to provide K-12 students with hands-on authentic STEM experiences in a way that is accessible to diverse groups of students. I believe there is a fruitful future in continuing to integrate research and educational goals to both advance our understanding of the impacts of environmental change and provide students with transformative opportunities to engage with scientific practices and tools to study change in their local environments.

References

Boyd PW, Cornwall CE, Davison A, Doney SC and others (2016) Biological responses to environmental heterogeneity under future ocean conditions. Glob Chang Biol 22:2633-2650.

Byrne M, Przeslawski R (2013) Multistressor impacts of warming and acidification of the ocean on marine invertebrates' life histories. Integr Comp Biol 53: 582-596

Noisette F, Hurd C (2018) Abiotic and biotic interactions in the diffusive boundary layer of kelp blades create a potential refuge from ocean acidification. Funct Ecol. 32:1329-1342

Kishida O, Trussell GC, Mougi A, Nishimura K (2010) Evolutionary ecology of inducible morphological plasticity in predator–prey interaction: toward the practical links with population ecology. Popul Ecol 52:37-46

Kordas RL, Harley CDG, O'Connor MI (2011) Community ecology in a warming world: the influence of temperature on interspecific interactions in marine systems. J Exp Mar Biol Ecol 400:218–226

Kroeker KJ, Kordas RL, Crim R, Hendriks IE, Ramajo L, et al. (2013) Impacts of ocean acidification on marine organisms: Quantifying sensitivities and interaction with warming. Glob Chang Biol 19:1884-1896

Kroeker KJ, Sanford E, Jellison BM, Gaylord B (2014) Predicting the effects of ocean acidification on predator-prey interactions: a conceptual framework based on coastal molluscs. Biol Bull 226:211-222

Kroeker KJ, Kordas RL, Harley CD (2017). Embracing interactions in ocean acidification research: confronting multiple stressor scenarios and context dependence. Biol Lett 13: 20160802.

Ruesink JL, Hong JS, Wisehart L, Hacker SD, and others (2010) Congener comparison of native (*Zostera marina*) and introduced (*Z. japonica)* eelgrass at multiple scales within a Pacific Northwest estuary. Biol Invasions 12: 1773-1789.

Tollrian R, Harvell CD (1999) The ecology and evolution of inducible defenses. Princeton University Press, Princeton, NJ

APPENDIX A: CHAPTER 2 SUPPLEMENTAL MATERIALS

Previously published at: http://www.int-res.com/articles/suppl/m607p001_supp/

Text S1 ***Membranipora*** **population dynamics model equations and assumptions**

Zooids increase their available energy content via feeding such that

$$q_{f_j} = A \cdot c_j \cdot F \cdot f \cdot S_j \cdot D_j .$$

Here, A is the algal concentration of the environment (cells/ml), c_J is the clearance rate of zooid j (ml/day), F is the food quality of algal cells (J/cell), f is the assimilation efficiency associated with trophic energy transfer, and S_j is a spination coefficient varying between 0 – 1.0. Zooids that are undefended have high S_j values whereas defended zooids have lower S_j values to reflect interference with feeding currents by induced spines (Grünbaum, 1997). Feeding is also constrained proportionally to developmental state, D_j, because newly formed zooids slowly gain the capacity to feed as they develop lophophores (McKinney and Jackson, 1991). In zooids with energy available for growth D_j increases up to the fully developed state D_{max} as

$$\frac{dD_j}{dt} = \begin{Bmatrix} d_j ;\ D < D_{max} ;\quad E_{tot_j} > 0 \\ otherwise: 0 \end{Bmatrix}.$$

Available energy decreases as it is used to form tissue and to metabolize. The rate of energy allocated for growth is described by the equation:

$$q_{g_j} = g_j \cdot Q_m \cdot (M_{max} - M_j)$$

where g_j is the rate of energy put towards tissue and mass production (day^{-1}), Q_m is the mass to energy conversion rate (J/g), M_{max} is the maximum possible zooid mass (g) and M_j is the current zooid mass. As zooids mature, maximum size is attained and q_{g_j} approaches zero. Zooid mass, M_j, increases as described by the following relationship:

$$\frac{dM_j}{dt} = \frac{q_{g_j}}{Q_m}$$

such that mass no longer increases when $q_{g_j} = 0$. E_{tot_j} is also decreased via metabolism whereby

$$q_{m_j} = q_0$$

where q_0 is the basal metabolic rate of a zooid (J/day).

Translocation of energy between zooids

Zooids can import energy from up to four neighbors: two upstream axial neighbors, and both lateral neighbors. They can also export energy to up to four neighbors, two downstream axial neighbors and both lateral neighbors. Zooids can translocate energy if their available energy

content is above a threshold energy requirement, E_r. The rate of energy input to zooid *j* due to translocation is described by

$$q_{in_j} = r_{t_a} \cdot a_{j-1,j}(E_{tot_{j-1}} - E_r) + r_{t_a} \cdot a_{j-2,j}(E_{tot_{j-2}} - E_r) + r_{t_l} \cdot l_{lat1,j}(E_{tot_{lat1}} - E_r) + r_{t_l} \cdot l_{lat2,j}(E_{tot_{lat2}} - E_r)$$

Here r_{t_a} is the energy translocation rate (day^{-1}) between axially-connected zooids and r_{t_l} is the energy translocation rate between laterally-connected zooids. $a_{j-i,j}$ and $l_{lat1,j}$ are the fractions of available energy transferred axially, from zooid z_{j-1} to zooid z_j, and laterally, from zooid z_{lat1} to zooid z_j, respectively (see Figure 2) and sum to 0.5. A similar relationship describes the energy export rate.

$$q_{out_j} = r_{t_a} \cdot a_{j+1,j}(E_{tot_j} - E_r) + r_{t_a} \cdot a_{j+2,j}(E_{tot_j} - E_r) + r_{t_l} \cdot l_{j,lat1}(E_{tot_j} - E_r) + r_{t_l} \cdot l_{j,lat2}(E_{tot_j} - E_r)$$

where a zooid's own excess available energy is distributed among four downstream neighbors based on the respective translocation rates of the neighbor's orientation to the focal zooid. Zooids can translocate energy if they are located in the colony interior, or form daughters in addition to transferring energy if they are on the colony edge, if they have sufficient energy available above E_r. Daughter zooids are born with an initial energy content, E_{min}, which is initially subtracted from the energy pool of the zooid that produced it, and an initial mass, M_{min}. Energy translocation cannot result in negative energy transfer for any zooid in a colony. In the model, zooids can detect existing zooids, including those belonging to other colonies, and do not create daughters if unoccupied space is unavailable.

Table S1 *Membranipora* population dynamics model parameters. Parameter values controlling zooid-level energy processes were informed by experiments (parts 1-3) or approximated and calculated from literature ranges and values.

Parameter	Definition	Value	Units	Source
p	Zooid side length	0.54041	mm	Experimental estimate
θ	Acute zooid angle	$\pi/6$	radians	Experimental estimate
F	Food quality	1.15 x 10^{-6} (1e-10 g dry wt/cell T.iso[1]) x (5.5 g cal/g dry wt[2])	J/cell	[1]Yoshioka et al., 2012 [2]Parsons et al., 1977
S_j	Spination coefficient of zooid *j*	1.0 unspined zooid 0.7 spined zooids	none	Grünbaum, 1997
A	Algal density	50,000	cells/ml	Experimental value
E_r	Threshold energy needed to send energy downstream	7.0	J	
M_{min}	Starting mass of zooid *j*	1 x 10^{-8}		Experimental estimate
M_{max}	Maximum size (tissue mass) of any zooid	1.96 x 10^{-7} From g skeleton / colony area estimates assuming skeleton is 70% of the total weight	g	Experimental estimate Hyman, 1959
Q_m	Mass – energy conversion factor	4.184 x 10^4 1 gC ~ 10-12 Kcal general conversion	g/J	McLusky, 1981
D_{min}	Starting developmental state of zooid *j*	0.1	none	
D_{max}	Maximum size developmental state of any zooid	1.0	none	
E_{min}	Starting energy content of every zooid	0.001	J	
f	Assimilation efficiency	0.7	none	
c_j	Clearance rate of zooid *j* (feeding)	22.08 (0.92 ml/hr/zooid)	ml/day	Riisgard and Manriquez 1997
$a_{j,k}$	Fraction of available energy transferred between axially connected zooid *j* – zooid *k*	0.25	none	Miles et al., 1995
$l_{j,k}$	Fraction of available energy transferred between laterally connected zooid *j* – zooid *k*	0.25	none	Miles et al., 1995
r_{t_a}	Energy translocation rate between axial zooids	2.0	day^{-1}	Miles et al., 1995
r_{t_l}	Energy translocation rate between lateral zooids	6.0	day^{-1}	Miles et al., 1995
g_j	Rate of energy used for growing tissue and mass	0.5	day^{-1}	
d_j	Developmental rate of zooid *j*	0.3	day^{-1}	Experimental estimate
q_0	Basal metabolic rate of zooid *j*	0.05 (0.025 – 0.144 J/day for *Bugula neritina*)	day^{-1}	Petterson et al., 2016

Table S1 References

Grünbaum D (1997) Hydromechanical mechanisms of colony organization and cost of defense in an encrusting bryozoan, Membranipora membranacea. Limnology and Oceanography. 42:741-752

Hyman LH (1959) The Invertebrates: Smaller Coelomate Groups, Chaetognatha, Hemichordata, Pogonophora, Phoronida, Ectoprocta, Brachiopoda, Sipunculida, the Coelomate Bilateria, Vol. 5. McGraw- Hill, New York.

McKinney FK, Jackson JB (1991) Bryozoan evolution. University of Chicago Press.

McLusky DS (1981) The estuarine ecosystem. Blackie Press, Glasgow.

Miles JS, Harvell CD, Griggs CM, Eisner S (1995) Resource translocation in a marine bryozoan: quantification and visualization of 14C and 35S. Marine Biology, 122:439-445

Parsons TR, Takahashi M, Hargrave B (1977) Biological oceanographic processes. Pergamon Press, Oxford.

Pettersen AK, White CR, Marshall DJ (2016) Metabolic rate covaries with fitness and the pace of the life history in the field. Proc. R. Soc. B. 283:20160323

Riisgard HU, Manriquez P (1997) Filter-feeding in fifteen marine ectoprocts (Bryozoa): particle capture and water pumping. Marine Ecology Progress Series. 154:223–239

Yoshioka M, Yago T, Yoshie-Stark Y, Arakawa H, Morinaga T (2012) Effect of high frequency of intermittent light on the growth and fatty acid profile of *Isochrysis galbana*. Aquaculture. 338:111-117

Figure S1: Experimental setup diagram depicting four pH treatments in larger tanks each with 8 chambers. Twelve colonies were divided into quarters and distributed across four pH treatments either exposed or not exposed to predator cues. Colony section positions in diagram do not reflect actual locations in chambers as colony section locations were randomized and rotated across chambers of the same predation treatment within pH treatment every two days to control for any chamber effects. Numbers refer to individual colonies (genotypes) and letters refer to the subsection of that genotype placed in a pH treatment (a = pH 7.9, b = pH 7.6, c = pH 7.3, d = pH 7.0). Nudibranch chambers contained predators to create waterborne cue pumped to predator treatments.

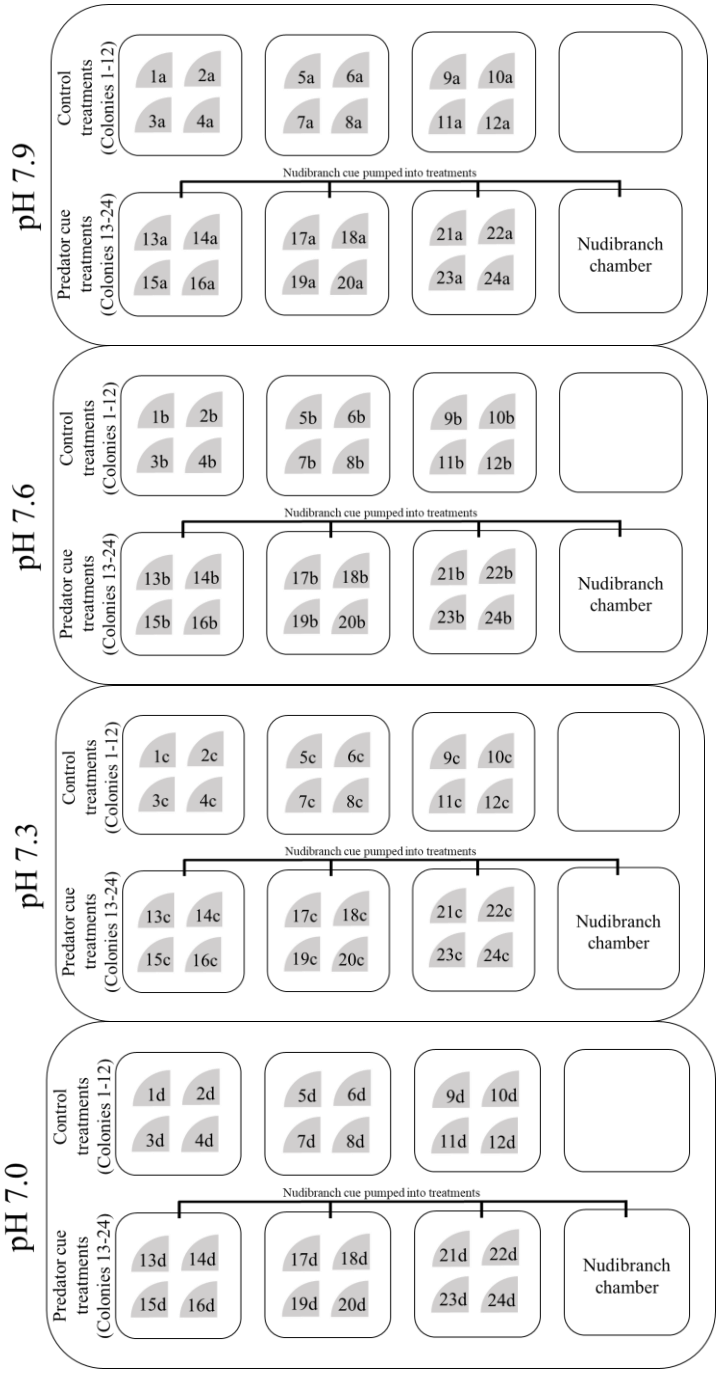

Table S2.1 Bryozoan growth rate models and AIC values used for model selection. Best fit model indicated in bold.

Model	**AIC**
Growth rate ~ 1 + (1|colony)	-465.2
Growth rate ~ pH + (1|colony)	-485.5
Growth rate ~ predation cue + (1|colony)	-467.8
Growth rate ~ pH + predation cue + (1|colony)	-488.1
Growth rate ~ pH * predation cue + (1|colony)	-498.3
Growth rate ~ pH + pH^2 + (1|colony)	-508.4
Growth rate ~ pH * predation cue + pH^2 + (1|colony)	-527.2
Growth rate ~ pH * predation cue + pH^2 * predation cue + (1|colony)	**-537.5**

Table S2.2 Best Fit Model Summary. Asterisk indicates significant P values at alpha = 0.05

Fixed effects

Parameter	**Estimate**	**SE**	**T**	**P**
Intercept	-10.32290	1.34700	-7.664	< 0.0001 *
pH	2.73056	0.35941	7.597	< 0.0001 *
Predation cue	7.42088	1.94776	3.810	0.0003 *
pH^2	-0.17888	0.02395	-7.470	< 0.0001 *
pH : predation cue	-1.94605	0.51971	-3.745	0.0004 *
pH^2 : predation cue	0.12721	0.03463	3.674	0.0005 *

Random effects

Effects	**Variance**	**SD**
Colony	7.684e-05	0.008766
Residual	1.006e-04	0.010032

Deviance = -553.5, df = 84

Table S3.1 Colony senescence models and AIC values used for mortality model selection. Best fit model indicated in bold. *Note: pH was centered to allow for model convergence*

Model	**AIC**
Proportion dead ~ 1 + (1|colony)	29344.84
Proportion dead ~ pH + (1|colony)	12290.83
Proportion dead ~ predation cue + (1|colony)	29345.49
Proportion dead ~ pH + predation cue + (1|colony)	12289.96
Proportion dead ~ pH * predation cue + (1|colony)	10794.83
Proportion dead ~ pH + pH^2 + (1|colony)	7862.155
Proportion dead ~ pH * predation cue + pH^2 + (1|colony)	6614.426
Proportion dead ~ pH * predation cue + pH^2 * predation cue + (1|colony)	**5485.83**

Table S3.2 Best Fit Model Summary. Asterisk indicates significant P values at alpha = 0.05

Fixed effects

Parameter	**Estimate**	**SE**	**Z**	**P**
Intercept	-3.50941	0.20079	-17.48	< 0.0001 *
pH (centered)	-3.85900	0.04126	-93.53	< 0.0001 *
Predation cue	0.68312	0.29032	2.35	0.0186 *
pH^2 (centered)	14.21632	0.21023	67.62	< 0.0001 *
pH: predation cue	1.59555	0.06386	24.99	< 0.0001 *
pH^2: predation cue	-10.26004	0.30616	-33.51	< 0.0001 *

* indicates significant P values at alpha = 0.05

Random effects

Effects	**Variance**	**SD**
Colony	0.4759	0.6898

Deviance = 5471.8, df = 85

Table S4.1 Spine length models and AIC values used for model selection. Best fit model indicated in bold.

Model	**AIC**
Spine length ~ 1 + (1|colony) + (1|colony : colony section)	13232.26
Spine length ~ pH + (1|colony) + (1|colony : colony section)	13227.55
Spine length ~ predation cue + (1|colony) + (1|colony : colony section)	13187.92
Spine length ~ pH + predation cue + (1|colony) + (1|colony : colony section)	**13183.21**
Spine length ~ pH * predation cue + (1|colony) + (1|colony : colony section)	13184.73

Table S4.2 Best Fit Model Summary. Asterisk indicates significant P values at alpha = 0.05

Fixed effects

Parameter	**Estimate**	**SE**	**T**	**P**
Intercept	-141.896	61.274	-2.316	0.02346 *
pH	21.527	8.108	2.655	0.00983 *
Predation cue (defended)	117.104	9.580	12.223	< 0.0001 *

Random effects

Effects	**Variance**	**SD**
Colony section	425.8	20.63
Colony	405.6	20.14
Residual	853.5	29.22

Deviance = 13171.2, df = 1344

Figure S2 To further explore differences in the abundance of spines with respect to pH in predation cue (black) and control treatments (grey), the following plot shows the proportion of spines present at random sampling locations along photo transects, with plotted prediction from the best fit model as determined by AIC. Models used a binomial response distribution and logit link function and considered colony a random effect.

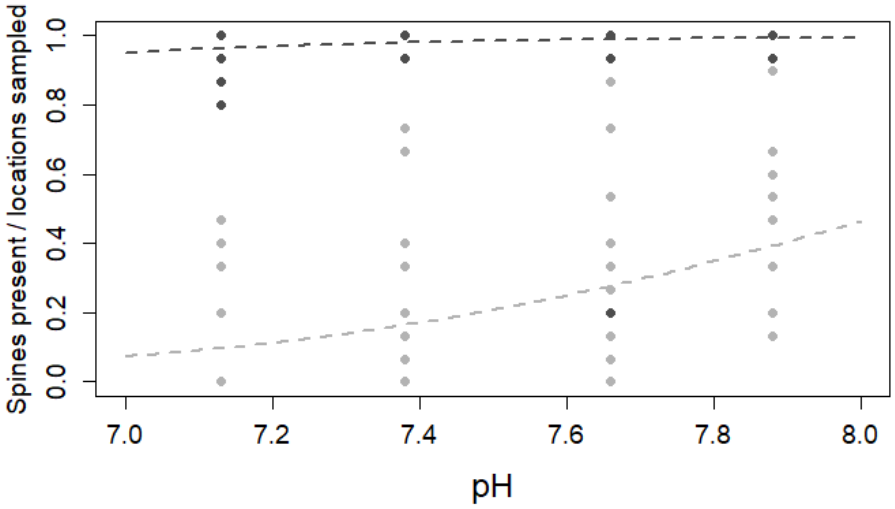

Table S5.1 Spine metric models and AIC values used for model selection. Best fit model indicated in bold.

Model	**AIC**
Spination metric ~ 1 + (1|colony)	101.46
Spination metric ~ pH + (1|colony)	100.05
Spination metric ~ predation cue + (1|colony)	69.13
Spination metric~ pH + predation cue + (1|colony)	**67.42**
Spination metric ~ pH * predation cue + (1|colony)	67.79

Table S5.2 Best Fit Model Summary. Asterisk indicates significant P values at alpha = 0.05

Fixed effects

Parameter	**Estimate**	**SE**	**T**	**P**
Intercept	-19.215	10.122	-1.898	0.0576
pH	2.383	1.328	1.795	0.0726
Predation cue	5.493	1.282	4.285	< 0.0001 *

* indicates significant P values at alpha = 0.05

Random effects

Effects	**Variance**	**SD**
Colony	0.4826	0.6947

Deviance = 59.4, df = 88

Table S6.1 Nudibranch zooid consumption models and AIC values for model selection. Best fit model indicated in bold.

Model	**AIC**
Zooids consumed ~ nudibranch length + (1|colony) + (1|nudibranch) + (1|colony size)	978.03
Zooids consumed ~ nudibranch length + pH + (1|colony) + (1|nudibranch) + (1|colony size)	979.76
Zooids consumed ~ nudibranch length + predation cue + (1|colony) + (1|nudibranch) + (1|colony size)	976.85
Zooids consumed ~ nudibranch length + pH + predation cue + (1|colony) + (1|nudibranch) + (1|colony size)	978.56
Zooids consumed ~ nudibranch length + pH * predation cue + (1|colony) + (1|nudibranch) + (1|colony size)	**975.09**

Table S6.2 Best fit model summary. Asterisk indicates significant P values at alpha = 0.05

Fixed effects

Parameter	**Estimate**	**SE**	**Z**	**P**
Intercept	0.65689	3.02767	0.217	0.82824
Nudibranch length	0.30969	0.09478	3.267	0.00109 *
pH	0.24648	0.40458	0.609	0.54238
Predation cue (defended)	6.82416	2.98450	2.287	0.02222 *
pH: predation cue	-0.95386	0.39693	-2.403	0.01626 *

Random effects

Effects	**Variance**	**SD**
Colony	0.2534	0.5034
Nudibranch	0.3468	0.5889
Colony size	0.1211	0.3480

Deviance = 959.1, df = 84

Table S7.1 Skeletal density (Ca per unit mm of skeleton) models and AIC values for model selection. Best fit model indicated in bold.

Model	**AIC**
Ca per area ~ 1 + (1|colony)	-1051.2
Ca per area ~ pH + (1|colony)	-1069.3
Ca per area ~ predation cue + (1|colony)	-1049.2
Ca per area ~ pH + predation cue + (1|colony)	-1067.3
Ca per area ~ pH * predation cue + (1|colony)	-1065.4
Ca per area ~ pH * predation cue + ph^2 + (1|colony)	-1079.0
Ca per area ~ pH * predation cue + ph^2 * predation cue + (1|colony)	-1078.1
Ca per area ~ pH + pH^2 + (1|colony)	**-1082.9**

Table S7.2 Best fit model summary. Asterisk indicates significant P values at alpha = 0.05

Fixed effects

Parameter	**Estimate**	**SE**	**T**	**P**
Intercept	-0.1339793	0.0310058	-4.321	< 0.0001 *
pH	0.0358173	0.0083360	4.297	< 0.0001 *
pH^2	-0.0023485	0.0005594	-4.198	< 0.0001 *

Random effects

Effects	**Variance**	**SD**
Colony	1.432e-07	0.0003784
Residual	2.270e-07	0.0004764

Deviance = -1092.9, df = 85

Figure S3 To further explore differences in the skeletal quality and composition with respect to pH treatment and predation cue, the following plot shows that proportion of the skeleton weight that is calcium, as a proxy for calcium carbonate, with plotted predictions from the best fit model as determined by AIC. Models used a Gaussian response distribution and identity link function and considered colony a random effect.

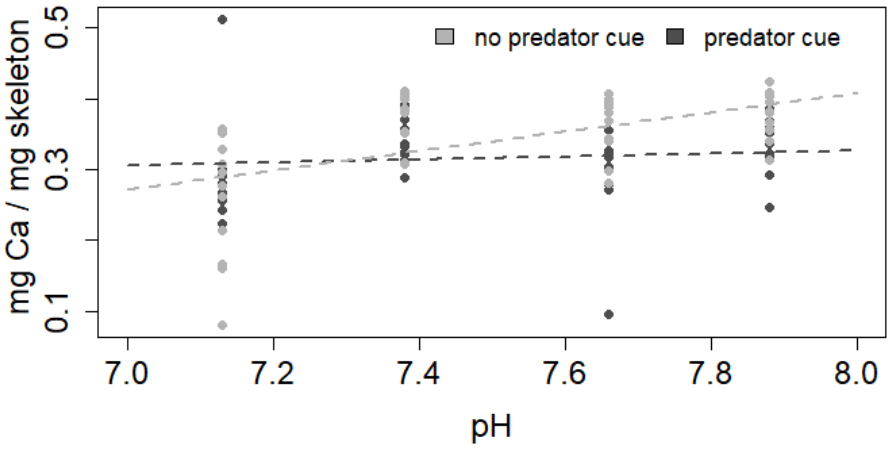

Table S8.1 Skeletal composition (mg Ca per mg of skeleton) models and AIC values for model selection. Best fit model indicated in bold.

Model	**AIC**
Ca per weight ~ 1 + (1|colony)	-227.6
Ca per weight ~ pH + (1|colony)	-236.3
Ca per weight ~ predation cue + (1|colony)	-228.9
Ca per weight ~ pH + predation cue + (1|colony)	-238.0
Ca per weight ~ pH * predation cue + (1|colony)	**-242.7**

Table S8.2 Best fit model summary. Asterisk indicates significant P values at alpha = 0.05

Fixed effects

Parameter	**Estimate**	**SE**	**T**	**P**
Intercept	-0.68307	0.23403	-2.919	0.0044 *
pH	0.13637	0.03113	4.381	< 0.0001 *
Predation cue	0.84465	0.33189	2.545	0.0126 *
pH: predation cue	-0.11579	0.04415	-2.623	0.0102 *

Random effects

Effects	**Variance**	**SD**
Colony	0.00	0.00
Residual	0.003456	0.05879

Deviance = -254.7, df = 84

Model simulation videos available at: http://www.int-res.com/articles/suppl/m607p001_supp/

Video S1
One representative model simulation with 8 colonies growing at pH 7.9 undefended growth rates (blue) and 8 colonies growing at pH 7.9 defended growth rates (pink). Light blue and light pink indicate developing zooids along the perimeter of colonies. Simulation used to determine the inter-population cost of defense.
File: pH7.9_model_example.avi

Video S2
One representative model simulation with 8 colonies growing at pH 7.6 undefended growth rates (blue) and 8 colonies growing at pH 7.6 defended growth rates (pink). Light blue and light pink indicate developing zooids along the perimeter of colonies. Simulation used to determine the inter-population cost of defense.
File: pH7.6_model_example.avi

Video S3
One representative model simulation with 8 colonies growing at pH 7.3 undefended growth rates (blue) and 8 colonies growing at pH 7.3 defended growth rates (pink). Light blue and light pink indicate developing zooids along the perimeter of colonies. Simulation used to determine the inter-population cost of defense.
File: pH7.3_model_example.avi

Video S4
One representative model simulation with 8 colonies growing at pH 7.0 undefended growth rates (blue) and 8 colonies growing at pH 7.0 defended growth rates (pink). Light blue and light pink indicate developing zooids along the perimeter of colonies. Simulation used to determine the inter-population cost of defense.
File: pH7.0_model_example.avi

APPENDIX B: CHAPTER 3 SUPPLEMENTAL MATERIALS

Supplemental analysis for Part 1:

Table S1.1 Linear models for field data with corresponding AIC values for model selection. Best fit model highlighted in bold.

Model	**AIC**
ln(Colony area) = population density * settlement time + intercept	522.76
ln(Colony area) = population density + settlement time + intercept	**520.77**
ln(Colony area) = settlement time + intercept	540.08
ln(Colony area) = population density + intercept	645.78
ln(Colony area) = intercept *(model of the mean)*	662.81

Table S1.2 Best fit model summary. Asterisk indicates significance.

Parameter	**Estimate**	**SE**	**T**	**P**
Intercept	10.193	0.234	43.554	< 0.0001*
Population density	-0.054	0.011	-4.707	< 0.0001*
Settlement time	-0.093	0.007	-13.219	< 0.0001*

Supplemental analysis for Part 2:

Table S2.1: Regression model summary for comparison of field and model colony areas

Parameter	**Estimate**	**SE**	**T**	**P**
ln(Percent occupied - model)	1.05	0.033	31.71	< 0.0001*

Supplemental analysis for Part 3:

Analysis of simulation data with population densities of 16, 20, 24, 28, 32, 36 colonies and pH conditions of 7.9 (ambient), 7.6 and 7.3. Corresponds with data presented in Figure 4a-d.

Table S3.1: Full statistical model set to describe effects of population density and pH on the four calculated metrics from simulation data **(**normalized COD = ***nCOD***, normalized defended colony size =$N_{d,t}$, relative COD = ***rCOD***, relative defended colony size = $R_{d,t}$). AIC values for all models are presented. Selected best fit model is highlighted in bold. If AIC values were within 2 units, the more parsimonious model was chosen.

Model	***nCOD***	$N_{d,t}$	***rCOD***	$R_{d,t}$
Response = population density * pH + intercept	-6462.7	-7875.4	-1314.1	-1314.11
Response = population density + pH + intercept	**-6464.2**	**-7878.1**	**-1315.8**	**-1315.83**
Response = population density + intercept	-6263.0	-7618.8	-1058.0	-1058.0
Response = pH + intercept	-5773.0	-6568.0	-1276.75	-1276.8
Response = intercept *(model of the mean)*	-5677.5	-6501.2	-1029.10	-1029.1

Table S3.2 Best fit model summary for normalized COD **(*nCOD*)**. Asterisk indicates significance.

Parameter	**Estimate**	**SE**	**T**	**P**
Intercept	-2.524	0.044	-57.069	< 0.0001*
Population density	-0.055	0.002	-35.789	< 0.0001*
pH 7.6	0.250	0.026	16.973	< 0.0001*
pH 7.3	0.190	0.026	-7.319	< 0.0001*

Table S3.3 Best fit model summary for normalized defended colony size ($N_{d,t}$). Asterisk indicates significance.

Parameter	**Estimate**	**SE**	**T**	**P**
Intercept	-2.857	0.021	-136.167	< 0.0001*
Population density	-0.039	0.001	-53.413	< 0.0001*
pH 7.6	-0.134	0.012	-10.933	< 0.0001*
pH 7.3	0.078	0.012	6.366	< 0.0001*

Table S3.4 Best fit model summary for relative COD (***rCOD***). Asterisk indicates significance.

Parameter	**Estimate**	**SE**	**T**	**P**
Intercept	0.565	0.016	34.903	< 0.0001*
Population density	-0.004	0.001	-6.469	< 0.0001*
pH 7.6	0.097	0.009	10.212	< 0.0001*
pH 7.3	-0.067	0.009	-7.089	< 0.0001*

Table S3.5 Best fit model summary for relative defended colony size (***$R_{d,t}$***). Asterisk indicates significance.

Parameter	**Estimate**	**SE**	**T**	**P**
Intercept	0.435	0.016	26.890	< 0.0001*
Population density	0.004	0.001	6.469	< 0.0001*
pH 7.6	-0.097	0.009	-10.212	< 0.0001*
pH 7.3	0.067	0.009	7.089	< 0.0001*

Analysis of simulation data with population densities of 16, 20, 24, 28, 32, and 36 colonies, settlement times of 0, 5, 10, and 20 days, and pH conditions of 7.9 (ambient), 7.6 and 7.3. Corresponds with data presented in Figure 5a-d.

Table S3.6: Full statistical model set to describe the effects of population density (density), settlement time (settlement) and pH on the four metrics calculated from simulation data (normalized COD = ***nCOD***, normalized defended colony size =$N_{d,t}$, relative COD = ***rCOD***, relative defended colony size = $R_{d,t}$). AIC values for all models are presented. Selected best fit model is highlighted in bold. If AIC values were within 2 units, the more parsimonious model was chosen. See next page for full table

Table 3.6

Model	***nCOD***	$N_{d,t}$	***rCOD***	$R_{d,t}$
Response = density + settlement + pH + pH*density + pH*settlement + density*settlement + pH*density*settlement + intercept	-11576.5	-14051.6	-654.1	-654.1
Response = density + settlement + pH + pH*density + pH*settlement + density*settlement + intercept	**-11578.5**	**-14050.4**	-656.1	-656.1
Response = density + settlement + pH + pH*settlement + density*settlement + intercept	-11558.5	-14031.5	-658.7	-658.7
Response = density + settlement + pH + pH*density + density*settlement + intercept	-11567.9	-14040.5	-660.1	-660.1
Response = density + settlement + pH + pH*density + pH*settlement + intercept	-11523.8	-14000.3	-657.8	-657.8
Response = density + settlement + pH + settlement*density + intercept	-11548.2	-14021.8	-662.6	-662.6
Response = density + settlement + pH + pH*settlement + intercept	-11504.5	-13982.0	-660.3	-660.3
Response = density + settlement + pH + pH*density + intercept	-11513.7	-13990.8	-661.8	-661.8
Response = density + settlement + pH + intercept	-11494.6	-13972.7	**-664.3**	**-664.3**
Response = density + settlement + intercept	-11313.0	-13759.4	-426.7	-426.7
Response = settlement + pH + intercept	-10896.5	-12513.1	-655.3	-655.3
Response = density + pH + intercept	-11093.8	-13307.6	-584.0	-584.0
Response = settlement + intercept	-10765.6	-12417.4	-419.2	-419.2
Response = density + intercept	-10947.9	-13158.9	-356.6	-356.6
Response = pH + intercept	-10601.1	-12188.2	-575.6	-575.6
Response = intercept *(model of the mean)*	-10490.1	-12108.6	-349.4	-349.4

Table S3.7 Best fit model summary for normalized COD (***nCOD***). Asterisk indicates significance.

Parameter	**Estimate**	**SE**	**T**	**P**
Intercept	5.451e-02	1.860e-03	29.297	< 0.0001*
Density	-1.340e-03	7.321e-05	-18.308	< 0.0001*
Settlement	-1.545e-03	1.252e-04	-12.336	< 0.0001*
pH 7.6	6.847e-03	2.227e-03	3.075	0.002*
pH 7.3	-1.321e-02	2.227e-03	-5.934	< 0.0001*
Density: pH (7.6)	-8.775e-05	8.549e-05	-1.026	0.305
Density*pH (7.3)	3.109e-04	8.549e-05	3.637	0.0003*
Settlement*pH (7.6)	-1.176e-04	7.551e-05	-1.557	0.120
Settlement*pH (7.3)	1.689e-04	7.551e-05	2.236	0.025*
Density*Settlement	3.572e-05	4.719e-06	7.569	< 0.0001*

Table S3.8 Best fit model summary for normalized defended colony size ($N_{d,t}$). Asterisk indicates significance.

Parameter	**Estimate**	**SE**	**T**	**P**
Intercept	4.625e-02	9.363e-04	49.398	< 0.0001*
Density	-9.579e-04	3.684e-05	-25.999	< 0.0001*
Settlement	-9.125e-04	6.302e-05	-14.479	< 0.0001*
pH 7.6	-2.848e-03	1.121e-03	-2.541	0.011*
pH 7.3	6.913e-03	1.121e-03	6.169	< 0.0001*
Density*pH (7.6)	2.796e-05	4.303e-05	0.650	0.516
Density*pH (7.3)	-1.627e-04	4.303e-05	-3.783	0.0002*
Settlement*pH (7.6)	1.298e-04	3.800e-05	3.415	0.0006*
Settlement*pH (7.3)	1.624e-05	3.800e-05	0.427	0.669
Density*Settlement	1.722e-05	2.375e-06	7.251	< 0.0001*

Table S3.9 Best fit model summary for relative COD (***rCOD***). Asterisk indicates significance.

Parameter	**Estimate**	**SE**	**T**	**P**
Intercept	0.527	0.020	26.323	< 0.0001*
Population density	-0.002	0.001	-3.309	0.0009*
Settlement time	-0.006	0.001	-9.161	< 0.0001*
pH 7.6	0.073	0.012	6.269	< 0.0001*
pH 7.3	-0.112	0.012	-9.667	< 0.0001*

Table S3.10 Best fit model summary for relative defended colony size ($R_{d,t}$). Asterisk indicates significance.

Parameter	**Estimate**	**SE**	**T**	**P**
Intercept	0.473	0.020	23.614	< 0.0001*
Population density	0.002	0.001	3.309	0.0009*
Settlement time	0.006	0.001	9.161	< 0.0001*
pH 7.6	-0.073	0.012	-6.269	< 0.0001*
pH 7.3	0.112	0.012	9.667	< 0.0001*

Supplemental Equations

1. Definitions of basic metrics from Methods section

1. Mean undefended colony sizes for type *s*, *m*, and *c* algal blades, which designate the blade densities of sparse (*s*), medium (*m*) and crowded (*c*), are

$$\bar{a}_{u,h} = \frac{1}{n_{u,h}} \sum_{i=0}^{n_{u,h}} a_{i,u,h}$$

where $h = s,m,c$ respectively, and $n_{u,h}$ is the number of undefended colonies.

2. Mean defended colony sizes for *s*, *m*, and *c* blades are

$$\bar{a}_{d,h} = \frac{1}{n_{d,h}} \sum_{i=0}^{n_{d,h}} a_{i,d,h}$$

where $n_{d,h}$ is the number of defended colonies.

3. Normalized cost of defense for *s*, *m*, and *c* blades are

$$nCOD = \frac{\bar{a}_{u,h} - \bar{a}_{d,h}}{A}$$

where *A* is the blade (model domain) area.

4. Relative cost of defense

$$rCOD = \frac{\bar{a}_{u,h} - \bar{a}_{d,h}}{\bar{a}_{u,h}}$$

5. Normalized undefended colony size

$$N_{u,h} = \frac{\bar{a}_{u,h}}{A}$$

6. Normalized defended colony size

$$N_{d,h} = \frac{\bar{a}_{d,h}}{A}$$

7. Relative defended colony size

$$R_{d,h} = \frac{\bar{a}_{d,h}}{\bar{a}_{u,h}}$$

2. Population-level scenario

We consider a scenario in which a population of *M. membranacea* inhabits a set of *B* algal blades. For simplicity, we consider only one cohort of settling larvae, assumed to have the same settlement time.

At $t = 0$, these blades have one of three levels of settlement density:

- A fraction f_s have sparse settlement, with $n_{u,s}$ undefended and $n_{d,s}$ defended colonies per blade
- A fraction f_m have medium settlement, with $n_{u,m}$ undefended and $n_{d,m}$ defended colonies per blade
- A fraction f_c have crowded settlement, with $n_{u,c}$ undefended and $n_{d,c}$ defended colonies per blade

The analysis generalizes easily to an arbitrary number of settlement density classes.

2.1 Relative (blade-level) expected fitness of undefended vs. defended colonies

Using area as a proxy for fitness, the total expected reproductive output of the undefended colonies on a single blade of type *h* is

$$R_{u,h} = n_{u,h}\bar{a}_{u,h}$$

For defended colonies, it is

$$R_{d,h} = n_{d,h}\bar{a}_{d,h}$$

We can now ask: On a blade of type *h*, what is the relative expected fitness decrease of a defended colony compared to an undefended colony? The answer is:

$$rCOD_h = \frac{\frac{R_{u,h}}{n_{u,h}} - \frac{R_{d,h}}{n_{d,h}}}{\frac{R_{u,h}}{n_{u,h}}}$$

$$= \frac{\bar{a}_{u,h} - \bar{a}_{d,h}}{\bar{a}_{u,h}}$$

2.2 Habitat-wide expected fitness of undefended vs. defended colonies

We can also ask: What is the absolute expected fitness of an undefended colony compared to a defended colony across an entire habitat consisting of multiple algal blades?

Using area as a proxy for fitness, the total expected reproductive output of the undefended fraction of the total population is

$$R_{u,tot} = \phi B\,(f_s R_{u,s} + f_m R_{u,m} + f_c R_{u,c})$$

where ϕ is the reproductive output per unit area of colony. Similarly, the total expected reproductive output of the defended fraction of the total population is

$$R_{d,tot} = \phi B\,(f_s R_{d,s} + f_m R_{d,m} + f_c R_{d,c})$$

Then, the average reproductive output of undefended colonies per unit blade area is

$$\begin{aligned}
\rho_{u,tot} &= \frac{R_{u,tot}}{AB} \\
&= \frac{\phi B\left(f_s R_{u,s} + f_m R_{u,m} + f_c R_{u,c}\right)}{AB} \\
&= \phi\,\frac{\left(f_s R_{u,s} + f_m R_{u,m} + f_c R_{u,c}\right)}{A} \\
&= \phi\,\frac{\left(f_s n_{u,s}\bar{a}_{u,s} + f_m n_{u,m}\bar{a}_{u,m} + f_c n_{u,c}\bar{a}_{u,c}\right)}{A} \\
&= \phi\left[f_s n_{u,s}\frac{\bar{a}_{u,s}}{A} + f_m n_{u,m}\frac{\bar{a}_{u,m}}{A} + f_c n_{u,c}\frac{\bar{a}_{u,c}}{A}\right] \\
&= \phi\left[f_s n_{u,s} N_{u,s} + f_m n_{u,m} N_{u,m} + f_c n_{u,c} N_{u,c}\right]
\end{aligned}$$

where $N_{u,h}$ is the normalized undefended colony size.

Likewise, the average reproductive output of defended colonies per unit blade area is

$$\begin{aligned}
\rho_{d,tot} &= \frac{R_{d,tot}}{AB} \\
&= \phi\left[f_s n_{d,s} N_{d,s} + f_m n_{d,m} N_{d,m} + f_c n_{d,c} N_{d,c}\right]
\end{aligned}$$

where $N_{d,h}$ is the normalized defended colony size.

The difference between the undefended and the defended colonies in average reproductive output per unit blade area is

$$\Delta\rho_{tot} = \rho_{u,tot} - \rho_{d,tot}$$

$$= \frac{R_{u,tot}}{AB} - \frac{R_{d,tot}}{AB}$$

$$= \phi\left[f_s(n_{u,s}N_{u,s} - n_{d,s}N_{d,s}) + f_m(n_{u,m}N_{u,m} - n_{d,m}N_{d,m}) + f_c(n_{u,c}N_{u,c} - n_{d,c}N_{d,c})\right]$$

Here, the fractions of blades of various densities (f_s, f_m, f_c) and the numbers of the defended and undefended colonies are weighting coefficients for the contributions of the normalized colony sizes to the aggregate, habitat-wide reproductive output per unit area.

We emphasize that the contributions of intra-blade competition depend on the number of both defended and undefended colonies. Our simulation results inform only the special case of equal numbers of undefended and defended colonies on each blade, i.e. $n_s = n_{u,s} = n_{d,s}$, $n_m = n_{u,m} = n_{d,m}$, $n_c = n_{u,c} = n_{d,c}$.

In this special case,

$$\Delta\rho_{tot,eq} = \rho_{u,tot} - \rho_{d,tot}$$

$$= \frac{R_{u,tot}}{AB} - \frac{R_{d,tot}}{AB}$$

$$= \phi\left[f_s n_{u,s}\left(N_{u,s} - N_{d,s}\right) + f_m n_{u,m}\left(N_{u,m} - N_{d,m}\right) + f_c n_{u,c}\left(N_{u,m} - N_{d,m}\right)\right]$$

$$= \phi\left[f_s n_s nCOD_s + f_m n_m nCOD_m + f_c n_{u,c} nCOD_c\right]$$

The above equation makes explicit the way in which the metric $nCOD_h$ determines the difference in average reproductive output per unit blade in habitats with various distributions of blade densities.

2.3 Generalization to m blade density classes

In summation notation, for an arbitrary set of blade crowding categories $H = h_1, h_2, \ldots, h_m$, the formulas above translate to:

$$R_{u,tot} = \phi B \sum_{h \in H} f_h R_{u,h},$$

$$R_{d,tot} = \phi B \sum_{h \in H} f_h R_{d,h},$$

$$\rho_{u,tot} = \phi \sum_{h \in H} f_h n_{u,h} N_{u,h},$$

$$\rho_{d,tot} = \phi \sum_{h \in H} f_h n_{d,h} N_{d,h} \ ,$$

$$\Delta\rho_{tot} = \phi \sum_{h \in H} f_h \left(n_{u,h} N_{u,h} - n_{d,h} N_{d,h} \right) \ ,$$

$$\Delta\rho_{tot,eq} = \phi \sum_{h \in H} f_h \, n_h nCOD_h$$

APPENDIX C: CHAPTER 4 SUPPLEMENTAL MATERIALS

Experimental setup

Figure S1: Experimental setup for Experiment 1. Experiment 2 and 3 used this similar set up. Experiment 3 used larger buckets (only 4 per water bath) to accommodate increased space needed for larger predators.

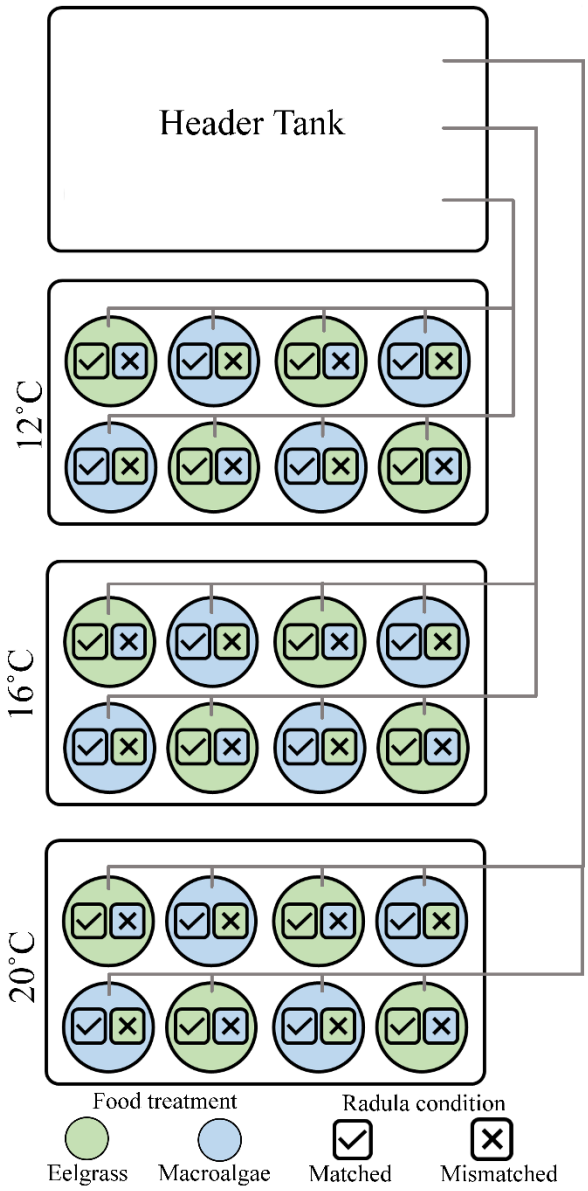

Analysis for Experiment 1:

Table S1.1 Regression for egg mass area vs. number of eggs contained in egg mass (data in Fig 1a). Asterisk indicates significance.

Parameter	**Estimate**	**SE**	**T**	**P**
Intercept	11.3510	1.8344	6.188	< 0.0001*
Egg mass area	3.3645	0.2485	13.539	< 0.0001*

R^2 = 0.788, F(1,48)=183.3, p < 0.0001

Table S1.2 Two-way ANOVA table for reproductive output by temperature and diet treatments (data in Fig 1b). Asterisk indicates significance.

Parameter	**DF**	**SS**	**MS**	**F**	**P**
Diet	3	105.78	35.26	34.945	< 0.0001*
Temperature	2	0.19	0.10	0.095	0.910
Diet * Temperature	6	4.15	0.69	0.685	0.663
Residuals	36	36.32	1.01		

Table S1.3 Tukey's HSD post hoc test results for ANOVA comparisons of reproductive output across diet treatments above in Table S1.2. Asterisk indicates significance.

Treatment	**p-value**
Eelgrass Match * Eelgrass Mismatch	< 0.0001*
Macroalgae Match * Eelgrass Match	< 0.0001*
Macroalgae Mismatch * Eelgrass Match	< 0.0001*
Macroalgae Match * Eelgrass Mismatch	0.0012
Macroalgae Mismatch * Eelgrass Mismatch	0.8958
Macroalgae Mismatch * Macroalgae Match	0.0002

Table S1.4 Two-way ANOVA table for fecal pellet production after 24 hours (time point 1) by temperature and diet treatments (data in Fig 1c.). Asterisk indicates significance.

Parameter	**DF**	**SS**	**MS**	**F**	**P**
Diet	3	1415.2	471.7	77.992	< 0.0001*
Temperature	2	0.9	0.5	0.078	0.925
Diet * Temperature	6	25.3	4.2	0.697	0.653
Residuals	36	217.7	6.0		

Table S1.5 Tukey's HSD post hoc test results for ANOVA comparisons of fecal pellet production across diet treatments above in Table S1.4. Asterisk indicates significance.

Treatment	**p-value**
Eelgrass Match * Eelgrass Mismatch	< 0.0001*
Macroalgae Match * Eelgrass Match	< 0.0001*
Macroalgae Mismatch * Eelgrass Match	< 0.0001*
Macroalgae Match * Eelgrass Mismatch	< 0.0001*
Macroalgae Mismatch * Eelgrass Mismatch	< 0.0001*
Macroalgae Mismatch * Macroalgae Match	0.1133

Table S1.6 Two-way ANOVA table for fecal pellet production after 24 hours (time point 2) by temperature and diet treatments (data in Fig 1d.). Asterisk indicates significance.

Parameter	**DF**	**SS**	**MS**	**F**	**P**
Diet	3	1100.8	366.9	29.633	< 0.0001*
Temperature	2	17.5	8.7	0.707	0.500
Diet * Temperature	6	20.5	3.4	0.276	0.945
Residuals	36	445.8	12.4		

Table S1.7 Tukey's HSD post hoc test results for ANOVA comparisons of fecal pellet production across diet treatments above in Table S1.6. Asterisk indicates significance.

Treatment	**p-value**
Eelgrass Match * Eelgrass Mismatch	0.9744
Macroalgae Match * Eelgrass Match	< 0.0001*
Macroalgae Mismatch * Eelgrass Match	< 0.0001*
Macroalgae Match * Eelgrass Mismatch	< 0.0001*
Macroalgae Mismatch * Eelgrass Mismatch	< 0.0001*
Macroalgae Mismatch * Macroalgae Match	0.9924

Table S1.8 Two-way ANOVA table for fecal pellet production after 24 hours (time point 3) by temperature and diet treatments (data in Fig 1e.). Asterisk indicates significance.

Parameter	**DF**	**SS**	**MS**	**F**	**P**
Diet	3	1603.8	534.6	61.485	< 0.0001*
Temperature	2	5.7	2.9	0.330	0.721
Diet * Temperature	6	49.5	8.2	0.949	0.473
Residuals	35	304.3	8.7		

Table S1.9 Tukey's HSD post hoc test results for ANOVA comparisons of fecal pellet production across diet treatments in Table S1.8. Asterisk indicates significance.

Treatment	**p-value**
Eelgrass Match * Eelgrass Mismatch	0.09661
Macroalgae Match * Eelgrass Match	< 0.0001*
Macroalgae Mismatch * Eelgrass Match	< 0.0001*
Macroalgae Match * Eelgrass Mismatch	< 0.0001*
Macroalgae Mismatch * Eelgrass Mismatch	< 0.0001*
Macroalgae Mismatch * Macroalgae Match	0.8282

Analysis for Experiment 2:

Table S2.1 Two-way ANOVA table for egg hatching time by temperature and substrate (data in Figure 2a). Asterisk indicates significance.

Parameter	**DF**	**SS**	**MS**	**F**	**P**
Temperature	2	27.54	13.77	5.281	0.010*
Substrate	1	18.92	18.92	7.256	0.011*
Temperature * Substrate	2	28.99	14.50	5.561	0.008*
Residuals	32	83.42	2.61		

Table S2.2 Tukey's HSD post hoc test results for ANOVA comparisons of egg hatching time above in Table S2.1. Asterisk indicates significance.

Treatment	**p-value**
16˚C Eelgrass * 12˚C Eelgrass	0.3349
20˚C Eelgrass * 12˚C Eelgrass	0.9840
12˚C Macroalgae * 12˚C Eelgrass	0.9989
16˚C Macroalgae * 12˚C Eelgrass	0.6331
20˚C Macroalgae * 12˚C Eelgrass	0.0015*
20˚C Eelgrass * 16˚C Eelgrass	0.5968
12˚C Macroalgae * 16˚C Eelgrass	0.3168
16˚C Macroalgae * 16˚C Eelgrass	1.0000
20˚C Macroalgae * 16˚C Eelgrass	0.0258
12˚C Macroalgae * 20˚C Eelgrass	0.9991
16˚C Macroalgae * 20˚C Eelgrass	0.8731
20˚C Macroalgae * 20˚C Eelgrass	0.0021*
16˚C Macroalgae * 12˚C Macroalgae	0.7206
20˚C Macroalgae * 12˚C Macroalgae	0.0007*
20˚C Macroalgae * 16˚C Macroalgae	0.1542

Figure S2 Egg mass area plotted against hatching time. There was no significant relationship between egg mass area and hatching time.

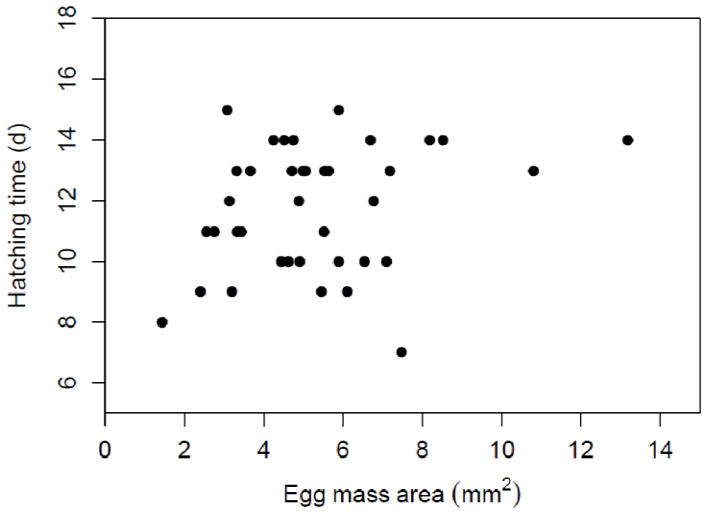

Table S2.3 Regression for egg mass size area vs. hatching time (data in Figure S2). There was no significant relationship between egg mass size and hatching time.

Parameter	**Estimate**	**SE**	**T**	**P**
Intercept	10.5212	0.8305	12.668	< 0.0001*
Egg mass area	0.2337	0.1435	1.629	0.112

R^2 = 0.042, F(1,36)= 2.652, p = 0.112

Analysis for Experiment 3:

Table S3.1 Generalized linear models with Poisson distribution to test the effect of temperature and predator type on number of snails eaten. Corresponding AIC values for each model are listed to determine model selection. Best fit model highlighted in bold.

Model	**AIC**
Snails eaten = predator type ***** temperature + intercept	201.52
Snails eaten **=** predator type **+** temperature **+** intercept	201.26
Snails eaten = predator type + intercept	**199.97**
Snails eaten = temperature	236.11
Snails eaten = intercept *(model of the mean)*	234.82

Table S3.2 Best fit model summary from selected model in Table S3.1. Asterisk indicates significance.

Parameter	**Estimate**	**SE**	**Z**	**P**
Intercept	1.006	0.110	9.105	< 0.0001*
Predator type (Sea Star)	-1.316	0.240	-5.480	< 0.0001*

Null deviance: 126.457, df = 59
Residual deviance: 89.608, df = 58

Table S3.3 Two-way ANOVA table for snail size consumed by predator type and temperature treatment (data in Figure 3b). Asterisk indicates significance.

Parameter	**DF**	**SS**	**MS**	**F**	**P**
Predator Type	1	0.78	0.7831	0.551	0.460
Temp	2	3.26	1.6275	1.145	0.323
Predator Type * Temp	2	0.08	0.0386	0.027	0.973
Residuals	96	136.49	1.4217		

Table S3.4 ANCOVA table to test the relationship between predator size and prey size for both predator types (data in Figure 3c). Asterisk indicates significance.

Parameter	**SS**	**DF**	**F**	**P**
Intercept	133.536	1	94.3536	< 0.0001*
Predator size	1.113	1	0.7865	0.3960
Predator type	0.101	1	0.0715	0.3773
Predator type * Predator size	0.275	1	0.1947	0.7898
Residuals	138.697	98		0.6600

APPENDIX D: CHAPTER 5 SUPPLEMENTAL MATERIALS

1. Snail catcher statistics

Table S1.1 One-way ANOVA table for new recruits (shell size < 1mm) caught in snail catchers Asterisk indicates significance.

Parameter	DF	SS	MS	F	P
Snail catcher	5	66.63	13.327	3.182	0.020*
Residuals	30	125.63	4.188		

Table S1.2 Tukey's HSD post hoc test results for ANOVA comparisons of number of new recruits (shell size < 1mm) across snail catchers above in Table S1.2. Asterisk indicates significance. Snail catchers 1A and 1B are from an macroalgae dominated site, 2A and 2B are in the transition zone between macroalgae and eelgrass, 3A and 3B are from an eelgrass dominated site.

Pairwise comparison	p-value
1B-1A	0.999
2A-1A	0.801
2B-1A	0.297
3A-1A	0.088
3B-1A	0.193
2A-1B	0.689
2B-1B	0.212
3A-1B	0.057
3B-1B	0.132
2B-2A	0.951
3A-2A	0.656
3B-2A	0.868
3A-2B	0.986
3B-2B	0.999
3B-3A	0.999

Table S1.3 One-way ANOVA table for number of adults (shell size < 1mm) caught in snail catchers.

Parameter	**DF**	**SS**	**MS**	**F**	**P**
Snail catcher	5	41.53	8.306	2.279	0.072
Residuals	30	109.31	3.644		

Table S1.2 Tukey's HSD post hoc test results for ANOVA comparisons of number of adults (shell size < 1mm) across snail catchers above in Table S1.2. Asterisk indicates significance. Snail catchers 1A and 1B are from an macroalgae dominated site, 2A and 2B are in the transition zone between macroalgae and eelgrass, 3A and 3B are from an eelgrass dominated site.

Pairwise comparison	**p-value**
1B-1A	0.978
2A-1A	0.999
2B-1A	0.989
3A-1A	0.342
3B-1A	0.503
2A-1B	0.942
2B-1B	0.764
3A-1B	0.092
3B-1B	0.161
2B-2A	0.998
3A-2A	0.446
3B-2A	0.619
3A-2B	0.709
3B-2B	0.857
3B-3A	0.999

2. Current sensor statistics

Table S2.1 ANOVA table comparing flow regimes across field sites. Values were log-transformed to satisfy Levene's Test of homogeneity of variances prior to running the ANOVA. Asterisk indicates significance.

Parameter	**DF**	**SS**	**MS**	**F**	**P**
Site	3	19.274	6.425	14.35	0.002*
Residuals	7	3.135	0.448		

Table S2.2 Linear models to determine relationship between the proportion of snails with matched radulae and current speed by habitat. Corresponding AIC values for each model are listed to determine model selection. Best fit model highlighted in bold.

Model	**AIC**
Snails matched = flow regime * habitat + intercept	**-9.35**
Snails matched = flow regime + habitat + intercept	-0.24
Snails matched = habitat + intercept	-0.98
Snails matched = flow regime + intercept	11.22
Snails matched = intercept *(model of the mean)*	10.15

Table S2.3 Best fit model summary from selected model in Table S2.2.

Parameter	**Estimate**	**SE**	**T**	**P**
Intercept	0.141	0.076	1.843	0.108
Flow regime	0.889	0.512	1.735	0.126
Habitat	0.873	0.117	7.447	< 0.001*
Flow regime * Habitat	-29.515	8.441	-3.497	0.010*

3. Current sensor calibrations and data

Figure S1: Current sensor calibrations for all four sensors used from pre- and post- deployments. Standard water flow speeds were set in a flume and the number of propeller rotations were counted over ten replicate 30 second periods. Sensors had the following deployment locations: Sensor B - MC Eelgrass, Sensor C - MC Macroalgae, Sensor D - FB macroalgae and Sensor E - FB eelgrass. Calibration relationships for each sensor were determined by linear regression.

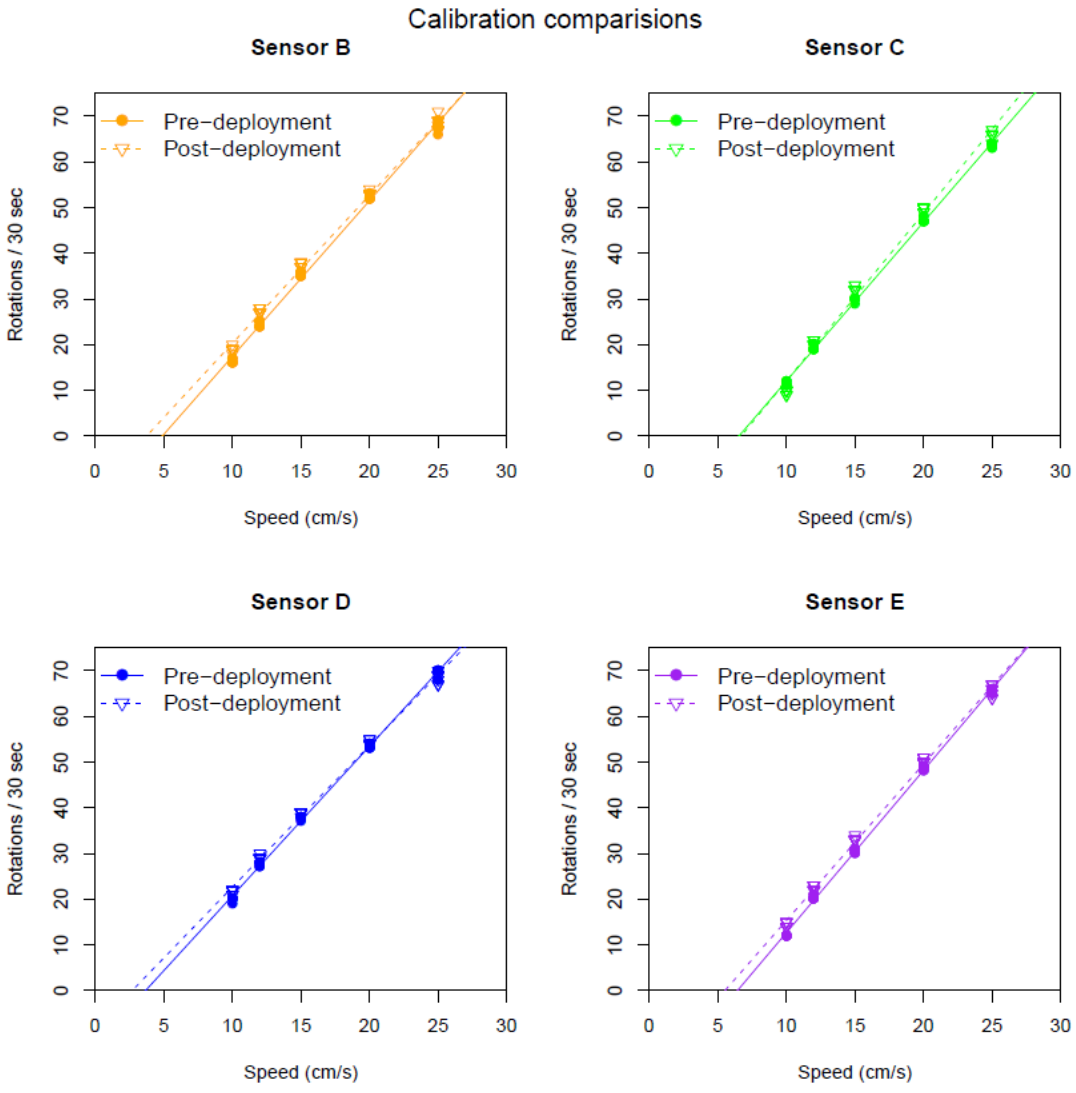

Figure S2: Current speed data from the Merrifield Cove Macroalgae site. Red dashed lines indicate the 10 cm/s threshold.

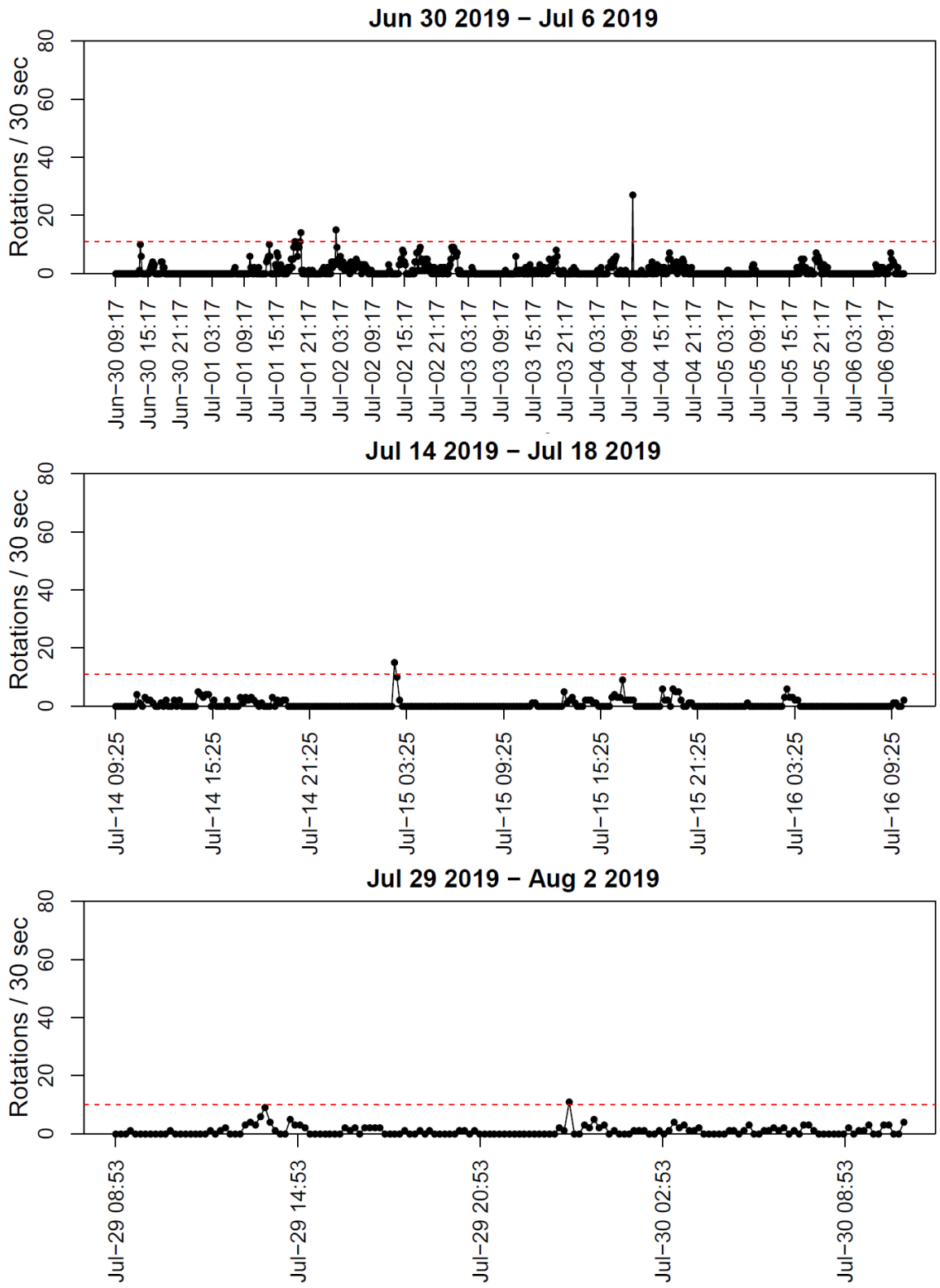

Figure S3: Current speed data from the False Bay Macroalgae site. Red dashed lines indicate the 10 cm/s threshold.

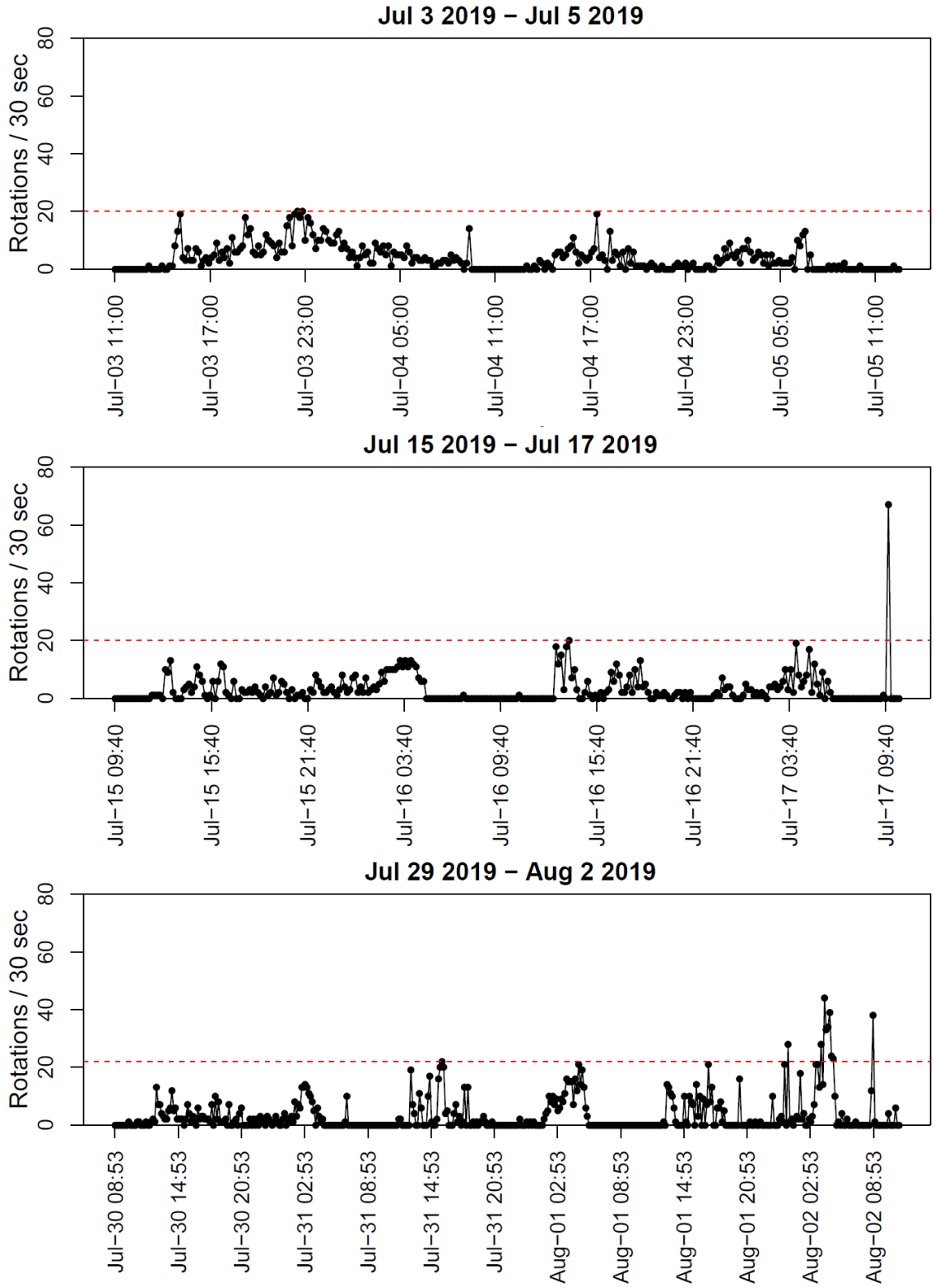

Figure S4: Current speed data from the Merrifield Cove Eelgrass site. Red dashed lines indicate the 10 cm/s threshold. Two maximum rotation points not plotted (Top: 1039, Middle: 396).

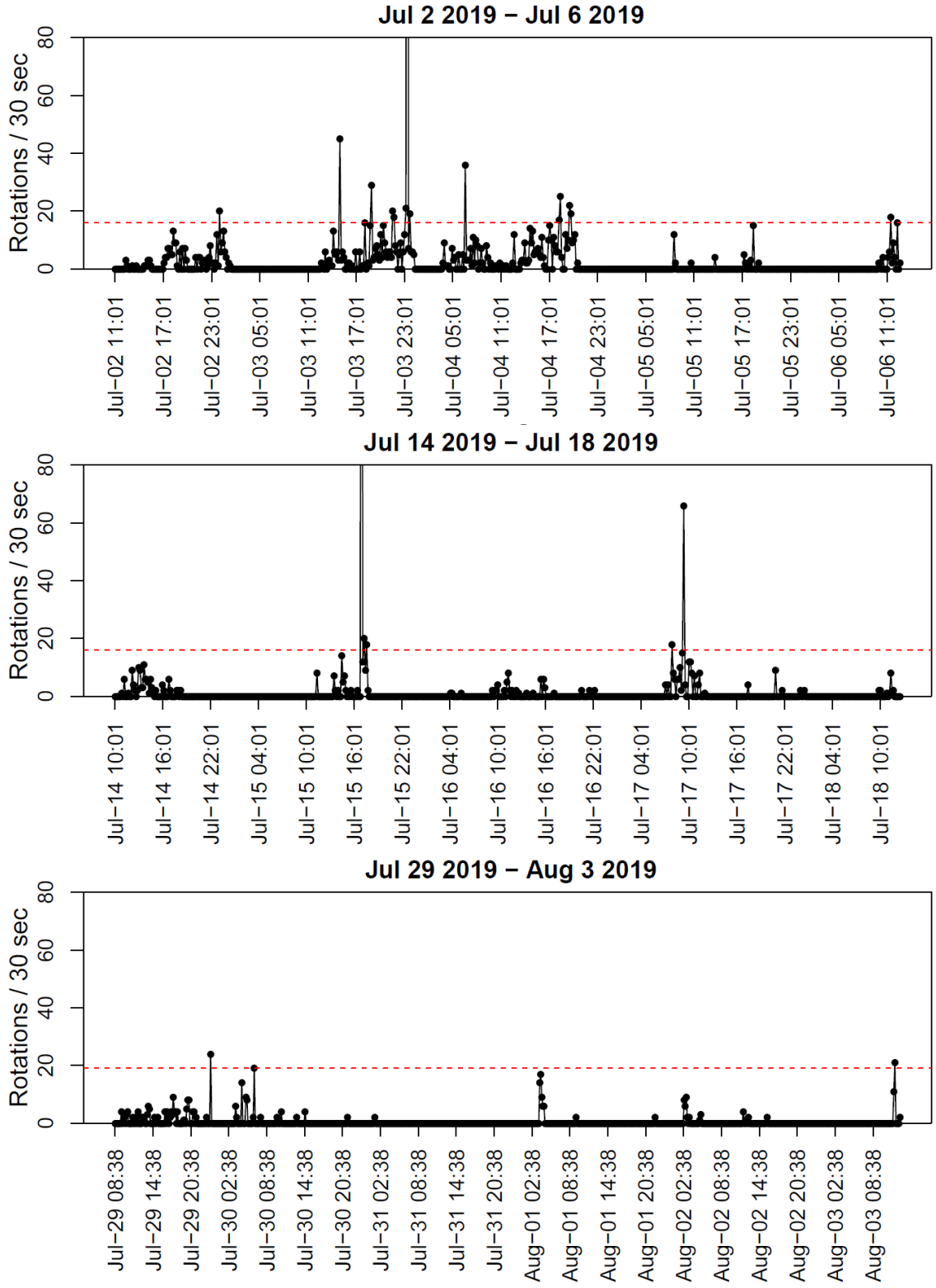

Figure S5: Current speed data from the False Bay Eelgrass site. Red dashed lines indicate the 10 cm/s threshold.

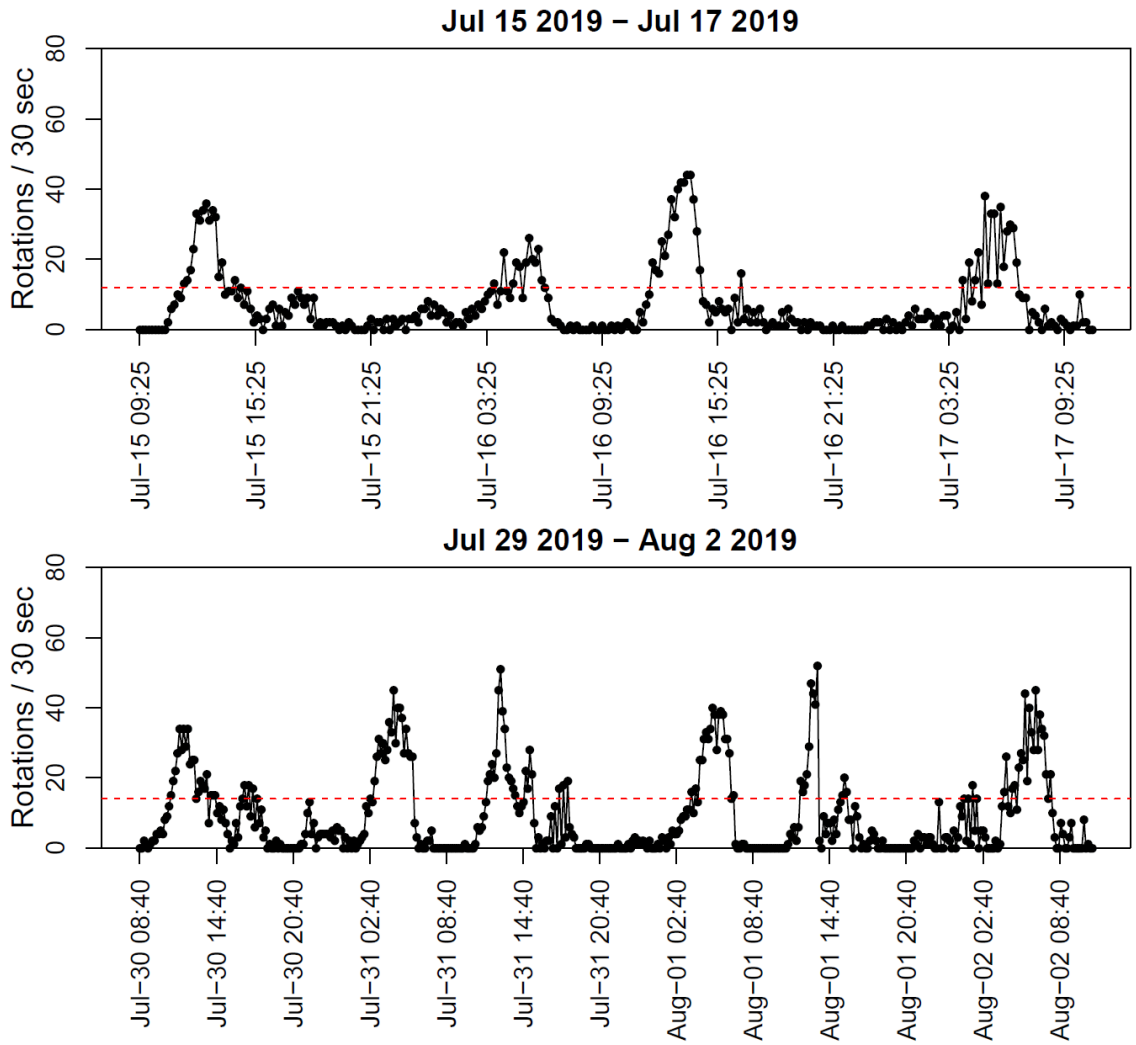

APPENDIX E: CHAPTER 6 SUPPLEMENTAL MATERIALS

Previously published at: https://doi.org/10.1080/10899995.2019.1702868

Student feedback question: How engaged were you during this lab? Did you enjoy it? If so why, or why not?

Responses received:

- I was engaged! Fun to create something that works!
- Yes! Was lit! 10/10 would recommend
- I was gone for the first two days so I was not very engaged in the lab. I think I would have liked it more if I was here the first couple of days
- 7/10
- On day 2, when the UW people were here, I was very engaged. I read all the instructions and led my lab. The next day I wasn't so much because we started to experience difficulties. I enjoyed this lab because I felt 'like a scientist' in a way. Instead of determining pH with strips we did it the harder way but the results were more specific.
- I was pretty engaged, I enjoyed this lab because it was interesting.
- I was very engaged, I did indeed enjoy this lab because it was fun.
- I was completely engaged during most of the lab. I did enjoy it. I was interested to try a lab that college students designed.
- I was not very engaged in this lab. I did not enjoy it only because something about the sensor was messed up so we go to do nothing besides wait and try to fix the issue which did not happen.
- I was very engaged in this lab because I got to write code. However, I was only here for one day, the first day of the lab, so my understanding still needs help. I very much enjoyed this lab because writing code is very cool.
- I was pretty engaged. Like 8/10. I enjoyed building the system.
- I enjoyed this lab very much and was engaged
- I was fully engaged in this lab. I enjoyed every bit because this lab was fun by identifying pH of solutions. I like using computers so this experiment was enjoyable.
- I was very engaged during this lab. I did enjoy the lab because we got to make a sensor and type commands into a computer.
- I was engaged in mainly in troubleshooting. Our lab didn't work so I tried to figure out why. Despite out lab being a failure, I do enjoy (trying to) fixing things. It'd be more enjoyable if everything worked though.
- I didn't enjoy it so much because I was confused about what we were doing but I think it was a very cool lab.
- I was very engaged in this lab even though it didn't work for us day 1. Overall, on day 2 we got it to work so then I enjoyed it. I really liked to try other ways besides titration and strips to find the pH of a solution.
- I really liked the lab. I really liked putting the parts together and trying to figure out what you are doing.
- I was very engaged during the lab.

- I enjoyed the lab because the colors were cool and our data was pretty close to the class average.
- I was pretty engaged. It was fun because cabbage juice is pretty.
- I enjoyed this lab because it involved using technology that is usually not used which was engaging.
- I was very engaged during this lab and enjoyed it very much mainly because I was learning new things and seeing strange equipment though I also appreciated the colors.
- I was engaged thoroughly in the lab and enjoyed it a lot like how to try and build sensors.
- I was very engaged and I enjoyed it because it was real science and I didn't have to write anything down. Also, the oceanographers were nice.
- I felt that during this lab I was engaged, I found the lab had a good connection between class and real world science.
- This lab was fun and engaging. I enjoyed assembling the spectrophotometer and using the computer software program to see the results of pH. Wish there would have been more time to do a more thorough analysis of the data/results.
- I was very engaged in this lab. I enjoyed it because we learned how to build a sensor and record different pH levels like scientists.
- I was sort of engaged. I knew what was going on. I enjoyed it because building the spectrophotometer was fun.
- It was fun but I wanted to actually get a pH around 8 since that was the accepted value
- I was quite engaged due to the interesting nature of the lab.
- Very engaged. It was cool to see a realistic application of what we are learning, so yes I enjoyed it.
- I was fairly engaged. I really enjoyed the lab and it gave me more knowledge on the process of finding pH and why it is important.
- I was very engaged physically in the lab but not mentally. The lab I found was pointless and a waste of time because there are machines already made to detect pH.
- My lab group and I worked hard for once during this lab, making it enjoyable, especially creating the sensor and using BeagleTerm to code really helped us work hard.
- On a scale of 1-10 I would say a 7 because I liked the hands-on aspect of building the sensor and getting the pH samples but it was frustrating trying to get the BeagleTerm to work for us. But I did enjoy the lab and I thought it was fun and interesting.
- I was very engaged. I enjoyed the lab very much because of the hands-on activity.
- Easy to understand. Some technical issues. All in all I felt the lab was simple if you actually followed and read the instructions given. The computer part of the job was simple for my lab group
- This lab was super fun and easy, really simple! The lab was easy to understand and not at all hard to do, it really encourages hands-on labs such as itself. Overall really enjoyable and awesome!
- I wasn't here on Wednesday but Tuesday was fun creating the box thing and actually seeing the technicalities that go into it and getting it to work with pH balances of things.
- I was engaged during this lab. I enjoyed it because it was simple and easy to follow.
- Overall, I enjoyed it for the most part. The first day it was fun but the second day wasn't when we would try to get data and it would be different every single time.

- I was pretty engaged until the computer stopped working and we couldn't do anything. That's when it got lame. I kinda enjoyed it, I like working with my hands so building the sensor was the best part for me. Overall this lab was okay, just need to work on the bugs on the computer and it would be sweet.
- I was engaged and enjoy working with electronics
- I liked the lab overall because it combines engineering and science.
- I thought it was a fun lab and I enjoyed it and using the light sensor
- Yes it was fun, mostly boring doing the same thing over and over again
- I enjoyed the lab, it was fun making electronics and working with programming.
- I wanted to be engaged but having three people in a group made it so that one was always shut out. I think pairs might be better for this lab so everyone can participate.
- I was engaged and enjoyed it because we got to build a sensor
- I found this lab engaging and interesting. It had applications for future everyday use.
- I enjoyed the lab
- I thought this lab was engaging. However, the directions were confusing and three people per group was too crowded.
- I wasn't really engaged in the lab but mainly because electric/sensors aren't really my cup of tea. But it would be very cool for someone who finds that interesting